

Aus der
Klinik und Poliklinik für Dermatologie und Allergologie
Klinik der Universität München
Direktor: Prof. Dr. Lars French



Role of B-cell Antigenicity in the Psoriatic Autoimmune Response against Melanocytes

Dissertation
zum Erwerb des Doktorgrades der Medizin
an der Medizinischen Fakultät
der Ludwig-Maximilians-Universität zu München

vorgelegt von
Mengwen He

aus
Guangxi, China

Jahr
2024

Mit Genehmigung der Medizinischen Fakultät
der Universität München

Berichterstatter:	Prof. Dr. Jörg C. Prinz
Mitberichterstatter:	Prof. Dr. Markus Braun-Falco
	PD Dr. Franziska Thaler
	PD Dr. Reinhard Obst
Mitbetreuung durch den promovierten Mitarbeiter:	Dr. Akiko Arakawa
Dekan:	Prof. Dr. med. Thomas Gudermann
Tag der mündlichen Prüfung:	18.09.2024

Table of contents

Zusammenfassung.....	1
Summary.....	3
1. Introduction.....	5
1.1 Concepts in the Pathogenesis of Psoriasis.....	5
1.1.1 Genetic Predisposition of Psoriasis	5
1.1.2 Function of HLA-class I Alleles in Psoriasis	6
1.1.3 Immunological Aspects of Psoriasis	8
1.1.4 Antigen Recognition of CD8 ⁺ T cells in Psoriasis	8
1.1.5 Streptococcal-Driven Psoriasis.....	11
1.2 MHC-class I Antigen Presentation.....	13
1.2.1 The Immune System.....	13
1.2.2 Characteristics of MHC Molecules	14
1.2.3 Antigen Presentation by MHC-class I Molecules	16
1.3 Discovery of T-cell Epitopes.....	18
1.3.1 Polyspecificity of T cells.....	18
1.3.2 Immunogenicity of T-cell Epitopes.....	19
1.3.3 Current Approaches for the Discovery and the Prediction of T-cell Epitopes.....	20
1.4 Objective	22
2. Materials	24
2.1 Devices	24
2.1.1 Cell Culture and Cell Analysis	24
2.1.2 Nucleic Acid Analysis.....	24
2.1.3 Centrifuges	25
2.1.4 Rotors	25
2.1.5 Coolers.....	25
2.1.6 Other Devices	25
2.2 Consumables and Chemicals.....	25
2.2.1 Consumables.....	25
2.2.2 Chemicals	26
2.3 Mediums.....	27
2.4 Buffers and Solutions.....	28
2.5 Commercial Kits and Specific Reagents.....	29
2.6 Oligonucleotides.....	30
2.6.1 Primers for Polymerase Chain Reaction.....	30
2.6.2 Primers for Sequencing	30
2.6.3 siRNAs	30
2.7 Plasmids and Vectors	31
2.8 Synthetic Peptides	31

2.9 Antibodies	32
2.9.1 Primary Antibodies.....	32
2.9.2 Directly Conjugated Antibodies	32
2.10 Bacterial Strains (<i>E. coli</i>)	33
2.11 Cells Lines/ Cells	33
2.12 Software	34
3. Methods.....	35
3.1 Cell Biological Methods.....	35
3.1.1 Cultivation of Suspension Cells	35
3.1.2 Cultivation of Adherent Cells.....	35
3.1.3 Determination of the Cell Number	35
3.1.4 Cryopreservation and Thawing of Eukaryotic Cells	36
3.1.5 Activation of V α 3S1/V β 13S1-TCR Hybridoma Cells by CD3 Cross-linking.....	36
3.1.6 Subcloning of the V α 3S1/V β 13S1-TCR Hybridoma.....	37
3.1.7 Cell Isolation or Separation	37
3.1.7.1 Isolation of PBMCs	38
3.1.7.2 Cell Separation and Depletion by Magnetic-activated Cell Sorting.....	38
3.1.7.3 Cell Sorting by Fluorescence-activated Cell Sorting for Co-culture Experiments	39
3.1.8 Co-culture Assays.....	42
3.1.9 Flow Cytometry Analysis of sGFP Expression in V α 3S1/V β 13S1-TCR Hybridoma Cells.....	42
3.1.10 Flow Cytometry Analysis of HLA-class I Expression	43
3.1.11 Cell Proliferation Assays	43
3.1.11.1 [3 H]-Thymidine Incorporation Assay	43
3.1.11.2 BrdU Cell Proliferation Assay.....	44
3.1.11.3 CFSE Labeling Assay.....	44
3.2 Molecular Biology Methods.....	45
3.2.1 Handling of <i>E.coli</i> Cultures	45
3.2.1.1 Cultivation of Bacteria.....	45
3.2.1.2 Preservation and Thawing of Bacterial Strains	46
3.2.1.3 Transformation of Bacteria.....	46
3.2.2 Generation of Peptide-Coding Plasmids	46
3.2.2.1 Primer Design of Peptide-Coding Plasmids	46
3.2.2.2 Cloning Peptide-Coding Sequence into Expression Vector	47
3.2.2.3 Plasmid DNA Isolation and Purification	48
3.2.3 Genomic DNA Extraction and Purification	49
3.2.4 Determination of DNA/RNA Concentration.....	49
3.2.5 Sequencing of DNA Samples	49
3.2.6 Transfection of Plasmid DNA and siRNA	50
3.2.6.1 Plasmid DNA Transfection of Cells with FuGENE.....	50
3.2.6.2 Plasmid DNA and siRNA Transfection of Cells with Nucleofector	50
3.2.7 Gel Electrophoretic Analysis of DNA.....	52
3.2.8 The Polymerase Chain Reaction (PCR)	52

3.2.9 HLA typing.....	53
3.3 Biochemistry Methods	54
3.3.1 Peptide Synthesis.....	54
3.3.2 MHC Immunoprecipitation (MHC-IP).....	54
3.3.3 Liquid Chromatography-Tandem Mass Spectrometry (LC-MS/MS)	55
3.3.4 Spectral Annotation and Database Search.....	56
3.4 Computational Methods	56
3.4.1 Determination of the V α 3S1/V β 13S1 TCR Ligand Motif.....	56
3.4.2 Screening HLA-C*06:02-Peptidomes for V α 3S1/V β 13S1-TCR Ligands.....	58
3.4.3 Screening for V α 3S1/V β 13S1-TCR Ligands in the Human Proteome.....	59
3.4.3.1 Motif-based Screening.....	59
3.4.3.2 MHC Binding Prediction of Selected Candidate Peptides	60
3.4.3.3 Narrowing Down the Search by Combinatorial Strategies	60
3.4.4 Analysis of the HLA-C*06:02 Peptidomes from B cell lines	60
3.5 Statistical Analyses	61
4. Results	63
4.1 Subcloning of the V α 3S1/V β 13S1-TCR Hybridoma.....	63
4.2 Stimulation of the V α 3S1/V β 13S1-TCR Hybridoma by B cells	63
4.2.1 Hybridoma Stimulation by Tonsillar B cells.....	63
4.2.2 Activation of the V α 3S1/V β 13S1 TCR by B cells is HLA-C*06:02-Restricted	66
4.2.3 Hybridoma Activation by Blood B cells	68
4.2.4 Co-culture of the V α 3S1/V β 13S1-TCR Hybridoma with Various Cell Types.....	70
4.3 Peripheral Blood B Cells Promote Autostimulation of CD8 ⁺ T cells in Psoriasis Patients	71
4.3.1 Increased Spontaneous Proliferation of PBMCs in Psoriasis Patients Compared to Healthy Donors.....	71
4.3.2 Spontaneous Cell Proliferation of PBMCs in Psoriasis Patients is Induced by B cells	72
4.3.3 B-cell Induced Autoproliferation of PBMCs is Significant in CD8 ⁺ T cells	73
4.3.4 Blocking HLA-ABC Reduces Autoproliferation of PBMCs	74
4.4 Determination of the V α 3S1/V β 13S1 TCR-Recognition Motif	75
4.4.1 Analysis of Mimotopes.....	76
4.4.2 Analysis of Human Self-Peptides and Environmental Peptide Ligands	78
4.4.3 Alanine Substitution Scan and Amino Acid Mutation Analysis	80
4.4.4 Summarized Recognition Motif of the V α 3S1/V β 13S1 TCR.....	83
4.4.5 The Motifs for Screening Human Proteome and HLA-C*06:02 Peptidomes.....	85
4.5 Screening of V α 3S1/V β 13S1-TCR Ligands in Peptidomes of HLA-C*06:02-C1R or -721.221	86
4.5.1 Candidate Peptides Derived from HLA-C*06:02-C1R and HLA-C*06:02-721.221	87
4.5.2 Examination of HLA-C*06:02-C1R or HLA-C*06:02-721.221 cell lines	88
4.6 Motif-based Database Search and Candidate Peptide Screening in B cell Transcriptomes	91
4.6.1 TCR-hybridoma Stimulation with Selected Candidate Peptides.....	91
4.6.2 siRNA Knockdown Experiments	94
4.7 Screening of V α 3S1/V β 13S1-TCR Ligands from HLA-C*06:02 homozygous B-cell Peptidomes	96
4.7.1 TCR Activation by Various HLA-C*06:02 Homozygous B cells	96

4.7.2 Analysis of HLA-C*06:02 Peptidomes	98
4.7.2.1 Yields and Length Distributions of HLA-C*06:02-Peptides	98
4.7.2.2 Peptide-binding Motifs of HLA-C*06:02 Molecules.....	101
4.7.2.3 Differences of Peptide Repertoires Regarding ERAP1 Haplotypes.....	103
4.7.3 Screening of Autoantigen Candidates from HLA-C*06:02-Peptidomes of B cells.....	106
4.7.3.1 TCR-Hybridoma Activation by Selected Candidate Peptides.....	107
4.7.3.2 Solubility Analysis	110
5. Discussion.....	113
5.1 Identification of B Cells as Initiators of the Psoriatic Autoimmune Response.....	114
5.2 Attempts to Identify the Psoriatic Autoantigen(s) in B cells	117
5.3 Streptococcal Angina Triggers B-cell-dependent Autoimmunity Against Melanocytes.....	121
5.4 HLA-C*06:02 Peptidome Analysis Depending on ERAP1 Variants	124
5.5 Impacts, Limitations, and Future Perspectives.....	127
5.6 Conclusions	129
6. Supplements.....	130
6.1 Primers for Double-strand DNA Coding Short Peptides	130
6.2 Plasmids	140
6.3 Information on Psoriasis Patients or Healthy Donors	146
6.4 Sequences of siRNAs for Target Proteins.....	147
6.5 Raw Data of HLA-C*06:02 Peptidomes.....	148
References	149
Appendixes.....	158
1. Abbreviations	158
2. Index of Figures	160
3. Index of Tables.....	161
4. Vector Map.....	162
Acknowledgements.....	163
Affidavit	165

Zusammenfassung

Psoriasis ist eine komplexe T-Zell-vermittelte Autoimmunerkrankung der Haut. Klinisch ist sie gekennzeichnet durch scharf abgegrenzte rötliche Plaques, die von silbriger Schuppung bedeckt sind und infolge einer entzündlichen Hyperproliferation von Keratinozyten entstehen. Psoriasis entwickelt sich auf einer komplexen genetischen Veranlagung, wobei das Humane Leukozyten Antigen (HLA) Klasse I-Allel HLA-C*06:02 das eigentliche Psoriasis-Risikogen darstellt. HLA-Klasse-I-Moleküle präsentieren Peptide an CD8⁺ T-Zellen, die aus zytoplasmatischen Proteinen generiert werden. Hierdurch lenken sie die T-Zell-Reaktion gegen bestimmte Zielzellen, die das elterliche Protein des antigenen Epitops exprimieren. Durch die Analyse eines pathogenen V α 3S1/V β 13S1-T-Zell-Rezeptors (TZR) aus einem läsionalen psoriatischen CD8⁺ T-Zell-Klon hatte unsere Forschungsgruppe nachgewiesen, dass HLA-C*06:02 als zugrundeliegender Pathomechanismus der HLA-Assoziation bei Psoriasis eine Autoimmunreaktion gegen Melanozyten durch die Präsentation eines autoantigenen Peptids von ADAMTS-like Protein 5 (ADAMTSL5) vermittelt.

Die Schuppenflechte ist aber keine kongenitale Erkrankung, sondern entwickelt sich im Laufe des Lebens. Das T-Zell-Rezeptor-Repertoire ist bei der Geburt weitgehend festgelegt, und sowohl das Autoantigen als auch potenziell autoreaktive T-Zellen sind bereits vor dem Ausbruch der Krankheit vorhanden, bleiben aber immunologisch inaktiv. Daher geht man davon aus, dass Umweltfaktoren, Lebensstil und Infektionen die Psoriasis auslösen, indem sie potenziell autoreaktive T-Zellen aktivieren. Die genauen Mechanismen der Gen-Umwelt-Interaktion bei der Entwicklung von Psoriasis sind jedoch noch nicht geklärt.

Streptokokken-Infektionen der Tonsillen sind häufige Auslöser für das erstmalige Auftreten und für Schübe der Psoriasis. Identische T-Zell-Klone in Tonsillen und Hautläsionen von Patienten mit streptokokkenbedingter Psoriasis, Besserung der Psoriasis nach therapeutischer Hemmung der T-Zell-Emigration aus sekundären lymphatischen Organen durch den S₁P₁-Rezeptor-Agonisten Ponesimod und die Abheilung der Psoriasis nach Tonsillektomie deuten darauf hin, dass die Induktion und Aufrechterhaltung der läsionalen psoriatischen T-Zell-Antwort von einer ständigen Rekrutierung pathogener T-Zellen aus sekundären lymphatischen Organen in die Haut abhängig ist.

Das Hauptziel meiner Arbeit war es, herauszufinden, wie die Streptokokken-Angina die autoimmune psoriatische T-Zell-Antwort induziert. Dazu habe ich den in einer Reporter-Maus-T-Hybridom-Zelllinie exprimierten psoriatischen V α 3S1/V β 13S1 TZR verwendet, um potenzielle Zielzellen und Antigene in den Tonsillen zu identifizieren. Zunächst kultivierte ich

das V α 3S1/V β 13S1-TZR-Hybridom zusammen mit primären menschlichen Zellen, die ich aus den Tonsillen und dem Blut HLA-C*06:02-positiver Psoriasis-Patienten isoliert habe, sowie mit Zelllinien verschiedener Herkunft. Auf diese Weise konnte ich nachweisen, dass neben Melanozyten auch B-Zellen sowohl den V α 3S1/V β 13S1-TZR als auch CD8⁺ T-Zellen von Psoriasis-Patienten spezifisch aktivieren. Die Schwierigkeit bei der Identifizierung von T-Zell-Antigenen liegt in der Komplexität der TZR-Antigenerkennung. TZRen sind polyspezifisch und können bis zu einer Million verschiedener antigener Peptide erkennen, die von dem restringierenden HLA-Molekül präsentiert werden, wenn sie dem Peptiderkennungsmotiv des TZRs entsprechen. Ich habe das Peptiderkennungsmuster, das den V α 3S1/V β 13S1-TZR ligiert, genauer charakterisiert. Mit diesem Motiv habe ich das Transkriptom und das HLA-C*06:02-Immunozeptidom von B-Zellen nach möglichen B-Zell-Antigenen des V α 3S1/V β 13S1-TZR durchsucht. Mit verschiedenen experimentellen Ansätzen konnte ich letztendlich mehrere Selbst-Peptide im HLA-C*06:02-präsentierten Immunozeptidom von B-Zellen identifizieren, die den V α 3S1/V β 13S1 TCR stimulieren und sich dabei vom Melanozytenautoantigen unterscheiden. Meine Ergebnisse deuten darauf hin, dass die starke Entzündungsreaktion während der Streptokokken-Angina eine Autoimmunaktivierung von CD8⁺ T-Zellen gegen B-Zell-Antigene in den Tonsillen auslöst, die sekundär gegen Melanozyten in der Haut kreuzreagieren und so die Psoriasis auslösen. Eine gegen B-Zellen gerichtete Immunaktivierung autoreaktiver CD8⁺ T-Zellen in sekundären lymphatischen Organen kann somit Effektor-T-Zellen generieren und vermehren, die die pathogene Autoimmunreaktion gegen Melanozyten in der Haut von Psoriasis-Patienten vermitteln. Diese Daten klären einen wesentlichen Schritt in der Induktion und Aufrechterhaltung der psoriatischen Autoimmunreaktion auf, und sie identifizieren einen bisher unbekannten Pathomechanismus, durch den Streptokokkeninfektionen Autoimmunität auslösen können.

Summary

Psoriasis is an inflammatory skin disease caused by a T-cell-mediated autoimmune response, clinically characterized by distinct reddish plaques covered with a thick layer of silvery scales resulting from excessive proliferation of keratinocytes. Psoriasis arises from a complex genetic predisposition, with the human leukocyte antigen (HLA) class I-allele HLA-C*06:02 representing the actual psoriasis risk gene. HLA-class I molecules on the cell surface present endogenous peptides originating from cytoplasmic proteins to CD8⁺ T cells, thereby guiding the T-cell reaction against specific target cells that express the parental protein containing the antigenic epitope. Using a pathogenic V α 3S1/V β 13S1 T-cell receptor (TCR) from a lesional psoriatic CD8⁺ T-cell clone, our research group demonstrated that HLA-C*06:02, as the underlying pathomechanism of the HLA association, facilitates an autoimmune reaction against melanocytes in psoriasis by presenting an autoantigenic peptide from ADAMTS-like protein 5 (ADAMTSL5).

Psoriasis is not a congenital condition but rather develops at some point during the life course. The T-cell receptor (TCR) repertoire is largely fixed at birth, and both the autoantigen and potentially autoreactive T cells are present prior to the onset of the disease but remain immunologically quiescent. Consequently, environmental factors, lifestyle, and infections are thought to induce psoriasis by priming potentially autoreactive T cells. The precise mechanisms of the gene-environment interaction in the development of psoriasis, however, are still not clear.

Streptococcal angina is the most common trigger for psoriasis onset and relapses. Identical T-cell clones in tonsils and skin lesions identified in patients with streptococcal-driven psoriasis, improvement of psoriasis by therapeutic blockade of T cell emigration from secondary lymphoid organs by an S₁P₁-receptor agonist ponesimod, and resolution of psoriasis following tonsillectomy collectively indicate that induction and maintenance of the pathogenic T-cell response in lesion rely on continuous recruitment of pathogenic T cells from secondary lymphoid organs into the skin.

The primary objective of my thesis was to identify how streptococcal angina induces the autoimmune psoriatic T-cell response. For this, I used a reporter mouse T-hybridoma cell line, in which the psoriatic V α 3S1/V β 13S1 TCR was reconstituted to identify potential target cells and antigens in the tonsils. I first co-cultured the V α 3S1/V β 13S1-TCR hybridoma with primary human cells obtained from the tonsils and blood of HLA-C*06:02⁺ psoriasis patients and with cell lines of various origins. This way, I showed that besides melanocytes, B cells specifically activate both the V α 3S1/V β 13S1 TCR and CD8⁺ T cells of psoriasis patients. The difficulty of

the identification of T-cell antigens lies in the complexity of TCR antigen recognition. TCRs are polyspecific and can recognize up to a million different antigenic peptides associated with the cognate HLA molecule if the peptides correspond to the peptide recognition motif of that TCR. I further precisely characterized the peptide recognition pattern ligating the V α 3S1/V β 13S1 TCR. With this motif, I searched the transcriptome and the HLA-C*06:02 immunopeptidome of B cells for possible B cell antigens of the V α 3S1/V β 13S1 TCR. Employing various experimental approaches, I finally identified several self-peptides in the HLA-C*06:02 immunopeptidome of B cells that stimulate the V α 3S1/V β 13S1 TCR and are distinct from the melanocyte autoantigen. My results suggest that the strong inflammatory reaction during streptococcal angina triggers activation of self-reactive CD8⁺ T cells against B cells in the tonsils, which then cross-react against melanocytes in the skin and cause psoriasis. The B-cell-directed immune activation of CD8⁺ T cells in secondary lymphoid organs may thus activate and expand the effector T cells that mediate the pathogenic autoimmune response against melanocytes in the skin of psoriasis patients. These data clarify an essential step in the induction and perpetuation of the psoriatic autoimmune response and they identify a formerly unknown pathomechanism by which streptococcal infections may initiate autoimmunity.

1. Introduction

1.1 Concepts in the Pathogenesis of Psoriasis

Psoriasis is a complex T-cell-mediated inflammatory skin disorder that affects roughly 2% of the Western population (Bowcock and Krueger, 2005). Plaque psoriasis (also known as psoriasis vulgaris), the most prevalent type of psoriasis, is clinically manifested by slightly elevated reddish patches or papules covered with intensive silvery scales. The inflammatory changes lead to a strong increase in keratinocyte proliferation (Griffiths *et al.*, 2021; Prinz, 2017b). The epidermopoiesis, i.e., the time span in which the epidermis regenerates completely, is shortened from approximately 28 days to less than five days. In up to 30% of psoriasis patients, inflammation also involves the joints, sometimes leading to severe arthritis (Prinz, 1997).

Psoriasis is caused by a combination of variables, involving the interplay between inherited susceptibility alleles and infectious, environmental, and lifestyle factors. Psoriasis has been identified as a T-cell-mediated disorder in the past two decades upon the basis of a strong disease association with HLA-C*06:02 and the favorable outcomes of T-cell-directed therapies (Griffiths *et al.*, 2021; Prinz, 2018). In our previous study, we have proven that psoriasis is an autoimmune disease by demonstrating that HLA-C*06:02 mediates an autoimmune response against melanocytes via the presentation of an autoantigenic peptide from ADAMTSL5 (Arakawa *et al.*, 2015).

The psoriatic immune response is characterized by a complex cytokine pattern dominated by the cytokines IL-17A, IL-22, and IFN- γ (Perera *et al.*, 2012). Even though the cytokine network of psoriasis has been dissected in great depth, the mechanisms inducing and maintaining the autoimmune response against melanocytes have remained unknown. Identification of these specific mechanisms may provide insights into the pathogenic understanding of the T-cell-mediated autoimmune response in psoriasis but also provide a concept for the pathogenic understanding of chronic immune-mediated inflammation in other HLA-class I-associated immune-mediated inflammatory disorders (IMIDs).

1.1.1 Genetic Predisposition of Psoriasis

Psoriasis genetic susceptibility is demonstrated by familial clustering and high disease concordance in monozygotic twins compared to dizygotic twins. Linkage analysis, which

permits the localization of disease-risk genes to well-defined chromosomal regions, was utilized to examine the genetic architecture of psoriasis (Capon, 2017). However, linkage studies turn out not to be suitable for the analysis of multifactorial diseases, though they have been proven highly useful in mapping gene loci underlying monogenic conditions. Nine different psoriasis susceptibility regions 1-9 (known as PSORS 1-9) have been mapped by linkage analysis, among which only PSORS1, corresponding to *HLA-C*06:02*, conveys a distinct predisposition to psoriasis (The International Psoriasis Genetics Consortium, 2003).

The advancement in high-throughput genotyping technologies allowed an alternative to linkage studies, i.e., genome-wide association studies (GWAS). In addition to GWAS, targeted genotyping technologies (e.g., ImmunoChip), which specifically analyzes single nucleotide polymorphisms (SNPs) associated with IMIDs, and the Exome chip, which focuses on markers within coding regions, were applied to examine the genetic architecture of psoriasis. At the time of my dissertation, a total of 63 susceptibility loci for psoriasis have been uncovered through comprehensive analyses using GWAS, exome-wide association studies, and ImmunoChip (47 identified in GWAS, 15 in ImmunoChip studies, and one in an exome-wide survey) (Capon, 2017; Ogawa and Okada, 2020; Tsoi *et al.*, 2012; Tsoi *et al.*, 2015).

The candidate genes identified can be clustered according to distinct immune pathways that they are involved in, such as antigen presentation (*HLA-C* and *ERAPI*), innate antiviral immunity (*DDX58*, *IFIH1*, *TYK2*, *RNF114*), as well as the activation, differentiation, and signaling of Th/c17 cells (*IL23A*, *IL23R*, *IL12B*, *TRAF3IP2*, *NFKBIZ*) (Capon, 2017). Notably, *HLA-C*06:02*, located in PSORS1 on chromosomal band 6p21.3 within the major histocompatibility complex (MHC), has been established as the main psoriasis risk gene based on sequence-based approaches in large samples (Nair *et al.*, 2006; Zhou *et al.*, 2016). This gene accounts for approximately half of the psoriasis risk (Burden *et al.*, 1998). The early onset, severity, and familial clustering of psoriasis are determined by the presence of *HLA-C*06:02*, which has a non-additive risk effect. The gene variants outside MHC contribute an estimated 20% of the psoriasis risk. Many of them, however, are pleiotropic in that they affect the risk of various IMIDs (Tsoi *et al.*, 2012). Psoriasis patients are inevitably heterogeneous regarding these gene variants, which may rather modulate disease phenotype or onset than provide a direct genetic cause (Nikamo *et al.*, 2015). The remaining around 30% of disease risk in genetically predisposed individuals is attributed to environmental, infectious, and lifestyle factors (Grjibovski *et al.*, 2007).

1.1.2 Function of HLA-class I Alleles in Psoriasis

Psoriasis belongs to the group of HLA-associated IMIDs, which also includes ankylosing spondylitis, rheumatoid arthritis, inflammatory bowel disease, multiple sclerosis, Behçet's disease, and others. Though IMIDs share a significant number of non-HLA loci, the associated HLA-class I or class II alleles are often disease-specific.

To date, a mere three out of over 25,000 HLA-class I alleles that have been identified exhibit a robust association with diseases: *HLA-B*51* is linked to Behçet's disease, *HLA-C*06:02* to psoriasis, and *HLA-B*27* to ankylosing spondylarthritis (Prinz, 2018). Diverse peptide-binding grooves arising from HLA allele polymorphisms ultimately determine distinct HLA allele-specific peptide repertoires (Falk *et al.*, 1991; Vyas *et al.*, 2008). Therefore, an autoimmune response against selected self-peptides presented by certain HLA molecules would be the most straightforward explanation for the HLA-class I association of diseases (Prinz, 2017a). However, this inference was disputed due to a strong linkage disequilibrium of HLA-class I alleles with other gene variants in the MHC and the lack of functional imputation of the actual pathogenic significance of *HLA-C*06:02* in psoriasis. Sequencing of the HLA-class I region finally confirmed that *HLA-C*06:02* is indeed the actual risk gene (Nair *et al.*, 2006; Zhou *et al.*, 2016).

The antigens presented by HLA-class I to T cells have a fundamentally distinct origin from those by II molecules (Rock *et al.*, 2016). HLA-class II molecules are expressed nearly exclusively on professional antigen-presenting cells and are responsible for presenting extracellular antigens to CD4⁺ T cells. Autophagy introduces organelles, mitochondria, ribosomes, or tiny quantities of cytosol into the HLA-class II-presentation pathway as well (Crotzer and Blum, 2009; Roche and Furuta, 2015; Stern and Santambrogio, 2016). In comparison, endogenous antigens are generated from cytoplasmic proteins and subsequently bound on HLA-class I molecules. Cytoplasmic proteins are initially degraded by the cellular proteasome and translocated into the endoplasmic reticulum (ER), where a fraction of the peptides is subsequently subjected to NH₂-terminal trimming by the endoplasmic reticulum aminopeptidase 1 (ERAP1). The peptides can be loaded into the peptide-binding groove of the HLA-class I molecules if they contain the anchor amino acid residues and are of appropriate size at 8 to 10 amino acids. After that, the expression of the “antigen-MHC-I complex,” which consists of one HLA-class I molecule and a peptide antigen, on the cell membrane enables recognition by the cognate αβ T-cell receptors (TCRs) of CD8⁺ T cells.

The fact that HLA-class I molecules present endogenous peptide antigens originating from cytoplasmic proteins implies that an HLA-class I-restricted autoimmune response has to be

directed against a particular target cell expressing the parental protein of the antigenic peptide epitope. This principle is the basis for understanding HLA-class I-restricted immune responses, regardless of whether the protein originates from an infectious intracellular pathogen or an intrinsic protein.

1.1.3 Immunological Aspects of Psoriasis

The involvement of T cells in the psoriasis pathogenesis was supported by growing evidence, including the presence of activated CD4⁺ T cells and CD8⁺ T cells in psoriatic plaques and peripheral blood of psoriasis patients, clonally expanded TCRs in psoriasis skin lesions and the therapeutic success of T cell-targeted drugs such as immunosuppressants or monoclonal antibodies. Various studies showed that epidermal recruitment, activation, and clonal expansion of CD8⁺ T cells are essential for the occurrence of psoriasis plaques, implying that CD8⁺ T cells are the actual pathogenic effector cells of psoriasis (Chang, J. C. *et al.*, 1994; Conrad *et al.*, 2007; Di Meglio *et al.*, 2016; Kim *et al.*, 2012; Paukkonen *et al.*, 1992).

The psoriatic immune response mediated by T cells is characterized by a complex cytokine network, with the IL-23/IL-17 axis playing a crucial role in the immunopathogenesis of psoriasis among diverse signaling pathways. T-helper/cytotoxic 17 cells (Th/c17 cells) are both defined by the production of interleukin-17 (IL-17). Lesionally infiltrating T cells produce the Th/c17 hallmark cytokines IL-17A, IL-17F, IL-22, TNF- α , and IFN- γ (Ortega *et al.*, 2009; Vural *et al.*, 2021). These cytokines further promote the proliferation of keratinocytes, the recruitment of neutrophils, and the generation of antimicrobial peptides, as well as inflammatory cytokines and chemokines. IL-23, which is generated by local dendritic cells and keratinocytes, in turn, maintains the activation of the psoriatic Th/c17 cells in the skin lesion (Prinz, 2018). Thus, a local immune-keratinocyte positive loop is formed in the psoriatic lesions. Therapeutic blockades of TNF- α , IL-17A, or IL-23 are currently the most effective therapy modalities for psoriasis (Griffiths *et al.*, 2021).

While the T-cell-dependent cytokine network in psoriasis is increasingly better understood, the mechanisms of psoriatic T-cell activation still raise many questions.

1.1.4 Antigen Recognition of CD8⁺ T cells in Psoriasis

According to my previous explanations, novel psoriatic lesions develop upon the recruitment and clonal expansion of CD8⁺ T cells in the epidermis that produce the pathogenic cytokines

IL-17A and IL-22, which indicate that CD8⁺ T cells are continuously recruited and activated by local autoantigen presentation (Prinz, 2017b).

The TCRs of the pathogenic CD8⁺ T cells that determine both HLA restriction and T-cell specificity are obviously significant for understanding the pathogenesis of the disease. Today's knowledge of the mechanisms of T-cell activation in psoriasis lesions comes from the analysis of TCR rearrangements of the T cells infiltrating the psoriatic lesions. The observation that psoriatic CD8⁺ T cells in the epidermis preferentially rearrange the TCR V β 3 or V β 13S1 variable region gene, together with the sequence analysis of the CDR3 regions of the TCR β -chains of the pathogenic T cells, which showed a clear oligoclonality or even monoclonality indicate that the immune response in psoriasis is resulting from antigen-specific activation (Chang, J. C. *et al.*, 1994). In our laboratory, an unbiased approach for characterizing $\alpha\beta$ TCRs of single T cells has been established (Kim *et al.*, 2012). With this technique, we identified predominant lesional CD8⁺ T-cell clones and examined the gene rearrangements of their paired TCR α - and β -chain. The TCRs from clonally expanded CD8⁺ T cells were reconstituted in a mouse 58 α/β - T-hybridoma recipient cell line with missing endogenous TCR α and β chains that carried all CD3 molecules and the signaling cascade to secrete IL-2 after TCR activation (Letourneur and Malissen, 1989). Consequently, these TCR hybridomas carry the specificity of the psoriatic immune response.

For sensitively detecting T-cell activation, the nuclear factor of activated T cells- superfolder green fluorescent protein (NFAT-sGFP) reporter system was introduced (Seitz *et al.*, 2006). When the TCR recognizes a specific antigen, the NFAT molecule is dephosphorylated in the hybridoma cell by the calcium-calciueurin-NFAT signal transmission pathway and then transferred into the nucleus, where it binds to the IL-2 promoter and switches on the IL-2 gene and induces the production of sGFP (Hooijberg *et al.*, 2000). In conjunction with the co-transfection of the specific TCR, human CD8 $\alpha\beta$ chains, and NFAT-sGFP, these T hybridoma cells can report TCR signaling by robust expression of sGFP when they recognize the appropriate antigen(s), which can be evaluated with fluorescence microscopy and flow cytometry analysis (Siewert *et al.*, 2012).

In our investigations, we utilized the V α 3S1/V β 13S1 TCR as a representative TCR since the rearrangement of the V13S1 TCR gene is a characteristic feature of CD8⁺ T cells lesional infiltrating in psoriatic lesions. The observations that the corresponding lesional CD8⁺ T cell clone of the V α 3S1/V β 13S1 TCR was ubiquitous and found in two separate biopsy samples from an HLA-C*06:02⁺ psoriasis patient indicate the pathogenic significance for the psoriatic

immune response in that patient. Therefore, the V α 3S1/V β 13S1 TCR from that patient was used in the TCR-hybridoma report assay for defining HLA restriction as well as the target cells and autoantigen of the T-cell-mediated psoriatic immune response (**Figure 1.1.4.1**) (Arakawa *et al.*, 2015; Kim, 2011).

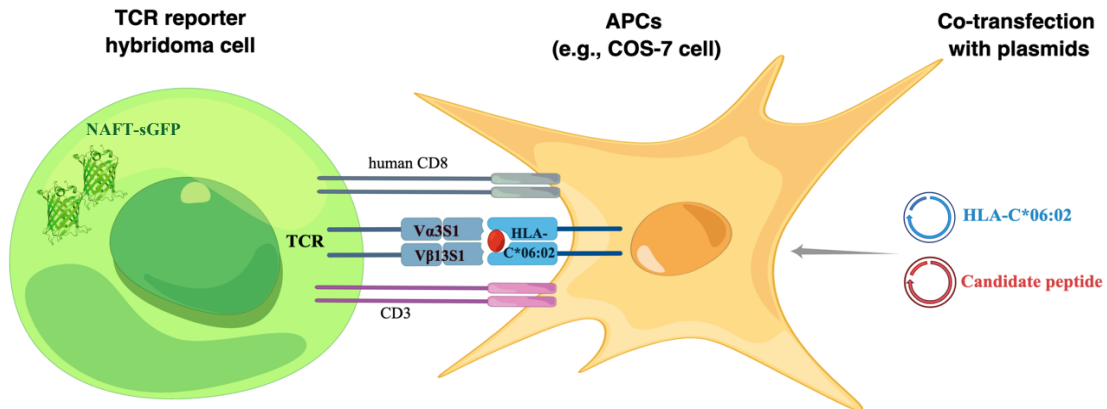


Figure 1.1.4.1 Schematic overview of the V α 3S1/V β 13S1-TCR hybridoma reporter assay. The TCR reporter hybridoma cell carries CD3 and a V α 3S1/V β 13S1 TCR, originating from a lesional CD8⁺ T cell clone isolated from an HLA-C*06:02-positive patient. We employed COS-7 cells as antigen-presenting cells, which were transiently co-transfected with HLA-C*06:02 and plasmid-encoded candidate peptides. This led to the expression of HLA-C*06:02 that had bound the candidate peptide on the surface of APCs. Once the V α 3S1/V β 13S1 TCR recognized the HLA-C*06:02-presented peptide, the TCR hybridoma reported on TCR signaling by strong sGFP production through the co-transfection of human CD8 α and NFAT-sGFP (figure by Figdraw).

In our previous work, we conducted a series of co-culture experiments of the V α 3S1/V β 13S1-TCR hybridoma with various human cell types from the skin and other tissues and revealed that the V α 3S1/V β 13S1 TCR was activated by primary melanocytes or melanocytic cell lines only when they carry HLA-C*06:02, irrespective of their origin from psoriasis patients or healthy donors. Extensive screening of a combinatorial peptide library co-expressed with HLA-C*06:02 in COS-7 cells further identified various mimotopes, i.e., artificial peptide antigens that ligated the V α 3S1/V β 13S1 TCR. The amino acid sequence of these peptides revealed the peptide recognition motif of the V α 3S1/V β 13S1 TCR. Finally, searching the human proteome for proteins containing peptides corresponding to the motif enabled the identification of a 9-mer peptide from ADAMTSL5 as the HLA-C*06:02-presented autoantigen on melanocytes for psoriasis. In accordance with the reactivity of the V α 3S1/V β 13S1 TCR against the melanocytic peptide, lesional CD8⁺ T cells react against melanocytes, and the ADAMTSL5 peptide proved to be highly immunogenic for psoriasis patients, inducing the production of IL-17A in CD8⁺ blood T cells (**Figure 1.1.4.2**) (Arakawa *et al.*, 2015).

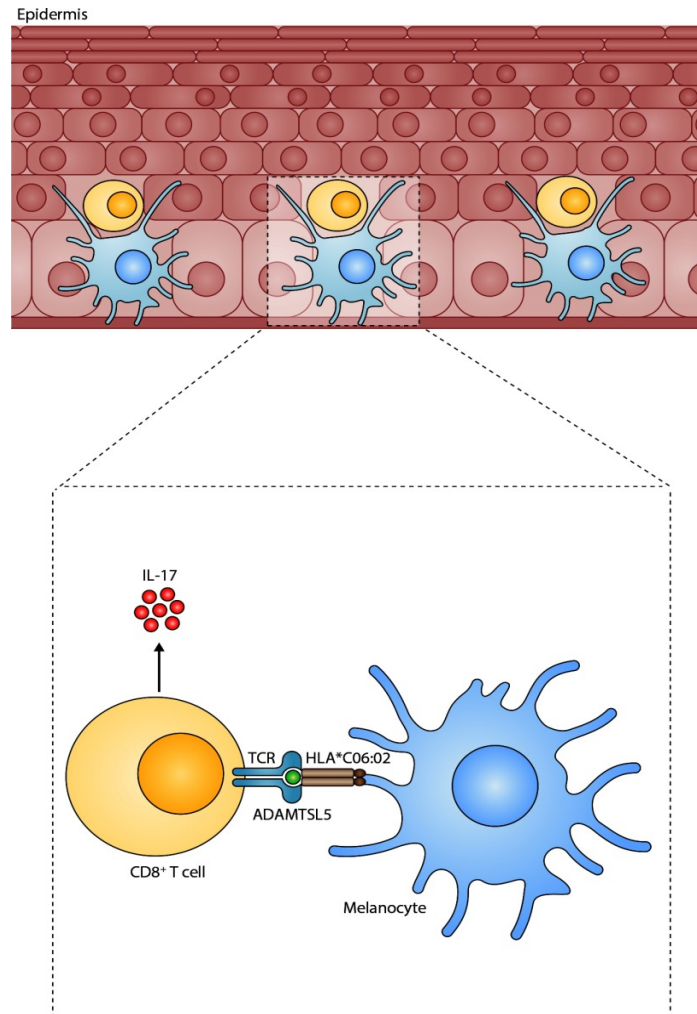


Figure 1.1.4.2 CD8⁺ T cells infiltrating in psoriatic lesions recognize ADAMTSL5 peptide as a psoriasis autoantigen presented by HLA-C*06:02 on melanocytes and produce the psoriasis hallmark cytokine IL-17 following activation (Krueger, 2015).

1.1.5 Streptococcal-Driven Psoriasis

Polyspecificity of TCRs implies that pathogenic T cells may recognize different peptides sharing similar amino acid patterns. The HLA-presented immunopeptidome contains thousands of different self-peptides. The TCR repertoire is largely fixed at birth, implying that potentially autoreactive T cells are already present before disease onset but remain quiescent (Sewell, 2012). Therefore, triggering events through external antigens or highly inflammatory conditions during a lifetime could break self-tolerance and lead to T-cell priming against self-peptides, initiating the psoriatic autoimmune response against melanocytes.

An essential question to be answered is whether the effector CD8⁺ T cells in the lesion are skin-resident memory T cells or a result of continuous T-cell recruitment. The development of psoriatic hyperplasia in skin grafts taken from the edge of psoriatic plaques and transplanted

into immunodeficient mice was completely prevented when the migration of CD8⁺ T cells into the epidermis was blocked (Boyman *et al.*, 2004; Conrad *et al.*, 2007; Di Meglio *et al.*, 2016). Accordingly, psoriasis metamorphosis requires the recruitment of T cells into the epidermis. This was also proven by the disease resolution after therapeutic application of the S₁P₁ receptor modulator ponesimod that inhibits T-cell emigration from secondary lymphoid organs or by treatment of patients with the LFA-1 antibody efalizumab that blocks migration of T cells from the circulation into psoriasis lesion (D'Ambrosio *et al.*, 2016; Jullien *et al.*, 2004; Ryan and Menter, 2014).

Psoriatic manifestations are often provoked by throat infections with different groups of β -hemolytic *Streptococci* (Groups A, B, C, and G) (Sigurdardottir *et al.*, 2013), and *HLA-C*06:02*-positive patients are particularly sensitive to the streptococcal trigger, as supported by genetic association studies (Haapasalo *et al.*, 2018; Mallbris *et al.*, 2009; Thorleifsdottir, Sigurdardottir, *et al.*, 2016). In streptococcal-induced psoriasis, the same T-cell clones identified in psoriatic lesions and the fraction of tonsillar T cells that express the cutaneous lymphocyte-associated antigen (CLA) (Diluvio *et al.*, 2006), together with the clinical observations that patients experienced significant improvement in their psoriasis after tonsillectomy (Wilson *et al.*, 2003), indicate that T cells may represent the link between streptococcal angina and psoriatic skin inflammation and that ongoing psoriasis requires continuous recruitment of T cells from secondary lymphoid organs, rather than a persistent activation of skin-resident T cells (Diluvio *et al.*, 2006; Gaide *et al.*, 2015).

Self-reactivity is controlled by the mechanisms of both central tolerance and peripheral tolerance (Prinz, 2022). In the thymus, central tolerance mechanisms effectively eliminate autoreactive T cells with TCRs exhibiting inadequate affinity towards cognate MHC or showing excessive response to self-peptide/MHC complexes. Although those T cells responding strongly to self-peptides are deleted during central tolerance induction, some T cells with a low level of self-reactivity may survive and be released into the periphery. They may be activated and directed against self either through molecular mimicry, a cross-recognition by pathogen-driven peptides, or through proinflammatory signals during activation of innate immunity.

According to the correlation between streptococcal infections and psoriasis, molecular mimicry between streptococcal antigens and self-peptides from keratinocytes has been proposed as a possible mechanism for triggering an autoimmune response in psoriasis. The principle of molecular mimicry is based on the fact that sequence homologies between a bacterial, viral, or

parasitic antigen and an endogenous protein may trigger a cross-reactive autoimmune response. Once such T cells are activated into effector T cells by pathogen-derived peptides, they could thereby cross-recognize a self-peptide and cause autoimmune disease (**Figure 1.1.5**) (Curtsinger *et al.*, 1998; Sewell, 2012; Veiga-Fernandes *et al.*, 2000). This concept is in accordance with the clinical fact that many autoimmune disorders are precipitated by infections. However, the identification of melanocytes but not keratinocytes as targets of the psoriatic autoimmune response contradicts this hypothesis and argues for a different mechanism.

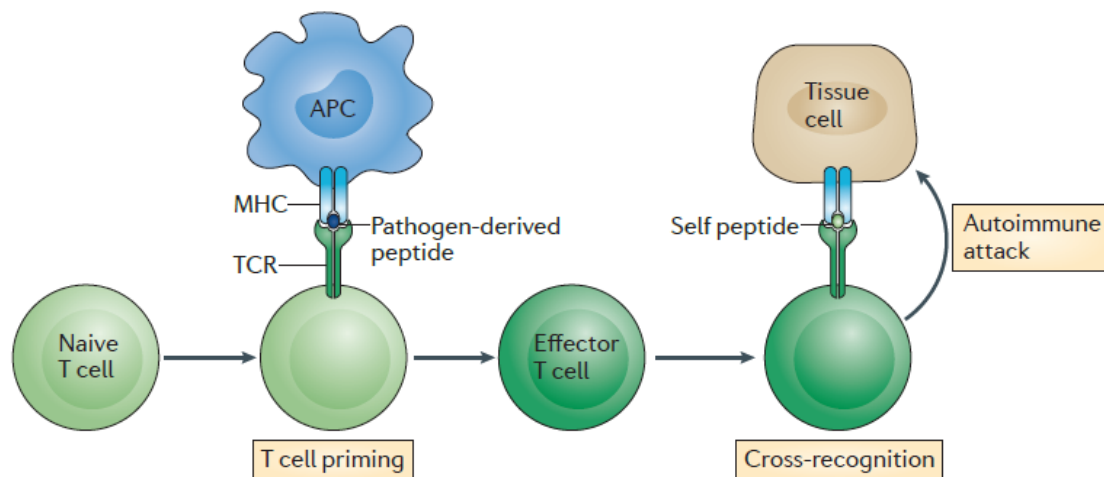


Figure 1.1.5 Cross-activation of T cells against self-peptides may be induced by exogenous antigens sharing similar amino acid patterns (Sewell, 2012).

1.2 MHC-class I Antigen Presentation

1.2.1 The Immune System

In mammalian organisms, the immune system is not only a defense organ protecting the organism against external pathogens but also acts as an overarching surveillance machinery to maintain tissue homeostasis and system integrity (Sattler, 2017). There are two distinct recognition systems within the immune system, namely innate and adaptive, with extensive crosstalk between them (**Figure 1.2.1**) (Dranoff, 2004).

The innate immune system is comprised of diverse cellular components, which encompass phagocytic cells (neutrophils, macrophages), dendritic cells (DCs), mast cells, natural killer (NK) cells, and other innate lymphoid cells, and humoral components such as the complement system. When specialized cell receptors recognize common features of many pathogens that have managed to penetrate the host, the defense mechanisms of innate immunity are triggered,

which are characterized by phagocytosis, recruitment of additional immune cells, the release of antiviral interferons, and opsonization of pathogens. Innate immunity mediates a fast response against common intruders and keeps reactions local (Medzhitov and Janeway, 2000).

The response of the adaptive immune system can be elicited by a wide variety of microbial and nonmicrobial substances. Adaptive immune cells recognize pathogenic structures, called antigens, with highly variable receptors. Further, they respond much more vigorously to subsequent infection by the identical pathogen, known as immunological memory. Lymphocytes and their secreted products are the distinctive elements of adaptive immunity: B lymphocytes, also known as B cells, express immunoglobulin molecules as antigen receptors on the cell surface; T lymphocytes, also known as T cells, exhibit immunoglobulin-like molecules called TCR as their surface antigen receptors. The antigen receptors secreted by B cells in the form of antibodies, which serve to neutralize toxins and viruses, as well as label extracellular pathogens for subsequent immune responses. $CD8^+$ T cells or $CD4^+$ T cells are activated by peptide antigens presented by the cognate MHC-class I or MHC-class II molecules, respectively. These activated T cells then drive the further immune response by releasing mediators or exerting various other effector mechanisms (den Haan *et al.*, 2014).

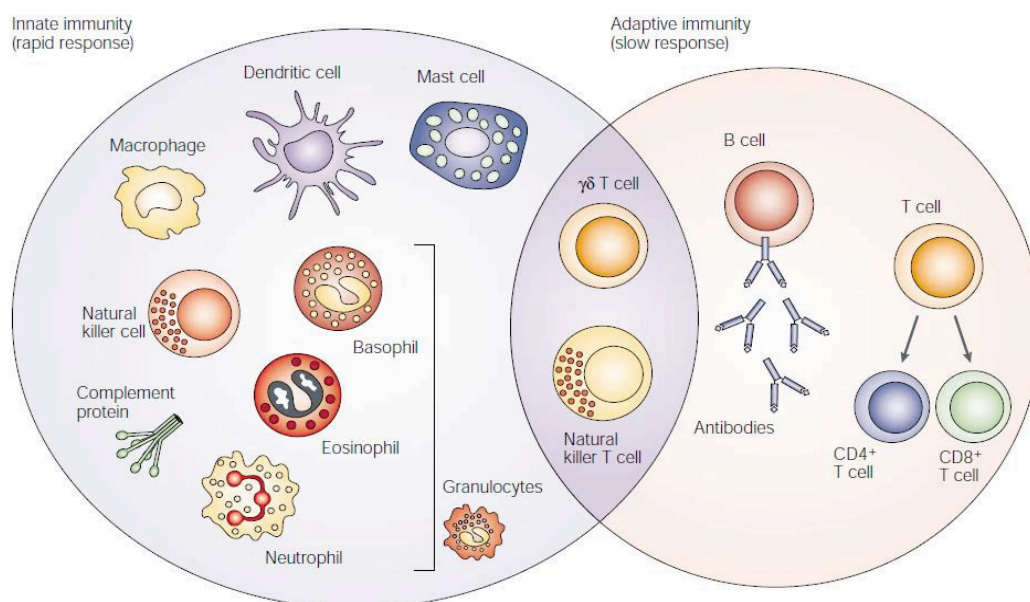


Figure 1.2.1 The innate and adaptive immunity (Dranoff, 2004).

1.2.2 Characteristics of MHC Molecules

The major histocompatibility complex (MHC) is a collection of genes that encode proteins expressed on the cell surface, facilitating the recognition of antigens by T cells. Antigen

presentation by MHC molecules is essential for adaptive immunity (Wieczorek *et al.*, 2017), shaping both the repertoire of peptides presented and the subsequent T-cell responses. In human beings, the MHC molecules are termed the human leukocyte antigens (HLA).

MHC protein molecules can be classified into two major types: class I and class II. MHC Class I molecules span the membrane of almost all nucleated cells in an organism. MHC-class II molecules are restricted to professional antigen-presenting cells (APCs), including DCs, B cells, and macrophages. Furthermore, MHC-class II molecules can be expressed on certain non-professional APCs upon proinflammatory signals such as keratinocytes or endothelial cells. TCRs can recognize antigens on the premise of MHC I or MHC II molecules presenting the antigen on the cell surface (Neefjes *et al.*, 2011). Hence, in the context of antigen recognition, T cells are guided towards interacting with cells rather than being “attracted” by free antigens. Furthermore, the different expression patterns of MHC I and II molecules direct different T cell subsets to interact differently with the appropriate types of cells. Specifically, MHC-class I and class II molecules present peptides on the surface of certain cells to CD8⁺ or CD4⁺ T cells, respectively (Rock *et al.*, 2016).

The extreme polymorphism of MHC I and MHC II molecules makes them unique in the proteome. There have been over 25,000 distinct HLA class I alleles discovered to the present (Barker *et al.*, 2023). Polymorphic residues on the top of α -chains of MHC molecules interact with the TCR, which allows TCRs to recognize simultaneously antigenic peptides and specific alleles of MHC molecules, which is referred to as MHC restriction. Polymorphic residues inside the MHC peptide binding groove form pockets that can bind their complementary amino acid side chains from peptides, which are termed anchor residues (**Figure 1.2.2**). Other than the two or three anchor residues, the remaining amino acid positions in a peptide can be occupied by (almost) any of the 20 amino acids. The specificity of pockets is defined by a small range of anchor residues for peptide binding, while the remaining 6 to 10 amino acids of the peptide can be varied with many possibilities. This results in a very wide repertoire of different peptides (up to a million) that can be presented by each MHC molecules. Peptide-binding grooves that are specific for different HLA alleles further determine distinct HLA-ligand repertoires. Moreover, cells can present a large peptidome with 3 to 6 different MHC I molecules and 3 to 12 distinct MHC II molecules (Rock *et al.*, 2016).

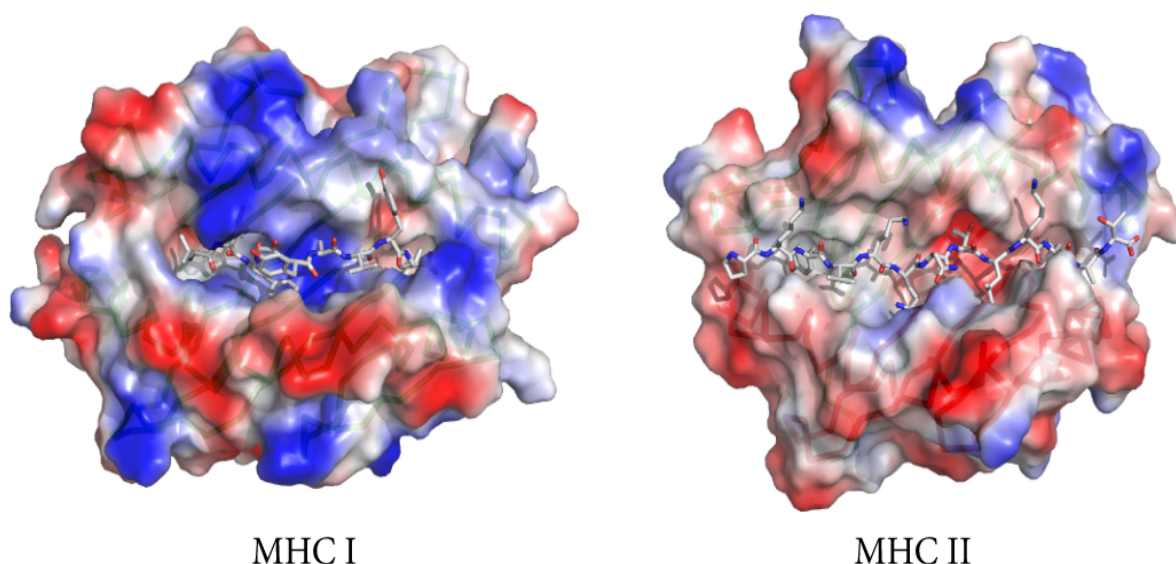


Figure 1.2.2 Peptide-binding groove of MHC I and MHC II molecules (Sanchez-Trincado *et al.*, 2017). The figure depicts the molecular surface from the perspective of TCR. MHC I molecules have a closed peptide-binding groove and are able to bind short peptides (8-11 amino acids), whereas MHC II molecules have an open binding groove and can bind longer peptides (9-22 amino acids). Crystal structures were determined by X-ray crystallography and generated using the APBS Tools plug-in within PyMOL.

1.2.3 Antigen Presentation by MHC-class I Molecules

MHC I molecules present peptides derived from cytoplasmic and nuclear proteins. The CD8⁺ T cells in healthy individuals are tolerant to peptides derived from autologous proteins. However, when cells are expressing mutated proteins (e.g., in cancers) or microbial genes (e.g., viral infections), these ‘altered-self’ or ‘non-self’ antigenic peptides that are included in the immunopeptidome would activate CD8⁺ T cells to detect and destroy these cells (**Figure 1.2.3.1**).

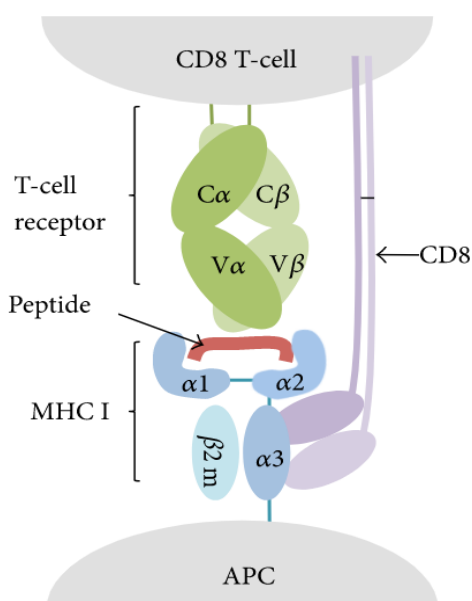


Figure 1.2.3.1 Peptide presentation by MHC I molecules and their recognition by CD8⁺ T cells (Sanchez-Trincado *et al.*, 2017).

During the initial stage of antigen processing, both normal and pathogenic proteins undergo degradation into peptide fragments by the proteasome. A majority of these fragments are subjected to further trimming and destruction by cytosolic peptidases, while a minority of fragments survive and escape into the ER via a peptide transporter termed transporter associated with antigen processing (TAP), which is embedded within the ER membrane. Subsequently, in the ER, a complex for loading peptides is formed, which consists of tapasin, a dedicated chaperone, along with empty MHC I molecules awaiting peptides, and two common chaperones, calreticulin, and protein disulfide isomerase ERp57. Tapasin helps to maintain the empty MHC I molecules in a peptide-receptive state and promotes the binding of peptides to MHC I molecules at a slow-off rate, which allows the test of appropriate peptides by MHC I molecules. Appropriate peptides would be translocated by TAP and loaded on MHC I molecules (Neefjes *et al.*, 2011).

The peptides with appropriate anchor residues are usually 8-10 amino acids long, owing to the closed ends at both sides of the binding groove of MHC class I molecules. Peptides at excessive length may be trimmed to a length of 8-10 amino acids by an ER resident aminopeptidase, endoplasmic reticulum aminopeptidase 1 (ERAP1), before being viewed by the MHC molecules (**Figure 1.2.3.2**). Notably, peptides at a length of 9-16 residues can strongly trigger the conformational change in ERAP1 and the lengths transported efficiently into the ER by TAP (Chang, S. C. *et al.*, 2005).

ERAP1 trims approximately one-third of NH₂-elongated precursor peptides down to 8-9 amino acids, the final sizes that can adapt into the binding grooves of MHC I molecules. Overtrimming can also destroy peptides, preventing binding to the MHC I molecules. Other peptides that are not capable of binding to an MHC I molecule will, in the end, be ultimately degraded in the cytosol. The gene for ERAP1 has different variants that combine to form 10 different haplotypes with different enzymatic activities (Hap1 to Hap10) (Ombrello *et al.*, 2015). Of these, ERAP1 Hap2 increases the risk of psoriasis in epistasis with *HLA-C*06:02* through high enzymatic activity and autoantigen production, while Hap10 generates only little autoantigen and protects *HLA-C*06:02* carriers from developing psoriasis (Arakawa *et al.*, 2021; Strange *et al.*, 2010).

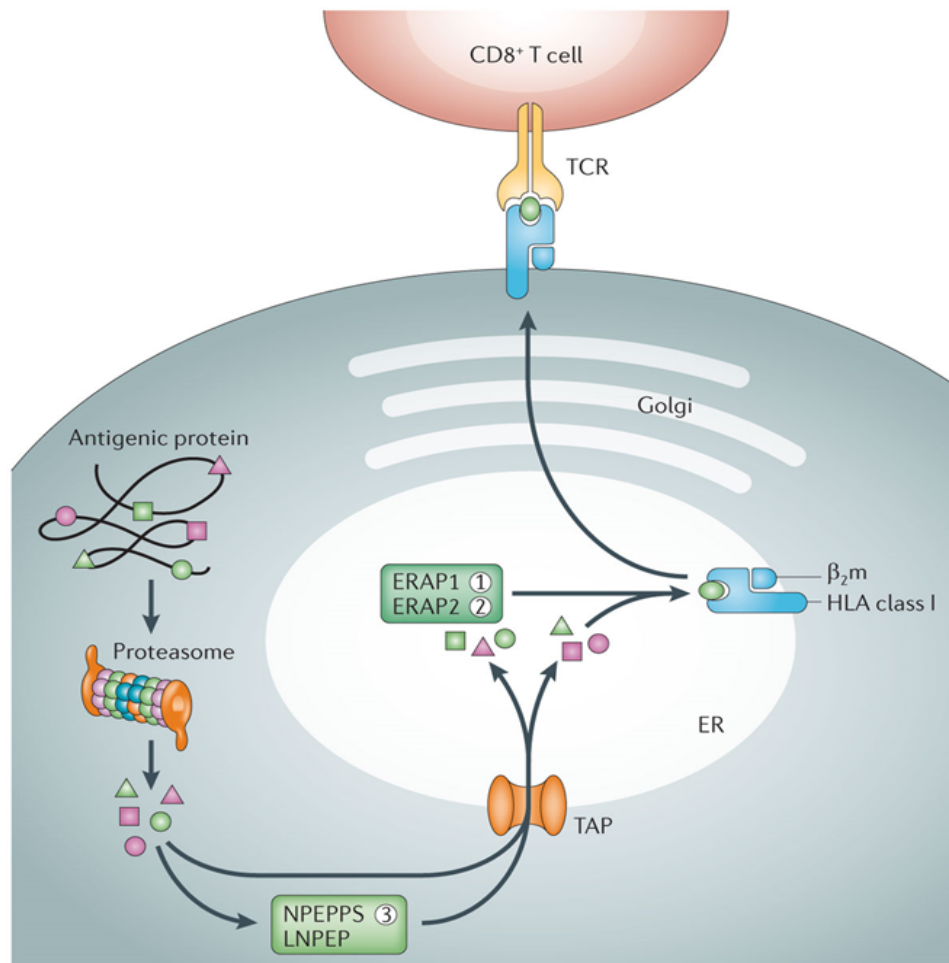


Figure 1.2.3.2 Autologous proteins are degraded in the proteasome, trimmed by cytoplasmic aminopeptidases, transferred into the endoplasmic reticulum, where a fraction is further digested by ERAP1, and loaded on MHC I molecules to be presented on the cell surface (Parkes *et al.*, 2013).

1.3 Discovery of T-cell Epitopes

1.3.1 Polyspecificity of T cells

According to the clonal selection theory, an immunological model that explains the cell functions in response to foreign antigens, one individual lymphocyte (T cell or B cell) recognizes only a single antigen, and the recognition of alternative ligands is unlikely (Jerne, 1955). However, this theory has been called for abandonment and a replacement for the notion that T cells must be extremely cross-reactive since the number of recognized antigens is much larger than the TCR repertoire (Sewell, 2012).

The antigen specificity of T cells depends on the clonotypic heterodimeric $\alpha\beta$ TCR, which consists of two chains (α chain and β chain) that are formed by somatic gene recombination of variable (V), diversity (D, β -chain only), joining (J) and constant (C) gene fragments. During

the gene rearrangement, nucleotides are inserted and deleted at the V(D)J junctions, and the two chains are separately rearranged. As a result of V(D)J junction ‘randomization’ and separated rearrangement of the two chains of a TCR, there is an estimated repertoire of $<10^8$ unique $\alpha\beta$ TCRs in humans (Dupic *et al.*, 2019; Sewell, 2012). The number of peptides that can bind to self-MHC molecules is gigantic, owing to the huge number of peptides that can be presented by a single HLA molecule (up to 4.8×10^{16}) and a vast pool of over 25,000 alleles, from which an individual human haplotype can encode up to six different HLA molecules (Barker *et al.*, 2023; Watkins and Miles, 2021).

While B cell receptors undergo affinity maturation through somatic recombination, the protein sequence of TCRs is fixed at birth. Therefore, the TCRs expressed by naive T cells never encountered foreign antigens but are required to respond to the full spectrum of foreign antigens. Given the limited number of distinct TCRs, the extensive cross-reactivity of T cells holds the key to the broad coverage of antigen diversity, which allows a single TCR to recognize over one million peptides in the context of an individual HLA-I molecule (Sewell, 2012). Specifically, TCRs are polyspecific and recognize peptides sharing certain amino acid patterns, not defined epitopes. In other words, a single T cell can react against many different peptides if they share the recognition motif specific to the TCR of the respective T cell.

However, the effect of T cell cross-reactivity to recognize a vast number of distinct peptides simultaneously leads to potential adverse consequences for causing autoimmunity that targets self-peptides.

1.3.2 Immunogenicity of T-cell Epitopes

Characterizing TCR specificity aims to identify the specific short peptide in an antigen with immunogenicity, that is, the capacity to activate $CD4^+$ or $CD8^+$ T cells (Ahmad *et al.*, 2016). The immunogenicity of T-cell epitopes is primarily determined by three fundamental processes: antigen processing, binding of peptides to MHC molecules, and recognition of peptide-loaded MHC complexes (pMHCs) by a cognate TCR (Sanchez-Trincado *et al.*, 2017).

Of these events, peptide binding to MHC is regarded as the most selective and possibly most well-understood step in antigen presentation, and much work has been focused on this step for predicting the binding affinity and stability factor of peptides on MHC molecules. However, the rules determining the recognition of a cognate pMHC by T cells are poorly known, though the recognition initiates the formation of a dynamic immunological synapse (IS) and eventually leads to the adaptive immune response (Schmidt *et al.*, 2021; Wu *et al.*, 2019).

1.3.3 Current Approaches for the Discovery and the Prediction of T-cell Epitopes

The difficulty in the identification of T-cell antigens lies in the complexity of antigen-specific T-cell activation, which involves several aspects (Prinz, 2023; Sharma *et al.*, 2019). Firstly, the presence of an enormous number of short peptides in an immunopeptidome results in a vast spectrum of T-cell epitopes for the search. Secondly, each individual HLA allele has a specific preference for binding peptides and ligating TCRs, and the respective HLA allele in an immune response needs to be defined from the multiple HLA alleles in a haplotype for the antigen search. The third factor that influences the immunogenicity of pMHC is the variation in antigenic protein expression levels within cells and biases in proteolytic processing. Finally, compared with epitope recognition by antibodies, TCR/pMHC interactions are transient, promiscuous, and have relatively low affinity.

Various function-based approaches for T-cell epitope discovery have been successfully developed (**Figure 1.3.3.1**). Candidate or random antigenic peptides are expressed on the cell surfaces of APCs with various assays illustrated in the figure. Subsequently, APCs expressing these peptides are tested to evaluate their immunogenicity by T-cell-based read-out assays, such as measurement of released cytokines or the detection of activation of NFAT-linked reporter T cells (Sharma and Holt, 2014; Sharma *et al.*, 2019).

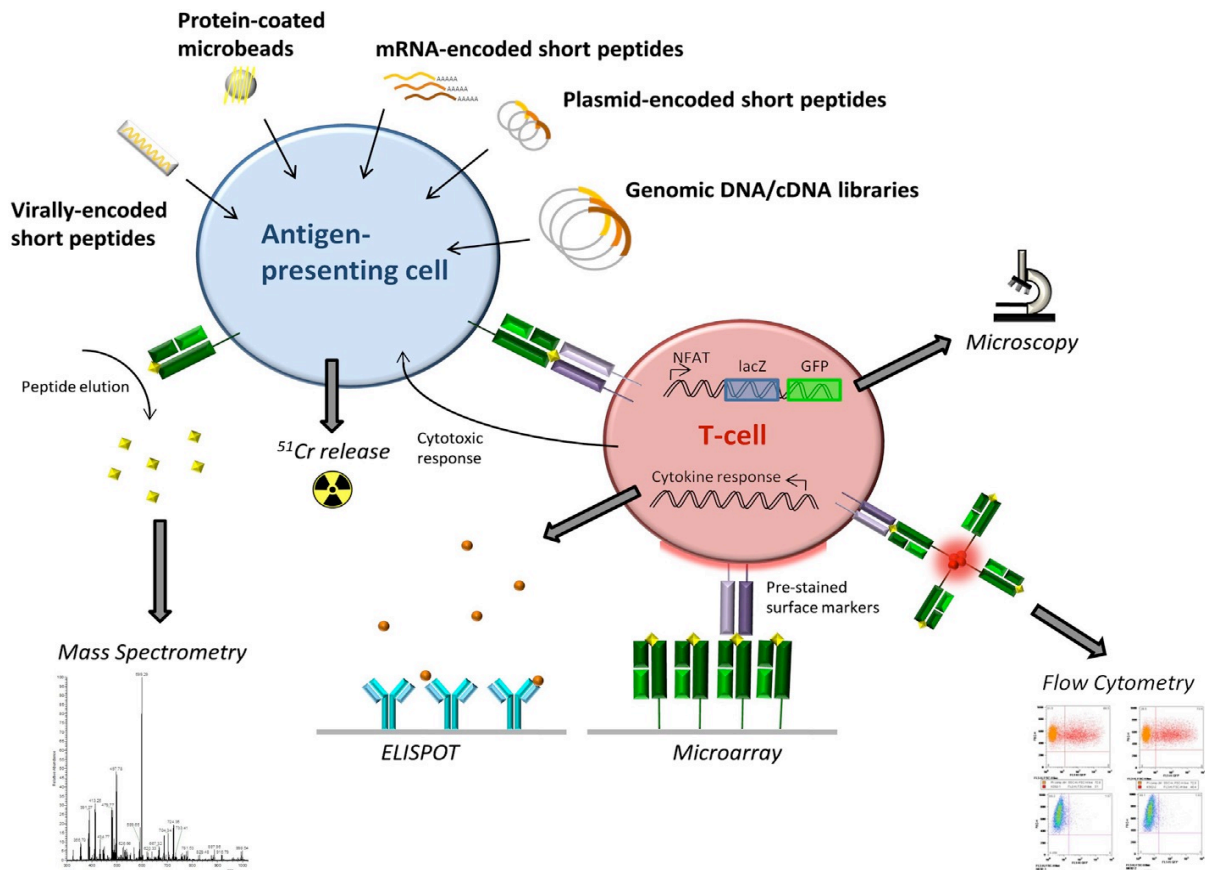


Figure 1.3.3.1 An overview of the multiple approaches applied in the discovery of T-cell epitopes (Sharma and Holt, 2014).

In the past two decades, along with the development of bioinformatics and computational biology, computational methods based on antigen processing and presentation simulation (such as NetChop, NetCTL, NetMHCpan, and MHCflurry) and epitope immunogenicity prediction (such as INeo-epp, NetTepi-1.0, IEDB T Cell Epitopes-Immunogenicity Prediction tool) have been developed to predict human antigen and neoantigen epitopes that are presented by particular HLA molecules (Calis *et al.*, 2013; Sanchez-Trincado *et al.*, 2017; Trolle and Nielsen, 2014; Wang *et al.*, 2020).

Furthermore, some studies have improved the predictions for peptides binding to MHC I molecules by considering molecular dimensions encoded in the pMHC complex, e.g., molecular docking, rather than considering properties of the peptide's amino acid sequence alone (Mobbs *et al.*, 2017; Riley *et al.*, 2019; Zhang, X. W., 2013).

Psoriasis shows a clear autoimmune pathomechanism. The mono- or oligoclonality of CD8⁺ T cell infiltrates in psoriatic skin lesions is a clear indication that only one or very few autoantigens stimulate the psoriatic autoimmune response. To date, four psoriasis autoantigens have been discovered, i.e., cathelicidin LL-37, ADAMTSL5 from melanocytes, lipid antigen PLA2G4D, and keratin 17 (**Figure 1.3.3.2**) (Ten Bergen *et al.*, 2020). The specific autoreactive T cells targeting the above autoantigens were observed in, respectively, part of psoriasis patients rather than in all patients. However, of these autoantigens, only the identification of the autoantigenicity of ADAMTSL5 is based on the analysis of the reactivity of a pathogenic psoriatic TCR and is thus definitely proven.

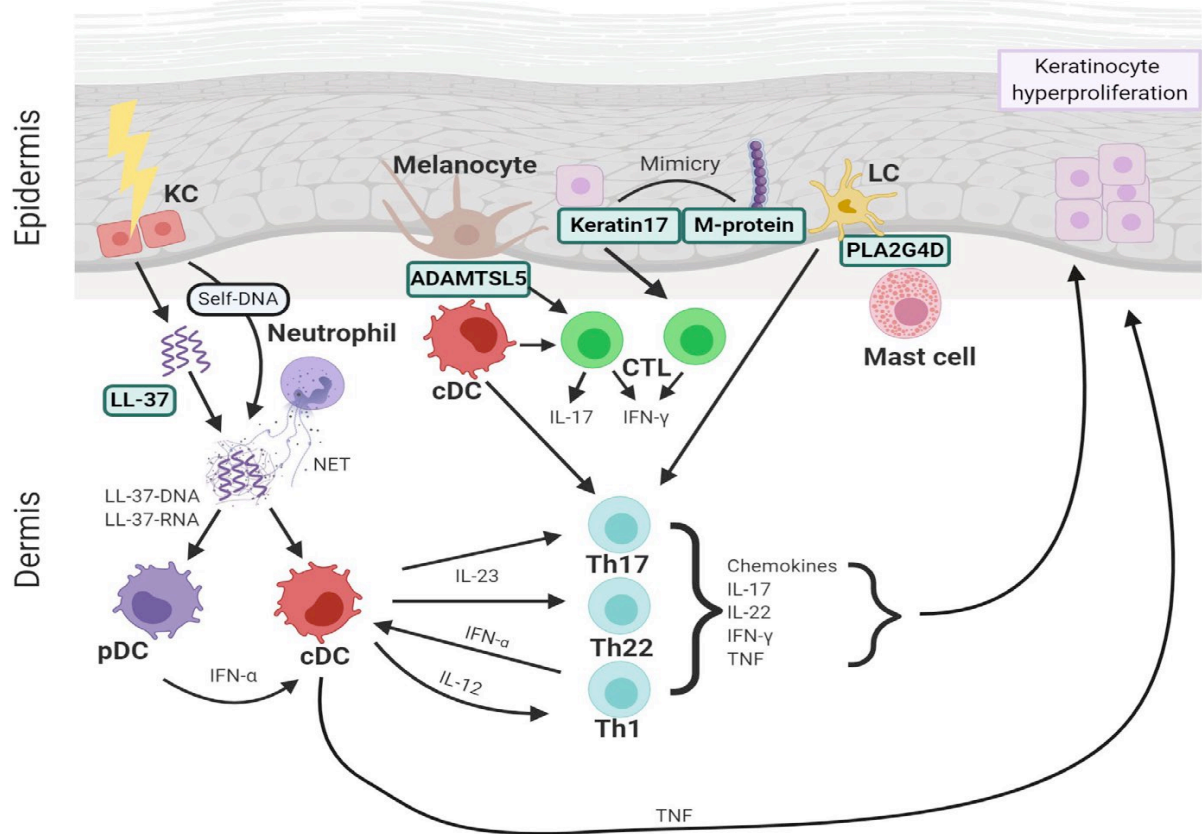


Figure 1.3.3.2 The potential pathogenesis of psoriatic skin induced by possible autoantigens (Ten Bergen *et al.*, 2020).

1.4 Objective

Using the lesional psoriatic V α 3S1/V β 13S1 TCR, we had formerly identified a melanocytic ADAMTSL5 peptide as a pathogenic psoriatic autoantigen presented by HLA-C*06:02 (Arakawa *et al.*, 2015). However, the triggering mechanisms activating the pathogenic CD8⁺ T cell response against melanocytes remain unknown.

The initial onset or relapses of psoriasis are closely linked to the occurrence of streptococcal tonsillitis, and HLA-C*06:02⁺ individuals are particularly susceptible to the streptococcal stimulus. This implies that the pathogenic effector T cells may be activated in the tonsils from where they enter the skin. Consistent with this, T cells clonally expanded in psoriasis lesions were identified in the tonsils of psoriasis patients who had undergone tonsillectomy for streptococcal-driven psoriasis. Accordingly, the psoriatic T-cell response in skin lesions involves a recruitment of pathogenic T cells from secondary lymphoid organs. Therefore, the general aim of my thesis was to identify possible stimulators for the pathogenic psoriatic autoimmune response against melanocytes in the tonsils.

In order to address this issue, the following objectives will be accomplished in my thesis using the psoriatic V α 3S1/V β 13S1 TCR:

- i. Identifying target cells that may stimulate the pathogenic psoriatic T cells in tonsils or other secondary lymphoid organs;
- ii. Proving the autostimulatory capacity of target cells for T cells in psoriasis patients;
- iii. Identifying potential self-peptides in the target cells stimulating the psoriatic T cells in the tonsils:
 - Search for candidate epitopes in the proteome of the target cells
 - Characterize the HLA-C*06:02 immunopeptidome of the target cells
 - Identify candidate epitopes in the immunopeptidome of HLA-C*06:02 derived from the target cells

2. Materials

2.1 Devices

2.1.1 Cell Culture and Cell Analysis

HB2472 sterile bench	Heraeus
SterilGARD® Class II Type A2 Biosafety Cabinet	Baker
Incubator Biometra BFED53	WTC Binder
Heracell CO ₂ Incubators 150i	Unity Lab Services
Incubator Shaker Innova 4230	New Brunswick Scientific
Incubator Shaker CH-4103	INFORS HT
Flow Cytometry:	
FACSCalibur™	Beckton Dickinson
FACSCanto™ II	Beckton Dickinson
FACSAria™ II Fusion	Beckton Dickinson
Light microscopy:	
Invert microscope, Axiovert25	Zeiss
Invert microscope, CK2	Olympus
Light microscope, BH series	Olympus
Fluorescence microscope	Zeiss
Nucleofection:	
Amaxa™ 4D-Nucleofector™ Core Unit	Lonza
Amaxa™ 4D-Nucleofector™ X Unit	Lonza
Pipette:	
PIPETMAN Classic P2 (0.2-2 µL)	Gilson
PIPETMAN Classic P10 (1-10 µL)	Gilson
PIPETMAN Classic P20 (2-20 µL)	Gilson
PIPETMAN Classic P200 (20-200 µL)	Gilson
PIPETMAN Classic P1000 (100-1,000 µL)	Gilson
Multipette 4780	Eppendorf
Multipette® plus	Eppendorf
Pipetboy acu Classic Pipette Controller	Integra Biosciences
Neubauer counting chamber	BRAND
Cell Harvester System	Inotech Biosystems International

2.1.2 Nucleic Acid Analysis

Electrophoresis chamber, horizontal	Life Technology
PS 500XT Power Supply	Hoeffer Scientific Instrument
Gel documentation system GenDoc2000	Bio-Rad
Spectrophotometer	Smartspec 3000
PCR Thermo cycler, Genamp 9700	Perkin Elmer

PCR Thermo cycler, Veriti	Applied Biosystem
Thermomixer 5436	Eppendorf
Vac-Man® Laboratory Vacuum Manifold	Promega
Microwave oven	Siemens

2.1.3 Centrifuges

Centrifuge, Rotixa / RP	Hettich
Universal benchtop centrifuge	Hettich
Benchtop centrifuge 5415C, 5415R	Eppendorf
Vacuum pump, Univapo 150H / 100H	Uniequip
Mini-centrifuge, 3-1810	Neolab

2.1.4 Rotors

A8.24	Hermle
Sorvall H 6000 A	DuPont Instruments
Sorvall GSA	DuPont Instruments
Rotor for 2 × 8, 0.2 ml PCR-Strips	Neolab

2.1.5 Coolers

Refrigerator KSV32123	Bosch
-20 °C Freezer GEM-432/8	Philipp Kirsch GmbH
-20 °C Profi Premiumline Freezer GGPv 6590	Liebherr
Ultra-low temperature freezer 820CV	Unity Lab Services
Ultra-low temperature freezer HDE series	Unity Lab Services

2.1.6 Other Devices

Fine balance	Sartorius
pH meter PH 523	WTW
IKAMAG RCT magnetic stirrer	IKA laboratory technology
Water bath	Julabo Labortechnik GmbH
Vortexer-2 genius	Scientific Industries
Reax-top Vortexer	Heidolph
50 L Upright Autoclave HV-50	Hirayama
Multiskan FC Microplate Photometer	ThermoFisher Scientific

2.2 Consumables and Chemicals

2.2.1 Consumables

Reagents	Manufacturer
5 ml Test Tube with Cell Strainer Snap Cap	Falcon, Becton Dickinson
5 ml Round Bottom Polystyrene Test Tube	Falcon, Becton Dickinson
Cryo.s™ 2 ml Freezing Tubes	Greiner Bio-One
Mr. Frosty™ Freezing Container	ThermoFisher Scientific
1.40 ml round bottom tubes	Micronic
MS Column	Miltenyi Biotec
LS Columns	Miltenyi Biotec
Falcon™ 50 ml Conical Tube	Becton Dickinson
Falcon™ 15 ml Conical Tube	Becton Dickinson
Vacutainer® Evacuated Blood Collection Tubes.	Becton Dickinson
1.5 ml Microcentrifuge Tubes	Eppendorf
2.0 ml Microcentrifuge Tubes	Eppendorf
Tissue culture petri dishes 94/16	Greiner Bio-One
Costar® Multiple Well Cell Culture Plates	Corning
25cm ² Tissue culture flask	Greiner Bio-One
75cm ² Tissue culture flask	Greiner Bio-One
Sterilin™ Serological pipettes	ThermoFisher Scientific
0.22 µm Millex® GP, Polyethersulfon, 33 mm	Merck
0,22 µm Stericup® Quick Release Sterile Vacuum Filtration System	Merck
DURAN® Erlenmeyer Beaker/ Flask/ Bottle	DWK Life Sciences
0.2ml Thin-wall 8-tube strip	KISKER BIOTECH GmbH
SafeSeal-Tips® Premium Pipette Filter tips	Biozym

2.2.2 Chemicals

Reagents	Manufacturer
Antibiotics for selection:	
Ampicillin	Sigma-Aldrich
Kanamycin	Sigma-Aldrich
Hygromycin	Invitrogen
Puromycin	Gibco
G418	Genaxxon bioscience
Blasticidin	Gibco
Agarose, Universal	VWR International GmbH
Select Agarose	Sigma-Aldrich
RedSafe™ Nucleic Acid Staining Solution (20,000x)	iNtRON Biotechnology
Dimethyl Sulfoxide (DMSO)	Sigma-Aldrich
Dithiothreitol (DTT)	Thermo Scientific™
Sodium Chloride (NaCl)	Merck
Bacto™ Tryptone	Becton Dickinson
Bacto™ Yeast Extract	Becton Dickinson

Ethylenediamine tetraacetic acid (EDTA), >99%	Sigma-Aldrich
---	---------------

2.3 Mediums

Reagents	Manufacturer	Applied Cells
<u>10% FCS RPMI Complete medium:</u>		
500 ml RPMI 1640 with L-glutamine	Gibco	Tonsil cells, lymphocytes
10% Fetal Calf Serum (FCS)	Sigma-Aldrich	
1% Penicillin / Streptomycin (10,000 U/ml)	Gibco	
1% Sodium Pyruvate (100 mM)	Sigma-Aldrich	
1% non-essential amino acids (100x)	Sigma-Aldrich	
0.5% Ciprofloxazin (Ciprobay®) 200mg / 100 ml	Bayer	
<u>10% AB RPMI Complete medium:</u>		
500 ml RPMI 1640 with L-glutamine	Gibco	PBMCs, primary lymphocytes
10% Human AB serum	Blood Bank, Red Cross	
1% Penicillin / Streptomycin (10,000 U/ml)	Gibco	
0.1% Human Interleukin-2 (1,000 U/ml)	Roche	
<u>15% FCS RPMI Complete medium:</u>		
500 ml RPMI 1640 with L-glutamine	Gibco	Epstein-Barr Virus (EBV)-transformed B cell lines: D22, PSO7, P16488, GM11930, HG00142, GM20771, HG00131, GM12286, GM12046
10% Fetal Calf Serum (FCS)	Sigma-Aldrich	
1% Penicillin / Streptomycin (10,000 U/ml)	Gibco	
1% Sodium Pyruvate (100 mM)	Sigma-Aldrich	
1% non-essential amino acids (100x)	Sigma-Aldrich	
0.5% Ciprofloxazin (Ciprobay®) 200mg / 100 ml	Bayer	
<u>10% FCS DMEM Complete medium:</u>		
500 ml DMEM with D-Glucose, L-glutamine	Gibco	NCI-H1975 MCF7 KHOS HEK293T
10% Fetal Calf Serum (FCS)	Sigma-Aldrich	
1% Penicillin / Streptomycin (10,000 U / ml)	Gibco	
1% Sodium Pyruvate (100 mM)	Sigma-Aldrich	
1% non-essential amino acids (100x)	Sigma-Aldrich	
0.5% Ciprofloxazin (Ciprobay®) 200mg / 100 ml	Bayer	
<u>Selection medium for the Vα3S1/Vβ13S1-TCR hybridoma:</u>		
100 ml 10% FCS RPMI Complete medium	See above	Vα3S1/Vβ13S1-TCR hybridoma
3ml G418 (50 mg/ml)	Genaxxon bioscience	
600 µl Hygromycin B (50 mg/ml)	Invitrogen	
100 µl Puromycin (1 mg/ml)	Gibco	
Fresh added in every passage:		
3 µl / 10 ml Blasticidin (10 mg/ml)	Gibco	

Selection medium for the HLA-C*06:02-721.221cell line:

100 ml 10% FCS RPMI Complete medium	See above	HLA-C*06:02
1ml Hygromycin B (50 mg/ml)	Invitrogen	transfected-721.221 cell line

Selection medium for COS-7-HLA-C*06:02 & HLA-C*06:02-C1R cell lines:

100 ml 10% FCS RPMI Complete medium	See above	COS-7-HLA-C*06:02, HLA-C*06:02 transfected-
2ml G418 (50 mg/ml)	Genaxxon bioscience	CR1 cell line

Freezing medium:

10% DMSO	Sigma-Aldrich	All cell lines
FCS	Gibco	

Collecting medium for sorted subpopulations:

10% AB RPMI Complete medium	See above	FACS Sorted cells
25 mM HEPES	Sigma-Aldrich	

Luria Bertani (LB)-medium:

10 g Bacto-Tryptone		
5 g Bacto-Yeast Extract	Becton-Dickinson	<i>E.coli</i>
7.5 g NaCl	Becton-Dickinson	
add (dH ₂ O) to 1L	Merck	

LB-Agar-Plates:

1 L LB-medium	See above	<i>E.coli</i>
15 g Select Agarose	Sigma-Aldrich	

SOC medium

Invitrogen	<i>E.coli</i>
------------	---------------

2.4 Buffers and Solutions

Reagents	Manufacturer	Applications
<u>Phosphate-buffered saline (PBS):</u>	Hospital Pharmacy, University Hospital of the LMU Munich	Reagent dissolution and dilution
<u>1x TBE DNA loading buffer:</u>	Sigma-Aldrich	DNA-Gel electrophoresis
90 mM Tris-HCl pH 8.0	Sigma-Aldrich	
90 mM Boric acid	Sigma-Aldrich	
2 mM EDTA		
H ₂ O		
<u>MACS Separation Buffer:</u>	Sigma-Aldrich	Cell separation
0.5% FCS	Sigma-Aldrich	
2 mM EDTA	See above	
PBS	Merck	
Filter sterilized		

Trypan blue solution:

1 vol. Trypanblue
3 vol. PBS

Sigma-Aldrich
See above

Dead cell staining

FACS buffer:

1% FCS
PBS

Sigma-Aldrich
See above

Flow Cytometry

EDTA detachment solution:

0.2% EDTA
PBS

Sigma-Aldrich
See above

Cell detachment

FACS sorting buffer:

2% Human AB serum
2 mM EDTA
25 mM HEPES
PBS

Blood Bank, Red Cross
Sigma-Aldrich
Sigma-Aldrich
See above

Cell sorting

0.5% Trypsin / EDTA (10x)

Gibco

Cell detachment

0.4% Trypan blue solution

Sigma-Aldrich

Dead cell staining

Ficoll Separating Solution

Merck

Cell separation

0.5% Phenol Red solution

Sigma-Aldrich

Cell culture

OPTI-MEM (1x)

Gibco

DNA Transfection

2.5 Commercial Kits and Specific Reagents

Product	Manufacturer	Application
Accudrop Beads	BD FACS™	FACS Cell sorting test
Blood and Tissue Genomic DNA Miniprep System	Viogene	Genomic DNA Extraction
CutSmart® Buffer (10x)	New England Biolabs	DNA digestion
CutSmart® Restriction Enzyme	New England Biolabs	DNA digestion
DAPI Solution (1 mg/ml)	ThermoFisher Scientific	Fluorescent staining
DNA Molecular Weight Marker IV	Roche	DNA Gel electrophoresis
DNA Molecular Weight Marker V	Roche	DNA Gel electrophoresis
dNTP Solution Mix (50 mM each)	Invitrogen	PCR
EB Buffer	Qiagen	DNA experiments
FuGENE® HD Transfection Reagent	Promega	Plasmid transfection
KoD XL DNA Polymerase	Merck	PCR
Mini & Midi MACS™ Starting Kits	Miltenyi Biotec	Cell separation
CD19 MicroBeads, human	Miltenyi Biotec	Cell separation
CD3 MicroBeads, human	Miltenyi Biotec	Cell separation
CD4 MicroBeads, human	Miltenyi Biotec	Cell separation
CD8 MicroBeads, human	Miltenyi Biotec	Cell separation
pcDNA™ 3.1/V5-His TOPO™ Expression Kit	Invitrogen	Cloning and expression of peptides
PCR Buffer (10x)	Roche	PCR

Pwo DNA Polymerase	Roche	PCR
QIAquick® Gel Extraction Kit	Qiagen	DNA purification
QIAquick® PCR-Purification Kit	Qiagen	Purification of PCR-products
Sall-HF Restriction Enzyme (20,000 U/ml)	New England Biolabs	DNA digestion
SF Cell Line 4D-Nucleofector™ X Kit S	Lonza	Nucleofection in eukaryotic cells
Taq DNA Polymerase, recombinant	Invitrogen	PCR
SmaI (10 U/μl)	Thermo Scientific™	HLA Genotyping
Wizard® Plus SV minipreps DNA Purification System	Promega	Plasmid isolation
Plasmid Maxi Kit	Qiagen	Plasmid isolation
BrdU Cell Proliferation Assay Kit	Cell signaling	Assessment of cell proliferation
[³ H]-thymidine	Hartmann Analytic	Assessment of cell proliferation
CFSE	eBioscience™	Assessment of cell proliferation

2.6 Oligonucleotides

Sequence information for mRNA and genomic DNA was obtained from the National Center for Biotechnology Information (www.ncbi.nlm.nih.gov). All primers in HPLC-purified quality were purchased from biomers.net and dissolved in nuclease-free sterile water to a concentration of 100 mM. Primers for PCR reactions producing double-strand DNA-coding short peptides are listed in separate tables in Section 6.1.

2.6.1 Primers for Polymerase Chain Reaction

HLA C_for_Sal	5'-TTG AGG ATT CTC CAC TCC CCT GAG-3'
HLA C_rev_Bam	5'--CTG TGC CTG GCG CTT GTA CTT-3'

2.6.2 Primers for Sequencing

T7 promoter-forward	5'- TAA TAC GAC TCA CTA TAG GG -3'
M13-Forward	5'- TGT AAA ACG ACG GCC AGT -3'
M13-Reverse	5'- CAG GAA ACA GCT ATG AC -3'

2.6.3 siRNAs

siRNA products were ordered from ThermoFisher Scientific, QIAGEN, or Eurofins. All siRNAs were dissolved in RNase-free water to a concentration of 20 μM and stored in aliquots at -80 °C. Sequences of Silencer® Select Validated siRNAs and Silencer® Select Pre-designed

siRNAs from ThermoFisher Scientific are available at PubChem Database by the IDs (<https://pubchem.ncbi.nlm.nih.gov>) and also given in Section 6.4. Sequences of two Silencer® Select Custom-Synthesized siRNAs and ADAMTSL5 siRNAs from QIAGEN and Eurofins are listed as follow:

Negative control Co-3 sense strand	5'- GCG CAU UCC AGC UUA CGU A TT -3'
Negative control Co-4 sense strand	5'- GCG CUA UCC AGC UUA CGU A TT -3'
ADAMTSL5-1(QIAGEN) sense strand	5'- AUG CCU AAC CAG GCA CUG UAA TT -3'
ADAMTSL5-2 (Eurofins) sense strand	5'- CAA CCC UGG CAU CGA GUU U TT -3'

Product	Manufacturer	Target gene
Silencer® Select Negative control #1 siRNA	ThermoFisher Scientific	Negative control
Silencer® Select Negative control #2 siRNA	ThermoFisher Scientific	Negative control
Silencer® Select Custom-Synthesized siRNA-Negative control Co-3	ThermoFisher Scientific	Negative control
Silencer® Select Custom-Synthesized siRNA-Negative control Co-4	ThermoFisher Scientific	Negative control
ADAMTSL5-1 siRNA	QIAGEN	ADAMTSL5
ADAMTSL5-2 siRNA	Eurofins	ADAMTSL5
Silencer® Select Validated siRNAs, ID: s27996	ThermoFisher Scientific	TAOK3
Silencer® Select Validated siRNAs, ID: s19459	ThermoFisher Scientific	HDAC6
Silencer® Select Pre-designed siRNAs, ID: s1854	ThermoFisher Scientific	B2M
Silencer® Select Pre-designed siRNAs, ID: s36919	ThermoFisher Scientific	PIF1
Silencer® Select Pre-designed siRNAs, ID: s36920	ThermoFisher Scientific	PIF1
Silencer® Select Pre-designed siRNAs, ID: s36921	ThermoFisher Scientific	PIF1
Silencer® Select Pre-designed siRNAs, ID: s42641	ThermoFisher Scientific	LRRC28
Silencer® Select Pre-designed siRNAs, ID:cs42642	ThermoFisher Scientific	LRRC28
Silencer® Select Pre-designed siRNAs, ID: s42643	ThermoFisher Scientific	LRRC28
Silencer® Select Pre-designed siRNAs, ID: s41144	ThermoFisher Scientific	ZNF670
Silencer® Select Pre-designed siRNAs, ID: s41145	ThermoFisher Scientific	ZNF670
Silencer® Select Pre-designed siRNAs, ID: s41146	ThermoFisher Scientific	ZNF670
Silencer® Select Pre-designed siRNAs, ID: s40543	ThermoFisher Scientific	KIFC2
Silencer® Select Pre-designed siRNAs, ID: s40544	ThermoFisher Scientific	KIFC2
Silencer® Select Pre-designed siRNAs, ID: s458471	ThermoFisher Scientific	FBXL19
Silencer® Select Pre-designed siRNAs, ID: s458473	ThermoFisher Scientific	FBXL19

2.7 Plasmids and Vectors

A map of the vector pcDNA™ 3.1D/V5-His-TOPO® applied in the study is shown in Appendix 4, and the plasmids used in this work are shown in Section 6.2.

2.8 Synthetic Peptides

All synthetic peptides were ordered from ThermoFisher Scientific Custom Peptide synthesis service (purity >95%). Sequences of synthetic peptides were listed as follows:

Peptide	Sequence
FALK	NH2-V-R-H-D-G-G-N-V-L-COOH

<i>Mycobacterium tuberculosis</i> -9mer	NH2-R-R-T-R-R-T-R-R-L-COOH
RASSF10-9mer	NH2-R-R-Q-R-R-S-R-R-L-COOH
ADAMTSL5-9mer	NH2-V-R-S-R-R-C-L-R-L-COOH
ADAMTSL5-8mer	NH2-R-S-R-R-C-L-R-L-COOH
PIF1-9mer	NH2-R-R-F-L-R-T-L-R-L-COOH
FBXL19-9mer	NH2-R-R-C-P-R-L-R-R-L-COOH
LRRC28-9mer	NH2-L-R-A-L-R-H-L-R-L-COOH
RANBP2-9mer	NH2-M-R-R-E-Q-V-L-K-V-COOH
FGR-9mer	NH2-T-R-G-D-H-V-K-H-Y-COOH
TIPARP-9mer	NH2-Y-R-I-L-Q-I-L-R-V-COOH
TPGS1-9mer	NH2-T-Y-S-E-L-L-R-R-I-COOH
CIZ1-9mer	NH2-R-Y-F-K-T-P-R-K-F-COOH
ETF1-9mer	NH2-K-R-H-N-Y-V-R-K-V-COOH
STAT6-9mer	NH2-Y-Q-R-D-P-L-K-L-COOH

2.9 Antibodies

2.9.1 Primary Antibodies

Clone	Specificity	Isotype and origin	Manufacturer
17A2	Purified anti-mouse CD3 antibody	Mouse IgG2a, κ	Biolegend
OKT3	Purified anti-human CD3 antibody	Mouse IgG2a, κ	Biolegend
W6/32	Ultra-LEAF™ Purified anti-human HLA-A, B, C antibody	Mouse IgG2a, κ	Biolegend
DT-9	Purified Azide-free anti-Human HLA-C	Mouse IgG2b, κ	Biolegend
MOPC-173	Ultra-LEAF™ Purified Mouse IgG2a	Mouse IgG2a, κ	Biolegend
MG2b-57	Ultra-LEAF™ Purified Mouse IgG2b	Mouse IgG2b, κ	Biolegend

2.9.2 Directly Conjugated Antibodies

Clone	Conjugation	Specificity	Isotype and origin	Manufacturer
OKT3	PE	anti-human CD3	Mouse IgG2a, κ	eBioscience
OKT4	PE	anti-human CD4	Mouse IgG2b, κ	eBioscience
OKT4	FITC	anti-human CD4	Mouse IgG2b, κ	Biolegend
SK1	PerCP /Cyanine5.5	anti-human CD8	Mouse IgG1, κ	Biolegend
3.9	FITC	anti-human CD11c	Mouse IgG1, κ	Biolegend
2H7	APC	anti-human CD20	Mouse IgG2b, κ	Biolegend
2H7	FITC	anti-human CD20	Mouse IgG2b, κ	eBioscience
63D3	APC	anti-human CD14	Mouse IgG1, κ	Biolegend
HI30	PerCP/Cyanine5.5	anti-human CD45	Mouse IgG1, κ	Biolegend
HCD56	PE/Cyanine7	anti-human CD56	Mouse IgG1, κ	Biolegend
EPR3113	PE	anti-human CD304 (anti-Neuropilin 1)	Rabbit IgG	abcam
DT-9	PE	anti-human HLA-C	Mouse IgG2b, κ	BD Biosciences
W6/32	PE	anti-human HLA-ABC	Mouse IgG2a, κ	BD Biosciences

L243	PerCP/Cyanine5.5	anti-human HLA-DR	Mouse IgG2a, κ	Biologend
L243	Alexa Fluro 647	anti-human HLA-DR	Mouse IgG2a, κ	Biologend
MOPC-21	PE	mouse IgG1	Mouse IgG1, κ	BD Biosciences
MPC-11	PE	mouse IgG2b	Mouse IgG2b, κ	BD Biosciences
MOPC-173	PE	mouse IgG2a	Mouse IgG2a, κ	BD Biosciences

2.10 Bacterial Strains (*E. coli*)

Bakterienstamm	Genotype	Company
OneShot [®] TOP10 Chemically Competent	F- <i>mcrA</i> Δ (<i>mrr-hsdRMS-mcrBC</i>) Φ 80 <i>lacZ</i> Δ M15 Δ <i>lacX74</i> <i>recA1</i> <i>araD139</i> Δ (<i>araleu</i>) 7697 <i>galU</i> <i>galK</i> <i>rpsL</i> (StrR) <i>endA1</i> <i>nupG</i>	Invitrogen
NEB [®] 10-beta Competent <i>E. coli</i> (High Efficiency)	Δ (<i>ara-leu</i>) 7697 <i>araD139</i> <i>fhuA</i> Δ <i>lacX74</i> <i>galK16</i> <i>galE15</i> <i>e14-</i> ϕ 80 <i>dlacZ</i> Δ M15 <i>recA1</i> <i>relA1</i> <i>endA1</i> <i>nupG</i> <i>rpsL</i> (StrR) <i>rph</i> <i>spoT1</i> Δ (<i>mrr-hsdRMS-mcrBC</i>)	New England Biolabs

2.11 Cells Lines/ Cells

Name	Type	Source of supply
V α 3S1/V β 13S1-TCR hybridoma	V α 3S1/V β 13S1-TCR CD8 ⁺ 58 α ⁻ β ⁻ mouse T hybridoma cell	Generated in the lab (Kim, 2011)
HEK293T	Immortalized human embryonic kidney cells	Invitrogen
COS-7-HLA-C*06:02	African green monkey SV40 transformed kidney fibroblast-like cell line, HLA-C*06:02 stably transfected	Generated in the lab with commercial COS-7 cell line
WM278	Human melanoma cell lines	originally obtained from the Wistar Institute
U937	Human monocytic cell line	Cell Line Service (CLS)
NCI-H1975	Human non-small cell lung cancer cell line	Kindly given by Division of Respiratory Medicine and Thoracic Oncology, Department of Medicine, LMU, Munich
MCF7	Human breast carcinoma cell line	Kindly given by Department of Gynecology and Obstetrics, LMU, Munich
KHOS	Human osteosarcoma cell line	Kindly given by Hopp Children's Cancer Center Heidelberg, Heidelberg
HaCaT	Human spontaneously immortalized keratinocyte cell line	PromoCell GmbH

Autologous EBV transformed B cell line PSO7	EBV immortalized B cell line from psoriasis patient that provided the V α 3S1/V β 13S1 TCR	PD Dr. Klaus Dornmair, Institute for Neuroimmunology, Max Planck Institute, Martinsried
EBV transformed B cell line Fey, P16488, P17490	B cell lines immortalized by EBV from an HLA-C*06:02-negative subject without psoriasis	PD Dr. Klaus Dornmair, Institute for Neuroimmunology, Max Planck Institute, Martinsried
EBV transformed B cell lines D22 and e9453	B cell lines immortalized by EBV from two HLA-C*06:02-positive volunteers without psoriasis	Prof. Rudolf Wank, Immunotherapy Research Center Munich, Munich
HLA-C*06:02-721.221 cell line	HLA-class I-deficient EBV-transformed Burkitt's lymphoblastoid cell line 721.221 (ATCC®CRL-1855), HLA-C*06:02 stably transfected	Generated in the lab
HLA-C*06:02-C1R cell line	EBV-transformed human B lymphoblastoid C1R cell line expressing low endogenous HLA, HLA-C*06:02 stably transfected	Prof. Dr. Stefan Stevanović, Interfaculty Institute for Cell Biology (IFIZ), University of Tübingen, Tübingen
EBV immortalized B cell lines GM11930, HG00131, HG00142, GM20771, GM12286, GM10246	B cells immortalized by EBV from homozygous HLA-C*06:02 individuals without psoriasis from the 1000 Genomes project	Coriell Institute for Medical Research, Camden, NJ, USA

2.12 Software

Software	Manufacturer
Sequence scanner 2.0	Applied Biosystem
Quantity One V 4.6.5	Bio-Rad
FlowJo V 886	Tree Star
Graphpad prism 9 Software	Graphpad Software, LLC

3. Methods

3.1 Cell Biological Methods

3.1.1 Cultivation of Suspension Cells

The V α 3S1/V β 13S1-TCR hybridoma, peripheral blood mononuclear cells (PBMCs), various Epstein-Barr Virus (EBV)-immortalized B cell lines and other suspension cell lines were maintained as suspension cultures. The composition of the culture media for each cell type is given in Section 2.3. The cell lines required passaging when the density reached approximately 1×10^6 /ml. Specifically, part of the cells was discarded, and the remaining cells were diluted with fresh culture medium in tissue culture flasks of different sizes at a temperature of 37 °C and a CO₂ concentration of 5%.

3.1.2 Cultivation of Adherent Cells

The cell lines COS-7-HLA-C*06:02, HEK293T, NCI-H1975, MCF7, and other adherent cell lines grow adherently in their respective culture medium. Once the cell confluence reached 80%, the cells were diluted. After discarding the supernatant, cells were digested with Trypsin/EDTA at 37 °C and 5% CO₂ for 5 to 10 minutes to singularize and detach cells from the surface of culture flasks. Part of the digested cells was discarded, and the remaining cells were diluted with fresh culture medium in tissue culture flasks of different sizes at 37 °C and 5% CO₂. Section 2.3 gives a summary of the medium for each adherent cell line.

3.1.3 Determination of the Cell Number

The number of living cells was determined with the Neubauer counting chamber. The cells were diluted 1:1 or 1:10 in trypan blue solution and placed in the counting chamber, depending on the cell density (Section 2.4). Trypan blue solution was used as a counter stain to identify dead cells. Dead cells appeared darkly colored in the microscope because they absorbed the dye due to defects in the cell membrane allowing transmigration of the colorant; such cells were not included in the count. After counting the four quadrants, the concentration of cells in the original suspension was determined by employing the following formula:

$$\text{Cell concentration} = \text{average number of cells per quadrant} \times \text{dilution} \times 10^4 / \text{ml.}$$

3.1.4 Cryopreservation and Thawing of Eukaryotic Cells

For long-term preservation, singularized adherent cells and suspended cells were centrifuged, counted, and resuspended in the freezing medium (Section 2.3) to a final concentration of 10^6 cells/ml. Up to 1.5 ml cell suspension was then transferred in 1.8 ml cryogenic vials and transferred into Mr. Frosty™ freezing container (ThermoFisher Scientific) for a slow cooling rate in a freezer at -80 °C. After two days, cryogenic vials were transferred into liquid nitrogen tanks and stored there.

To recover the cells, they were thawed as quickly as possible in a 37 °C water bath and transferred to a 50 ml Falcon tube filled with an appropriate medium in order to dilute the DMSO (Sigma-Aldrich). After centrifugation at 1,600 rpm for 5 minutes, the cells were first cultivated in a medium without selection antibiotics for two days and then transferred into the medium with appropriate antibiotics (Section 2.3).

3.1.5 Activation of V α 3S1/V β 13S1-TCR Hybridoma Cells by CD3 Cross-linking

The surface of cell culture plates was coated with an anti-mouse CD3 antibody (Section 2.9.1) diluted 1:500 in PBS overnight at 37 °C. After removal of the supernatant, V α 3S1/V β 13S1-TCR hybridoma cells were added. After 24 hours, induction of sGFP expression in activated V α 3S1/V β 13S1-TCR hybridoma cells was assessed by fluorescence microscopy and flow cytometry. Anti-human CD8 antibody is applied to stain V α 3S1/V β 13S1-TCR hybridoma cells to distinguish them from APCs in flow cytometry analysis.

The gating strategy for examining sGFP expression in V α 3S1/V β 13S1-TCR hybridoma cells is illustrated in **Figure 3.1.5** (Arakawa *et al.*, 2021).

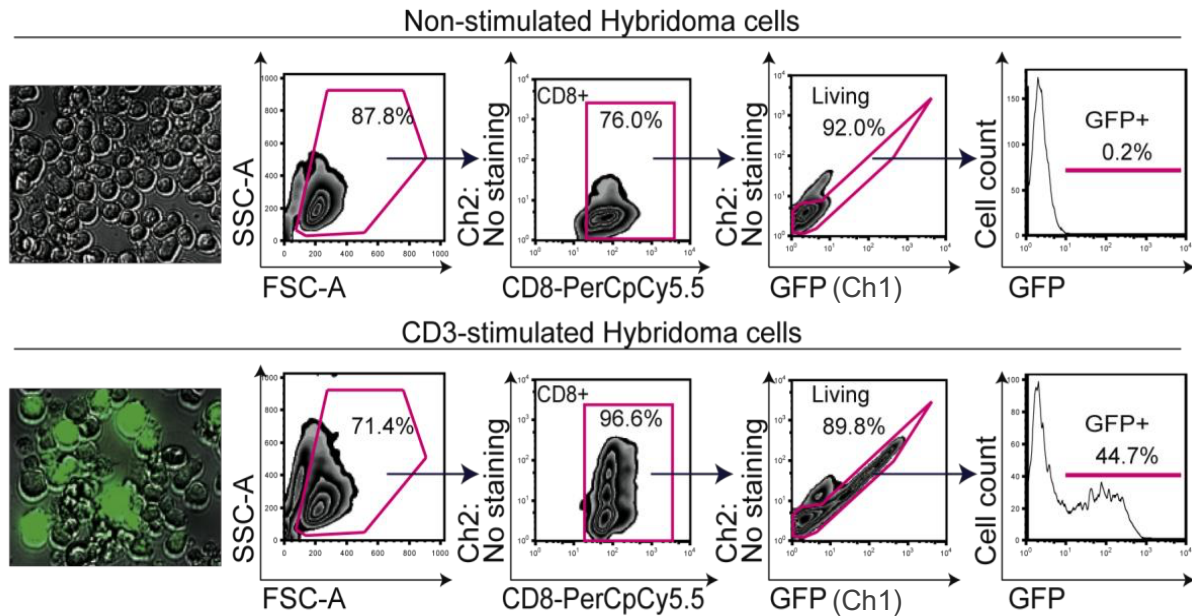


Figure 3.1.5 Gating strategy to assess sGFP induction in $V\alpha 3S1/V\beta 13S1$ -TCR hybridoma stimulation experiments. In co-culture experiments with APCs (e.g., HEK293T, COS-7 cells), hybridoma cells were stained with anti-human CD8 antibody to discriminate $V\alpha 3S1/V\beta 13S1$ -TCR hybridoma from APCs. TCR-hybridoma cells with high autofluorescence in Ch1 and Ch2 were excluded from analyses. The GFP⁺ gate is set to 0.2% of GFP⁺ cells in non-stimulated hybridoma cells. In sGFP⁺ hybridoma cells, the mean fluorescence intensity (MFI) of sGFP is determined.

3.1.6 Subcloning of the $V\alpha 3S1/V\beta 13S1$ -TCR Hybridoma

The $V\alpha 3S1/V\beta 13S1$ -TCR hybridoma cells require occasional recloning to maintain high stimulatory responsiveness. The $V\alpha 3S1/V\beta 13S1$ -TCR hybridoma clone H2II formerly generated in the laboratory was diluted to 2 cells/ml in a 10% FCS RPMI complete medium (Section 2.3). The cell suspension was seeded at 0.1 ml/well in 96 well-round bottom microtiter plates to a final density of 0.2 cells/well to obtain hybridoma subclones from single cells. The plates were cultivated in a CO₂ incubator. The development of cell colonies was analyzed daily by inverted microscopy. Hybridoma subclones growing from single cells were transferred and expanded in 48-well plates with the hybridoma selection medium (Section 2.3) (500 μ l/well). GFP expression in the $V\alpha 3S1/V\beta 13S1$ -TCR hybridoma subclones was induced by CD3 crosslinking and analyzed by flow cytometric analysis. Subclones with high induction of sGFP were expanded and frozen for further use.

3.1.7 Cell Isolation or Separation

3.1.7.1 Isolation of PBMCs

Peripheral blood samples of psoriasis patients were obtained from the Psoriasis Center, Clinic and Polyclinic of Dermatology and Allergy of the University Hospital of Munich. All patients and voluntary donors had been informed about the purpose of the investigation and gave their written consent. The study was approved by the Ethics Committee of the Medical Faculty, Ludwig-Maximilian-University of Munich, and performed in accordance with the ethical principles of the Declaration of Helsinki. HLA-C*06:02 status, age, and gender of patients were recorded in anonymous form (see Supplements 6.3).

Peripheral blood was collected in Vacutainer® Evacuated Blood Collection Tubes (BD). PBMCs were isolated from the blood samples donated by volunteers using Ficoll density gradient centrifugation. Each 15 ml of blood was diluted with 20 ml of PBS. 35 ml of the diluted blood suspension were slowly and smoothly layered onto 15 ml of Ficoll separating solution (Merck) in a 50 ml Falcon tube and centrifuged at 2,040 rpm (brake 0, acceleration time 150 s) for 30 minutes at 20 °C. This separated white blood cells from erythrocytes. The white blood cell buffy coat overlying the Ficoll gradient was carefully collected with a pipette, avoiding disturbance of other layers as much as possible, and transferred to a fresh Falcon tube. The collected cells were diluted with RPMI 1640 (Gibco) and then centrifuged at 1,600 rpm for 10 minutes. The supernatant was discarded after centrifugation, and the cellular pellet was washed twice in RPMI 1640 and then resuspended in 2 ml fresh 10% AB RPMI Complete medium (Section 2.3) for subsequent applications.

3.1.7.2 Cell Separation and Depletion by Magnetic-activated Cell Sorting

Cell subsets of PBMCs or tonsil cells were isolated by the magnetic-activated cell sorting (MACS) assay. As the steps for different cell separations are similar, the general procedure of magnetic sorting is described.

Cryopreserved tonsil cells were derived from psoriasis patients who had formerly been tonsillectomized because of recurrent streptococcal angina associated with severe psoriasis relapses (Diluvio *et al.*, 2006). They were thawed, washed once in pre-warmed (37 °C) 10% FCS RPMI complete medium, and cultured overnight. The isolation of PBMCs is described in the above section .

PBMCs or tonsillar cells with an initial number of 10^7 were washed and resuspended in 80 μ l MACS separation buffer (Section 2.4). The cells were then incubated in the refrigerator (2-8

°C) for 20 minutes with 20 µl antibody-conjugated magnetic microbeads (Section 2.5) per 10^7 total cells. Numerous cell types and cell subsets can be separated with specific MACS MicroBeads. After 20 minutes of incubation, the cells were labeled with microbeads and then washed once with 1-2 ml of MACS separation buffer, pelleted by centrifugation, and resuspended in 500 µl buffer.

The cell suspension was run through an a priori equilibrated MACS column set in the MACS Separator's magnetic field (Miltenyi Biotec). Cells labeled with magnetic beads are preserved within the column, while unlabeled cells in the flow were collected as depleted cell fractions. After three washing steps by adding MACS separation buffer (MS: 3×500 µl, LS: 3×3 ml), the column with labeled cells being adsorbed in was removed from the magnetic field, leading to the elution of target cells from the column. Both fractions (labeled and unlabeled cells) were pelleted by centrifugation, washed in RPMI 1640 medium, and resuspended in the according medium for further use. For example, for the separation and the depletion of B cells, B cells were separated from PBMCs by applying human CD19 Microbeads. In this way, two parts of PBMCs were obtained: B cells and B cell-depleted PBMCs. If necessary, higher purification of target cell fractions can be achieved by repeating the above separation process.

3.1.7.3 Cell Sorting by Fluorescence-activated Cell Sorting for Co-culture Experiments

PBMCs can be sorted into more than two sub-groups by fluorescence-activated cell sorting (FACS), a flow cytometry technology that targets and isolates cell populations using fluorescent labeling. Following the process through a cytometer, cells are sorted based on light scattering, and the cell surface marker is labeled with fluorescent dyes (**Figure 3.1.7.3.1**).

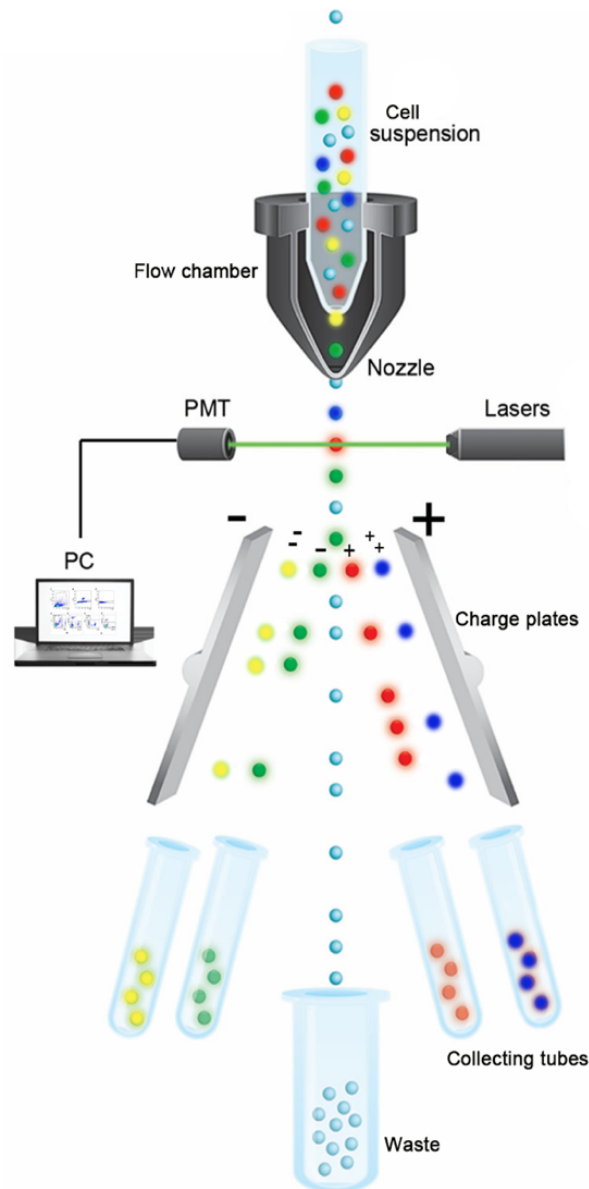


Figure 3.1.7.3.1 Schema of fluorescence-activated cell sorting (FACS) modified from previous work of Hodne and Weltzien (Hodne and Weltzien, 2015). The cell suspension of PBMCs is subjected to labeling with distinct fluorescent tags, which vary based on the experimental setup. A laser-detector system is employed to monitor the fluorescent and light scatter characteristics, enabling the detection of cell flow passing through. Subsequently, cells are sorted into several collecting tubes according to their charge in an electric field, while unlabeled cells are separated into a waste tube.

Freshly isolated PBMCs were stained with multiple fluorescing antibodies for 30 minutes in the dark at room temperature (RT). **Table 3.1.7.3** displays the antibody marker panels applied to label target cells. With labeling ways in the marker panels, the gating strategies depicted in **Figure 3.1.7.3.2** were applied to enable the gating of various cell populations of interest in PBMCs (B cells, CD4⁺ T cells, CD8⁺ T cells, NK cells, monocytes, and pDCs). Plasmacytoid DCs (pDCs) were chosen as one population of interest among subsets of DCs because they are the most abundant DC subset in the tonsils. Cell sorts were performed on a FACSAria™ II

Fusion cell sorter (BD). Setting optimization with Accudrop Beads (BD) and compensation was performed. Before loading the sorting samples, 10 μ l DAPI dye was added at 1/100 dilution per sample. FACS-separated cell populations were collected in the collecting medium (Section 2.3) and placed on ice during the sorting procedures. After collection, purity analysis was conducted to ensure that the cell population of interest was pure enough (>95%) for further co-culture experiments. The cell subgroups of PBMCs in collecting tubes were then obtained by centrifugation at 1,000 rpm for 3 minutes, and the supernatant was removed. The cell pellet was resuspended with a 10% FCS RPMI complete medium and co-cultured with hybridoma, as described in Section 2.3.

Panels	FITC	PE	PerCP/Cyanine5.5	PE/Cyanine7	APC
1	CD20	CD4	CD8	CD56	-
2	CD11c	CD304	HLA-DR	-	CD14

Table 3.1.7.3 Overview of antibody marker panels used in the cell sorting.

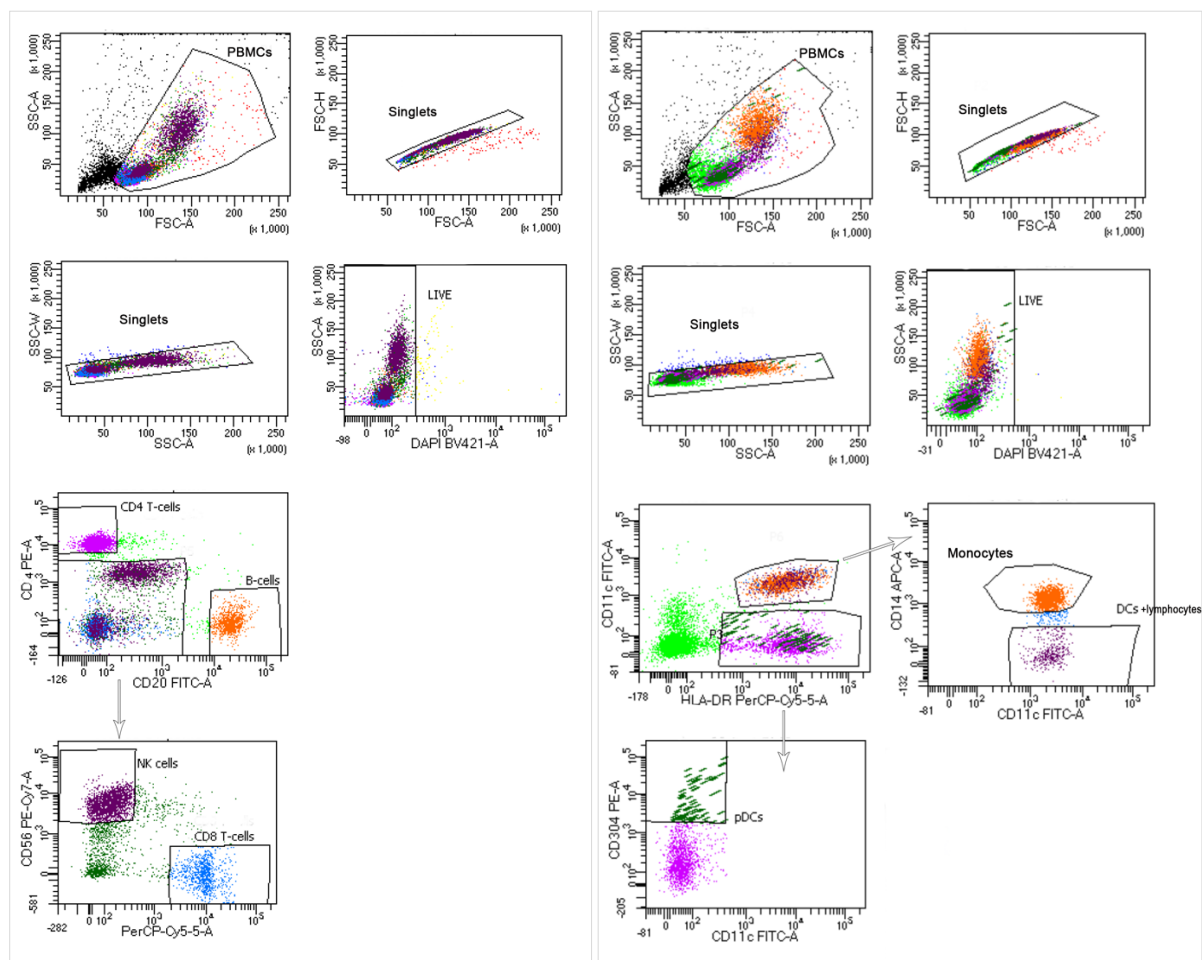


Figure 3.1.7.3.2 Gating strategies to determine B cells, CD4⁺ T cells, CD8⁺ T cells, NK cells, monocytes, and pDCs. B cells are CD20⁺ CD4⁻; CD4⁺ T cells are CD4⁺ CD20⁻; CD8⁺ T cells are CD20⁻ CD4⁺

CD8⁺; NK cells are CD20⁻ CD3⁻ CD56⁺; Monocytes are HLA-DR⁺ CD11c⁺ CD14⁺; pDCs are HLA-DR⁺ CD11c⁻ CD304⁺ (Durand and Segura, 2016).

3.1.8 Co-culture Assays

For the determination of potential target cells stimulating the Vα3S1/Vβ13S1 TCR, human cell lines of various origins were co-cultured with Vα3S1/Vβ13S1-TCR hybridoma cells in 48-well plates. Subsets of PBMCs or tonsil cells were co-cultivated with Vα3S1/Vβ13S1-TCR hybridoma in a 96-well plate in the appropriate medium without selection antibiotics. If cell lines to be tested were adherent cells, they were seeded in the plate 24 hours before adding 2.5×10⁴ cells/well of the Vα3S1/Vβ13S1-TCR hybridoma to reach 70%-80% confluence. Subsets of PBMCs or tonsil cells and Vα3S1/Vβ13S1-TCR hybridoma were seeded at 2×10⁴ and 1×10⁴ cells/well, respectively. After 24 hours of co-culture, the induction of sGFP in Vα3S1/Vβ13S1-TCR hybridoma cells was assessed by flow cytometry. As negative/positive controls, Vα3S1/Vβ13S1-TCR hybridoma cells were cultured without treatment or pre-coated anti-mouse CD3 antibody (1:500).

For determination of potential autoantigen(s) that are recognized by the Vα3S1/Vβ13S1 TCR, various HLA-C*06:02-transfected APCs (e.g., COS-7-HLA-C*06:02 cell line, HLA-C*06:02-721.221 cell line, HLA-C*06:02-transfected HEK293T cells) or naturally HLA-C*06:02-positive WM278 cells were used for presenting peptides, either in the form of peptide-coding plasmids or synthetic peptides, and co-cultured with the Vα3S1/Vβ13S1-TCR hybridoma. If APCs were adherent cells, they were seeded in the plate 24 hours before transfection to reach 70%-80% confluence. Plasmid-encoded peptides were co-transfected into APCs using FuGENE[®] HD reagent (Section 3.2.6.1), while synthetic peptides were added into cultures directly for presentation by APCs. After 24 hours of co-culture, the induction of sGFP in Vα3S1/Vβ13S1-TCR hybridoma cells was assessed by flow cytometry. Empty plasmids and pcDNA-GFP served as negative control and transfection control in stimulation experiments with peptide-encoding plasmids, while the FALK peptide (a synthetic HLA-C*06:02-presented peptide lacking antigenicity for the Vα3S1/Vβ13S1 TCR) was applied as negative control in the stimulation experiments with synthetic peptides (Falk *et al.*, 1993). The Vα3S1/Vβ13S1-TCR hybridoma cells cultured in pre-coated anti-mouse CD3 antibody (1:500) served as positive control.

3.1.9 Flow Cytometry Analysis of sGFP Expression in Vα3S1/Vβ13S1-TCR Hybridoma Cells

After 24 hours of co-culture with various APCs, V α 3S1/V β 13S1-TCR hybridoma cells were pelleted and stained with anti-human CD8 antibody conjugated with PerCP/Cyanine5.5 for 30 minutes at RT to allow differentiation of the V α 3S1/V β 13S1-TCR hybridoma from other cell types in FACS analysis. The cells were washed once, resuspended with 150 μ l FACS buffer in 1.40 ml round bottom tubes, and then analyzed using a FACSCanto™ II Flow Cytometry System (BD). The data were analyzed using FlowJo software (Tree Star).

3.1.10 Flow Cytometry Analysis of HLA-class I Expression

1×10^5 to 1×10^6 cells/well were seeded in 48 or 96 well plates prior to the staining. The adherent cells at 80-90 % confluence were detached the next day using EDTA detachment solution and washed once with 200 μ l FACS buffer. Suspension cells were directly collected and washed once. Subsequently, cells were incubated with anti-human HLA-C (DT-9), anti-human HLA-ABC (W6/32), and corresponding isotype antibodies conjugated with PE (Section 2.9) for 30 minutes at RT. The antibodies were diluted 1:1 in FACS buffer and applied at 1.4 μ l per 10^5 cells. The cells were washed once, resuspended with 150 μ l FACS buffer in 1.40 ml round bottom tubes, and then analyzed by a FACSCanto™ II flow cytometry system (BD). The data were analyzed by FlowJo (Tree Star).

3.1.11 Cell Proliferation Assays

Depending on the purpose, different cell proliferation assays were applied to assess the cell proliferation of PBMCs or lymphocytes.

3.1.11.1 [3 H]-Thymidine Incorporation Assay

[3 H]-thymidine incorporation assay was used to measure the proliferation of PBMCs by the incorporation of [3 H]-thymidine (Hartmann Analytic) into the DNA of the dividing cell. Cells were seeded and cultured in 96-well plates at 2×10^5 cells/well. Triplicates of PBMCs were pulsed overnight on day 4 with 24,500 bq/well [3 H]-thymidine (Hartmann Analytic), and proliferation was assessed according to the incorporated radioactivity. Harvesting and measurement of radioactive decay (counts per minute) were done using an automatic filter counting system (Inotech Biosystems, Derwood, USA). The intensity of radioactivity reflects the replication of cells. Stimulation of PBMCs with immobilized anti-human CD3 antibody served as positive control.

3.1.11. 2 BrdU Cell Proliferation Assay

Thymidine analog BrdU (5-Bromo-2'-Deoxyuridine) can also be used to measure cell proliferation. The BrdU cell proliferation assay examines the BrdU incorporated into cellular DNA during cell proliferation by employing a BrdU Cell Proliferation Assay Kit (Cell signaling). According to the manufacturer's protocol, the 10× BrdU solution was prepared in the first step. Cells were seeded and cultured in 96 well plates at 2×10^5 cells per well for three days. 24 hours before cells were to be harvested, 10× BrdU solution was added to the wells to a final 1× concentration (e.g., 20 µl of 10× BrdU solution in 200 µl medium per well in the plate). After 30 minutes of denaturing, one hour of incubation with BrdU mouse detection antibody and 30 minutes of incubation with horseradish peroxidase (HRP)-conjugated secondary antibody, the amount of BrdU incorporated into cells is proportional to the magnitude of the color-specific light absorbance, which is developed by the HRP substrate 3,3', 5,5'-Tetramethylbenzidine dihydrochloride hydrate (TMB) and measured by enzyme-linked immunosorbent assay (ELISA) with a microplate photometer. Stimulation of PBMCs with anti-human CD3 antibody served as positive control.

3.1.11.3 CFSE Labeling Assay

Carboxyfluorescein diacetate succinimidyl ester (CFSE) labeling assay is employed to detect cell proliferation either *in vitro* or *in vivo*, as incorporated fluorescence in progeny cells is decreased by half after each cell division. In viable cells, non-fluorescent CFSE is hydrolyzed by esterase enzymes in the cytoplasm, releasing fluorescent amine-reactive dyes. These dyes then form fluorescent conjugates by covalently reacting with the amine groups on intracellular proteins. 1×10^7 to 2×10^8 PBMCs were washed with RPMI medium twice and then resuspended with 1 ml RPMI medium. 5 µM CFSE (eBioscience™) stored in DMSO was diluted at 1:1,000 in PBS and added into the cell suspension. Then, the cells were vortexed for 30 seconds and incubated in the dark for 10 minutes at RT. Cells were washed with 2 ml serum-containing culture medium three times and cultured for five days. Before measuring the cell division by flow cytometry, the cells were stained with antibodies conjugated with appropriate fluorescent dyes avoiding FITC (CFSE-stained cells were analyzed in the FITC channel): APC-CD19, PE-CD3, PerCP/Cyanine5.5-CD8 or PerCP/Cyanine5.5-CD4. In this way, the proliferation rate of different types of cells ($CD8^+$ T cells, $CD4^+$ T cells, $CD3^+$ T cells, and B cells) can be assessed according to the decrease in fluorescence intensity. Anti-CD3 stimulation served as positive control. **Figure 3.1.11** shows the workflow of the above assays assessing cell proliferation for different applications in our study.

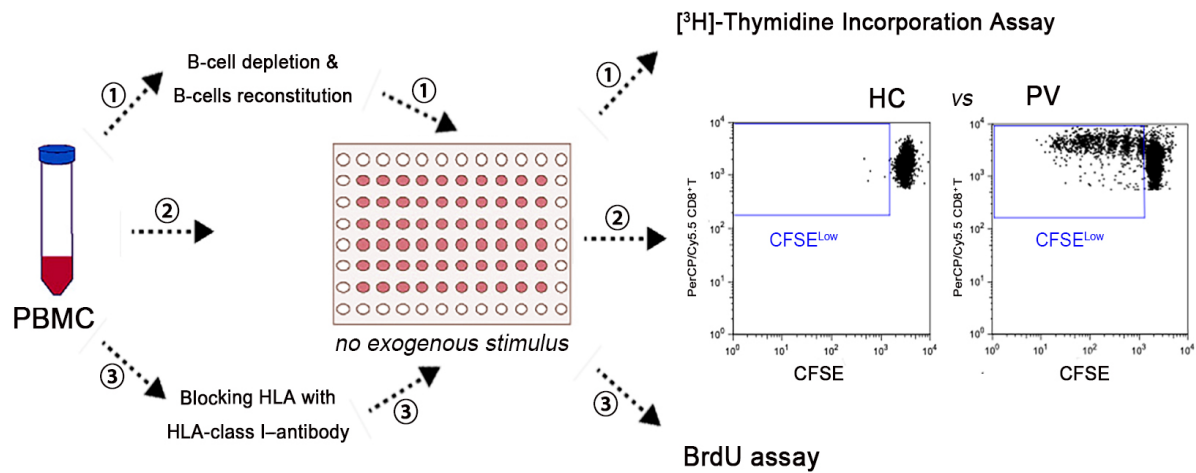


Figure 3.1.11 Workflow for assessing autoproliiferation of PBMCs under different conditions in vitro using three assays: ① ^3H -Thymidine incorporation assay; ②CFSE-labeled assay (CFSE^{low} population indicates proliferating cells); ③BrdU Cell Proliferation Assay. Cells were cultured in a serum-free medium and in the absence of exogenous stimulus for five days.

3.2 Molecular Biology Methods

3.2.1 Handling of *E.coli* Cultures

3.2.1.1 Cultivation of Bacteria

To prepare solid LB-agar plates, select agarose was added to the liquid LB medium (components see Section 2.3). After autoclaving the prepared LB medium, the desired antibiotic was incorporated at the appropriate concentration (final concentration: ampicillin at 100 $\mu\text{g}/\text{ml}$ or kanamycin at 50 $\mu\text{g}/\text{ml}$) when the temperature dropped to approximately 60 $^{\circ}\text{C}$. The liquid agar was carefully poured into plastic Petri dishes, ensuring that the bottom was well-covered and dried under sterile conditions at RT. The agar plates were stored at 4 $^{\circ}\text{C}$, and the selection antibiotics in the growth medium were stable for up to 2 weeks.

To grow the bacteria on the agar plates, for example, after transformation, 20-200 μl of the bacterial suspension was pipetted onto the agar plate and evenly distributed using a flamed Drigalski spatula. Plating out should take place immediately after application of the suspension to avoid diffusion into the agar. The culture dishes were placed in an incubator at 37 $^{\circ}\text{C}$ for overnight cultivation.

3.2.1.2 Preservation and Thawing of Bacterial Strains

Glycerin stocks were used to preserve bacterial strains. For this purpose, 800 µl of a freshly grown bacterial culture was mixed with 200 µl of 87% glycerol into a freezer tube and stored at -80 °C.

For thawing the preserved strains, a double-volume LB medium was added. Subsequently, the bacteria underwent centrifugation at 3,000 g and 4 °C for 15 minutes and were resuspended in a minimum of five times the original volume of LB amp medium. Following 1 hour of shaking at 225 rpm and 37 °C, the cells were diluted at a ratio of 1: 8 and subjected to additional shaking for approximately 5 hours prior to proceeding with subsequent procedures such as plasmid isolation.

3.2.1.3 Transformation of Bacteria

1-5 µl of DNA (usually ranging from 10 pg to 100 ng) were introduced into 15-20 µl of *E. coli* strain within a 1.5 ml microtube and gently homogenized. The resulting *E. coli* /DNA mixture was subjected to a 30-minute incubation on ice. Subsequently, each transformation tube underwent a heat shock process at 42 °C, accomplished by placing it into a Thermomixer for a duration of 30 to 60 seconds. Following the heat shock, the tubes were incubated on ice for 2 minutes.

After adding 50 µl SOC medium (Invitrogen, without antibiotic), the bacteria were grown in a shaking incubator at 37 °C for 20-60 minutes at 225 rpm. Then, some or all the transformation bacteria were placed onto an LB agar plate containing the appropriate antibiotic and cultured at 37 °C overnight.

3.2.2 Generation of Peptide-Coding Plasmids

3.2.2.1 Primer Design of Peptide-Coding Plasmids

Sequence information for mRNA and genomic DNA was obtained from the National Center for Biotechnology Information (www.ncbi.nlm.nih.gov). The corresponding sequence in the natural mRNA was validated with “Web BLAST” from the National Center for Biotechnology Information (<https://blast.ncbi.nlm.nih.gov/Blast.cgi>). If there was no corresponding natural mRNA sequence, nucleotide sequences were designed based on codon usage with The IDT Codon Optimization Tool (<https://eu.idtdna.com/CodonOpt>). Primers were designed according to the user manual (Version F, 10 November 2010) of the pcDNA™3.1 Directional TOPO®

Expression Kit (**Table 3.2.2.1**). Primers labeled with “for” (forward) elongate the coding strand of the DNA sequence encoding short peptides, while primers labeled with “rev” (reverse) elongate the non-coding strand. Peptide sequences were converted to the reverse DNA complement sequence with a web Reverse Complement tool (https://www.bioinformatics.org/sms/rev_comp.html). All forward and reverse oligonucleotides for PCR reactions producing double-strand DNA coding short peptides are listed in separate tables in Section 6.1.

		Overhang	Initiation codon	Sequence	Stop codon	
For(ward)	5’-	CACC -	ATG -	Peptide triplets	- TGA	-3’
Rev(erse)	3’-			Reverse complement sequence	- ACT	-5’

Table 3.2.2.1 Template design of primers for producing double-strand DNA encoding short peptides.

The nucleotide sequences were confirmed by translation with the ExPASy translation tool (<http://web.expasy.org/translate/>). All primers were purchased HPLC purified and in a “Dried” state from biomers.net. Primers were dissolved to a concentration of 100 mM and then stored at -80 °C.

3.2.2.2 Cloning Peptide-Coding Sequence into Expression Vector

For the generation of double-stranded DNA of short peptides with overhang, the forward and reverse oligonucleotides were initially subjected to denaturation at 95 °C for a duration of 5 minutes using the Veriti PCR Thermal Cycler and subsequent annealing carried out at 75 °C for 3 minutes, followed by a gradual cooling process with an intermediate step at 50 °C for 3 minutes to the final room temperature. The reaction system is shown in the following mix:

Volume	Reagent	Final Concentration
10 µl	x-for (100 µM)	20 µM
10 µl	x-rev (100 µM)	20 µM
10 µl	Pwo 10x PCR Puffer (with Mg ₂)	1×
70 µL	ddH ₂ O	

2 µl annealed inserts were diluted in 1,500 µl with ddH₂O (1:750). The backbone plasmid and the diluted inserts were ligated at RT for 20 minutes using the pcDNA3.1 Directional TOPO Expression Kit (Invitrogen) following the protocol. The reaction setup is shown as the following mix:

Volume	Reagent	Final Amount
1 µl	annealed insert DNA	4 to 5 ng
1 µl	salt solution	
1 µl	TOPO vector-pcDNA3.1	
3 µl	ddH ₂ O	

One sample containing H₂O instead of the annealed insert was applied as a negative control. 1 µl of the ligation mix was transformed into an *E. coli* strain One Shot® TOP10 (Invitrogen). The next day, three to five colonies were selected and cultivated in a 2 ml LB medium. Plasmids were isolated and purified following the instructions provided in Section 3.2.2.3 and subsequently sequenced as explained in 3.2.5. Spared plasmids from positive clones were kept at -20 °C.

3.2.2.3 Plasmid DNA Isolation and Purification

The isolation of plasmids was performed with Wizard® Plus SV minipreps DNA Purification System (Promega) following the manufacturer's instructions. Briefly, 2 ml of the grown bacterial culture was transferred to a 2 ml Eppendorf microcentrifuge tube, and the bacteria were pelleted by centrifugation for 5 minutes at top speed. The bacterial pellet was resuspended thoroughly in 250 µl Cell Resuspension Solution in the kit by vortexing, and the bacteria were then lysed with 250 µl Cell Lysis Solution and gently inverted 4 times to mix. 10 µl of Alkaline Protease Solution was added to the bacteria lysis, again gently inverted 4 times to mix, and incubated for 5 minutes at RT. After adding 350 µl of Neutralization Solution, the mixture was centrifuged for 10 minutes at top speed to separate the precipitated components, and the supernatant was transferred to a miniprep Spin Column.

The Vacuum Adapters were adapted to the manifold port, and then the Spin Columns were inserted into the Adapters. The liquid in Spin Columns was pulled through the column by applying a vacuum, and then the columns were washed two times with 750 µl of Wash Solution (ethanol added). The columns were transferred to a 2 ml Collection Tube and centrifuged at top speed for 2 minutes.

The plasmid DNA bound to the column membrane was eluted with 60 µl of nuclease-free water into a sterile 1.5 ml Eppendorf microcentrifuge tube. To ensure complete elution of the DNA, the column was incubated for 2 minutes at RT before the final centrifugation step. The plasmid DNA solutions were stored at 4 °C for further use or at -20 °C for long-term preservation.

The isolation of larger amounts of plasmids was carried out with the QIAGEN Plasmid Maxi Kit according to the manufacturer's instructions.

3.2.3 Genomic DNA Extraction and Purification

Genomic DNA was extracted and purified utilizing the Blood and Tissue Genomic DNA Miniprep System (Viogene) in accordance with the instructions provided by the manufacturer. In brief, up to 10^7 cells are lysed, and proteins denatured in the 20 μ l Proteinase K and 200 μ l EX lysis buffer at 60 °C for 20 minutes. During this step, the samples were vortexed every 3-5 minutes to mix. Subsequently, the samples were incubated at 70 °C for a duration of 20 minutes. Afterward, 200 μ l absolute ethanol or isopropanol was added to samples and mixed by vortexing. The mixture was transferred into the Genomic DNA Mini Column and placed onto a Collection Tube, followed by centrifugation at 8,000 rpm for 2 minutes. DNA selectively adhered to the column while other cellular components were allowed to pass through. After thoroughly washing to eliminate any remaining impurities, the high-molecular-weight DNA was eluted and precipitated using a 200 μ l preheated elution solution. The DNA solutions were stored at 4 °C or -20 °C.

3.2.4 Determination of DNA/RNA Concentration

The concentration of aqueous DNA solutions was measured photometrically by determining the optical density (OD) at a wavelength of 260 nm, at which the absorption maximum of single- and double-stranded DNA is. The concentration of the different types of nucleic acids is calculated from the absorption at 260 nm, including the dilution factor. The ratio of the absorbance at 260 and 280 nm ($A_{260/280}$) is utilized to assess the purity of nucleic acids. A value of $A_{260/280}$ at approximately 1.8 is deemed indicative of pure DNA, while for pure RNA $A_{260/280}$ is considered around 2.0. The measurement was carried out with the Smart-Spec 3000 spectrophotometer from Bio-Rad.

3.2.5 Sequencing of DNA Samples

For DNA to be sequenced, samples were prepared as follows:

Volume	Reagent	Final Concentration /Amount
0.5-2 μ l	Plasmid DNA	200-300 ng
0.5 μ l	T7 forward primer (3 mM)	0.7 mM
to 7 μ L	ddH ₂ O	

Sequencing analyses were carried out at the sequencing service at the faculty of biology of the Ludwig-Maximilian-University of Munich. The resulting DNA sequences were analyzed with

the software “Chromas Lite V2.01” and “Web BLAST” (Basic Local Alignment Search Tool v2.11.0) (NIH, National Institutes of Health).

3.2.6 Transfection of Plasmid DNA and siRNA

3.2.6.1 Plasmid DNA Transfection of Cells with FuGENE

In V α 3S1/V β 13S1-TCR hybridoma stimulation experiments, plasmid-encoded peptides were transfected into APCs using FuGENE[®] HD reagent in accordance with the instructions of the manufacturer. COS-7-HLA-C*06:02 cell line, HLA-C*06:02-721.221 cell line, WM278 cell line, and other cell lines served as commonly used APCs. Prior to transfection, APCs were seeded in 48-well plates in appropriate medium without selection antibiotics at densities of 2×10^4 cells/well 24 h before transfection (confluence of adherent APCs need to reach 70%-80% on the transfection day).

On the day of transfection, APCs were transfected using the FuGENE[®] HD transfection reagent (Section 2.5) with the peptide-coding plasmids listed in Section 6.2, which were prepared as described in Section 3.2.2. After 24 hours, the V α 3S1/V β 13S1-TCR hybridoma cells were introduced (Section 3.1.8). The following day, the induction of sGFP in hybridoma cells was examined using the fluorescence microscope and flow cytometry. The empty vector plasmid served as a negative control.

3.2.6.2 Plasmid DNA and siRNA Transfection of Cells with Nucleofector

The Amaxa[™] 4D-Nucleofector[™] System (Lonza), including the 4D-Nucleofector[™] Core Unit and 4D-Nucleofector[™] X Unit, was applied for plasmid DNA transfection of difficult-to-transfect cell types. In our case, we applied this system to transfect B cells.

B cells were subcultured 1-2 days before nucleofection to an optimal cell density in their logarithmic growth phase. Plasmid DNA and pmaxGFP vector were diluted to 0.2 $\mu\text{g}/\mu\text{l}$ and added to Nucleocuvette strip wells at 2 $\mu\text{l}/\text{well}$. For siRNA, 1 or 1.5 μl siRNA (20 μM) was added to each Nucleocuvette strip well to achieve the final concentrations of 1 μM and 1.5 μM in the cell suspension. Required cells were centrifuged at $90\times g$ for 10 minutes at RT and then resuspended carefully to a final concentration of 2×10^5 to 1×10^6 cells in 20 μl SF 4D Nucleofector[™] solution and subsequently added into the Nucleocuvette strip wells. Gently Tapping the Nucleocuvette[™] Strips ensured that the sample covers the bottom of the cuvette. Then, the Nucleocuvette[™] Strip was placed into the retainer of the 4D-Nucleofector[™] X Unit

with a closed lid for nucleofection. Immediately after the nucleofection, 80 μ l/well of pre-warmed (37 °C) 10% FCS RPMI medium was covered onto the Nucleocuvette strip wells and incubated without any further touching or pipetting for 10 minutes at 37 °C. After the recovery step, cells were gently transferred from the cuvette into a 96-well plate, which was pre-incubated with the appropriate medium and cultured in a 37 °C/5 % CO₂ incubator for further experiments.

The nucleofection process was running under program DN-100. The program for nucleofection varies depending on individual EBV-transformed B cell lines, and DN-100 achieved the best balance between transfection efficiency and cell survival rates among selected programs for the HLA-C*06:02-721.221 and HLA-C*06:02-C1R cell lines (**Figure 3.2.6.2**). The candidate programs used for nucleofecting EBV-transformed B cell lines on 4D-Nucleofector™ X Unit platform, i.e., CA-137, CB-138, CM-150, and DN-100, were selected by combining the information from the Knowledge Database of Lonza (<https://knowledge.lonza.com/>) and the recommendation from Lonza's Scientific Support Team.

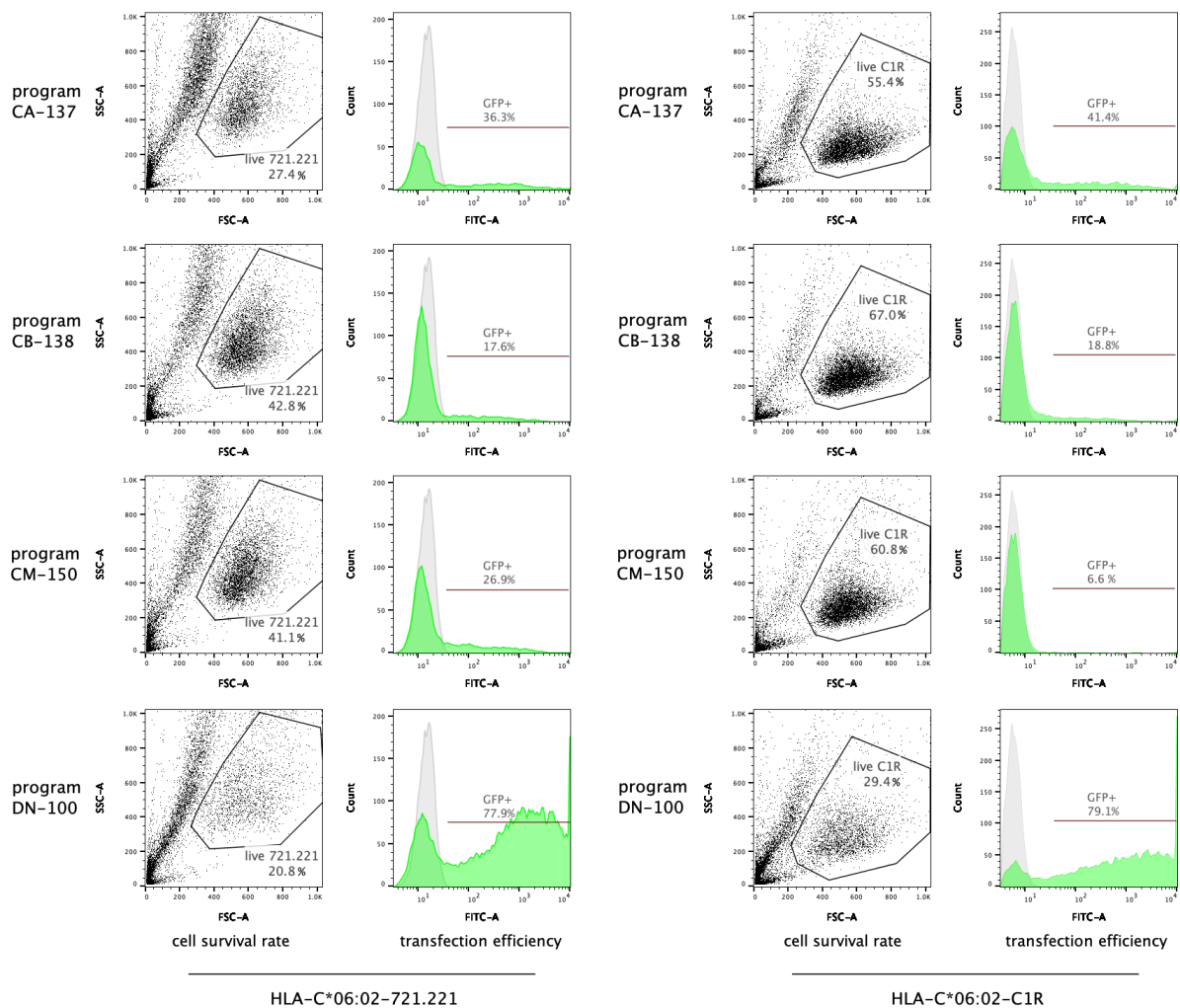


Figure 3.2.6.2 Representative flow cytometric panels showing transfection efficiency and cell survival rates under the settings of various nucleofection programs for HLA-C*06:02-721.221 and HLA-C*06:02-C1R. Panels in the column of “cell survival rates” show the proportion of viable cells after the nucleofection process. Histograms in the column of “transfection efficiency” illustrate the GFP expression of cells nucleofected with pmaxGFP plasmid (green) or empty vector control (gray), with numbers showing the frequency of the nucleofected cell rate with pmaxGFP.

3.2.7 Gel Electrophoretic Analysis of DNA

Agarose gel was prepared according to the size range of linear double-stranded DNA molecules. Briefly, the appropriate amount of agarose (VWR International) was dissolved in 100 ml 1× TBE buffer by heating in a microwave oven and poured into the gel mold with a comb after cooling down to 60-80 °C.

% Agarose concentration in gel (w/v)	Efficient separation range for linear double stranded DNA molecules (kb)
0.3	5-60
0.6	1-20
0.7	0.8-10
0.9	0.5-7
1.2	0.4-6
1.5	0.2-3
2.0	0.1-2

The agarose gel was transferred into the electrophoresis chamber and coated with 1× TBE buffer. 10 µl DNA solution (0.3-0.5 µg) was loaded into the slots with 3-5 µl loading buffer, carefully avoiding air bubbles. DNA ladders of known size were used as DNA size standards according to the size of DNA: DNA ladder V (8-587 bp) and DNA ladder VI (0.15-2.1 kbp). The electrophoresis was run under a voltage of 100-120 V and a current of 60 A, respectively, for approximately 1-1.5 hours. 5-10 µl of RedSafe™ Nucleic Acid Staining Solution/100 ml gel was used for staining for 20 minutes. This was followed by washing with distilled water for 10 minutes. The dye ethidium bromide intercalates into the helices of the DNA and stains them specifically. When exposed to UV light (wavelength: 320 nm), the dye shows fluorescence, and the DNA becomes visible. The gel documentation system GenDoc2000 was applied for the analysis and documentation.

3.2.8 The Polymerase Chain Reaction (PCR)

Polymerase Chain Reaction (PCR) is a method for the targeted amplification of a selected nucleic acid region. During the PCR process, specific primers are employed to anneal to the plus and minus strands of the template DNA and facilitate the amplification of the sequence of

interest. Alternating thermal cycles allow DNA denaturation, primer annealing, and DNA synthesis. Temperature-stable DNA polymerases, such as Taq DNA polymerase, allow repeated DNA synthesis and denaturation cycles of the newly synthesized DNA double strands to be carried out in a simple manner.

The standard PCR setup was as follows:

Reagent	Volume
DNA	2 µl
dNTP-Mix (2.5 mM)	2.5 µl
Primer for (2.5 pmol/µl)	2 µl
Primer rev (2.5 pmol/µl)	2 µl
10× PCR-Buffer	2.5 µl
DNA-Polymerase (5 U/µl)	0.5 µl
DMSO	1 µl
ddH ₂ O	12.5 µl
	25 µl

The standard PCR program was:

Step	Temperature (°C)	Dauer (Sec)
1. Initial denaturation	94	300
2. Denaturation	94	30
3. Annealing	depending on the primer pair	10
4. Elongation	72	30
5. Padding	72	15

Steps 2-4, as one cycle, are repeated 25-30 times, during which the annealing temperature is 3-5 °C lowered after every 5 cycles. After the PCR reaction, the PCR product was checked on a 1-2% agarose gel, as described in Section 3.2.7.

3.2.9 HLA typing

HLA haplotypes were ascertained through sequence-based typing at the Laboratory for Immunogenetics and Molecular Diagnostics, Ludwig-Maximilian-University of Munich. In specific instances, HLA-C*06:02 typing was conducted with PCR restriction fragment length polymorphism analysis in our laboratory. In brief, genomic DNA was extracted from Ficoll-separated PBMCs or cell lines described in Section 3.2.3 and then amplified by PCR in 25 µl reactions described in Section 3.2.8. Subsequently, a 10 µl aliquot of the PCR product was digested in a 20 µl reaction and incubated at RT for 4 hours.

The digestion step reaction was performed as follows:

Reagent	Concentration
PCR product	10 μ l
SmaI (10U/ μ l)	1 μ l
KCl (500 mM)	2 μ l
Tris-HCl (200 mM)	1 μ l
MgCl ₂ (50 mM)	2.8 μ l
DTT (100 mM)	0.2 μ l
ddH ₂ O	3 μ l
	20 μ l

After digestion, HLA-C*06:02 alleles were determined by electrophoresis with a 2% agarose gel according to cleaved products: in non-HLA-C*06:02 individuals, the 618 bp PCR product was cleaved to fragments of 348 and 270 bp, whereas HLA-C*06:02 carriage resulted in fragments of 348, 196 and 74 bp in the homozygous individuals and 348, 270, 196 and 74 bp in the heterozygous state.

3.3 Biochemistry Methods

3.3.1 Peptide Synthesis

The purity of all commercially available synthetic peptides was >95%, verified by high-performance liquid chromatography and mass spectrometry analysis. Peptide solubility was calculated with a tool from INNOVAGEN (<https://pepcalc.com/peptide-solubility-calculator.php>). According to their respective solubility, peptides were dissolved in the appropriate solution or buffer at a concentration of 1 mg/ml and stored at -80 °C.

Synthetic peptides were presented by APCs to the V α 3S1/V β 13S1-TCR hybridoma in co-culture assays to test the antigenicity of peptides as described in Section 3.1.8.

3.3.2 MHC Immunoprecipitation (MHC-IP)

HLA-class I molecules were isolated by standard MHC immunoprecipitation (MHC-IP). For sample preparation, an amount of 10⁸ to 10⁹ cells of EBV-immortalized B cell lines of interest was harvested by centrifugation at 1,600 rpm for 10 minutes at 4 °C. After two washing steps with cold PBS, cells were pelleted into a 2 ml microcentrifugation tube and quickly frozen with liquid nitrogen, then transferred and stored at -80 °C until IP.

Prior to IP, cell pellets were lysed in the CHAPS lysis buffer (Applichem, 10 mM in PBS), supplemented with a protease inhibitor cocktail (Roche), and by subsequent homogenization and ultrasonication. The Cell lysate underwent MHC-IP for overnight. Specifically, cell lysate was centrifuged at 4000 rpm for 45 minutes, and the resultant supernatant was filtrated and bound to serially connected columns with the pan-HLA-class I-specific monoclonal W6/32 antibody, which is covalently linked to CNBr- activated Sepharose (GE Healthcare). On the next day, columns were washed with ddH₂O for the first 30 minutes and with PBS for an additional 1 hour; thereby, pMHC complexes were eluted following 15-minute incubation with 100 μ l 0.2% trifluoroacetic acid (Merck) on a shaker, which was performed for a total of eight times. HLA-associated peptides were separated from larger MHC components in the elution, α -chain, and β 2-microglobulin (β 2m) by ultrafiltration using centrifugal filter units (3 kDa; Merck). Hydrophobic peptides were recovered by washing the filters with 500 μ l solution containing 32.5% acetonitrile (Merck) and 0.1% trifluoroacetic acid. All the above steps were carried out at 4°C or on ice, while the remaining steps were performed at RT. HLA ligands in the filtrates were concentrated to roughly 50 μ l with the use of vacuum centrifugation. Subsequently, purification and desalting of HLA ligands were achieved by employing ZipTip C18 pipette tips (Merck) and following elution with 35 μ l trifluoroacetic acid. Samples were entirely dried by vacuum centrifugation and resuspended in 25 μ l of 1% acetonitrile/0.05% trifluoroacetic acid. Samples were stored at -80 °C until LC-MS/MS analysis.

3.3.3 Liquid Chromatography-Tandem Mass Spectrometry (LC-MS/MS)

Peptide samples were subjected to separation and analysis by reversed-phase liquid chromatography (nanoUHPLC, UltiMate 3000 RSLCnano; Dionex) coupled tandem mass spectrometry (Orbitrap Fusion Lumos; Thermo Fisher Scientific), which is known as liquid chromatography-tandem mass spectrometry (LC-MS/MS). In brief, samples were analyzed in five technical replicates at 5 μ l for each. Each sample was loaded onto a 75 μ m \times 2 cm C18 trap column (Acclaim PepMap RSLC; ThermoFisher Scientific) at 4 ml/min for 5.75 minutes. Peptide separation was then carried out on a 50 μ m \times 25 cm separation column (Acclaim PepMap RSLC; Dionex) at 50 °C and a flow rate of 300 nl/min, with a linear gradient ranging from 2.4% to 32.0% acetonitrile in a duration of 90 minutes. Eluted peptides underwent nanospray ionization before being analyzed in the mass spectrometer under the TopSpeed mode, and survey MS scans were acquired in the Orbitrap with a resolution of 120,000. During the scan, precursor ions were selected in the quadrupole, fragmented via collision-induced

dissociation, and eventually recorded in the Orbitrap. For HLA class I ligands, precursors with a mass range of 400-650 m/z and charge states of 2+ to 3+ were selected for fragmentation.

3.3.4 Spectral Annotation and Database Search

Data were processed against the human proteome that is comprised in the Swiss-Prot database (<http://www.uniprot.org>, release September 27, 2020; containing 20,279 reviewed protein sequences), employing the SequestHT algorithm in the Proteome Discoverer software (version 1.3; Thermo Fisher). Precursor mass tolerance was configured at 5 ppm, while fragment mass tolerance was configured at 0.02 Da. The search was not limited to enzymatic specificity and oxidized methionine was permitted as a dynamic modification. The percolator-assisted false discovery rates (FDR) calculation was configured at a target value of $q \leq 0.05$ (5% FDR). Peptide lengths were limited to 8-12 amino acids for HLA class I ligands.

MHC-IP, LC-MS/MS and spectral annotation described above were performed by our collaborators, Prof. Andreas Schlosser and Melissa Bernhardt, from the Center for Integrative and Translational Bioimaging at Universität Würzburg, Würzburg.

3.4 Computational Methods

3.4.1 Determination of the V α 3S1/V β 13S1 TCR Ligand Motif

By screening a completely randomized plasmid-encoded combinatorial nonamer peptide library (PECPL) or libraries with predefined HLA-C*06:02 anchor residues, we had previously identified eight mimotopes stimulating the V α 3S1/V β 13S1 TCR. The library mimotopes showed a conserved amino acid pattern: they all carried arginine (Arg, R) at positions P2 and P8, leucine (Leu, L) at P9, and arginine (Arg, R) or leucine (Leu, L) at P7; Six mimotopes shared arginine (Arg, R) at P5, while P1, P3, P4, and P6 showed greater variability (Arakawa *et al.*, 2015).

Subsequent homology searches based on the convergent amino acid pattern and pre-determined library positions in accordance with known HLA-C*06:02 anchor positions (Falk *et al.*, 1993; Rasmussen *et al.*, 2014) had identified ten V α 3S1/V β 13S1-TCR epitopes in human proteins (**Figure 3.4.1.1**) (Arakawa *et al.*, 2015).

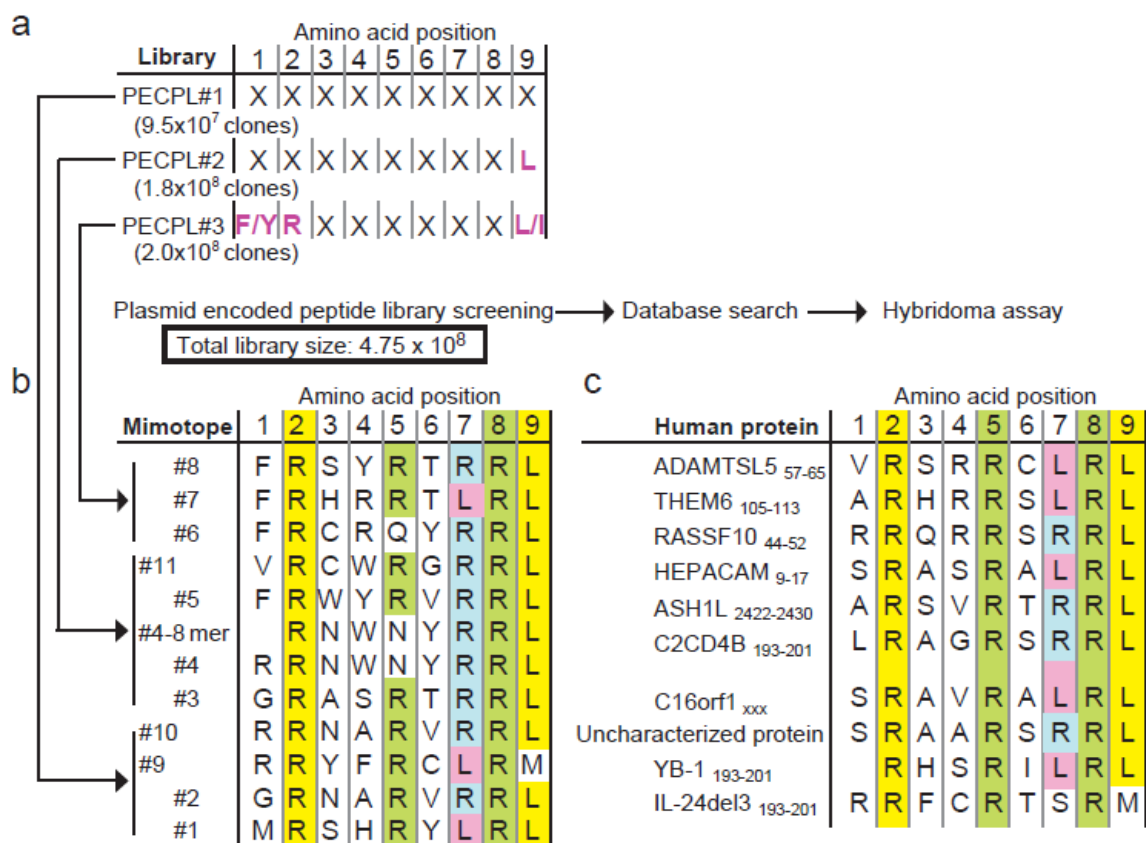


Figure 3.4.1.1 The procedure for identifying human candidate peptide antigens based on mimotope sequences. (a, b) Design of PECPLs #1-3 and Mimotopes derived from these PECPLs. (c) Human peptide ligands of the V α 3S1/V β 13S1 TCR (Arakawa *et al.*, 2015). Amino acids are designated by the one-letter code.

Screening for additional ligands had furthermore identified 25 epitopes stimulating the V α 3S1/V β 13S1-TCR in environmental antigens from plants, food, microbiome, pathogens, etc. (Ishimoto *et al.*, 2024).

The sequences of all the above stimulatory peptides were plotted into a frequency matrix/heat map of the amino acids at the respective peptide positions and correlated to the strength of the V α 3S1/V β 13S1 TCR responses. The sequence logo visualization of V α 3S1/V β 13S1 TCR-ligands was achieved by Seq2Logo 2.0, with selecting Kullback-Leibler logotype and default parameters (Thomsen and Nielsen, 2012). Anchor and auxiliary anchor positions were defined based on the sequence logo of nonamers and subsequently adopted for octamers. According to the frequency matrix/heat map and response strength, V α 3S1/V β 13S1 TCR-ligand motifs were determined.

In order to specify the critical amino acid residues for immunogenicity of antigens and define the motif recognized by the V α 3S1/V β 13S1 TCR comprehensively, we further compared the TCR response to wild-type antigenic peptides and mutated peptides using two different

strategies. The relevance of each amino acid position for the recognition motif of the V α 3S1/V β 13S1 TCR was verified by alanine scanning mutagenesis (Cunningham, B. C. and Wells, 1989). We further exchanged the HLA-C*06:02 anchor residues (P2, P7, P9) and the V α 3S1/V β 13S1-TCR recognition residues (P5, P8) to other plausible residues according to the physicochemical properties of amino acids and their side chains. **Figure 3.4.1.2** clearly depicts the HLA-C*06:02 anchor residues and the V α 3S1/V β 13S1-TCR recognition residues of the ADAMTSL5 peptide analogue in the crystal structure.

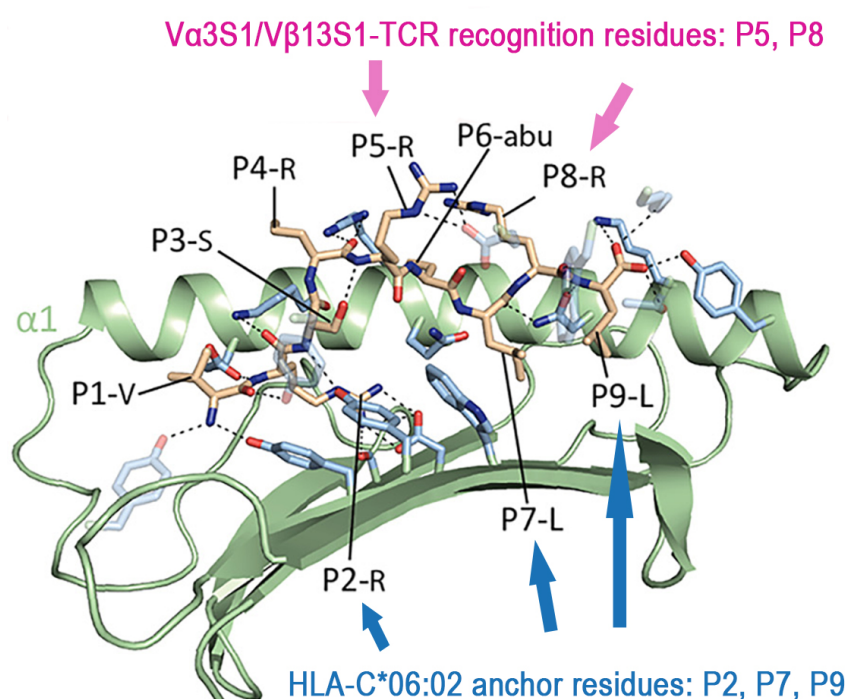


Figure 3.4.1.2 Crystal structure of HLA-C*06:02 with an analogue of ADAMTSL5 peptide (VRSRR-abu-LRL) in the peptide-binding grooves. Figure modified from Mobbs *et al.* (Mobbs *et al.*, 2017).

3.4.2 Screening HLA-C*06:02-Peptidomes for V α 3S1/V β 13S1-TCR Ligands

Initially, two HLA-C*06:02-immunopeptidomes from C1R and 721.221 cell lines were available for analysis (Di Marco *et al.*, 2017; Mobbs *et al.*, 2017). The course of experiments required the analysis of additional HLA-C*06:02 immunopeptidomes. For this purpose, six HLA-C*06:02 homozygous EBV-transformed B cell lines were identified from the HLA typing data from the 1000 Genomes Project (Abi-Rached *et al.*, 2018; Auton *et al.*, 2015) and obtained from the NIGMS Human Genetic Cell Repository and NHGRI Sample Repository for Human Genetic Research at the Coriell Institute for Medical Research (Camden, NJ, USA) (**Table 3.4.3**).

For the elution of endogenous HLA-C*06:02-peptides, the HLA-C*06:02-homozygous B cell lines were expanded, pelleted, and cryopreserved in liquid nitrogen in the laboratory. Four of the six cell lines were selected for the elution of HLA-C*06:02-associated peptides using LC-MS/MS since they had higher growth rates and carried specific gene variants of the ERAP1 that affect the risk of psoriasis. In psoriasis, the ERAP1 haplotype Hap2 is a risk haplotype in epistasis with the *HLA-C*06:02* allele through high autoantigen supply, while the haplotype Hap10 is protective in the disease by generating much lower amounts of the autoantigenic ADAMTSL5 peptide (Arakawa *et al.*, 2021).

The HLA-C*06:02 peptidomes from 721.221 and C1R cells and those eluted from the above four B cell lines were used to search for antigenic candidate self-peptides based on the previously defined V α 3S1/V β 13S1 TCR-ligand motifs. Peptides corresponding to the V α 3S1/V β 13S1 TCR-recognition motifs (see **Table 4.4.5**) were selected as candidate peptide antigens for subsequent stimulation of the V α 3S1/V β 13S1-TCR hybridoma. The coding cDNA of candidate peptide antigens were cloned into plasmids (Section 3.2.2) and co-expressed with HLA-C*06:02 in APCs to activate the V α 3S1/V β 13S1-TCR hybridoma in co-culture experiments (Section 3.2.6 and 3.1.8). The frequency matrix of V α 3S1/V β 13S1 TCR-ligands underwent dynamical adjustment according to newly identified candidate antigen peptides.

Cell line ID	HLA-A		HLA-B		HLA-C		HLA-DQB1		HLA-DRB1		ERAP1 haplotype
GM11930	02:01	24:02	13:02	13:02	06:02	06:02	02:02	06:02	07:01	15:01	Hap2A Hap2A
HG00142	02:01	29:02	57:01	45:01	06:02	06:02	03:01	03:03	04:01	07:01	Hap10 Hap10
GM20771	01:01	30:01	13:02	57:01	06:02	06:02	03:01	06:02	12:01	15:01	Hap10 Hap2A
GM12286	02:01	24:02	13:02	57:01	06:02	06:02	02:02	03:03	07:01	07:01	Hap3A Hap10
GM12046	01:01	02:05	57:01	50:01	06:02	06:02	02:01	02:02	03:01	07:01	Hap1A Hap8
HG00131	01:01	03:01	57:01	37:01	06:02	06:02	03:01	03:03	11:01	07:01	Hap1A Hap2A

Table 3.4.2 HLA-genotypes and ERAP1-Haplotypes of six HLA-C*06:02-homozygous B cell lines.

3.4.3 Screening for V α 3S1/V β 13S1-TCR Ligands in the Human Proteome

3.4.3.1 Motif-based Screening

We applied the Expasy ScanProsite tool (<https://prosite.expasy.org/scanprosite/>) to scan the conserved V α 3S1/V β 13S1-TCR recognition motifs against the *Homo sapiens* [9606] UniProt database (in total 20,431 proteins were registered in UniProt database, released September 2019) by submitting a group of motifs that were defined according to the peptide recognition motif of the V α 3S1/V β 13S1 TCR, as listed in **Table 4.4.5**.

3.4.3.2 MHC Binding Prediction of Selected Candidate Peptides

The binding affinity of peptides for HLA-C*06:02 was predicted using the NetMHCcons 1.1 server, a consensus method that integrates three cutting-edge approaches, namely NetMHC, NetMHCpan, and PickPocket, in order to provide the most reliable predictions. The prediction results are provided as “nM IC50” values and as “% Rank” in regard to a collection of 200,000 random natural peptides. The thresholds of “% Rank” for strong binders and weak binders were defined at 0.5 and 2, respectively, and the thresholds of “nM IC50” for strong binders and weak binders were defined at 50 nM and 500 nM, of which IC50 < 500 nM is suggested by a systematic assessment as a useful threshold to identify approximately 90% of MHC class I restricted T-cell epitopes (Sette *et al.*, 1994).

Candidate peptides defined as strong binders or weak binders to HLA-C*06:02 were selected for further examination, and the strong binders were preferentially tested.

3.4.3.3 Narrowing Down the Search by Combinatorial Strategies

Motif-based screening and HLA-C*06:02-binding predictions together determined a large number of candidate peptides to be tested as ligands of the V α 3S1/V β 13S1 TCR. Therefore, I further narrowed down the candidate peptides using a combinatorial strategy.

Firstly, the transcriptome of an EBV-immortalized B cell line e9453 was used for bioinformatic searches to narrow down candidate peptides from the human proteome to those that are only contained in the proteins expressed by B cells. Candidate peptides from protein genes with higher copy numbers of cDNA in the B-cell transcriptome were preferentially tested. The transcriptome analysis of e9453 was accomplished by Dr. Akiko Arakawa *et al.* in previous work, referring to the method described by Arakawa *et al.* (2015).

Next, I further selected candidate peptides according to: i) the protein expression level in tonsils or B cells in The Human Protein Atlas database; ii) the differential expression in lesional and non-lesional psoriatic skin in the GEO Dataset Browser-NCBI (e.g., No. GDS4602); iii) the differentiated gene expression during the activation of human tonsillar naïve B cells (Youming, 2018). Those peptides whose parental proteins are encoded by genes with extremely low or no expression in tonsils or B cells were excluded from the list of candidate peptides. Finally, a feasible number of candidate peptides remained for further functional experiments.

3.4.4 Analysis of the HLA-C*06:02 Peptidomes from B cell lines

The length distribution of different HLA-C*06:02 peptidomes was calculated, mainly including ligands with a length of 8-11 amino acids. Ligand overlap was determined using a web-based tool, InteractiVenn, which provides Venn diagrams to show the overlapping peptides among different HLA-C*06:02 peptidomes (Heberle *et al.*, 2015).

The peptide binding specificity of HLA-C*06:02 was visualized using the sequence logo generation tool Seq2Logo 2.0, with the selection of Kullback-Leibler logotype and default settings (Thomsen and Nielsen, 2012). Seq2Logo is a web tool to generate sequence logos for constructing and visualizing amino acid binding motifs and sequence profiles, incorporating various dimensions such as sequence weighting, pseudo counts, and a two-sided representation of amino acid enrichment and depletion.

Given that nonamers (9-mers) are the most prominent length variants in all HLA-C*06:02 peptidomes (Di Marco *et al.*, 2017; Mobbs *et al.*, 2017; Sarkizova *et al.*, 2020) and the ADAMTSL5 octamers (8-mers) and 9-mers showed the strongest immunogenicity to stimulate the V α 3S1/V β 13S1 TCR (Arakawa *et al.*, 2021), visualization of HLA-C*06:02 binding motifs based on 9-mers or 8-mers was carried out for each of the peptidomes.

The psoriasis risk in HLA-C*06:02 carriers is controlled by different ERAP1 haplotypes, each generating a different amount of autoantigen. Hap2 is the main risk haplotype of ERAP1 for psoriasis in HLA-C*06:02 carriers, while Hap10 is protective (Arakawa *et al.*, 2021; Ombrello *et al.*, 2015). Based on deep whole-genome sequencing of plenty of individuals in the 1000 Genomes Project, data of SNPs were available for the determination of the ERAP1 haplotypes of the B-cell lines obtained for the analysis of HLA-C*06:02 immunopeptidomes (**Table 3.4.2**). Donors of HLA-C*06:02-homozygous B cell lines GM11930 and HG00142 turned out to be homozygous Hap2 and Hap10 haplotype carriers, respectively. A comprehensive analysis of their HLA-C*06:02 peptidomes was conducted to understand the role of ERAP1 in B-cell-dependent autoimmune response.

3.5 Statistical Analyses

Statistical analyses were carried out using GraphPad Prism Software (version 9.4.1), and data storage was done with Microsoft Excel. Unless otherwise specified, this study presents medians, standard error of the mean (SEM), and *p* values from an unpaired two-tailed t-test. In cases where the data did not follow a normal distribution, the nonparametric Mann-Whitney U test was employed to compare two independent groups, while the Wilcoxon matched-pairs signed

rank test was utilized for paired sample comparisons. A significance level of $p < 0.05$ (two-tailed) was deemed statistically significant. The sample size was determined by preliminary data, previous publications, and observed effect sizes. In general, no data were intentionally excluded from the analyses. However, certain stimulation experiments were excluded due to the failure of positive control samples or GFP transfection.

4. Results

4.1 Subcloning of the V α 3S1/V β 13S1-TCR Hybridoma

The responsiveness of the V α 3S1/V β 13S1-TCR hybridoma to stimulation degenerates over time. This requires occasional recloning of the hybridoma to obtain subclones with high sensitivity for activation by TCR ligation. Therefore, I recloned the available V α 3S1/V β 13S1-TCR hybridoma clone Hyb 6.5 H2II clone at the beginning of my work to obtain well-activatable hybridoma cells for my intended experiments. The subclones were stimulated with CD3 antibody coated on flat bottom culture plates, and the induction of sGFP was measured by flow cytometry after 24 hours. Fourteen of all the harvested subclones showed stimulation-induced expression of sGFP in more than 30% of the hybridoma cells. The two V α 3S1/V β 13S1-TCR hybridoma clones with the highest sGFP induction (>65%) upon CD3 activation among all subclones, Hyb 6.5 11II and 16II (**Figure 4.1**), were expanded and used for further experiments.

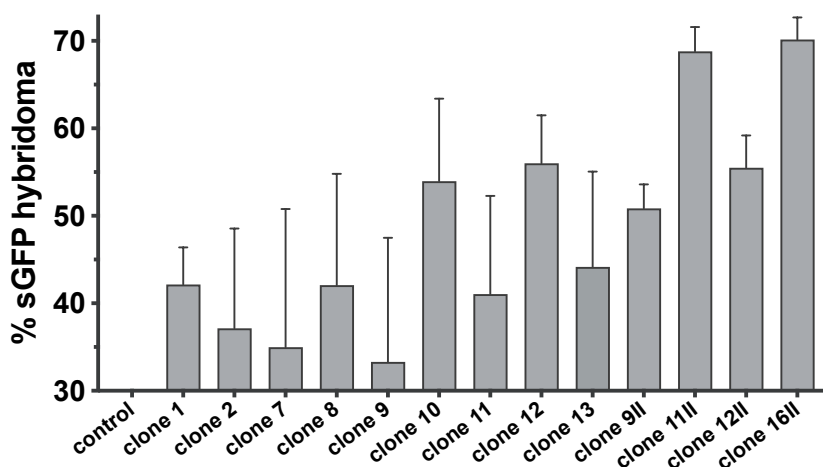


Figure 4.1 The induction of sGFP expression by anti-mouse CD3 antibody in different V α 3S1/V β 13S1-TCR hybridoma subclones. As a negative control, the V α 3S1/V β 13S1-TCR hybridoma cells were incubated in culture plates untreated with CD3 antibody. Clone 11II and clone 16II had the highest level of sGFP induction (>65%) among all subclones. Data were summarized from technical triplicates from two independent experiments.

4.2 Stimulation of the V α 3S1/V β 13S1-TCR Hybridoma by B cells

4.2.1 Hybridoma Stimulation by Tonsillar B cells

Psoriasis is triggered under genetic predisposition by environmental factors and infections in the life course. The most common trigger is tonsillitis caused by group A *S. pyogenes* and other streptococcal strains. The link between streptococcal angina and psoriasis is underlined by the fact that the presumably pathogenic lesional psoriatic T-cell clones are present in the fraction of those tonsillar T cells that are capable of entering the skin because they express the skin-homing receptor CLA (Diluvio *et al.*, 2006). This suggests that pathogenic psoriatic T cells are initially activated in the tonsils and then recruited into the skin, where they react against melanocytes and cause psoriatic skin lesions.

The first task of my doctoral thesis was to search for evidence of a possible trigger of the psoriatic T-cell response in the tonsils using the V α 3S1/V β 13S1 TCR. For this purpose, I had cryopreserved tonsil cells from three HLA-C*06:02-positive psoriasis patients available who had undergone tonsillectomy for streptococcal-induced psoriasis (Diluvio *et al.*, 2006). In all three patients, psoriasis had gone into remission after tonsillectomy. The V α 3S1/V β 13S1-TCR hybridoma cells were co-cultured with these tonsil cells for 24 hours and then analyzed for the induction of sGFP by fluorescence microscopy or flow cytometry analysis. Alexa Fluor 647 anti-HLA-DR antibody was applied to stain APCs such as B cells, monocytes, and dendritic cells since APCs but not T cells express HLA-class II molecules. A marked activation of the V α 3S1/V β 13S1-TCR hybridoma induced by tonsil cells from patients was observed both by flow cytometry analysis and fluorescence microscopy (**Figure 4.2.1.1**).

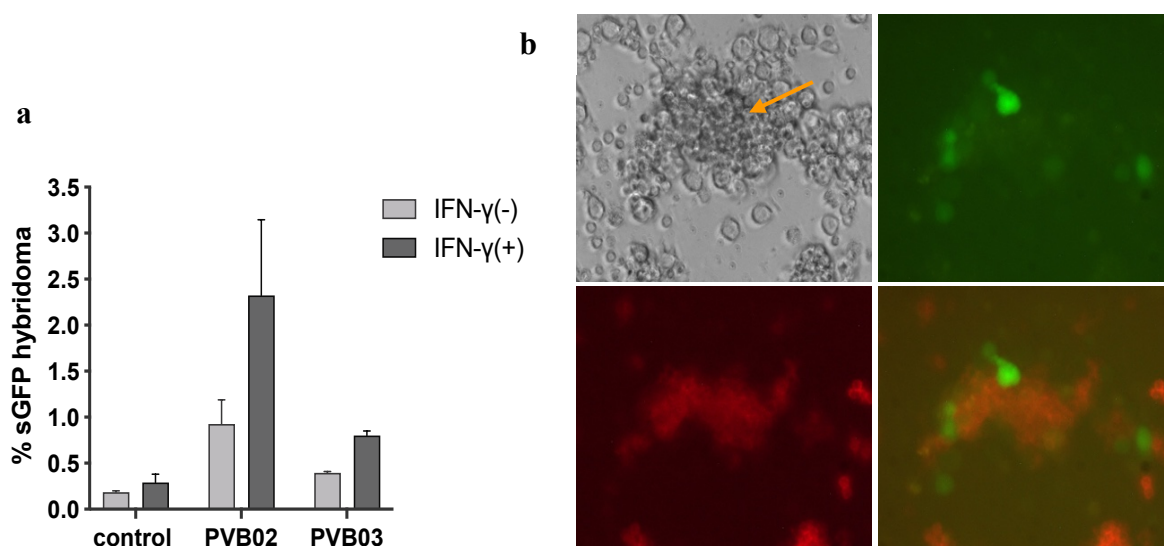


Figure 4.2.1.1 Tonsil cells from HLA-C*06:02-positive patients induced a marked activation of the V α 3S1/V β 13S1-TCR hybridoma. (a) TCR activation by tonsillar cells from different HLA-C*06:02-positive patients with or without preincubation with IFN- γ . The V α 3S1/V β 13S1-TCR hybridoma cells incubated in culture plates solely without tonsillar cells served as negative control. Data were summarized from technical triplicates from two or three independent experiments. (b) Activation of the V α 3S1/V β 13S1-TCR hybridoma in co-culture with tonsillar cells from PVB04 analyzed by

fluorescence microscopy. Most activated hybridoma cells (green fluorescence) were found in the cell clusters and had direct contact with HLA-DR-stained APCs (red fluorescence).

B cells and T cells are the main cell types in tonsillar tissue. To identify which cells in the complex tonsillar cell population stimulated the V α 3S1/V β 13S1 TCR, I enriched B cells and T cells from tonsillar cells by cell sorting assays using antibody-coated magnetic beads (MACS) or by FACS and achieved a cell purity of >95%. The remaining cell types were designated as “non-B/T cells”. The V α 3S1/V β 13S1-TCR hybridoma was co-cultured with these tonsillar cell fractions, and the expression of sGFP was analyzed by flow cytometry. Similar to the role of IFN- γ for the immunogenicity of melanocytes for the V α 3S1/V β 13S1 TCR, preincubation with IFN- γ of the fractionated tonsil cells for 24 hours was performed to increase the otherwise low HLA-C expression and HLA-C*06:02-restricted antigen presentation. Co-culture with B cells, but not T cells or non-B/T cells, induced a marked induction of sGFP in the TCR hybridoma that was further enhanced by IFN- γ . Thus, tonsillar B cells activated the V α 3S1/V β 13S1 TCR (**Figure 4.2.1.2**). A slight hybridoma activation without statistical difference by the other cell fractions is likely due to contaminating B cells.

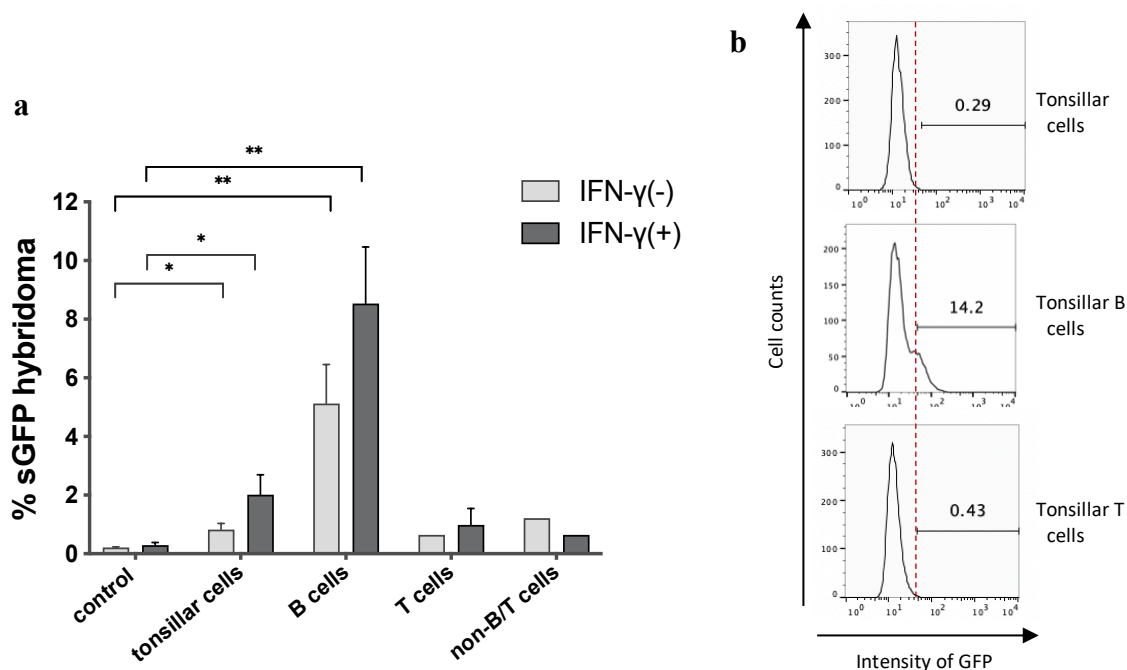


Figure 4.2.1.2 B cells from HLA-C*06:02-positive patients are target cells of the V α 3S1/V β 13S1 TCR in the tonsils. (a) TCR hybridoma activation by different tonsil cell subsets from HLA-C*06:02-positive patients with or without preincubation with IFN- γ (n=2). The V α 3S1/V β 13S1-TCR hybridoma cells incubated in culture plates solely without other cells served as a negative control. Data were summarized from technical triplicates from two independent experiments, compared by nonpaired t-test, and shown as mean \pm SEM, with statistical significance indicated as * p < 0.05, ** p < 0.01. (b) Representative flow cytometry histograms of sGFP induction by different tonsillar cell subsets from an HLA-C*06:02-positive patient.

4.2.2 Activation of the V α 3S1/V β 13S1 TCR by B cells is HLA-C*06:02-Restricted

To verify whether the activation is mediated by HLA-C*06:02-positive B cells, the V α 3S1/V β 13S1-TCR hybridoma was co-cultured with different HLA-typed EBV-transformed B cell lines (**Table 4.2.2**), of which the B cell line PSO7 originated from the patient from whom the V α 3S1/V β 13S1 TCR had been isolated (Section 2.11). Induction of sGFP in the V α 3S1/V β 13S1-TCR hybridoma cells was analyzed after 24 hours of co-culture by flow cytometry analysis. Only HLA-C*06:02-positive but not HLA-C*06:02-negative B cell lines stimulated the V α 3S1/V β 13S1 TCR. Preincubation of the B cell lines with the pan HLA-class I antibody, W6/32, completely inhibited the hybridoma activation (**Figure 4.2.2**). Further, an HLA-C*06:02-negative B cell line (P16488) became stimulatory following nucleofection with an HLA-C*06:02 plasmid. These results revealed that EBV-transformed B cell lines can act as surrogates for primary B cells in my experiments and that the activation of the V α 3S1/V β 13S1 TCR by B cells is restricted by HLA-C*06:02.

Cell lines	HLA-A		HLA-B		HLA-C		Hybridoma activation
Fey	0101	0101	0801	0801	0701	0701	–
P16488	2601	0201	3801	0801	1203	0701	–
P17490	0301	0201	3501	4001	03	04	–
PSO7	0235	3001	4427	1302	0602	0704	+
D22	02	02	57	57	0602	0602	++
e9453	0301	0201	35	37	0602	0401	++
GM20771	0101	3001	1302	5701	0602	0602	+++
GM11930	0201	2402	1302	1302	0602	0602	+
HG00131	0101	0301	5701	3701	0602	0602	++
HG00142	0201	2902	5701	4501	0602	0602	+
GM12286	0201	2402	1302	5701	0602	0602	++
GM12046	0101	0205	5701	5001	0602	0602	+
HLA-C*06:02-P16488	2601	0201	3801	0801	1203 0602	0701	+

Table 4.2.2 HLA-class I haplotypes of various EBV-transformed B cell lines and the corresponding hybridoma activation induced by co-culture with these cell lines. No activation (–) of V α 3S1/V β 13S1-TCR hybridoma was observed in co-culture with EBV-transformed B cell lines from HLA-C*06:02-negative healthy donors (Fey, P16488, P17490), while varying degrees (+ to +++) of hybridoma activation were observed in co-culture with EBV-transformed B cell lines from HLA-C*06:02-positive psoriasis patients or healthy donors, as determined by flow cytometry analysis.

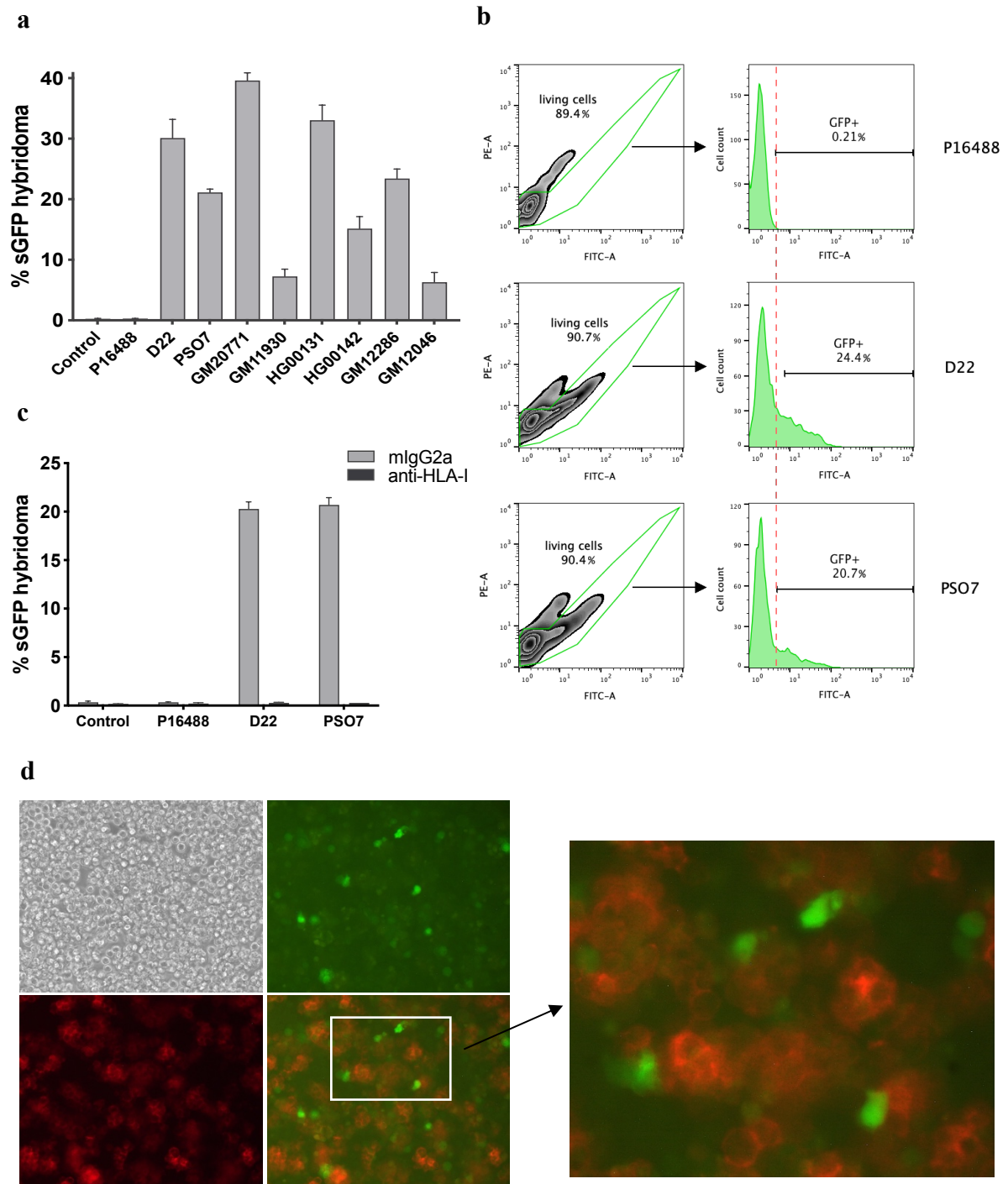


Figure 4.2.2 Activation of the $V\alpha 3S1/V\beta 13S1$ -TCR hybridoma in co-culture with HLA-C*06:02-positive EBV-transformed B cell lines. (a) EBV-transformed B cell lines from HLA-C*06:02-positive donors activated the $V\alpha 3S1/V\beta 13S1$ -TCR hybridoma to varying degrees, except for the HLA-C*06:02-negative cell line P16488. (b) Representative flow cytometry histograms of sGFP induction by HLA-C*06:02-negative cell line (P16488) and HLA-C*06:02-positive cell lines (D22 and PSO7). (c) Hybridoma activation by D22 and PSO7 was completely inhibited by anti-human HLA-class I antibody (W6/32). Mouse IgG2a was applied as isotype control in the blocking experiments. (d) Activation of the $V\alpha 3S1/V\beta 13S1$ -TCR hybridoma in co-culture with the autologous EBV-transformed B cell line PSO7, measured by fluorescence microscopy. The numerous green fluorescent cells are activated $V\alpha 3S1/V\beta 13S1$ -TCR hybridoma cells, while the red fluorescent cells are B cells stained with Alexa Fluor 647 anti-HLA-DR antibody. Magnification: EBV-transformed B cells form cell clusters,

activating the V α 3S1/V β 13S1-TCR hybridoma. The V α 3S1/V β 13S1-TCR hybridoma cells incubated in culture plates solely without other cells served as negative controls. Data were summarized from technical triplicates from two or three independent experiments.

4.2.3 Hybridoma Activation by Blood B cells

The co-culture experiments of the V α 3S1/V β 13S1-TCR hybridoma with tonsillar B cells and EBV-transformed B cell lines indicated that B lymphocytes may activate the psoriatic autoimmune response. In the next step, I investigated whether the antigenicity for the V α 3S1/V β 13S1 TCR is a general property of B cells. For this purpose, I fractionated freshly isolated PBMCs from HLA-C*06:02-positive psoriasis patients (n=4) and HLA-C*06:02-positive or HLA-C*06:02-negative healthy individuals (each n=3) into CD4⁺ or CD8⁺ T cells, B cells, monocytes, and plasmacytoid dendritic cells by fluorescence-activated cell sorting. The V α 3S1/V β 13S1-TCR hybridoma was co-cultured with total PBMC or each of these fractions for 24 hours with or without the addition of IFN- γ . Flow cytometry analysis of sGFP induction revealed that in these co-culture experiments, B cells but not other blood cell types from HLA-C*06:02⁺ psoriasis patients significantly stimulated the V α 3S1/V β 13S1 TCR (**Figure 4.2.3**). As with tonsillar B cells or HLA-C*06:02⁺ melanocytes, IFN- γ markedly increased the stimulatory capacity of the blood B cells from HLA-C*06:02⁺ psoriasis patients for the V α 3S1/V β 13S1 TCR. B cells from HLA-C*06:02⁺ healthy individuals induced only minor V α 3S1/V β 13S1 TCR stimulation, which was slightly enhanced by IFN- γ . It did not differ significantly from a discrete hybridoma activation by HLA-C*06:02-negative B cells, which may be involve allo-reactivity, as many CD8⁺ T cells are allo-HLA cross-reactive (D'Orsogna *et al.*, 2010). B cells from HLA-C*06:02⁺ psoriasis patients thus were particularly immunogenic for the V α 3S1/V β 13S1 TCR. The HLA-C*06:02 status, age, and gender of patients are given in Section 6.3.

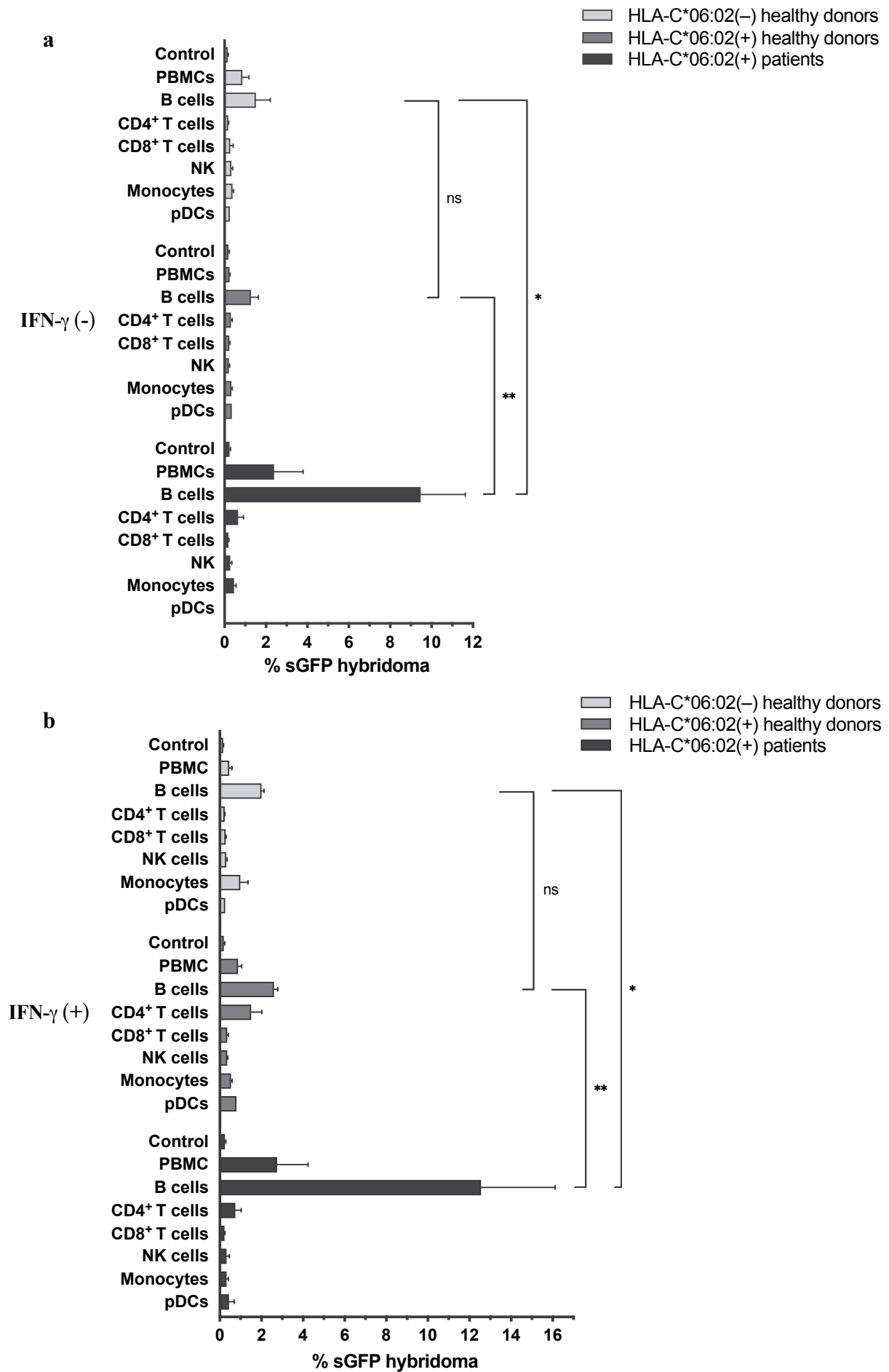


Figure 4.2.3 Primary B cells from the peripheral blood of HLA-C*06:02-positive psoriasis patients activate the V α 3S1/V β 13S1-TCR hybridoma. (a) V α 3S1/V β 13S1 TCR activation by different PBMC subsets from HLA-C*06:02⁺ psoriasis patients and HLA-C*06:02⁺ or HLA-C*06:02-negative healthy individuals without preincubation with IFN- γ , as determined by the induction of sGFP in hybridoma cells by flow cytometry. Among the different cell subsets, B cells from HLA-C*06:02⁺ psoriasis patients significantly activated the V α 3S1/V β 13S1-TCR hybridoma. (b) V α 3S1/V β 13S1 TCR activation by the different PBMC subsets following preincubation with IFN- γ . It enhanced the activation of the V α 3S1/V β 13S1 TCR hybridoma by B cells from HLA-C*06:02⁺ psoriasis patients significantly. Staining with PerCP /Cyanine5.5-labelled CD45 antibody differentiated PBMCs and their subsets from hybridoma cells. The V α 3S1/V β 13S1-TCR hybridoma cells incubated in culture plates solely without other cells served as negative controls. Data were summarized from technical triplicates, compared by nonpaired t-test, and shown as mean \pm SEM, with statistical significance indicated as * p < 0.05, ** p < 0.01 and ns denoting no statistical difference (HLA-C*06:02-negative healthy donors, n=3; HLA-C*06:02-positive healthy donors, n=3; HLA-C*06:02-positive patients, n=4).

4.2.4 Co-culture of the V α 3S1/V β 13S1-TCR Hybridoma with Various Cell Types

Psoriasis is a complex T cell-mediated disease that primarily affects the skin but also shows inflammatory changes in various other organs. To determine whether the reactivity of the V α 3S1/V β 13S1 TCR is selectively directed against B cells and melanocytes or whether additional cell types could be target cells for the V α 3S1/V β 13S1 TCR, I analyzed the reactivity of the V α 3S1/V β 13S1 TCR against human cell lines of various origins. Following transfection with HLA-C*06:02, cells were co-cultured with the V α 3S1/V β 13S1-TCR hybridoma and the induction of sGFP was determined by fluorescence microscopy and flow cytometry. None of the various human cell types tested activated the V α 3S1/V β 13S1 TCR, except B cells and melanocytes (Table 4.2.4).

Cells of various origins	Cell types	HLA-C*06:02 association	Hybridoma activation
Melanocytes*	Primary melanocytes	HLA-C*06:02-heterozygous	++
WM278*	Melanoma cell line	HLA-C*06:02-heterozygous	+
WM9*	Melanoma cell line	HLA-C*06:02-heterozygous	+
Keratinocytes*	Primary human keratinocytes	HLA-C*06:02-transfected	–
HaCaT*	Spontaneously immortalized human keratinocyte cell line	HLA-C*06:02-transfected	–
A431*	Human epidermoid carcinoma cell line	HLA-C*06:02-transfected	–
Fibroblasts*	Primary human skin fibroblasts	HLA-C*06:02-heterozygous	–
NCI-H1975	Human non-small cell lung cancer cell	HLA-C*06:02-transfected	–
MCF7	Human breast carcinoma cell line	HLA-C*06:02-transfected	–
KHOS	Osteosarcoma cell line	HLA-C*06:02-transfected	–
U937	Pro-monocytic, human myeloid leukemia cell line	HLA-C*06:02-transfected	–
PSO7	Autologous EBV-transformed primary human B cell line from patient that provide the V α 3S1/V β 13S1 TCR	HLA-C*06:02-heterozygous	++

Table 4.2.4 Stimulation of the V α 3S1/V β 13S1-TCR hybridoma by human cell lines of various origins. Data were assessed by multiparametric flow cytometry analysis.

*These cell lines were also previously tested by Dr. Arakawa *et al.* (2015)

Taken together, these experiments demonstrate that the HLA-C*06:02-restricted immunogenicity for the V α 3S1/V β 13S1 TCR is a specific property of melanocytes and B lymphocytes. While in former experiments HLA-C*06:02⁺ melanocytes had stimulated the V α 3S1/V β 13S1 TCR regardless of their origin from psoriasis patients or healthy HLA-C*06:02 carriers, B cells were particularly immunogenic for the V α 3S1/V β 13S1 TCR when derived from HLA-C*06:02⁺ psoriasis patients. The findings also suggest that streptococcal infection may trigger psoriasis primarily through initiating and maintaining an autoimmune response of CD8⁺ T cells against B cells in the tonsils, which then becomes cross-activated against melanocytes in the skin.

4.3 Peripheral Blood B Cells Promote Autostimulation of CD8⁺ T cells in Psoriasis Patients

Given the immunogenicity of B cells for the pathogenic psoriatic V α 3S1/V β 13S1 TCR, I next investigated whether B lymphocytes may stimulate CD8⁺ T cells of psoriasis patients. For this purpose, I cultured PBMCs from psoriasis patients and healthy controls without additional stimulation and measured the spontaneous proliferation by [³H]-thymidine incorporation, carboxyfluorescein diacetate N-succinimidyl ester (CFSE)-labeling assay and BrdU cell proliferation assay.

4.3.1 Increased Spontaneous Proliferation of PBMCs in Psoriasis Patients Compared to Healthy Donors

1.5×10⁵ PBMCs from each of seven psoriasis patients and seven healthy controls were seeded in culture. After 4 days, they were pulsed with [³H]-thymidine for 24 hours. The radioactivity incorporated into DNA by *de novo* DNA generation reflects the degree of cell proliferation. Measurement of [³H]-thymidine incorporation revealed a significantly increased spontaneous *in vitro* proliferation of PBMCs from psoriasis patients compared to healthy individuals. This indicates that psoriasis is associated with increased autostimulatory activation of blood cells (**Figure 4.3.1**).

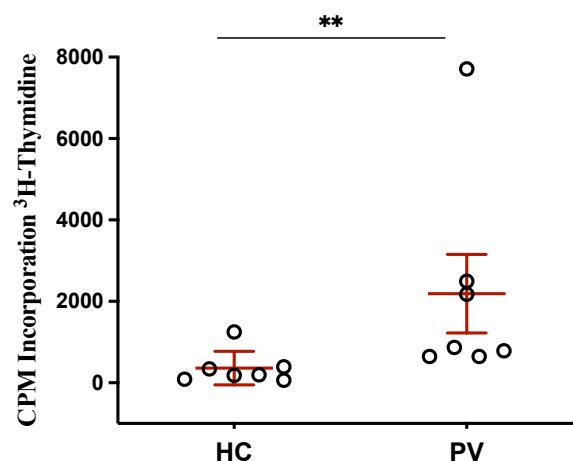


Figure 4.3.1 Spontaneous cell proliferation of PBMCs in HCs and PVs. Spontaneous cell proliferation of PBMCs was measured in triplicates by [^3H]-thymidine incorporation after 4 days of culture in healthy controls (HC, $n=7$) and patients with psoriasis (PV, $n=7$). Dots represent the mean values for each subject, and bars mark the mean \pm SEM of the group. Data were compared by the Mann-Whitney U-test, with statistical significance indicated as $**p < 0.01$.

4.3.2 Spontaneous Cell Proliferation of PBMCs in Psoriasis Patients is Induced by B cells

Because B cells selectively activate the $\text{V}\alpha 3\text{S}1/\text{V}\beta 13\text{S}1$ -TCR hybridoma in co-culture experiments, I examined if B cells may induce the increased autoproductive activation of PBMCs in psoriasis patients. For this, I depleted B cells from PBMCs. Subsequently, I compared [^3H]-thymidine incorporation of total PBMCs with that of B-cell depleted and B-cell reconstituted PBMCs in psoriasis patients and healthy controls. In order to obtain conclusive results, the proportion of reconstituted B cells in PBMCs was adjusted to 40%.

Figure 4.3.2 shows the spontaneous proliferation of PBMCs under these conditions, namely total PBMCs, B-cell depleted PBMCs, and B-cell reconstituted PBMCs. In healthy subjects, B-cell depletion and reconstitution had no consistent effect on [^3H]-thymidine incorporation. In contrast, in psoriasis patients, the depletion of B cells resulted in a significant decrease, and the reconstitution of B cells resulted in a significant increase in the autoproductive activation of PBMCs. Thus, B cells induce the autoproductive activation of PBMCs in psoriasis patients.

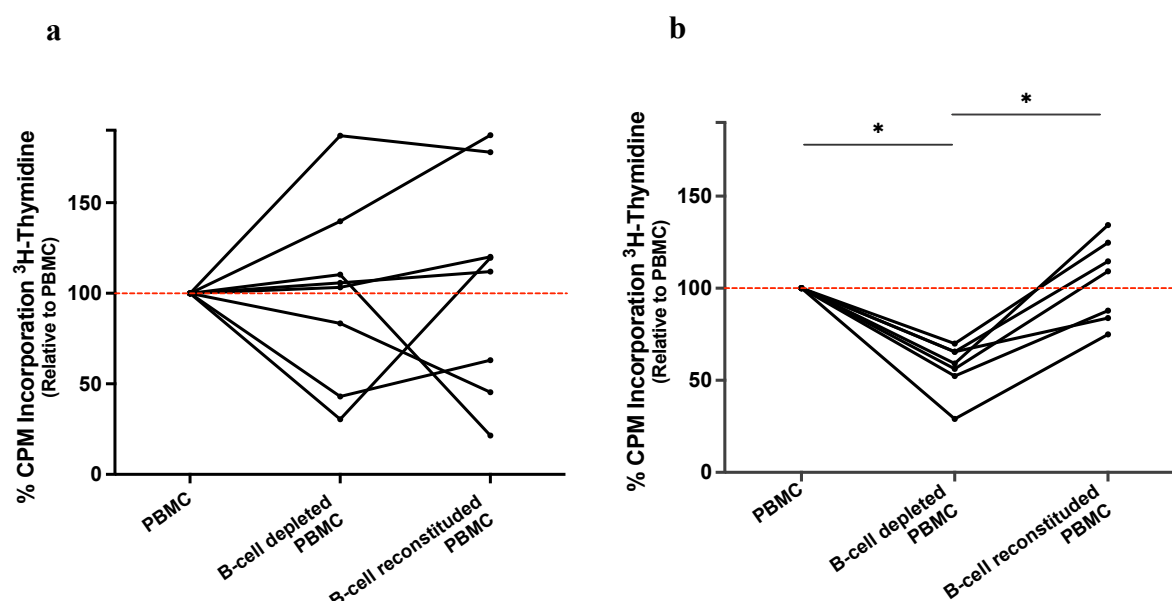


Figure 4.3.2 Spontaneous cell proliferation of PBMCs of B-cell depleted PBMCs and B-cell reconstituted PBMCs in healthy donors and psoriasis patients (relative to PBMCs). Spontaneous cell proliferation was measured in triplicates by [^3H]-thymidine incorporation on day 4 of PBMC culture in healthy controls (HC, $n = 7$) and patients with psoriasis (PV, $n = 7$). Lines represent the alterations in CPM for each subject, and dots mark mean values. Data were compared using the Wilcoxon matched-pairs signed rank test, with statistical significance indicated as $*p < 0.05$. (a) B-cell depletion and reconstitution did not consistently change the proliferation of PBMCs in healthy donors. (b) The proliferation of B-cell-depleted PBMCs decreased significantly compared to the spontaneous proliferation of PBMCs and increased again after the PBMCs were reconstituted with B cells.

4.3.3 B-cell Induced Autoproliferation of PBMCs is Significant in CD8^+ T cells

To determine which T-cell population was stimulated by B cells, I incubated the PBMCs with CFSE for five days. After harvesting, PBMCs were stained with fluorescently labeled antibodies for CD3, CD19, CD4, and CD8, and the cell division rate was measured by flow cytometry through the decrease in CFSE-dependent fluorescence intensity in these subpopulations (CD3^+ T cells, B cells, CD4^+ T cells, and CD8^+ T cells), which results from the dilution of the dye in the dividing cells.

No significant difference was observed in the frequency of proliferating CD3^+ T cells, CD4^+ T cells, or B cells between healthy controls and patients with psoriasis. However, PBMCs from psoriasis patients showed a significant increase in the frequency of proliferating CD8^+ T cells compared to healthy controls (**Figure 4.3.3**).

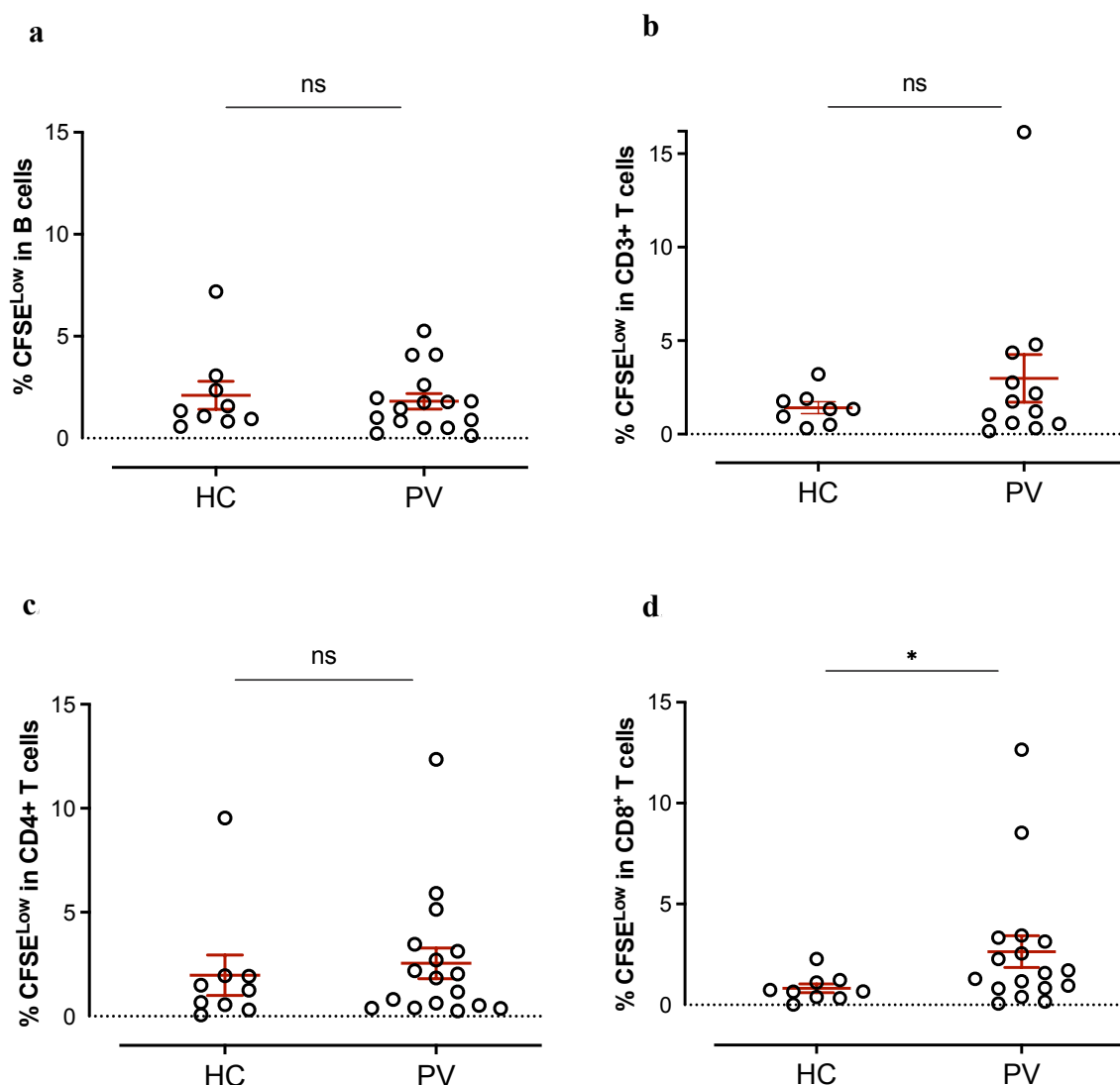


Figure 4.3.3 Degree of autoproliferation of various cell types from PBMCs (HCs vs. PVs), which is determined by the frequency of CFSE^{low} (low CFSE signal population) in each cell type. (a, b) No significant difference in proliferating B cells and T cells (CD3⁺ T cells) between HCs and PVs was observed ($p > 0.05$). (c, d) However, CFSE-staining revealed a significant increase of proliferating CD8⁺ T cells ($p = 0.03$) but not CD4⁺ T cells ($p > 0.05$) in PVs compared to HCs. Data were assessed by multiparametric flow cytometry analysis and compared by a two-tailed Mann-Whitney U test, with statistical significance indicated as * $p < 0.05$ and ns denoting no statistical difference. Each dot represents mean values from one subject.

4.3.4 Blocking HLA-ABC Reduces Autoproliferation of PBMCs

To investigate whether the T-cell proliferation is HLA-class I restricted, I analyzed the proliferation rate by cultivating the PBMCs in the presence or absence of the pan-HLA-class I antibody, W6/32. In this experiment, I measured cell proliferation by incorporating BrdU as a non-radioactive method. Bromodeoxyuridine is a thymidine analog that is incorporated into the DNA of dividing cells during cell proliferation and determined by intracellular antibody staining. The HLA-class I-antibody significantly decreased the number of proliferating cells in

PBMCs of psoriasis patients but not in PBMCs of healthy donors. This indicates that the autoproliferation of blood T cells induced by autologous B cells is HLA-class I-restricted (**Figure 4.3.4**).

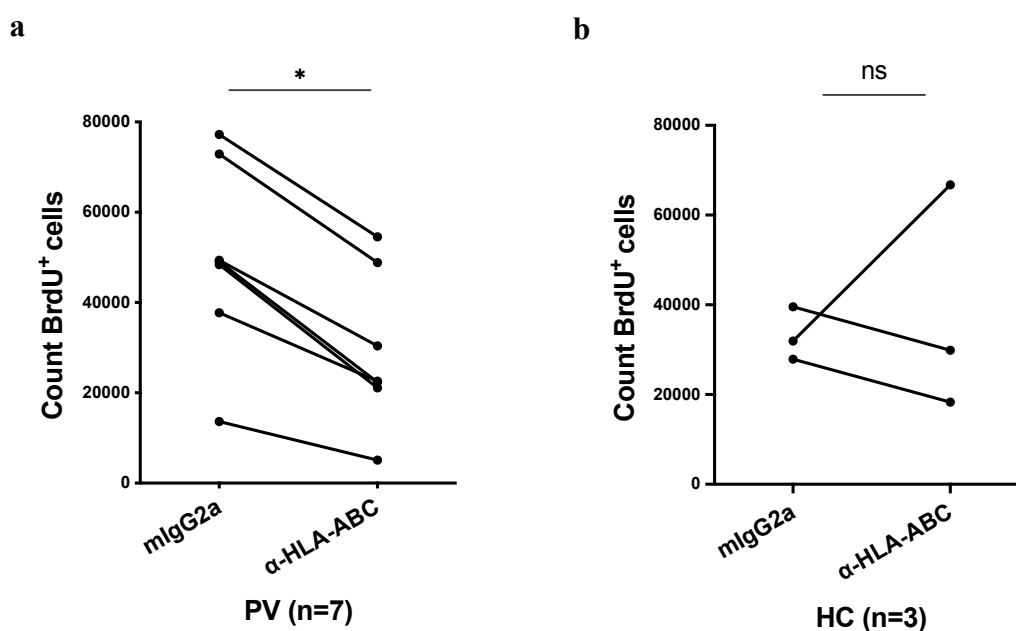


Figure 4.3.4 Inhibition of autoproliferation the PBMCs from PVs or HCs by preincubation with anti-human HLA-ABC antibody (W6/32), as assessed by the decrease of BrdU⁺ cell counts. Mouse IgG2a antibody served as isotype controls. (a) Cell proliferation of the PBMCs from PVs ($n = 7$) was significantly inhibited by anti-human HLA-ABC antibody. (b) In contrast, no statistical difference was observed in the cell proliferation of PBMCs from HCs ($n = 3$) after applying anti-human HLA-ABC antibody. Lines represent the values change of one subject, and dots mark mean values. Data were assessed by multiparametric flow cytometry analysis and compared using the Wilcoxon matched-pairs signed rank test, with statistical significance indicated as $*p < 0.05$, and ns denoting no statistical difference.

4.4 Determination of the Vα3S1/Vβ13S1 TCR-Recognition Motif

The results suggest that streptococcal angina may cause an HLA-C*06:02-restricted immune response of CD8⁺ T cells against B cells, which is subsequently cross-activated against melanocytes in the skin and thus triggers psoriasis. The autoimmune response against melanocytes is antigen-specific and directed against an epitope from ADAMTSL5 presented by HLA-C*06:02. This raises the question of which self-peptide is presented by HLA-C*06:02 on B lymphocytes and recognized by the Vα3S1/Vβ13S1 TCR and pathogenic psoriatic CD8⁺ T cells.

HLA-class I peptidomes consist of thousands of different self-peptides generated by processing from cytoplasmic proteins for HLA-class I presentation. Thus, an HLA-class I-restricted

autoimmune response is directed against a specific target cell expressing the parental protein of the self-peptide. TCRs, in turn, are not specific for a single epitope but recognize peptides sharing a recognition motif specific for the respective TCR. It usually consists of 2 anchor amino acids for the respective HLA allele and one or two amino acids contacting the TCR, while tolerating a broad amino acid diversity at the other positions of the antigenic nonamer. For the identification of an autoantigenic self-peptide, it is therefore necessary to determine the peptide recognition motif of the TCR of interest. In a second step, the transcriptome, proteome, or immunopeptidome of the target cell of the HLA-class I-restricted autoimmune response can then be analyzed for proteins containing peptide sequences that correspond to the respective TCR recognition motif (Prinz, 2023).

To identify the self-peptide presented by HLA-C*06:02 on B cells and recognized by the V α 3S1/V β 13S1 TCR, I first characterized the recognition motif of this pathogenic TCR in more detail. For this purpose, I employed the amino acid sequences of V α 3S1/V β 13S1 TCR ligands that had already been identified in previous experiments.

4.4.1 Analysis of Mimotopes

Peptide library screening using combinatorial peptide libraries had previously identified 11 mimotopes, which are presented by HLA-C*06:02 and ligate the V α 3S1/V β 13S1 TCR (Arakawa *et al.*, 2015). They were characterized by a convergent amino acid pattern with distinct residue preferences for arginine (Arg, R) at positions P2 and P8, leucine (Leu, L) at P9, and arginine (Arg, R) or leucine (Leu, L) at P7. Six mimotopes carried arginine (Arg, R) at P5, whereas P1, P3, P4, and P6 exhibited greater amino acid diversity (**Figure 4.4.1**). The conserved residues were located at the primary HLA-C*06:02 anchor positions P2, P9 as well as auxiliary anchor at P7, while P5 and P8 mediate the contact with the V α 3S1/V β 13S1 TCR (Falk *et al.*, 1993; Mobbs *et al.*, 2017; Rasmussen *et al.*, 2014).

a**Vα3S1/Vβ13S1-TCR contact residues**

Mimotopes	1	2	3	4	5	6	7	8	9	TCR-activation
Mimotope 1	M	R	S	H	R	Y	L	R	L	+++++
Mimotope 2	G	R	N	A	R	V	R	R	L	+++++
Mimotope 3	G	R	A	S	R	T	R	R	L	+++++
Mimotope 4	R	R	N	W	N	Y	R	R	L	+++++
Mimotope 4-8mer		R	N	W	N	Y	R	R	L	+++++
Mimotope 5	F	R	W	Y	R	V	R	R	L	+++++
Mimotope 6	F	R	C	R	Q	Y	R	R	L	+++++
Mimotope 7	F	R	H	R	R	T	L	R	L	+++++
Mimotope 8	F	R	S	Y	R	T	R	R	L	+++++
Mimotope 9	R	R	Y	F	R	C	L	R	M	+++++
Mimotope 10	R	R	N	A	R	V	R	R	L	+++++
Mimotope 11	V	R	C	W	R	G	R	R	L	+++++

HLA-C*06:02 anchor residues

b

Amino-acid	1	2	3	4	5	6	7	8	9
A	0	0	1	2	0	0	0	0	0
C	0	0	2	0	0	1	0	0	0
D	0	0	0	0	0	0	0	0	0
E	0	0	0	0	0	0	0	0	0
F	4	0	0	1	0	0	0	0	0
G	2	0	0	0	0	1	0	0	0
H	0	0	1	1	0	0	0	0	0
I	0	0	0	0	0	0	0	0	0
K	0	0	0	0	0	0	0	0	0
L	0	0	0	0	0	0	3	0	11
M	1	0	0	0	0	0	0	0	1
N	0	0	4	0	2	0	0	0	0
P	0	0	0	0	0	0	0	0	0
Q	0	0	0	0	1	0	0	0	0
R	3	12	0	2	9	0	9	12	0
S	0	0	2	1	0	0	0	0	0
T	0	0	0	0	0	3	0	0	0
V	1	0	0	0	0	3	0	0	0
W	0	0	1	3	0	0	0	0	0
Y	0	0	1	2	0	4	0	0	0
Sum	11	12	12	12	12	12	12	12	12


0  1
Proportion of amino acid residues

Figure 4.4.1 Mimotopes derived from plasmid-encoded combinatorial nonamer peptide libraries (PECPLs). (a) Amino acid sequence of mimotopes. HLA-C*06:02 anchor positions (P2, P7, P9) are mainly labeled in yellow, and V α 3S1/V β 13S1 TCR contact position (P5, P8) mainly in green. (b) Heat map of the amino acids at the different peptide positions. The numbers indicate the frequency of the amino acids at the respective positions of the mimotopes. The color intensity represents the proportion of amino acid residues; the darker the color, the higher the proportion. Amino acids are designated by the one-letter code. The strength of V α 3S1/V β 13S1 TCR stimulation is graded from no stimulation (-) to maximum (+++++) stimulation.

4.4.2 Analysis of Human Self-Peptides and Environmental Peptide Ligands

Subsequent bioinformatic searches against the human proteome had not identified parental proteins containing sequences fully identical to the mimotopes. The convergent amino acid pattern of mimotopes was used to select and test 180 natural human peptides for the identification of candidate antigens of the V α 3S1/V β 13S1 TCR. Thirteen 9-mer human self-peptides and corresponding 8-mer peptides starting at the NH₂-terminal anchor residue for HLA-C*06:02 derived from human protein had previously been identified as self-peptides ligands of the V α 3S1/V β 13S1-TCR using the hybridoma reporter assay, of which only the ADAMTSL5 peptide was generated from the parental protein for presentation (Introduction 1.1.4) (**Figure 4.4.2 a & b**). With the same method, various peptides from environmental antigens had been identified as potential environmental triggers of the psoriatic autoimmune response in another project as well (**Figure 4.4.2 b & d**) (Ishimoto *et al.*, 2024). All of them corresponded to the conserved amino acid motif of the mimotopes and contained Arg at P5 and P8, and the HLA-C*06:02-anchor residues Arg at P2, Leu at P9, and Arg or Leu at P7.

a

Human proteins	1	2	3	4	5	6	7	8	9	TCR-activation
ADAMTSL5 ₅₇₋₆₅	V	R	S	R	R	C	L	R	L	+++
THEM6 ₁₀₅₋₁₁₃	A	R	H	R	R	S	L	R	L	++++
RASSF10 ₄₄₋₅₂	R	R	Q	R	R	S	R	R	L	++
HEPACAM ₉₋₁₇	S	R	A	S	R	A	L	R	L	++
ASH1L ₂₄₂₂₋₂₄₃₀	A	R	S	V	R	T	R	R	L	+
C2CD4B ₁₉₃₋₂₀₁	L	R	A	G	R	S	R	R	L	++++
C16orf91 ₁₆₇₋₁₇₅	S	R	A	V	R	A	L	R	L	++
HCG1742967 ₃₄₋₄₂	S	R	A	A	R	S	R	R	L	++
YB-1 ₁₉₃₋₂₀₁	H	R	H	S	R	I	L	R	L	++
IL-24del3 ₁₉₃₋₂₀₁	R	R	F	C	R	T	S	R	M	++
ADAMTSL5-8mer ₅₈₋₆₅		R	S	R	R	C	L	R	L	+++
C2CD4B-8mer ₁₉₄₋₂₀₁		R	A	G	R	S	R	R	L	+++
YB-1-8mer ₁₉₄₋₂₀₁		R	H	S	R	I	L	R	L	+++

b

Environmental proteins	1	2	3	4	5	6	7	8	9	TCR-activation
<i>Coffea canephora</i> -unnamed protein product	Y	R	S	Y	R	T	R	R	M	+++++
<i>Spinacia oleracea</i> -RNA pseudouridine synthase 3	H	R	N	H	R	Y	L	R	L	++++
<i>Malus domestics</i> : Apple-1-LOC103417966	A	R	S	F	R	S	L	R	L	++++
<i>Malus domestics</i> : Apple-2-LOC103417966	A	R	S	S	R	S	L	R	L	+++
<i>Triticum aestivum</i> : Wheat-1-RGC1B		R	M	R	R	C	R	R	M	+++
<i>Triticum aestivum</i> : Wheat-2-unnamed protein product		R	A	G	R	V	L	R	V	+
<i>Saccharomyces cerevisiae</i> -Hsl1p		R	S	R	R	S	L	R	L	++++
<i>Serpula lacrymans</i> var. <i>lacrymans</i> S7.9-hypothetical protein SERLADRAFT_432168	H	R	T	R	R	T	R	R	L	+++
<i>Aspergillus niger</i> - hypothetical protein ANI_1_1926104	G	R	A	S	R	S	R	R	L	+++
<i>Trichophyton verrucosum</i> HKI 0517-signal transduction protein Syl1, putative	F	R	T	R	R	T	R	R	L	+
<i>Mycobacterium tuberculosis</i> -phenolphthiocerol synthesis type-I polyketide synthase PPSA	R	R	T	R	R	T	R	R	L	++
<i>Nocardia brasiliensis</i> NBRC 14402-NBRGN_050_00490	R	R	T	R	R	S	R	R	L	+
<i>Chlamydia trachomatis</i> -uncharacterized protein	F	R	S	Y	R	V	R	R	L	++++
<i>Klebsiella pneumoniae</i> -phage virion morphogenesis protein	K	R	S	R	R	V	L	R	L	+++
<i>Streptococcus agalactiae</i> -ABC transporter ATP binding protein		R	C	S	R	V	L	R	L	++
<i>dFlavonifractor plautii</i> - Hypothetical protein	E	R	A	A	R	T	R	R	L	++
<i>Clostridium</i> sp. D5-Alpha-galactosidase		R	S	V	R	T	R	R	L	+
<i>Actinomyces oris</i> -DUF3876 domain containing protein		R	S	G	R	T	R	R	L	+
<i>Pseudomonas syringae</i> -hypothetical protein	M	R	W	F	R	V	R	R	L	++++
<i>Desulfovibrio aminophilus</i> -hypothetical protein		R	A	S	R	T	R	R	L	+++
<i>Pectobacterium atrosepti</i> -acyl-CoA dehydrogenase	W	R	H	S	R	A	L	R	L	+++
<i>Streptomyces</i> -MULTISPECIES: hypothetical protein	A	R	C	R	Q	Y	R	R	L	++
<i>Myxococcus virescens</i> -hypothetical protein	F	R	C	R	T	Y	R	R	L	++
<i>Burkholderia lata</i> -hypothetical protein	G	R	T	S	R	T	R	R	L	+
Human herpesvirus 5(HHV-5)		R	T	F	R	L	R	R	L	+

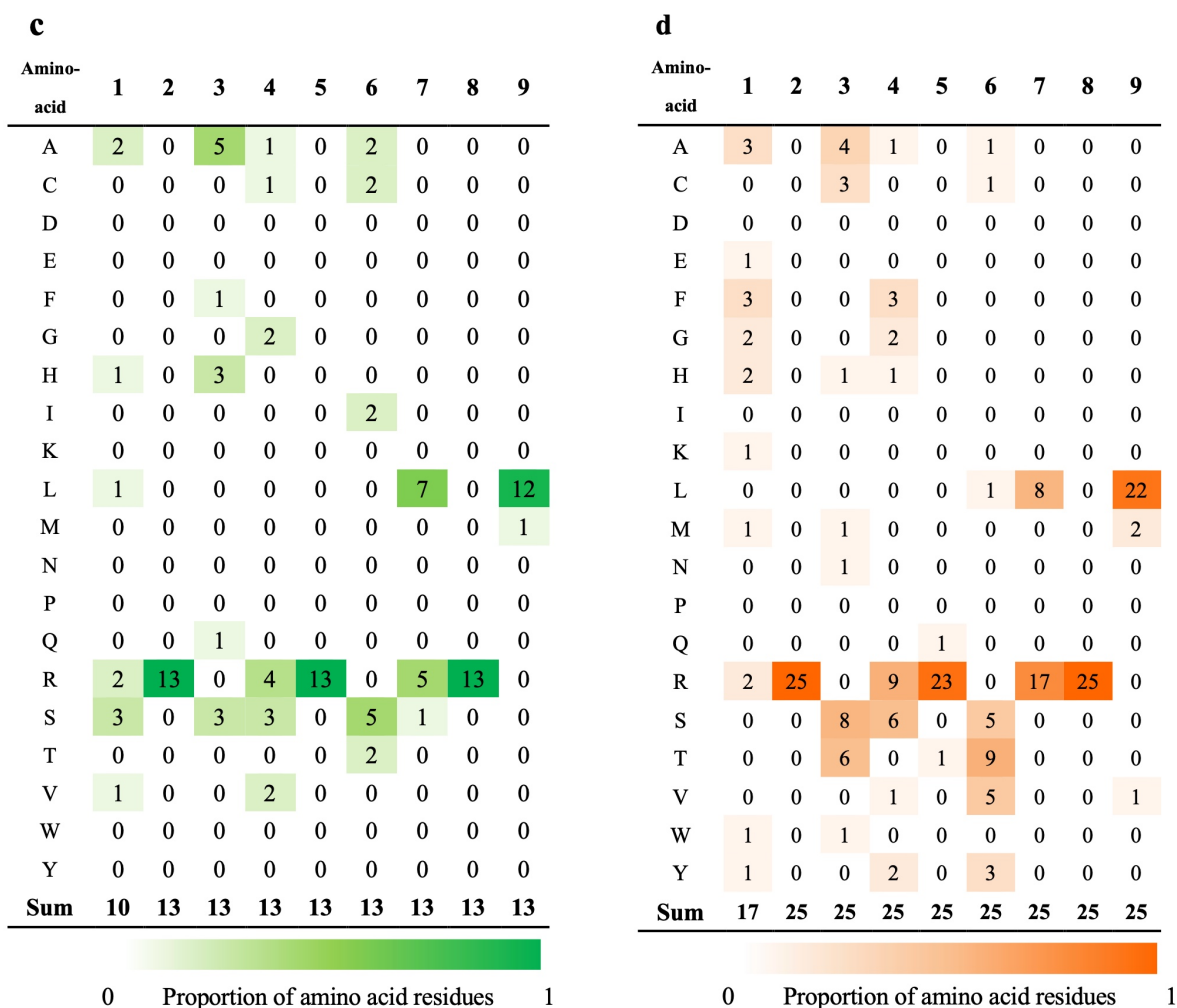


Figure 4.4.2 Amino acid sequences of natural human self-peptide ligands and environmental peptides stimulating the V α 3S1/V β 13S1 TCR and the frequency of the respective amino acid residues in heat maps. (a, b) Amino acid sequence of human self-peptides and environmental peptides stimulating the V α 3S1/V β 13S1 TCR. HLA-C*06:02 anchor positions (P2, P7, P9) are labeled in yellow, and V α 3S1/V β 13S1 TCR contact position (P5, P8) in green. Amino acids different from the autoantigenic ADAMTSL5 epitope are labeled red. (c, d) Heat map of the amino acids at the different peptide positions of human self-peptides and environmental peptides. Numbers indicate the frequency of amino acids present at the respective positions of the mimotopes. The color intensity represents the proportion of amino acid residues: the darker the color, the higher the proportion. Amino acids are designated by the one-letter code. The strength of V α 3S1/V β 13S1 TCR stimulation is graded from no stimulation (-) to maximum (+++++) stimulation.

4.4.3 Alanine Substitution Scan and Amino Acid Mutation Analysis

To confirm whether the antigenicity of peptides relies on this motif, we subjected the ADAMTSL5₅₇₋₆₅ epitopes to alanine (Ala, A) scanning mutagenesis analysis to test which positions are decisive for the antigenicity of peptides. Alanine is utilized due to its non-bulky and chemically inert nature, as well as its methyl functional group, imitating the secondary

structure preferences of numerous other amino acids. The full list of plasmids encoding cDNA sequences of these mutants, along with their corresponding primers, is given in **Table 6.1.1** and **Table 6.2.1** in the supplementary data.

I confirmed that arginine or leucine at HLA-C*06:02 anchor positions P2, P7, and P9 and arginine at positions P5 and P8 together determine the core peptide recognition motif of the V α 3S1/V β 13S1 TCR. The substitution of any amino acid residue at these positions with alanine resulted in the loss of V α 3S1/V β 13S1 TCR stimulation (**Figure 4.4.3.1**).

Human proteins	1	2	3	4	5	6	7	8	9	TCR-activation
ADAMTSL5-9mer ₅₇₋₆₅	V	R	S	R	R	C	L	R	L	+++
ADAMTSL5-A1 ₅₇₋₆₅	A	R	S	R	R	C	L	R	L	+++
ADAMTSL5-A2 ₅₇₋₆₅	V	A	S	R	R	C	L	R	L	-
ADAMTSL5-A3 ₅₇₋₆₅	V	R	A	R	R	C	L	R	L	+++
ADAMTSL5-A4 ₅₇₋₆₅	V	R	S	A	R	C	L	R	L	+++
ADAMTSL5-A5 ₅₇₋₆₅	V	R	S	R	A	C	L	R	L	-
ADAMTSL5-A6 ₅₇₋₆₅	V	R	S	R	R	A	L	R	L	++
ADAMTSL5-A7 ₅₇₋₆₅	V	R	S	R	R	C	A	R	L	-
ADAMTSL5-A8 ₅₇₋₆₅	V	R	S	R	R	C	L	A	L	-
ADAMTSL5-A9 ₅₇₋₆₅	V	R	S	R	R	S	R	R	A	-
ADAMTSL5-A58 ₅₇₋₆₅	V	R	S	R	A	S	L	A	L	-
ADAMTSL5-A578 ₅₇₋₆₅	V	R	S	R	A	S	A	A	L	-

Figure 4.4.3.1 Alanine scanning mutagenesis of the autoantigenic ADAMTSL5₅₇₋₆₅ peptide. ADAMTSL5₅₇₋₆₅ peptide lost its ability to stimulate TCR hybridoma upon the alanine substitution on P2, P5, P7, P8, and P9. HLA-C*06:02 anchor positions (P2, P7, P9) are labeled in yellow, and V α 3S1/V β 13S1 TCR contact position (P5, P8) in green. The alanine substitutions were marked with “A” in red. Amino acids are designated by the one-letter code. The strength of V α 3S1/V β 13S1 TCR stimulation is graded from no stimulation (-) to maximum (+++++) stimulation.

I further expanded the V α 3S1/V β 13S1 TCR-recognition motif by mutation analysis of ADAMTSL5 and RASSF10 at positions that are decisive for the antigenicity of these peptides. The amino acids were mutated mainly into amino acids having common physicochemical properties with the original conserved amino acid residues (Rausch *et al.*, 2005; Taylor, 1986). The full list of plasmids encoding cDNA sequences of ADAMTSL5 and RASSF10 mutants, along with their corresponding primers, is given in **Table 6.1.2** and **Table 6.2.2** in the supplementary data. I found that conserved amino acids at positions R2, R5, and R7 to R9 could be partially replaced by various other amino acids without the peptides losing their stimulatory property. However, this was dependent on the respective peptide. While the ADAMTSL5 peptide retained its stimulatory property upon exchange of amino acid L for V, I, F, or M at R9, the same exchange in peptide RASSF10 resulted in a loss of antigenicity for the V α 3S1/V β 13S1

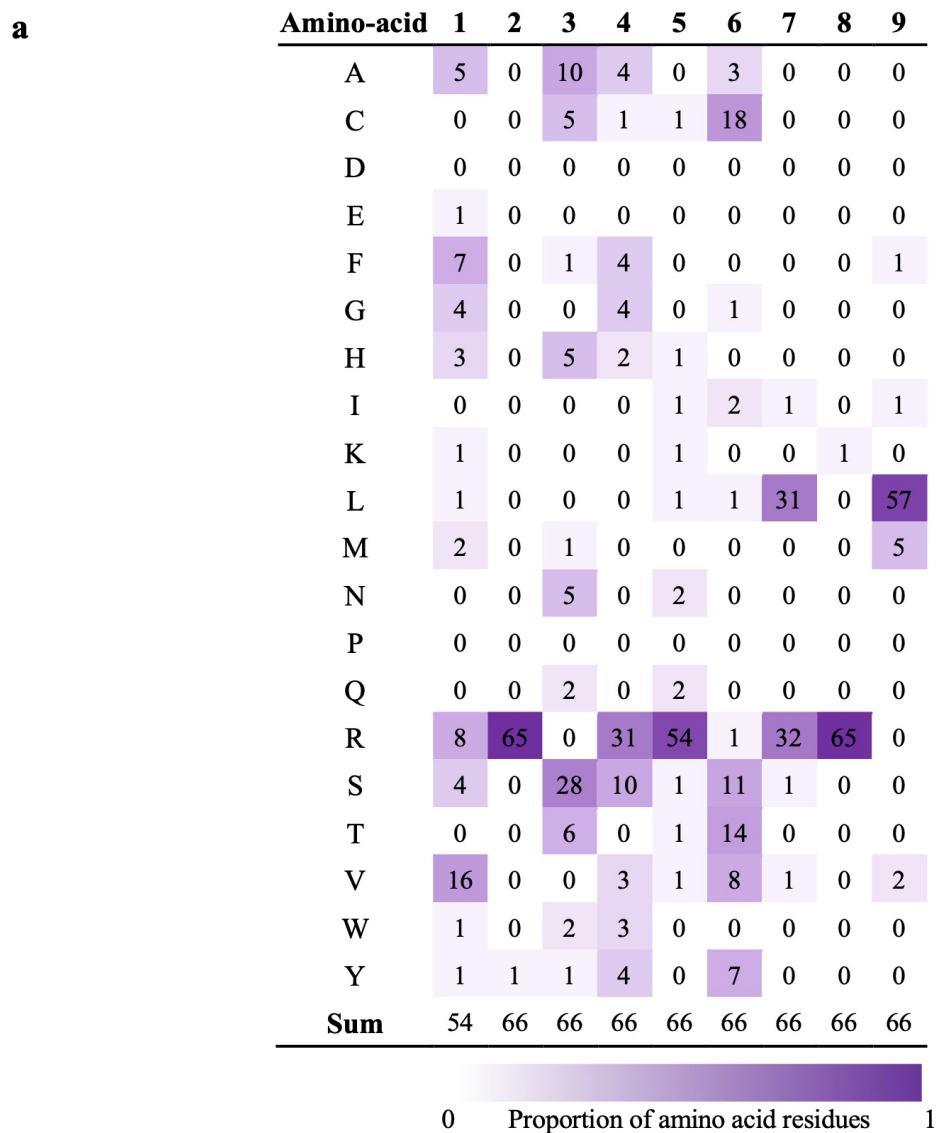
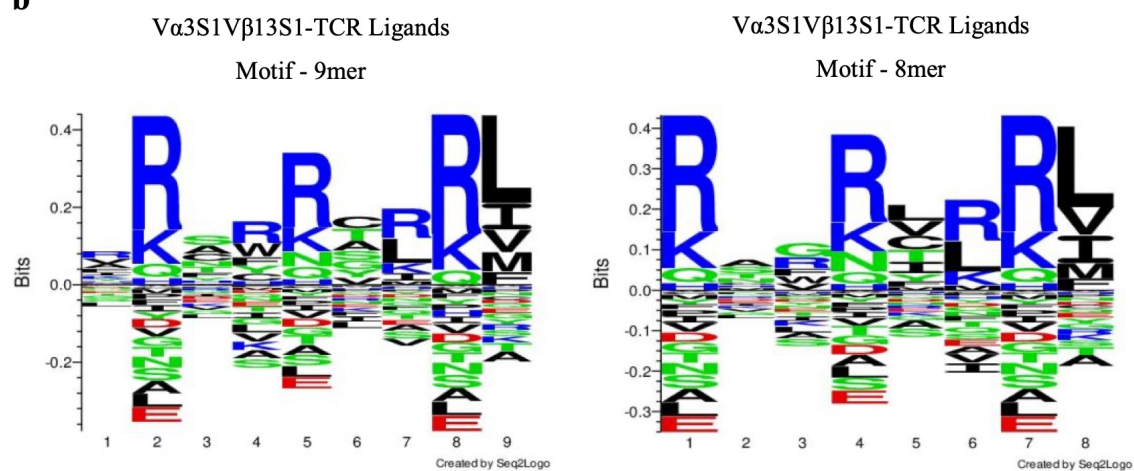
TCR. Thus, the actual peptide recognition motif of the V α 3S1/V β 13S1 TCR can only be complemented in a peptide-dependent manner at individual positions (**Figure 4.4.3.2**).

Human proteins	1	2	3	4	5	6	7	8	9	TCR-activation
ADAMTSL5-S1 ⁵⁷⁻⁶⁵	S	R	S	R	R	C	L	R	L	+++
ADAMTSL5-G2 ⁵⁷⁻⁶⁵	V	G	S	R	R	C	L	R	L	–
ADAMTSL5-T2 ⁵⁷⁻⁶⁵	V	T	S	R	R	C	L	R	L	–
ADAMTSL5-P2 ⁵⁷⁻⁶⁵	V	P	S	R	R	C	L	R	L	–
ADAMTSL5-Y2 ⁵⁷⁻⁶⁵	V	Y	S	R	R	C	L	R	L	–
ADAMTSL5-L2 ⁵⁷⁻⁶⁵	V	L	S	R	R	C	L	R	L	–
ADAMTSL5-C5R6 ⁵⁷⁻⁶⁵	V	R	S	R	C	R	L	R	L	+
ADAMTSL5-K5 ⁵⁷⁻⁶⁵	V	R	S	R	K	C	L	R	L	+
ADAMTSL5-H5 ⁵⁷⁻⁶⁵	V	R	S	R	H	C	L	R	L	+
ADAMTSL5-S5 ⁵⁷⁻⁶⁵	V	R	S	R	S	C	L	R	L	+
ADAMTSL5-L5 ⁵⁷⁻⁶⁵	V	R	S	R	L	C	L	R	L	+
ADAMTSL5-F5 ⁵⁷⁻⁶⁵	V	R	S	R	F	C	L	R	L	–
ADAMTSL5-I5 ⁵⁷⁻⁶⁵	V	R	S	R	I	C	L	R	L	+
ADAMTSL5-V5 ⁵⁷⁻⁶⁵	V	R	S	R	V	C	L	R	L	+
ADAMTSL5-G5 ⁵⁷⁻⁶⁵	V	R	S	R	G	C	L	R	L	–
ADAMTSL5-K7 ⁵⁷⁻⁶⁵	V	R	S	R	R	C	K	R	L	–
ADAMTSL5-K7 ⁵⁷⁻⁶⁵	V	R	S	R	R	C	Q	R	L	–
ADAMTSL5-K7 ⁵⁷⁻⁶⁵	V	R	S	R	R	C	I	R	L	++
ADAMTSL5-K7 ⁵⁷⁻⁶⁵	V	R	S	R	R	C	V	R	L	+
ADAMTSL5-K8 ⁵⁷⁻⁶⁵	V	R	S	R	R	C	L	K	L	++
ADAMTSL5-H8 ⁵⁷⁻⁶⁵	V	R	S	R	R	C	L	H	L	–
ADAMTSL5-L8 ⁵⁷⁻⁶⁵	V	R	S	R	R	C	L	L	L	–
ADAMTSL5-Y9 ⁵⁷⁻⁶⁵	V	R	S	R	R	C	L	R	Y	–
ADAMTSL5-V9 ⁵⁷⁻⁶⁵	V	R	S	R	R	C	L	R	V	+++
ADAMTSL5-F9 ⁵⁷⁻⁶⁵	V	R	S	R	R	C	L	R	F	++
ADAMTSL5-I9 ⁵⁷⁻⁶⁵	V	R	S	R	R	C	L	R	I	+++
ADAMTSL5-M9 ⁵⁷⁻⁶⁵	V	R	S	R	R	C	L	R	M	+++
RASSF10-Y2 ⁴⁴⁻⁵²	R	Y	Q	R	R	S	R	R	L	++
RASSF10-G2 ⁴⁴⁻⁵²	R	G	Q	R	R	S	R	R	L	–
RASSF10-T2 ⁴⁴⁻⁵²	R	T	Q	R	R	S	R	R	L	–
RASSF10-A2 ⁴⁴⁻⁵²	R	A	Q	R	R	S	R	R	L	–
RASSF10-P2 ⁴⁴⁻⁵²	R	P	Q	R	R	S	R	R	L	–
RASSF10-Q2 ⁴⁴⁻⁵²	R	Q	Q	R	R	S	R	R	L	–
RASSF10-G5 ⁴⁴⁻⁵²	R	R	Q	R	G	S	R	R	L	–
RASSF10-M9 ⁴⁴⁻⁵²	R	R	Q	R	R	S	R	R	M	–
RASSF10-T9 ⁴⁴⁻⁵²	R	R	Q	R	R	S	R	R	T	–
RASSF10-G9 ⁴⁴⁻⁵²	R	R	Q	R	R	S	R	R	G	–
RASSF10-I9 ⁴⁴⁻⁵²	R	R	Q	R	R	S	R	R	I	–
RASSF10-A9 ⁴⁴⁻⁵²	R	R	Q	R	R	S	R	R	A	–
RASSF10-V9 ⁴⁴⁻⁵²	R	R	Q	R	R	S	R	R	V	–
RASSF10-Y9 ⁴⁴⁻⁵²	R	R	Q	R	R	S	R	R	Y	–
RASSF10-F9 ⁴⁴⁻⁵²	R	R	Q	R	R	S	R	R	F	–
RASSF10-P9 ⁴⁴⁻⁵²	R	R	Q	R	R	S	R	R	P	–

Figure 4.4.3.2 Amino acid mutation analysis of the HLA-C*06:02 anchor positions P2, P7, and P9, and V α 3S1/V β 13S1 TCR-recognition positions P5 and P8 in the autoantigenic ADAMTSL5₅₇₋₆₅ peptide and the stimulatory RASSF10₄₄₋₅₂ peptide. HLA-C*06:02 anchor positions are labeled in yellow, and V α 3S1/V β 13S1 TCR contact position in green. The mutated amino acids were marked with red. Amino acids are designated by the one-letter code. The strength of V α 3S1/V β 13S1 TCR stimulation is graded from no stimulation (-) to maximum (+++++) stimulation.

4.4.4 Summarized Recognition Motif of the V α 3S1/V β 13S1 TCR

Thus, I was able to compile all peptide ligands of the V α 3S1/V β 13S1 TCR that had been identified in previous experiments. They consist of mimotopes identified by peptide library analysis, various natural human self-peptides, various peptides from environmental antigens, and several mutated peptides from the autoantigenic ADAMTSL5 and the stimulatory RASSF10 peptides. I generated a final frequency matrix/heat map of the amino acids at the different peptide positions and created a sequence logo of the peptide recognition motif by Seq2Logo 2.0 (**Figure 4.4.4**). Using this extended V α 3S1/V β 13S1 TCR recognition motif, I searched for homologous peptides in human proteins that can be presented by HLA-C*06:02 on B lymphocytes using different search strategies.

**b**

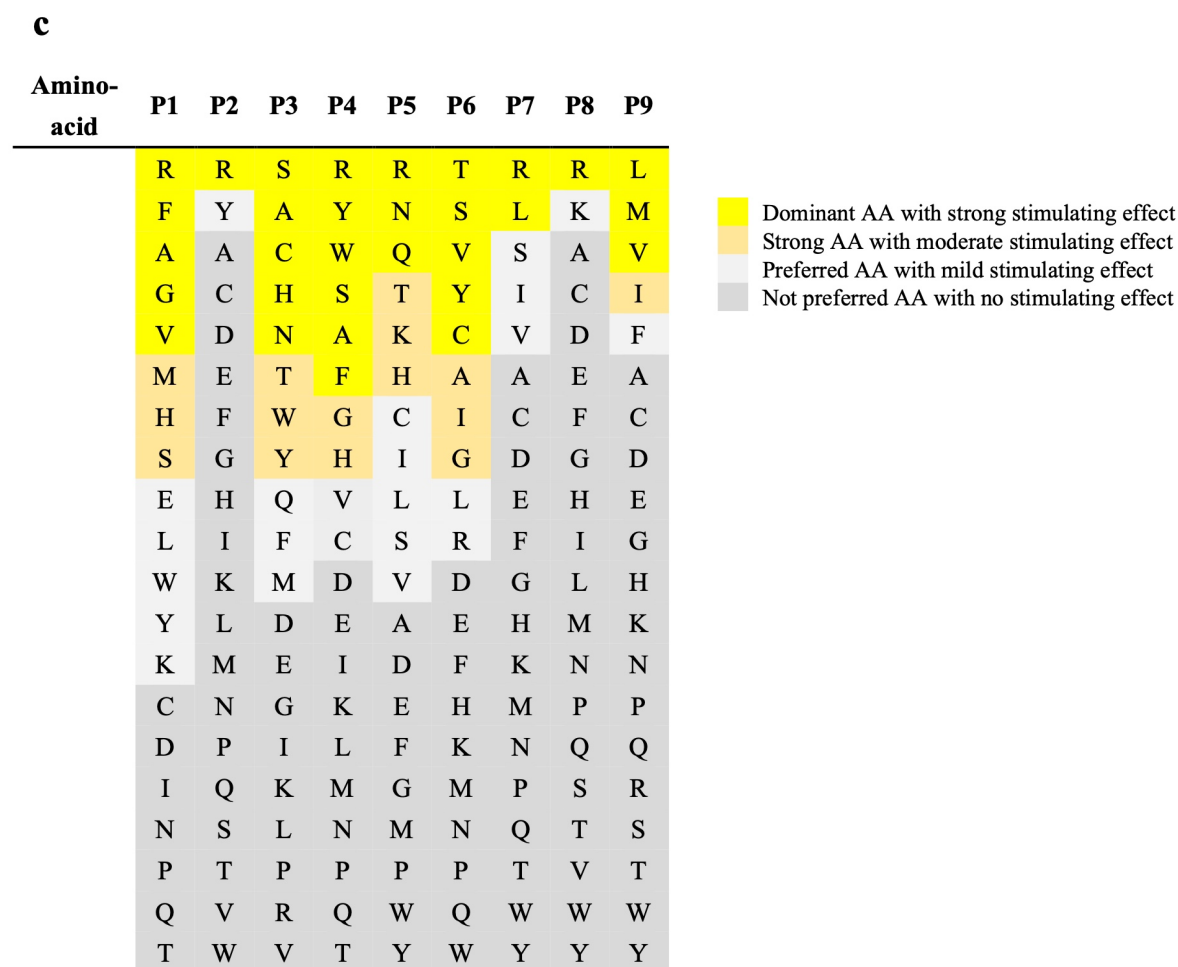


Figure 4.4.4 Frequency matrix/heat map of the amino acids at the different peptide positions and sequence logo of the peptide recognition motif. (a) Heat map of the amino acids at the different peptide positions in all the V α 3S1/V β 13S1 TCR peptide ligands. The numbers indicate the frequency of the amino acids at the respective positions of the mimotopes. The color intensity represents the proportion of amino acid residues; the darker the color, the higher the proportion. (b) 9-mer and 8-mer V α 3S1/V β 13S1 TCR-ligands recognition motifs were visualized employing Seq2Logo 2.0 and Kullback-Leibler logotype applying default settings (Thomsen and Nielsen, 2012). The size of the letter indicates the impact of the corresponding amino acid, presented by a given position in either a positive or negative fashion. (c) Frequency matrix of amino acids at the different peptide positions in all the peptide ligands of the V α 3S1/V β 13S1 TCR considering the stimulatory degree. Amino acids are designated by the one-letter code.

4.4.5 The Motifs for Screening Human Proteome and HLA-C*06:02 Peptidomes

In order to discover candidate self-peptides presented by HLA-C*06:02 on B cells, which could potentially activate the V α 3S1/V β 13S1 TCR, I utilized the compiled amino acid pattern of the V α 3S1/V β 13S1 TCR ligands to establish amino acid motifs for screening both the human proteome and the HLA-C*06:02 peptidomes derived from human B cells.

I examined only one candidate peptide at a time using the V α 3S1/V β 13S-TCR hybridoma reporter assay to enable high-sensitivity detection of positive TCR-antigen interactions. Therefore, the list of candidate peptide antigens to be tested with the V α 3S1/V β 13S-TCR hybridoma reporter assay had to be narrowed to a reasonable extent without missing the autoantigen(s). Thus, the motifs listed in **Table 4.4.5** were used for the screening proteome or peptidomes, in an order from strict motifs (fewer matches, high homology, at lower sensitivity) to less strict motifs (more matches, less homology, at higher sensitivity).

Order	Motifs (encoded in PROSITE format)
1	x-[RY]-x(2)-[RNQTKHCILSV]-x-[RLSIV]-[RH]-[LFMVIF]
2	x-[RY]-x(2)-[RNQTKH]-x-[RLSIV]-[RH]-[LFMVIF]
3	x-[RY]-x(2)-[RNQTKH]-x-[RLSIV]-R-[LFMVIF]
4	x-[RY]-x(2)-[RNQTKH]-x-[RL]-R-[LMVIF]
5	x-[RY]-x(2)-[RNQ]-x-[RL]-R-[LMV]
6	x-R-x(2)-[RNQ]-x-[RL]-R-[LMV]
7	x-R-x(2)-R-x-[RL]-R-[LMV]
8	x-R-x(2)-R-x-[RL]-R-L
9	x-R-x(2)-R-x-R(2)-L

Table 4.4.5 The motifs applied to screen against the human proteome and HLA-C*06:02 peptidome from human B cells, in an order from strict to less strict. The motifs are encoded in PROSITE format.

4.5 Screening of V α 3S1/V β 13S1-TCR Ligands in Peptidomes of HLA-C*06:02-C1R or -721.221

After determining the amino acid motifs of V α 3S1/V β 13S1-TCR ligands, the next step for the identification of autoantigen(s) presented by HLA-C*06:02 on B lymphocytes was to analyze the transcriptome or HLA-C*06:02 peptidome of B cells for peptide sequences homologous to the respective TCR recognition motif.

Firstly, I searched for published peptidome data and found two HLA-C*06:02 peptidomes determined from two B cell lines stably transfected with HLA-C*06:02, namely HLA-C*06:02-C1R and HLA-C*06:02-721.221 (Di Marco *et al.*, 2017; Mobbs *et al.*, 2017). Both C1R and 721.221 were immortalized by Epstein-Barr virus (EBV) and had lost (or had low) HLA expression following γ -ray radiation (Shimizu *et al.*, 1988; Storkus *et al.*, 1989). Since both of them have a functional antigen presentation pathway, they were transfected with the gene encoding HLA-C*06:02 and employed for ligand identification of HLA-C*06:02 (Di Marco *et al.*, 2017; Mobbs *et al.*, 2017). Therefore, we considered the immunopeptidomes of HLA-

C*06:02-C1R and HLA-C*06:02-721.221 as suitable screening pools for the identification of the self-peptide(s) ligating the V α 3S1/V β 13S1-TCR ligands on HLA-C*06:02⁺ B cell lines.

4.5.1 Candidate Peptides Derived from HLA-C*06:02-C1R and HLA-C*06:02-721.221

First, I examined whether the ADAMTSL5 peptide was present in the peptidomes of the two cell lines. This was not the case. Therefore, I had to assume that the V α 3S1/V β 13S1 TCR is stimulated by an HLA-C*06:02-presented B-cell peptide other than ADAMTSL5. I therefore screened the HLA-C*06:02-ligand repertoires published by Di Marco and Mobbs (in total around 3,000 peptides) (Di Marco *et al.*, 2017; Mobbs *et al.*, 2017) for peptides corresponding to the V α 3S1/V β 13S1-TCR ligand motifs (Section 4.4.5) and selected 29 peptides as candidate antigens for further testing (**Figure 4.5.1**). The cDNAs corresponding to these peptides were cloned into plasmids (the full list of primers and plasmids is given in **Table 6.1.3** & **Table 6.2.3**) and co-expressed with HLA-C*06:02 in COS-7 cells, which were used for antigen presentation to the psoriatic V α 3S1/V β 13S1-TCR hybridoma in co-culture experiments. However, none of the candidate antigens stimulated the V α 3S1/V β 13S1 TCR (**Figure 4.5.1**).

Human proteins	1	2	3	4	5	6	7	8	9	TCR-activation
AURKA ₁₈₈₋₁₉₆	L	R	H	P	N	I	L	R	L	—
ALG3 ₂₆₋₃₄	Q	R	A	W	Q	E	R	R	L	—
AQR ₄₆₇₋₄₇₅	L	R	N	F	N	L	F	R	L	—
NLRC5 ₁₃₃₅₋₁₃₄₃	F	R	P	E	H	V	S	R	L	—
UNC119B ₆₈₋₇₆	I	R	P	E	H	V	L	R	L	—
SND1 ₃₁₅₋₃₂₃	E	R	F	A	K	E	R	R	L	—
SF3B3 ₆₉₆₋₇₀₄	S	R	P	V	K	L	F	R	V	—
CSNK2A1 ₃₀₅₋₃₁₃	L	R	Y	D	H	Q	S	R	L	—
NXF1 ₃₄₃₋₃₅₁	E	R	F	P	K	L	L	R	L	—
PSMD2 ₂₆₀₋₂₆₈	S	R	F	P	E	A	L	R	L	—
SMG1 ₂₀₈₄₋₂₀₉₂	K	R	A	S	Y	I	L	R	L	—
AIFM2 ₂₅₂₋₂₆₀	Y	R	K	A	F	E	S	R	L	—
ATG2B ₅₀₁₋₅₀₉	S	R	P	E	L	I	F	R	L	—
ZNF282 ₁₇₇₋₁₈₅	N	R	N	F	W	V	L	R	L	—
CD70 ₁₃₇₋₁₄₅	S	R	S	I	S	L	L	R	L	—
ACACA ₁₄₅₋₁₅₃	F	R	N	E	R	A	I	R	F	—
ZNF574 ₅₈₆₋₅₉₄	V	R	F	H	R	P	Y	R	L	—
VPS51 ₁₉₄₋₂₀₂	G	A	Y	G	Q	A	V	R	Y	—
MFSD5 ₂₉₉₋₃₀₇	Y	R	I	A	T	S	K	R	Y	—
CSNK2A2 ₃₀₆₋₃₁₄	L	R	Y	D	H	Q	Q	R	L	—
PARP14 ₁₆₄₃₋₁₆₅₁	F	R	I	E	K	I	E	R	I	—
SF3B4 ₇₈₋₈₆	K	L	Y	G	K	P	I	R	V	—
FBXW8 ₂₉₄₋₃₀₂	H	R	F	E	H	D	A	R	I	—
SLC4A1AP ₂₅₇₋₂₆₅	V	H	V	G	H	V	V	R	F	—
CLASP2 ₂₀₅₋₂₁₃	I	R	H	T	H	V	P	R	L	—
NEMF ₃₂₆₋₃₃₄	V	R	K	D	H	E	N	R	L	—
RP9 ₁₄₉₋₁₅₇	K	R	H	E	K	D	V	R	I	—
MYH4 ₂₄₅₋₂₅₃	S	R	F	G	K	F	I	R	I	—
LSM7 ₁₇₋₂₅	K	Y	I	D	K	T	I	R	V	—

Figure 4.5.1 TCR-hybridoma stimulation by peptide antigens derived from HLA-C*06:02-C1R or HLA-C*06:02-721.221. The order of peptides in the figure from top to bottom represents the degree of homology to the respective TCR recognition motifs. No activation (—) of the V α 3S1/V β 13S1-TCR hybridoma was observed by these candidate peptides. Amino acids are designated by the one-letter code.

4.5.2 Examination of HLA-C*06:02-C1R or HLA-C*06:02-721.221 cell lines

Since top candidate peptides derived from the two publicly available HLA-C*06:02-peptidomes were not able to ligate the V α 3S1/V β 13S1 TCR, I decided to verify whether the HLA-C*06:02-C1R and HLA-C*06:02-721.221 cell lines would stimulate the V α 3S1/V β 13S1 TCR at all.

For this purpose, the two B cell lines were co-cultured with the V α 3S1/V β 13S1-TCR hybridoma. After 24 hours of co-culture V α 3S1/V β 13S1-TCR hybridoma cells were analyzed for the induction of sGFP by flow cytometry analysis. Neither HLA-C*06:02-C1R nor HLA-

C*06:02-721.221 or the HLA-C*06:02-negative B cell line P16488 induced sGFP expression in the V α 3S1/V β 13S1-TCR hybridoma cells. By contrast, the EBV-transformed B cell line D22 and primary B cells from PBMCs of an HLA-C*06:02 patient strongly stimulate the V α 3S1/V β 13S1-TCR hybridoma (Figure 4.5.2.1).

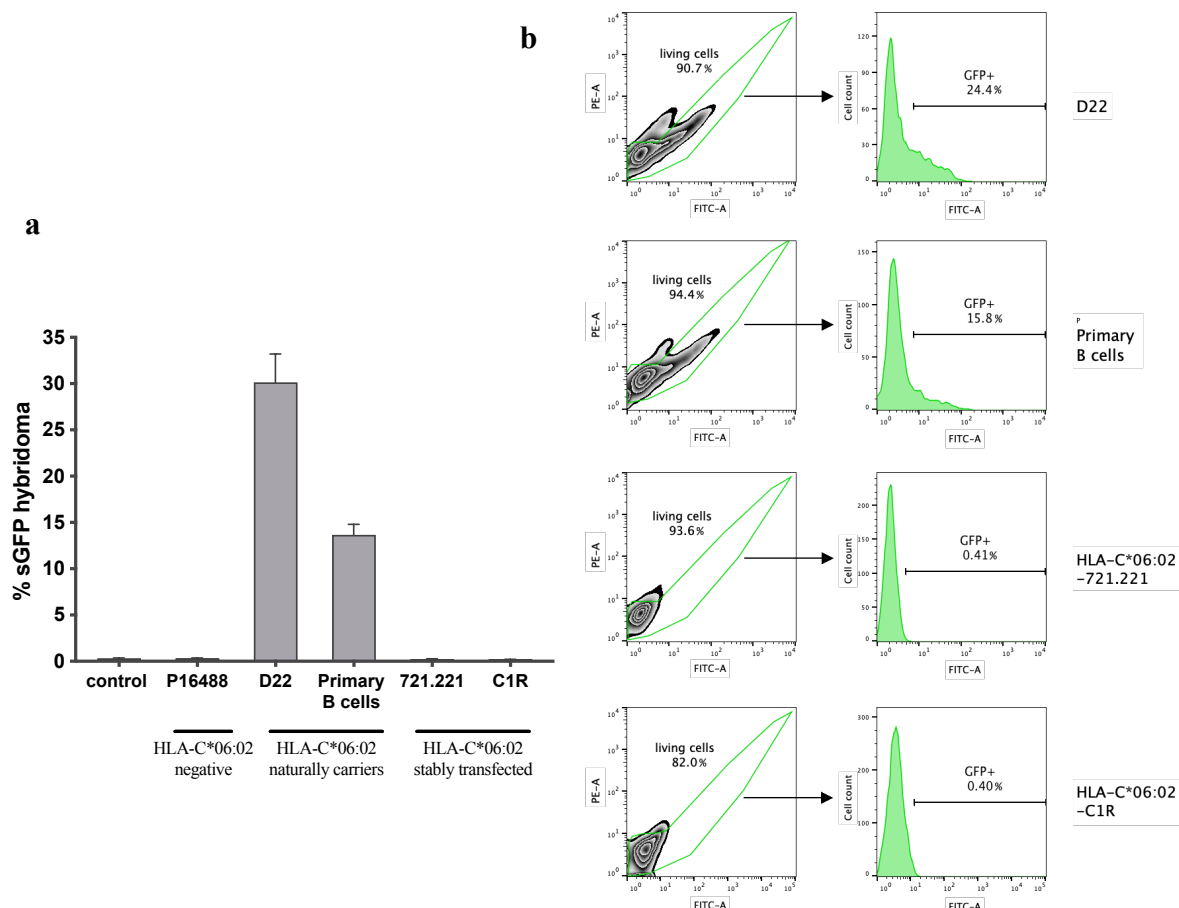


Figure 4.5.2.1 HLA-C*06:02-C1R and HLA-C*06:02-721.221 were not able to activate V α 3S1/V β 13S1-TCR hybridoma in co-culture experiments. (a) Activation of the V α 3S1/V β 13S1-TCR hybridoma in co-culture with various HLA-C*06:02-positive/negative B cell lines. The V α 3S1/V β 13S1-TCR hybridoma cells incubated in culture plates solely without other cells served as negative controls. EBV-transformed HLA-C*06:02⁺ B cell line D22 and primary B cells from psoriasis patient PVB01 served as positive controls. (b) Representative flow cytometry histograms of sGFP induction by D22, primary B cells, HLA-C*06:02-721.221, and HLA-C*06:02-C1R. Data were summarized from technical triplicates from two or three independent experiments.

Several reasons may explain why HLA-C*06:02-C1R and HLA-C*06:02-721.221 were not immunogenic for the V α 3S1/V β 13S1 TCR, though they were B cell lines. Apart from the possible cause that the autoantigens of B cells stimulating the V α 3S1/V β 13S1 TCR were not expressed at all in the two cell lines, a defect in antigen processing and presentation may also have resulted in the loss of immunogenicity of HLA-C*06:02-C1R and HLA-C*06:02-721.221.

Thus, I next examined whether HLA-C*06:02-C1R and HLA-C*06:02-721.221 could load and present peptides by HLA-C*06:02 by adding synthetic peptide ligands of the V α 3S1/V β 13S1

TCR in co-culture experiments. In all stimulation experiments, sGFP induction in V α 3S1/V β 13S1-TCR hybridoma cells was examined after 24 hours of co-culture by flow cytometry. COS-7-HLA-C*06:02 served as a control cell line for its known ability to process and present peptides. Synthetic ADAMTSL5 and *Mycobacterium tuberculosis* peptides stimulated the V α 3S1/V β 13S1-TCR hybridoma to varying degrees in all cell lines (**Figure 4.5.2.2**). This directly validated that the HLA-C*06:02-C1R and HLA-C*06:02-721.221 were able to present TCR peptide ligands sufficiently.

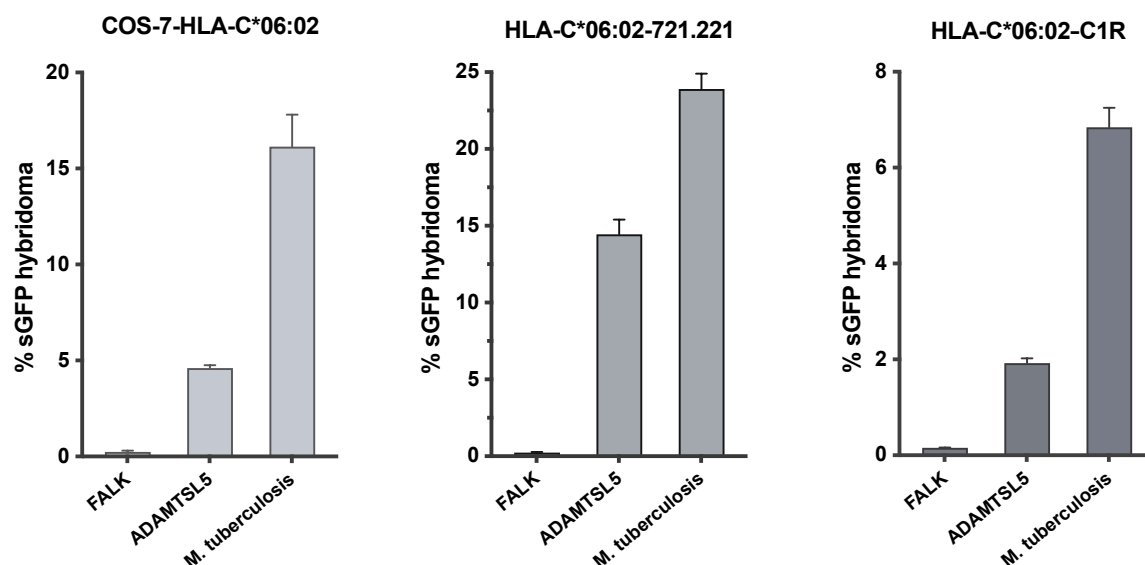


Figure 4.5.2.2 Activation of the V α 3S1/V β 13S1-TCR hybridoma cells by co-culture with COS-7 cells or the B cell lines 721.221 or C1R that were stably transfected with HLA-C*06:02 and loaded with synthetic peptides. Synthetic ADAMTSL5 and *M. tuberculosis* peptides are both ligands of the V α 3S1/V β 13S1 TCR. Synthetic FALK peptide served as negative control. Data were summarized from technical triplicates from two or three independent experiments.

I further overexpressed the plasmid-encoded ADAMTSL5 peptide “VRSRRCLRL” for presentation in HLA-C*06:02-C1R and HLA-C*06:02-721.221 cells by nucleofection. V α 3S1/V β 13S1-TCR hybridoma cells were added 24 hours later, and sGFP induction in hybridoma cells was examined after 24 hours of co-culture by flow cytometry. Despite that B cell lines are a notoriously difficult-to-transfect cell type, it was evident that both cell lines could express and present the ADAMTSL5 peptide by HLA-C*06:02 and stimulate the V α 3S1/V β 13S1 TCR (**Figure 4.5.2.3**).

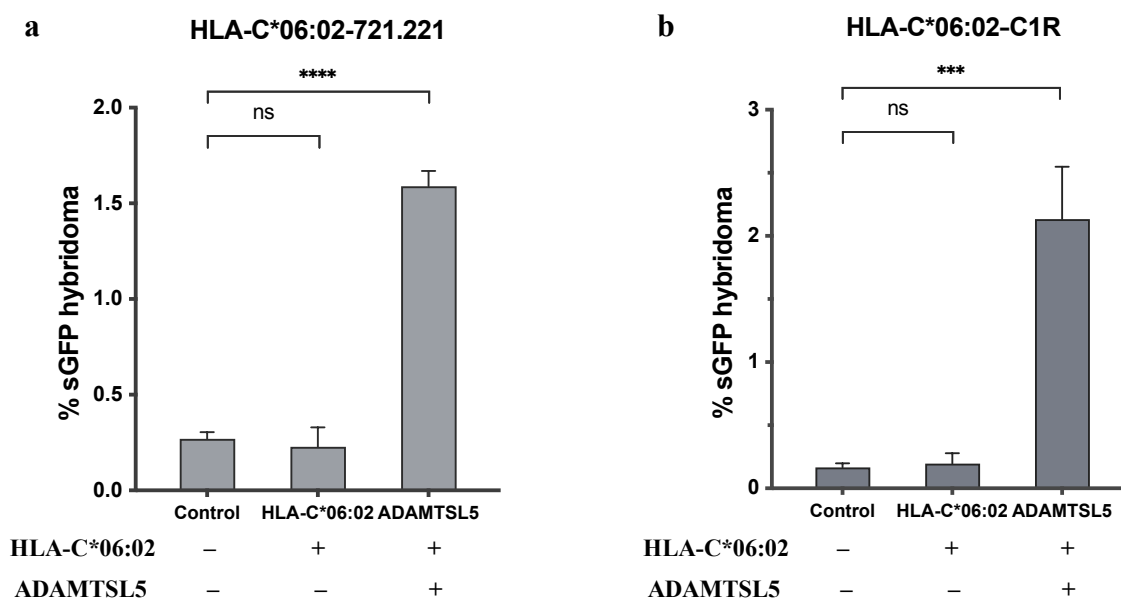


Figure 4.5.2.3 The co-nucleofection of plasmid-encoded ADAMTSL5 peptide and HLA-C*06:02, as opposed to the sole introduction of the HLA-C*06:02 plasmid, resulted in the activation of the V α 3S1/V β 13S1-TCR hybridoma in co-culture experiments with HLA-C*06:02-721.221 (a) or HLA-C*06:02-C1R cells (b). To serve as negative controls, the V α 3S1/V β 13S1-TCR hybridoma cells were co-cultured with HLA-C*06:02-721.221 or HLA-C*06:02-C1R that had not been transfected with plasmids. Data were summarized from technical triplicates from two or three independent experiments, compared by nonpaired t-test, and shown as mean \pm SEM, with statistical significance indicated as *** p < 0.001, **** p < 0.0001, and ns denoting no statistical difference.

From these experiments, I concluded that the antigenic peptide(s) stimulating the V α 3S1/V β 13S1 TCR in human B cells was not generated and presented by HLA-C*06:02-C1R and HLA-C*06:02-721.221 cells at all. This may be due to alterations induced by gamma-ray radiation of both C1R and 721.221 cell lines, which was the major difference between immunogenic EBV-transformed B cell lines and primary B cells from HLA-C*06:02 positive patients. Thus, the search for autoantigenic V α 3S1/V β 13S1 TCR peptides had to focus on the transcriptome and HLA-C*06:02 peptidome of the actual antigenic B cells.

4.6 Motif-based Database Search and Candidate Peptide Screening in B cell Transcriptomes

Since the transcriptome or immunopeptidome of HLA-C*06:02-C1R and HLA-C*06:02-721.221 may differ from the original transcriptome or immunopeptidome of human B cells, I performed a second attempt to identify the V α 3S1/V β 13S1 TCR ligands of B cells based on database screening.

4.6.1 TCR-hybridoma Stimulation with Selected Candidate Peptides

I screened 20,431 *Homo sapiens* “Reviewed (Swiss-Prot)” proteins in the UniProt database for antigenic peptides with the previously defined V α 3S1/V β 13S1 TCR-recognition motifs (**Table 4.4.5**). From the peptides identified by the screening strategies described in Section 3.4.3, I removed those peptides from the screening list that were present in the peptidomes of HLA-C*06:02-C1R and HLA-C*06:02-721.221, since both cell lines did not stimulate the V α 3S1/V β 13S1 TCR.

I selected 78 candidate peptides for screening out of the huge human peptide repertoire. The full list of plasmids encoding these peptides and their corresponding primers is given in **Tables 6.1.4** and **Table 6.2.4**. All of them were derived from proteins expressed in the transcriptome of human B cells. Candidate peptides defined as strong binders to HLA-C*06:02, as determined by the NetMHCcons 1.1 server, were preferentially to be examined. As a general experimental strategy, the coding cDNA of candidate peptide antigens was cloned into plasmids and co-expressed with HLA-C*06:02 in COS-7 cells or HEK293T cells to stimulate the V α 3S1/V β 13S1-TCR hybridoma in co-culture experiments.

I finally identified 13 peptides that stimulated the V α 3S1/V β 13S1 TCR when presented by COS-7 cells. None of them was present in the HLA-C*06:02 peptide repertoires isolated from HLA-C*06:02-C1R or HLA-C*06:02-721.221 (**Figure 4.6.1.1**).

a

Human proteins	1	2	3	4	5	6	7	8	9	TCR-activation
ADAMTSL5 ₅₇₋₆₅	V	R	S	R	R	C	L	R	L	100%
KIFC2 ₇₃₂₋₇₄₀	R	R	S	P	R	G	R	R	I	48%
PIF1 ₁₁₄₋₁₂₂	R	R	F	L	R	T	L	R	L	45%
HDAC6 ₈₂₈₋₈₃₆	R	R	Y	W	R	S	L	R	V	26%
ZNF670 ₂₉₀₋₂₉₈	F	R	C	S	R	V	L	R	V	24%
LRRC28 ₁₁₀₋₁₁₈	L	R	A	L	R	H	L	R	L	20%
FBXL19 ₆₄₉₋₆₅₇	R	R	C	P	R	L	R	R	L	16%
TAOK3 ₂₇₇₋₂₈₅	V	R	R	D	R	P	L	R	V	14%
BEX4 ₅₀₋₅₈	I	R	R	G	R	V	R	R	L	7%
CCDC71 ₄₄₂₋₄₅₀	Q	R	A	Q	R	I	L	R	V	6%
ALKBH7 ₁₉₀₋₁₉₈	R	R	I	P	R	G	R	R	I	6%
SCN9A ₁₆₁₅₋₁₆₂₃	A	R	I	G	R	I	L	R	L	5%
KCNMA1 ₂₇₁₋₂₇₉	L	R	F	L	R	A	L	R	L	4%
SLC47A1 ₂₀₋₂₈	V	R	G	S	R	C	L	R	L	4%

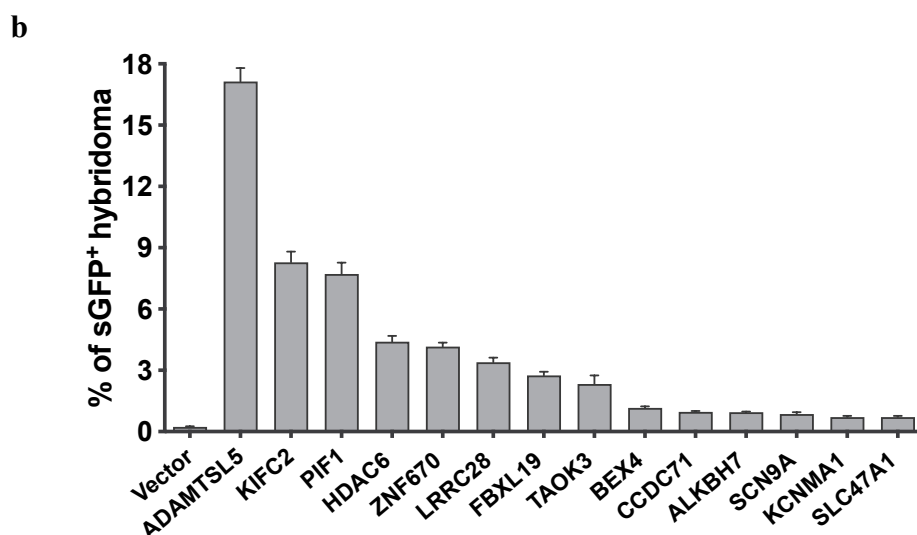


Figure 4.6.1.1 Candidate peptide antigens stimulating the V α 3S1/V β 13S1-TCR hybridoma that were identified in the human proteome and expressed in B cells. (a) Sequences of the candidate peptide antigens stimulating the V α 3S1/V β 13S1-TCR hybridoma. The percentages of TCR stimulation represent the peptide-induced stimulation relative to the ADAMTSL5 peptide. (b) TCR activation by different plasmid-encoded peptide antigens presented by COS-7-HLA-C*06:02. Empty vector served as a negative control. Data were summarized from technical triplicates from two or three independent experiments. Amino acids are designated by the one-letter code.

When co-expressed together with HLA-C*06:02 in HEK293T cells, only two out of the 13 peptides, PIF1 and LRRC28, were found to induce V α 3S1/V β 13S1 TCR activation (**Figure 4.6.1.2a**). HEK293T is a widely used human cell line for exogenous gene expression derived from a human embryonic kidney. HEK293T cells may possess distinct abilities in processing and presenting antigens compared to COS-7 cells, an African green monkey kidney fibroblast-like cell line.

In order to further clarify the antigenicity of the identified peptides, I employed synthetic peptides to stimulate the V α 3S1/V β 13S1 TCR hybridoma. For this purpose, I applied HLA-C*06:02 transfected COS-7 cells as antigen-presenting cells. In a comparable manner, three out of 13 peptide antigens examined, namely PIF1, LRRC28, and FBXL19, activated the V α 3S1/V β 13S1 TCR and thus were antigenic as synthetic peptides (as depicted in **Figure 4.6.1.2b**). I therefore assumed that these peptides are more likely to be autoantigens of B cells for the V α 3S1/V β 13S1 TCR.

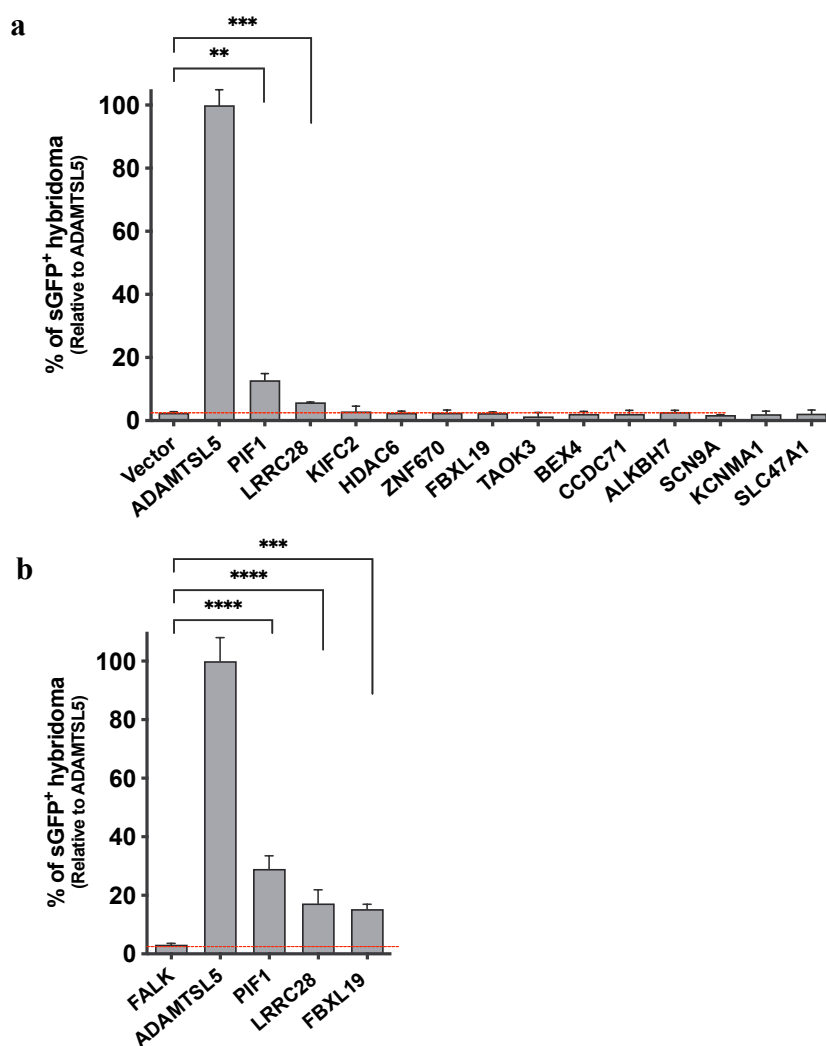


Figure 4.6.1.2 Candidate peptide antigens stimulating the V α 3S1/V β 13S1-TCR hybridoma that were identified in the human proteome and expressed in B cells. (a) Antigenic candidate peptide antigens verified by plasmid transfection in HEK293T cells. TCR activation by candidate peptide antigens is given relative to the stimulation induced by the ADAMTSL5 peptide. Empty vector served as a negative control. (b) V α 3S1/V β 13S1 TCR-hybridoma stimulation by synthetic peptides presented by COS-7-HLA-C*06:02. FALK peptide served as negative control. Data were summarized from technical triplicates from two or three independent experiments, compared by nonpaired t-test, and shown as mean \pm SEM, with statistical significance indicated as ** p < 0.01, *** p < 0.001, **** p < 0.0001.

4.6.2 siRNA Knockdown Experiments

Unlike self-peptides derived from the elution of HLA-C*06:02 on B cells, the candidate peptide antigens selected from the human proteome or B-cell transcriptome based on the V α 3S1/V β 13S1-TCR recognition motifs were solely predicted with computational prediction tools. A question remained of whether these peptides are actually presented by HLA-C*06:02 on B cells.

Consequently, I had to investigate whether these stimulating peptides could be generated through the processing of the parental proteins and subsequently be presented by HLA-C*06:02

on B cells to activate the V α 3S1/V β 13S1 TCR. To achieve this objective, I established protocols for nucleofection of B cell lines with siRNA to suppress the expression of the respective parental proteins, which were then used to stimulate the V α 3S1/V β 13S1-TCR hybridoma in co-culture experiments.

siRNAs targeting PIF1, LRRC28, and FBXL19 and several other parental proteins of stimulating peptides were applied (**Figure 4.6.2**). For the positive control, I used siRNA targeting β 2-microglobulin, which is part of the heterodimeric HLA-class I complex and required for the expression of MHC class I proteins on the cell surface for antigen presentation to CD8⁺ T cells. siNeg served as a negative control. Sequences of siRNAs are listed in Section 6.4.

Figure 4.6.2 demonstrates that neither at 48 h nor 72 h following nucleofection of the antigenic B cell line D22, any of the siRNAs targeting parent proteins of candidate peptide antigens were able to achieve a reduction in the antigenicity of B cells. Instead, TCR stimulation was strongly reduced by silencing of β 2-microglobulin. Thus, the knockdown experiments could not verify the stimulating peptides as antigens that are naturally generated from the parental proteins in B cells to stimulate the V α 3S1/V β 13S1 TCR.

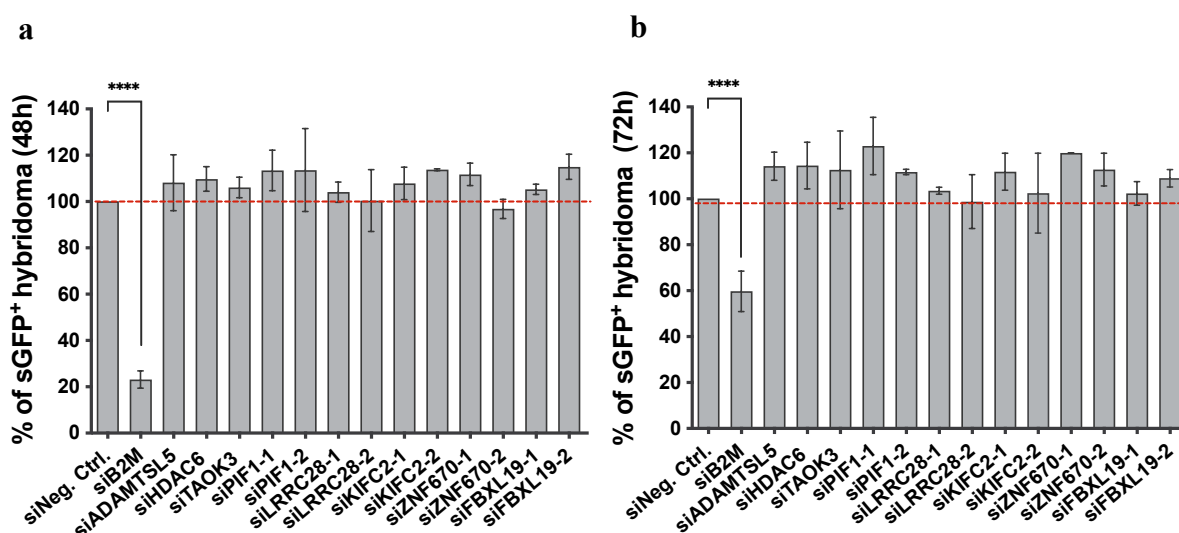


Figure 4.6.2 V α 3S1/V β 13S1 TCR activation by D22 assessed at 48 h (a) and 72 h (b) subsequent to nucleofection of D22 with various siRNAs targeting parental proteins of candidate peptide antigens. siB2M, siADAMTSL5, siTAOK3, siHDAC6 were validated siRNAs. siB2M served as a positive control, while the siNeg served as a negative control and reference value (100%). Only siB2M exhibited a significant reduction in the TCR activation of D22 among all tested siRNAs. Data were summarized from technical triplicates from two or three independent experiments, compared by nonpaired t-test, and shown as mean \pm SEM, with statistical significance indicated as **** p < 0.0001.

4.7 Screening of V α 3S1/V β 13S1-TCR Ligands from HLA-C*06:02 homozygous B-cell Peptidomes

The second approach to identify autoantigenic B-cell peptides based on the V α 3S1/V β 13S1-TCR recognition motifs against human proteome had also not yielded conclusive results. Therefore, I initiated another strategy. As described in Section 3.4.2, I obtained six EBV-transformed B cell lines homozygous for HLA-C*06:02. Since they were samples from the 1000 Genomes Project, their genetic information was available. Endogenous human B-cell HLA-C*06:02-peptidomes were eluted from four of these cell lines by applying LC-MS/MS. The presence of peptides in the HLA-C*06:02 peptidome stimulating the V α 3S1/V β 13S1 TCR would likely prove their role as psoriatic B cell autoantigens, that may cause a cross-reactive immune response against melanocytes.

4.7.1 TCR Activation by Various HLA-C*06:02 Homozygous B cells

First, I co-cultured the HLA-C*06:02-homozygous B cell lines with the TCR hybridoma to verify their antigenicity for the V α 3S1/V β 13S1 TCR. After 24 hours, induction of sGFP was determined by flow cytometry analysis. All six HLA-C*06:02-homozygous B cell lines induced activation of the V α 3S1/V β 13S1-TCR hybridoma to varying degrees. Among them, cell lines GM20771 and HG00131 induced the strongest stimulation of V α 3S1/V β 13S1-TCR hybridoma cells (**Figure 4.7.1 a**). Similar to primary melanocytes or primary B cells from blood or tonsils, IFN- γ enhanced the V α 3S1/V β 13S1-TCR stimulation in these B cell lines, but in a smaller magnitude.

To investigate the correlation of V α 3S1/V β 13S1-TCR hybridoma activation of HLA-C*06:02-homozygous B cell lines with the expression of HLA-C*06:02, I stained these B cell lines with anti-human HLA-C and anti-human HLA-ABC antibodies. By aligning hybridoma activation and HLA expression levels, I found that the expression of HLA-C, instead of the expression of HLA-ABC, was highly positively correlated to the degree of V α 3S1/V β 13S1-TCR hybridoma activation (**Figure 4.7.1 b and c**). Thus, expression levels of HLA-C*06:02 determined the stimulatory capacity of the B-cell lines.

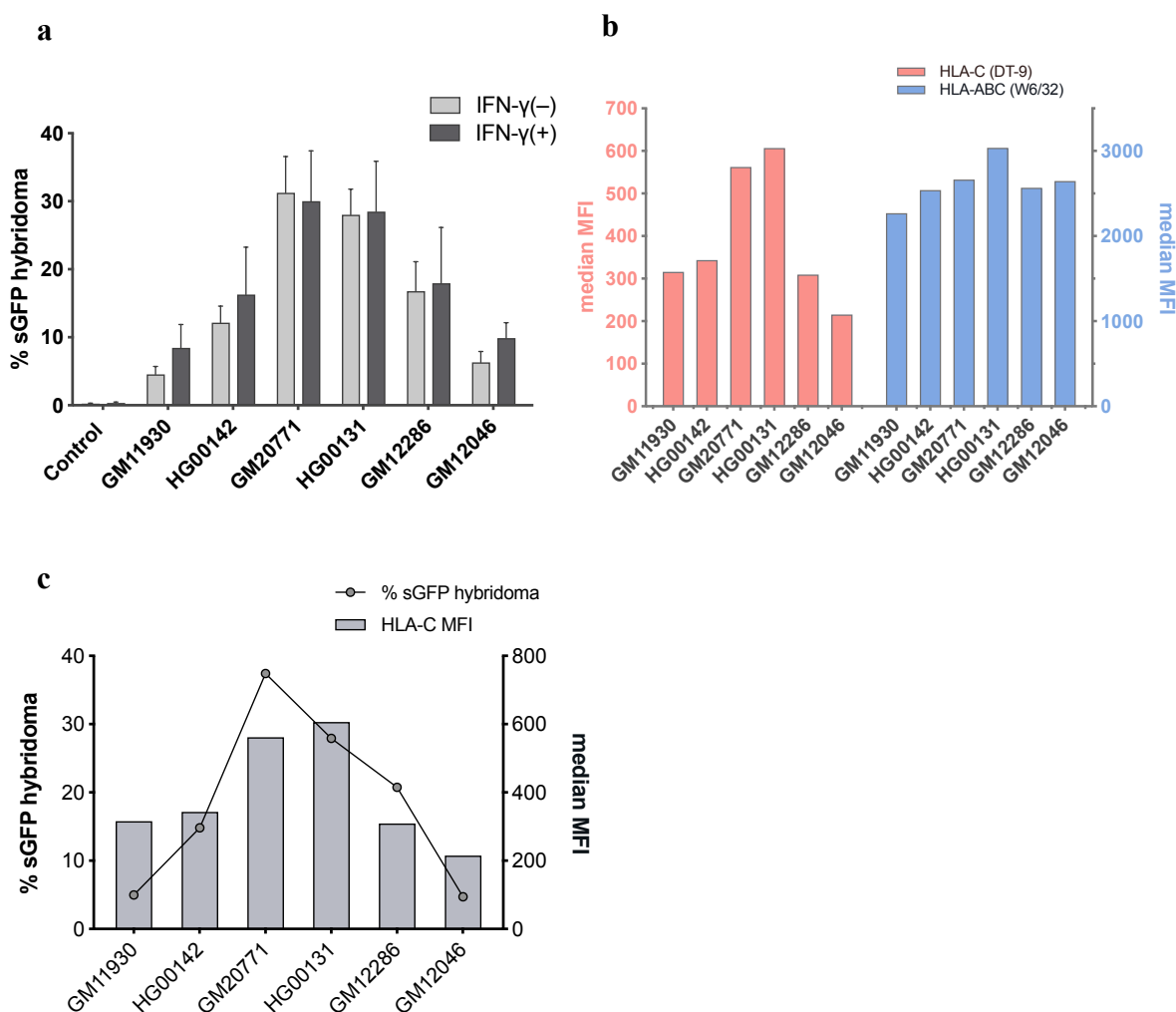


Figure 4.7.1 Induction of sGFP in the V α 3S1/V β 13S1-TCR hybridoma cell line by various HLA-C*06:02-homozygous B cell lines and correlation between TCR-hybridoma activation and HLA-C expression. (a) TCR-hybridoma activation by various HLA-C*06:02-homozygous B cell lines with or without preincubation with IFN- γ to enhance HLA-C expression. The V α 3S1/V β 13S1-TCR hybridoma cells incubated in culture plates solely without other cells served as negative control. (b) Mean fluorescence intensity (MFI) of HLA-C or HLA-ABC staining of various HLA-C*06:02-homozygous B cell lines was assessed by flow cytometry. The monoclonal antibodies for HLA-C or HLA-ABC staining were DT-9 and W6/32, respectively. (c) Alignment of TCR hybridoma stimulation (bars, without preincubation with IFN- γ) and MFI of HLA-C staining (black line with dots) of different HLA-C*06:02-homozygous B cell lines. Data were assessed by multiparametric flow cytometry analysis. Data were summarized from technical triplicates from two or three independent experiments.

According to our previous study, ERAP1 haplotypes control the level of autoimmunogenicity of melanocytes in psoriasis by different autoantigen yields. In melanocytes, the ERAP1 risk haplotype Hap2 generates significantly higher stimulatory amounts of the ADAMTSL5 epitope from precursor peptides and greater HLA-C expression than the protective haplotype, Hap10 (Arakawa *et al.*, 2021). Therefore, we determined the ERAP1 haplotype information of the six homozygous HLA-C*06:02 B cell lines from the genetic data of the 1000 Genomes Project (Table 3.4.2). Among them, GM11930 and HG00142 were homozygous for Hap2 or Hap10,

respectively, corresponding to the epistasis between *HLA-C*06:02* and *ERAP1* variants in psoriasis risk. Interestingly, these two cell lines stimulated the V α 3S1/V β 13S1 TCR the least. Because the generation of the ADAMTSL5 peptide from peptide precursors is ERAP1-dependent and much affected by the trimming activities of different ERAP1 haplotypes, this is another indication that B cells may present a different autoantigen than ADAMTSL5.

According to hybridoma activation results, ERAP1 haplotype information and growth rate of cells (GM12286 and GM10246 grew slowly, not depicted), four of the six *HLA-C*06:02*-homozygous B cell lines were selected for the elution of *HLA-C*06:02*-associated peptides: GM11930, HG00142, GM20771 and HG00131. I expanded these cell lines in culture to each 1×10^9 cells for peptide elution.

4.7.2 Analysis of *HLA-C*06:02* Peptidomes

In collaboration with Andreas Schlosser and Melissa Bernhardt, Center for Integrative and Translational Bioimaging in Universität Würzburg, we obtained a list of peptides eluted from *HLA-C*06:02* from the four *HLA-C*06:02*-homozygous B cell lines. None of them contained the ADAMTSL5 peptide or any of the 13 V α 3S1/V β 13S1 TCR ligands identified from the human proteome, further emphasizing that *HLA-C*06:02* presents another V α 3S1/V β 13S1 TCR ligand on B cells than on melanocytes.

Concurrently, a large HLA peptidome dataset, including an *HLA-C*06:02* peptidome, was released by Sarkizova and colleagues (Sarkizova *et al.*, 2020) by applying stable *HLA-C*06:02* transfectants of the 721.221 cell line. Together with *HLA-C*06:02* peptidomes unveiled by Di Marco and Mobbs, there were three *HLA-C*06:02* peptidomes eluted from C1R or 721.221 cell lines available then.

These matrices were analyzed comprehensively, not only to search for immunogenic self-peptide(s) in B cells but also to obtain deeper insights into peptide-binding specificities of *HLA-C*06:02* molecules and the association of ERAP1 haplotypes with *HLA-C*06:02*-restricted B-cell immunogenicity.

4.7.2.1 Yields and Length Distributions of *HLA-C*06:02*-Peptides

In total, between 234 and 2,281 *HLA-C*06:02* ligands could be identified for the respective *HLA-C*06:02*⁺ B cell lines. **Table 4.7.2.1** displayed the overall yields and amounts of specific

lengths of HLA-C*06:02-peptides. The yields and length distributions of respective HLA-C*06:02 peptidomes are also shown in **Figure 4.7.2.1.1**.

Source of Peptidome	8-mers	9-mers	10-mers	11-mers	> 11-mers	Yields
GM11930	122 (31.77%)	260 (67.71%)	1 (0.26%)	0 (0%)	1 (0.26%)	384 (100%)
HG00142	21 (8.97%)	210 (89.74%)	1 (0.43%)	2 (0.85%)	0 (0%)	234 (100%)
GM20771	101 (14.35%)	591 (83.95%)	8 (1.14%)	3 (0.43%)	1 (0.14%)	704 (100%)
HG00131	70 (15.12%)	390 (84.23%)	2 (0.43%)	1 (0.22%)	0 (0%)	463 (100%)
Di Marco	47 (4.93%)	870 (91.29%)	32 (3.36%)	4 (0.42%)	0 (0%)	953 (100%)
Sarkizova	277 (12.14%)	1628 (71.37%)	151 (6.62%)	77 (3.38%)	148 (6.49%)	2,281 (100%)
Mobbs	37 (1.84%)	750 (37.26%)	78 (3.87%)	59 (2.93%)	1088 (54.05%)	2,013 (100%)

Table 4.7.2.1 Yields and numbers of specific lengths of HLA-C*06:02-ligands in various HLA-C*06:02 peptidomes. Numbers present the amounts of specific peptide length (mainly 8- to 11-mers), and percentages shown in parentheses present the proportion of the length among all peptides.

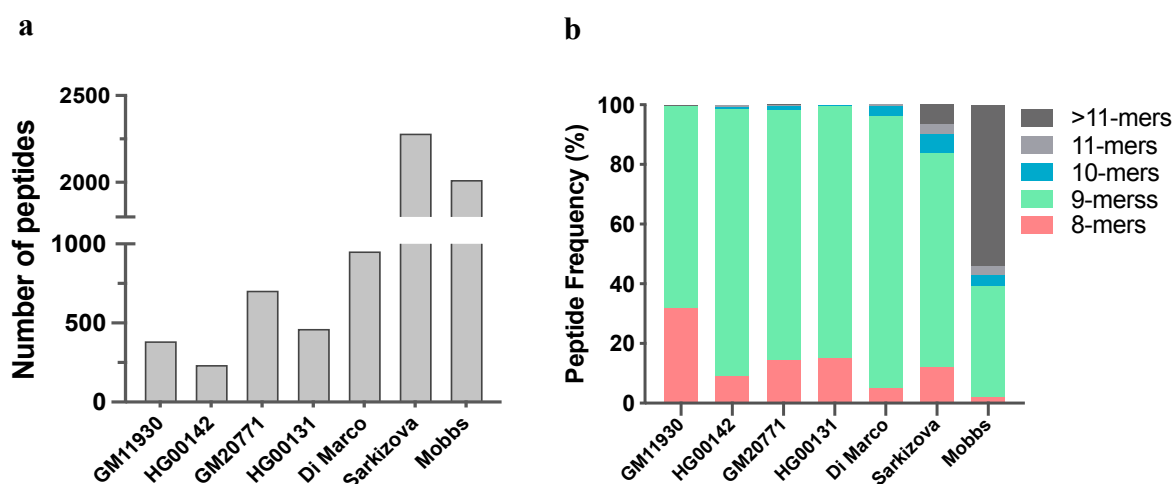


Figure 4.7.2.1.1 Yields and length distributions of respective HLA-C*06:02-peptidomes.

The binding groove of MHC class I molecules usually accepts peptides with a length of 8-10 amino acids and appropriate anchor residues. The length distribution of respective HLA-C*06:02 peptidomes exhibited a distinct composition of peptide lengths, with more than 90% of peptides being 8-10 amino acids long in the four HLA-C*06:02-homozygous B cell lines. The peptidomes published by Sarkizova and Mobbs instead contained a higher proportion of longer peptides (11-mers & >11-mers) (**Figure 4.7.2.1.1b**). There was a large probability that those long peptides were false binders due to different criteria and thresholds for defining true HLA-C*06:02 binders in different studies. This was indirect evidence that the peptidomes eluted from the four HLA-C*06:02-homozygous B cell lines more reliably represented the regular HLA-C*06:02 immunopeptidome of B cells, though with lesser yields.

We noticed that HLA-C*06:02 peptides eluted from C1R or 721.221 cell lines were much more abundant than those from HLA-C*06:02-homozygous B cell lines. Natural expression of HLA-

C shows a lower level at the cell surface and represents only ~10% of classical MHC-I molecules. Instead, the artificial HLA-C*06:02-transfectants C1R or 721.221 may have much higher HLA-C expression on the cell surface. The different degrees of HLA-C expression may lead to a difference in HLA-C*06:02 peptide yields. In order to verify this conjecture, I compared the HLA-C expression of several EBV-transformed B cell lines with the HLA-C*06:02-transfectant 721.221. **Figure 4.7.2.1.2** revealed that the artificial HLA-C*06:02-transfectant cell line HLA-C*06:02-721.221 with higher yields of HLA-C*06:02 ligands (2281 in Sarkizova's and 2013 in Mobbs') has a significantly higher HLA-C expression than the EBV-transformed B cell lines.

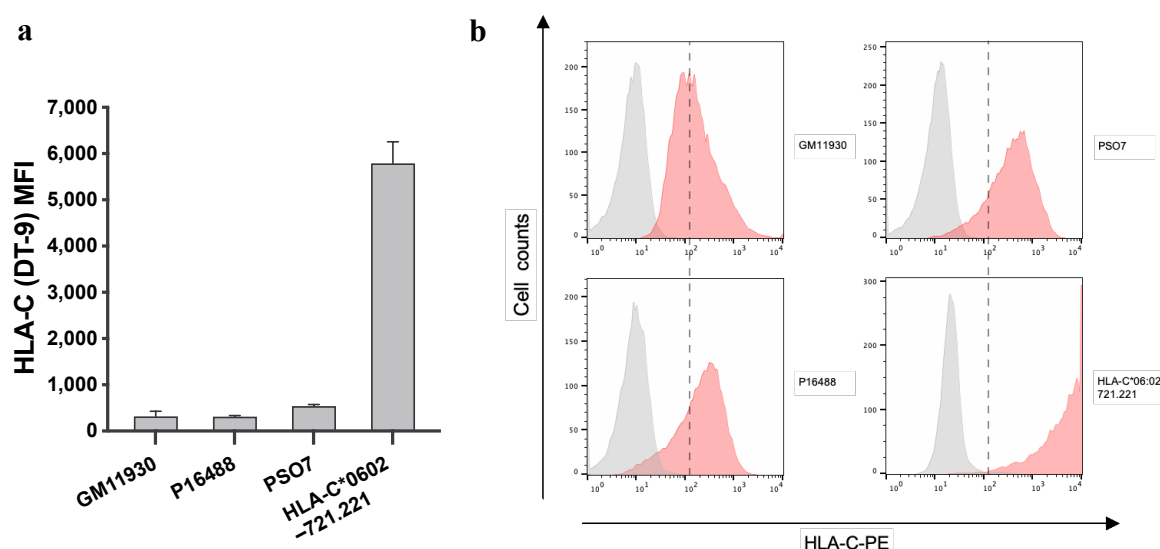


Figure 4.7.2.1.2 HLA-C*06:02 stably transfected 721.221 cells have much higher HLA-C expression than other HLA-C*06:02⁺ B cell lines with natural HLA-C expression. (a) Mean fluorescence intensity (MFI) of HLA-C (DT-9) staining of HLA-C*06:02 stably transfected 721.221 or various EBV-transformed B cell lines. (b) Representative flow cytometric panels of HLA-C (DT-9) staining with isotype control (gray) of HLA-C*06:02 stably transfected 721.221 or of various EBV-transformed B cell lines. GM11930, P16488, and PSO7 are HLA-C*06:02-homozygous, HLA-C*06:02-negative, or HLA-C*06:02-heterozygous B cell lines, respectively. Data were summarized from technical triplicates from two or three independent experiments.

While the HLA-C*06:02 immunopeptidomes isolated from C1R and 721.221 contained 4,411 individual peptides, the peptidomes isolated from all four B cell lines contained a total of 1,215 different peptides. The Venn diagram displayed in **Figure 4.7.2.1.3a** shows an overlap of 526 peptides between the HLA-C*06:02-peptidomes from the four homozygous HLA-C*06:02 B cell lines and the three HLA-C*06:02-peptidomes published for cell lines C1R or 721.221. There was a clear overlap in the peptidomes eluted from HLA-C*06:02 of the four EBV-transformed B cell lines, but only 53 peptides were found across all of them. In principle, the selection of candidate peptide antigens for the V α 3S1/V β 13S1 TCR should avoid peptide ligands eluted from HLA-C*06:02 of C1R and 721.221, because these cell lines did not

stimulate the V α 3S1/V β 13S1 TCR. Therefore, I excluded these peptides from my further antigen search and focused on the overlapping peptide repertoires from the four HLA-C*06:02 homozygous B cell lines, which all stimulated the V α 3S1/V β 13S1 TCR (**Figure 4.7.2.1.3b**). After calculation, the frequencies of unshared ligands in GM11930, HG00142, GM20771, HG00131 were 57.3%, 29.9%, 53.6%, 37.4% overall ligands, respectively.

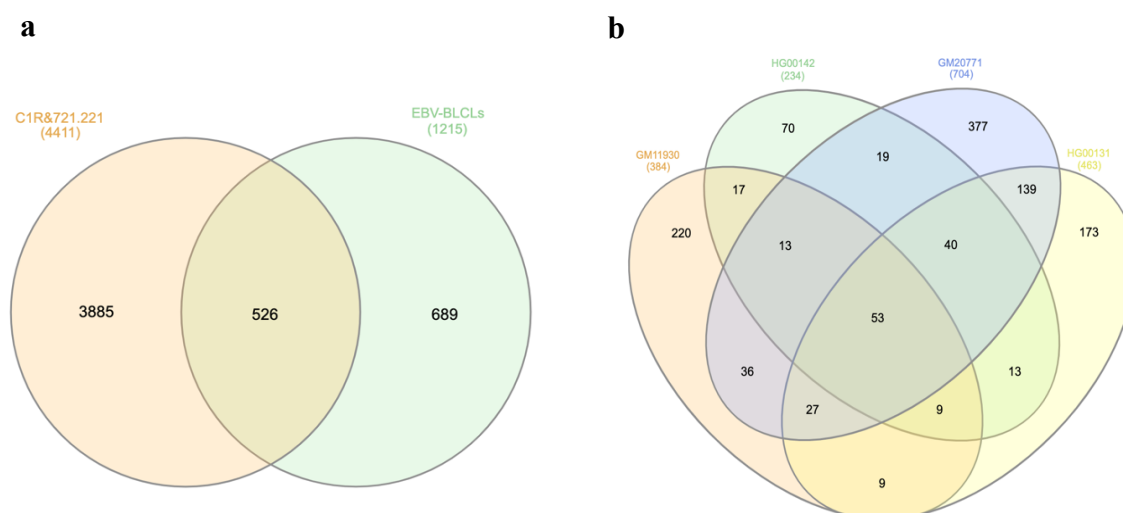


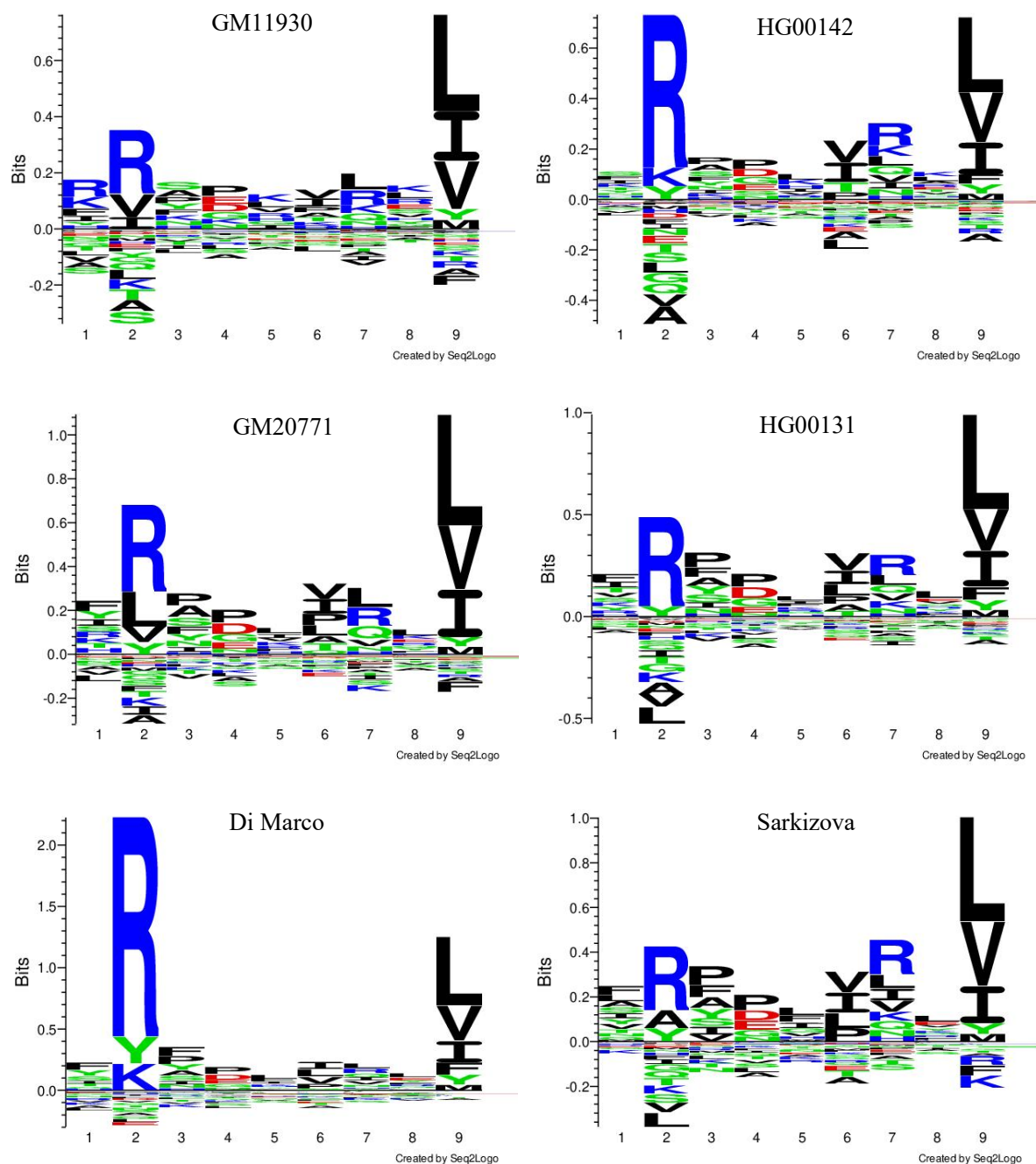
Figure 4.7.2.1.3 Overlap of different HLA-C*06:02-peptidomes. (a) Overlap of HLA-C*06:02 peptidomes from the four homozygous HLA-C*06:02⁺ B cell lines and HLA-C*06:02-transfected C1R or 721.221 cell lines (marked as “EBV-BLCLs” and “C1R & 721.221” respectively). When several peptidomes were aggregated into one group, the replicates were removed, leaving only the unique values for the Venn diagrams. (b) Overlap of peptides from four homozygous HLA-C*06:02 B cell lines. Venn diagrams were created by InteractiVenn (Heberle *et al.*, 2015), and numbers present the amounts of peptides in overlapping or non-overlapping areas.

4.7.2.2 Peptide-binding Motifs of HLA-C*06:02 Molecules

I visualized the peptide-binding motifs of HLA-C*06:02 molecules of the seven HLA-C*06:02 peptidomes by generating sequence logos of 9-mer peptides. For convenience of comparison, I placed the V α 3S1/V β 13S1-TCR ligand motif shown in Section 4.4.4 next to the peptide-binding motifs of the HLA-C*06:02 molecules from the different B-cell lines (**Figure 4.7.2.2**).

These peptide-binding motifs share dominant anchor residue arginine (Arg, R) and leucine (Leu, L) at anchor positions P2 and P9, respectively. Anchor residues valine (Val, V) and isoleucine (Ile, I) were also preferred by P9 in all motifs of peptidomes. Most motifs of peptidomes had a clear preference for arginine or leucine at the auxiliary anchor position P7, where lysine (Lys, K) was also accepted, such as in HG00142’s and Mobbs’ peptidomes. Only the peptide-binding motifs of HLA-C*06:02 in Di Marco’s peptidome had no preference for any amino acid residues at P7.

The motifs were much consistent with the V α 3S1/V β 13S1 TCR-ligands presented by HLA-C*06:02. As a difference, the V α 3S1/V β 13S1 TCR-ligands showed a strong preference for arginine and lysine at the TCR-contacting positions P5 and P8. The motif analysis indicated the reliability and feasibility of our autoantigen search based on the V α 3S1/V β 13S1 TCR-ligand motif.



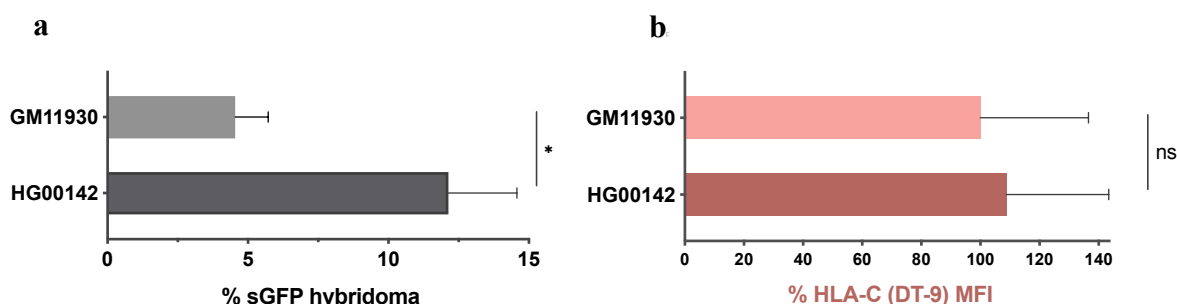


Figure 4.7.2.3.1 Comparison of hybridoma activation and HLA-C expression between GM11930 (Hap2/Hap2) and HG00142 (Hap10/Hap10). (a) Induction of sGFP in V α 3S1/V β 13S1-TCR hybridoma by HG00142 was significantly higher than that by GM11930. (b) Mean fluorescence intensity (MFI) of HLA-C of GM11930 and HG00142 was assessed by flow cytometry and normalized to means of HLA-C MFI of GM11930. Data were summarized from technical triplicates from two independent experiments, compared by nonpaired t-test, and shown as mean \pm SEM, with statistical significance indicated as $*p < 0.05$ and ns denoting no statistical difference.

The risk ERAP1 haplotype Hap2 generates a higher yield of the psoriatic autoantigenic ADAMTSL5 peptide from NH₂-elongated precursor peptides, compared with the protective haplotype Hap10 (Arakawa *et al.*, 2021). Consistent with these findings, my peptidome analysis revealed that GM11930 (Hap2/Hap2) supplied a significantly higher number of different HLA-C*06:02 peptides than HG00142 (Hap10/Hap10) (384 vs. 234, **Table 4.7.2.1**) and a higher proportion of HLA-C peptides among all HLA-class I peptides (**Figure 4.7.2.3.2a**).

The trimming experiments by Arakawa *et al.* have revealed that Hap2 cleaved the ADAMTSL5 precursor peptides much more efficiently than Hap10 did. By analysis of length differences in HLA-C*06:02 peptidomes between GM11930 and HG00142, the higher trimming efficiency of Hap2 than Hap10 was validated by the observation that the proportion of 8-mers in the overall ligands of GM11930 was higher than in HG00142 (**Figure 4.7.2.3.2b**).

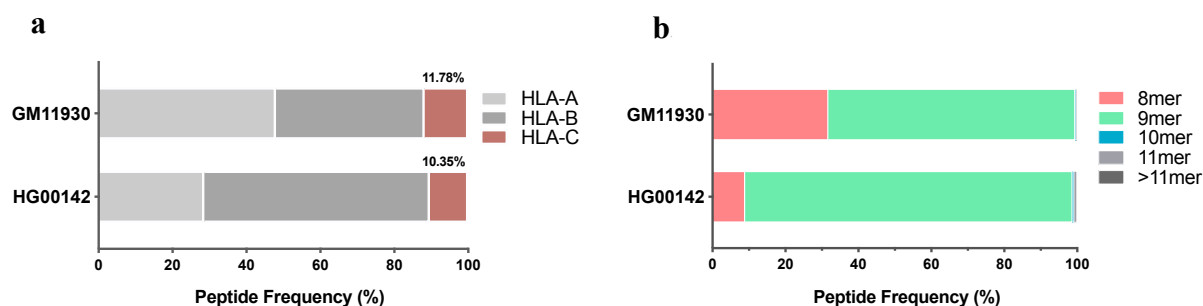


Figure 4.7.2.3.2 Differences in proportion and length distribution of HLA-C ligands between GM11930 and HG00142. (a) Proportion of HLA-A, B, C ligands in the overall HLA-class I ligands of GM11930 or HG00142. GM11930 (Hap2/Hap2) had a higher proportion of HLA-C ligands than HG00142 (Hap10/Hap10) (11.78% vs. 10.35%) among overall HLA-class I ligands. (b) Length distribution of HLA-C*06:02 peptidomes from GM11930 or HG00142. Proportion of 8-mers in the overall HLA-C*06:02 ligands of GM11930 was significantly higher than in HG00142.

ERAP1 is an aminopeptidase that creates the appropriate peptide length for HLA-C*06:02 presentation by trimming NH₂-terminally elongated peptide precursors. It is rational to presume that ERAP1 Hap2, with its higher trimming efficiency compared to Hap10, may produce peptides that mainly differ in N-terminal amino acid residues. This was supported by the bar chart showing the composition of amino acids at a given position in the peptides of the HLA-C*06:02 peptidomes. Except for P1 at the N-terminus, amino acids at other positions had a similar composition between GM11930 and HG00142. The frequencies of basic N-terminal residues K (lysine) and R (arginine) were much higher in peptides eluted from GM11930 than from HG00142, while hydrophilic neutral amino acids S (Serine), T (Threonine) and hydrophobic residues V (Valine) and Y (Tyrosine) had a higher proportion in peptides from HG00142 (**Figure 4.7.2.3.3**). Still, the detailed mechanisms of how Hap2 and Hap10 trim peptide precursors remain largely unknown.

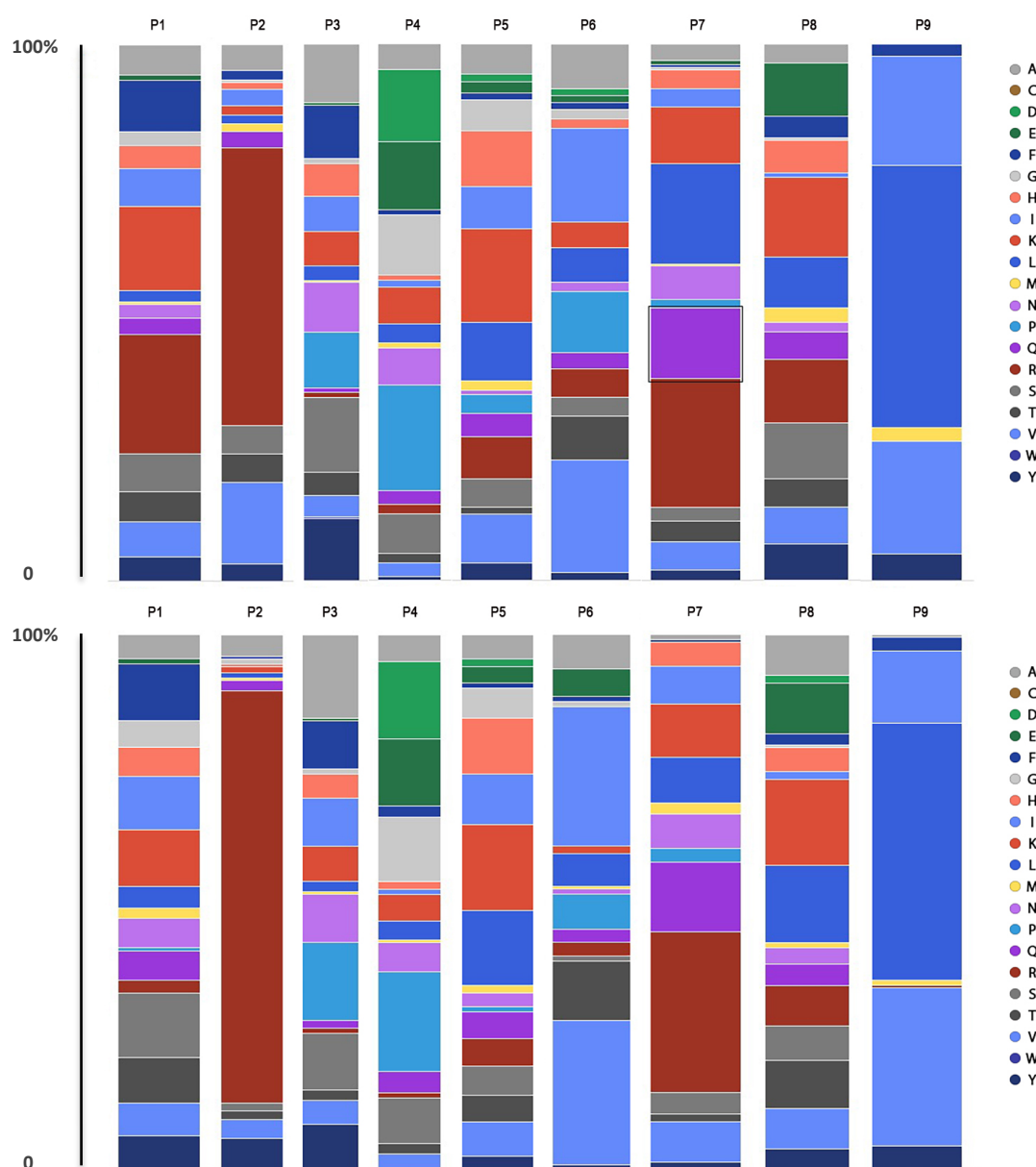


Figure 4.7.2.3.3 The bar chart showing the proportion of respective amino acids in the bar indicates the frequency of amino acids at a given position in the HLA-C*06:02 peptidome of GM11930 (upper) and HG00142 (lower).

However, it should be admitted that while GM11930 and HG00142 are both HLA-C*06:02 homozygous B cell lines showing immunogenicity to V α 3S1/V β 13S1-TCR hybridoma, the level of HLA-C expression and the elution of HLA-C*06:02 ligands may depend on multifactorial factors. The characteristics that they carry homozygous haplotypes of ERAP1 make them suitable for my study, but still, the cell lines are from different individuals. An unbiased comparison of functions of different ERAP1 haplotypes in the autoimmune response against B cells would require ERAP1^{-/-} B cells reconstituted with either Hap2 or Hap10. Nevertheless, this is another indication that the B-cell autoantigen may be subject to different processing and is distinct from the melanocyte autoantigen.

4.7.3 Screening of Autoantigen Candidates from HLA-C*06:02-Peptidomes of B cells

The comprehensive analysis of HLA-C*06:02-peptidomes from different sources provided me with much information for the next autoantigen search, given that the ADAMTSL5 peptide was not represented in these peptidomes. In the next step, I screened the four HLA-C*06:02 peptidomes obtained from Professor Schlosser for candidate peptide sequences corresponding to the V α 3S1/V β 13S1-TCR ligand motifs, excluding the peptides from the HLA-C*06:02 peptidomes from C1R or 721.221. A total of 689 peptides in four HLA-C*06:02 peptidomes (after removal of 526 peptides overlapping with C1R or 721.221) were included in my analysis.

According to the peptide recognition motif, I selected 81 peptides as candidate antigens of the V α 3S1/V β 13S1 TCR. The full list of these peptides is given in **Table 6.1.5** and **Table 6.2.5** in the supplementary data together with the encoding cDNA sequences and corresponding primers. Following the established protocols, the cDNAs corresponding to these peptides were cloned into plasmids and co-expressed with HLA-C*06:02 in COS-7 cells for antigen presentation to the psoriatic V α 3S1/V β 13S1 TCR in co-culture experiments. Unexpectedly, none of these promising candidate peptides exhibited antigenicity for the V α 3S1/V β 13S1 TCR when presented by COS-7-HLA-C*06:02.

I then chose WM278, a melanoma cell line naturally carrying HLA-C*06:02, as another APC to examine the antigenicity of the candidate peptides. This selection was based on the previous finding that WM278 cells are highly susceptible to transfection and effectively present plasmid-encoded peptide antigens to the V α 3S1/V β 13S1 TCR (Arakawa *et al.*, 2015; Arakawa *et al.*,

2021). WM278 cells themselves are antigenic for the V α 3S1/V β 13S1 TCR, as they naturally express and present the ADAMTSL5 peptide and, therefore, stimulate the V α 3S1/V β 13S1 TCR. Nevertheless, WM278 cells are suitable for this approach because their antigenicity for the V α 3S1/V β 13S1 TCR depends much on the addition of IFN- γ to increase the expression of ERAP1 and HLA-C*06:02 and is otherwise relatively low. Consequently, all stimulation values had to be normalized by accounting for this natural activation.

4.7.3.1 TCR-Hybridoma Activation by Selected Candidate Peptides

Among the 81 candidate antigens selected from the HLA-C*06:02 immunopeptidomes of the B cell lines, 7 peptides stimulated the V α 3S1/V β 13S1 TCR when expressed in WM278 cells but not in COS-7-HLA-C*06:02 cells (**Figure 4.7.3.1.1**). The ADAMTSL5 nonamer and the PIF1 peptides, which I had identified as V α 3S1/V β 13S1 TCR ligand using the motif-based database search in the human proteome, served as positive controls.

a

Human proteins	1	2	3	4	5	6	7	8	9	TCR-activation
ADAMTSL5 ₅₇₋₆₅	V	R	S	R	R	C	L	R	L	100%
PIF1 ₁₁₄₋₁₂₂	R	R	F	L	R	T	L	R	L	61%
TIPARP ₄₉₀₋₄₉₈	Y	R	I	L	Q	I	L	R	V	89%
FGR ₁₉₀₋₁₉₈	T	R	G	D	H	V	K	H	Y	82%
RANBP2 ₂₀₇₅₋₂₀₈₃	M	R	R	E	Q	V	L	K	V	55%
CIZ1 ₆₉₂₋₇₀₀	R	Y	F	K	T	P	R	K	F	50%
TPGS1 ₁₄₂₋₁₅₀	T	Y	S	E	L	L	R	R	I	42%
RNF111 ₂₀₈₋₂₁₅		R	R	L	P	C	R	K	R	40%
ETF1 ₁₉₇₋₂₀₅	K	R	H	N	Y	V	R	K	V	24%

b

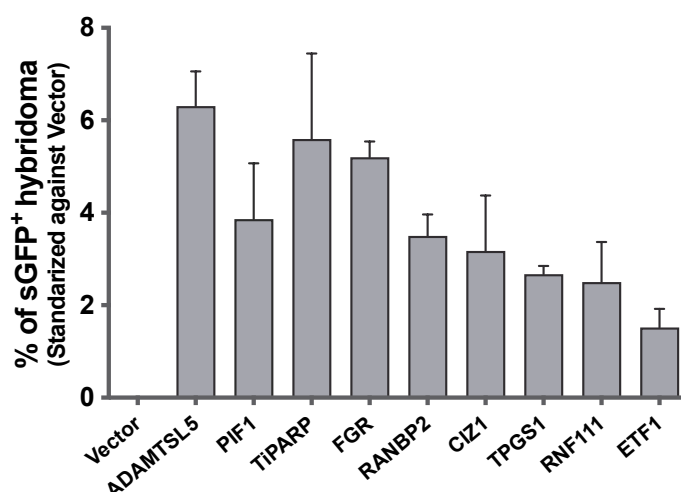


Figure 4.7.3.1.1 V α 3S1/V β 13S1 TCR peptide ligands identified through screening of HLA-C*06:02 peptidomes from HLA-C*06:02-homozygous B cell lines. (a) Sequences of candidate peptide antigens stimulating the V α 3S1/V β 13S1-TCR hybridoma. The percentages of TCR stimulation represent the peptide-induced stimulation relative to the ADAMTSL5 peptide. (b) V α 3S1/V β 13S1-TCR hybridoma activation by various peptides presented by WM278 as normalized to the basal activation by WM278 cell transfected with empty vector. ADAMTSL5 and PIF1 peptide served as positive controls. Data were summarized from technical triplicates from two or three independent experiments. Amino acids are designated by the one-letter code.

Thus, the HLA-C*06:02 immunopeptidomes of the B cell lines contained several peptides that were antigenic for the V α 3S1/V β 13S1 TCR and could serve as B-cell autoantigens to stimulate the melanocyte-directed autoimmune response in psoriasis. The lack of antigenicity of the plasmid-encoded peptides in COS-7 cells again suggests that the processing of particular peptides may depend on the respective cell type.

According to the presence of various stimulatory peptides in the HLA-C*06:02 peptidomes of the B-cell lines, the antigenicity of select peptides cannot be tested by knockdown experiments, as this would not affect the expression of the parental proteins of the other immunogenic peptides presented simultaneously. Therefore, I employed synthetic peptides to test their actual antigenicity when presented as exogenous antigens by HLA-C*06:02-721.221 or WM278 cell lines. Confirmation of the antigenicity of these peptides, especially in 721.221 cells, a cell line lacking antigenicity for V α 3S1/V β 13S1 TCR, would provide additional evidence for a role as pathogenic self-peptides in B cells. Moreover, by using synthetic peptides, stimulation was independent of cell type-specific processing of plasmid-encoded peptides.

The 7 peptides that showed antigenicity for the V α 3S1/V β 13S1 TCR in WM278 cells were selected for the test of synthetic peptides. The FALK peptide served as a negative control. Only the TiPARP peptide induced TCR activation when presented by HLA-C*06:02-721.221. While it activated a smaller number of hybridoma cells than did the ADAMTSL5 peptide, it exhibited a higher stimulatory capacity in terms of the strength of sGFP expression in activated V α 3S1/V β 13S1 TCR hybridoma cells (**Figure 4.7.3.1.2 a & b**): the mean fluorescence intensity (MFI) in hybridoma cells stimulated with the synthetic TiPARP peptide was substantially higher than that induced by synthetic ADAMTSL5 peptide (**Figure 4.7.3.1.2 c**). Similar results were obtained when WM278 cells were used as APC for stimulation of the V α 3S1/V β 13S1 TCR with synthetic peptides (**Figure 4.7.3.1.2 d**), confirming the results obtained with HLA-C*06:02-721.22 cells. Thus, the TiPARP peptide is indeed a B-cell autoantigen for the V α 3S1/V β 13S1 TCR.

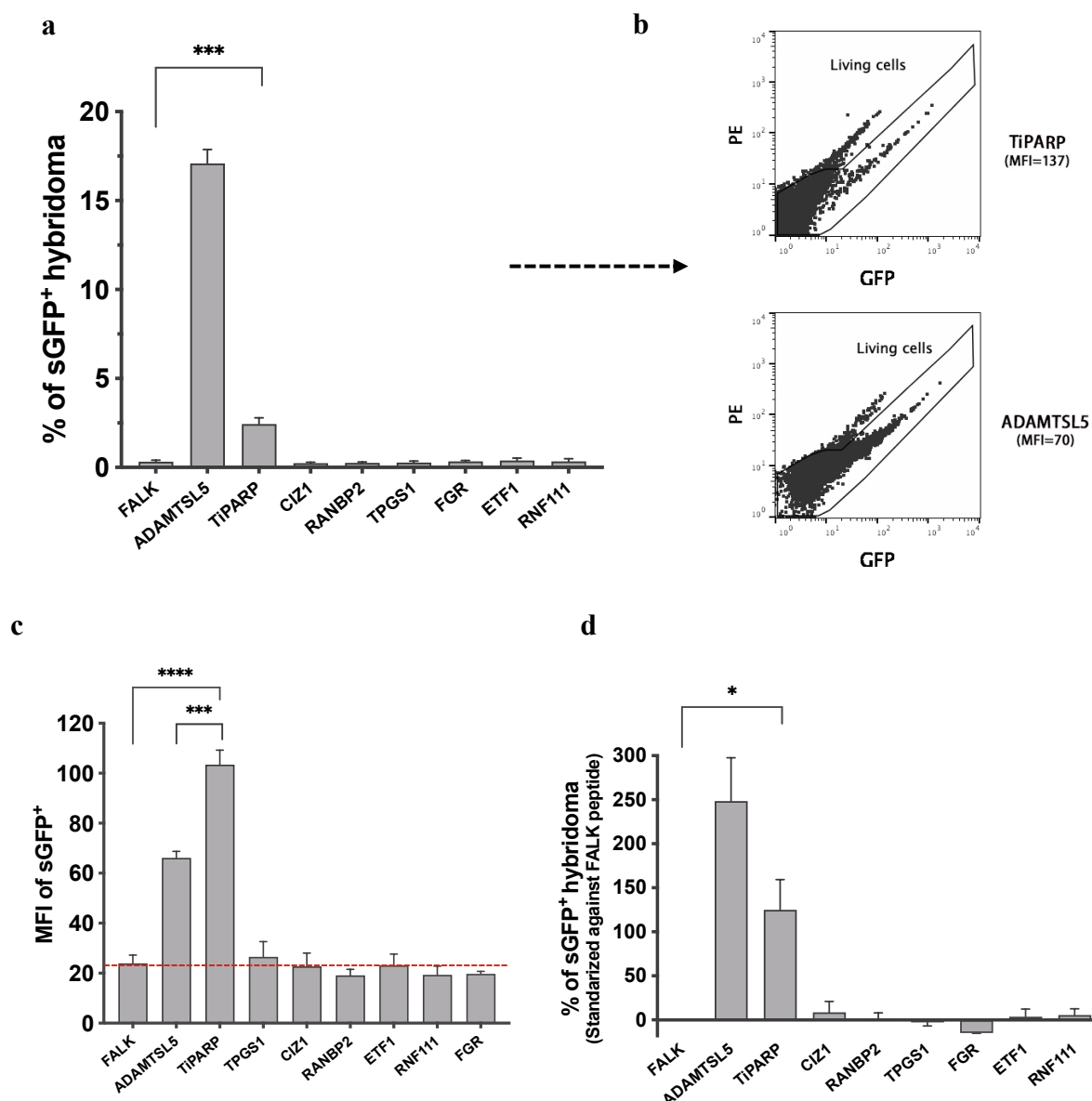


Figure 4.7.3.1.2 TCR activation by various synthetic candidate peptides identified by screening HLA-C*06:02 peptidomes from HLA-C*06:02-homozygous B cell lines. (a) TCR activation by various synthetic peptides presented by HLA-C*06:02-721.221. (b) Representative flow cytometric panels of TCR-hybridoma activation with TiPARP peptide (upper) or with ADAMTSL5 peptide (lower) presented by HLA-C*06:02-721.221. (c) Mean fluorescence intensity (MFI) of hybridoma cells stimulated by various synthetic peptides presented by HLA-C*06:02-721.221. (d) TCR activation by various synthetic peptides presented by WM278. The percentage of TCR stimulation by peptides is normalized to TCR activation by WM278 cells in the stimulation with synthetic FALK peptide as a negative control since WM278 causes basal V α 3S1/V β 13S1 TCR activation due to the inherent presentation of the ADAMTSL5 peptide. Since the TiPARP peptides were dissolved in DMSO at a concentration of 10mg/ml and subsequently diluted with distilled water to 1mg/ml, 10% v/v DMSO was added to the cultures of other synthetic peptides. Data were summarized from technical triplicates from two or three independent experiments, compared by nonpaired t-test, and shown as mean \pm SEM, with statistical significance indicated as * p < 0.05, *** p < 0.001, **** p < 0.0001.

4.7.3.2 Solubility Analysis

The synthetic TiPARP peptide had low solubility in aqueous medium. This was evident by undissolved crystals and a high hydrophobicity determined by the peptide solubility calculator, thereby requiring DMSO to make a stock solution. I therefore hypothesized that the lower number of activated hybridoma cells but the higher cellular sGFP intensity induced by TiPARP-stimulation was a result of poor peptide solubility in the culture medium. To investigate the impact of solubility on TCR activation by TiPARP peptide, I tested several of peptide mutants.

The hydrophobicity of various residues can be normalized by assigning a value of 100 to the most hydrophobic residue (Phe, F) when it is relative to neutral glycine (Gly, G), which is assigned a value of 0. The scales were extended to residues with greater hydrophilicity than glycine, as presented in **Table 4.7.3.2** (Monera *et al.*, 1995).

Very Hydrophobic		Hydrophobic		Neutral		Hydrophilic	
Amino acid	Value	Amino acid	Value	Amino acid	Value	Amino acid	Value
Phe, F	100	Tyr, Y	63	Thr, T	13	Arg, R	-14
Ile, I	99	Cys, C	49	His, H	8	Lys, K	-23
Trp, W	97	Ala, A	41	Gly, G	0	Asn, N	-28
Leu, L	97			Ser, S	-5	Glu, E	-31
Val, V	76			Gln, Q	-10	Pro, P	-46
Met, M	74					Asp, D	-55

Table 4.7.3.2 Hydrophobicity index for common amino acids, which shows the relative hydrophobicity (at pH 7). The value of the hydrophobicity index shown in the table has been normalized in such a way that the most hydrophobic residue is assigned a value of 100 in comparison to glycine, which is deemed neutral (a value of 0). The scales were then extended to residues that have a higher hydrophilicity than glycine. Amino acids are designated by the one- and three-letter code.

The TiPARP peptide “YRILQILRV” contains five “very hydrophobic” residues and one “hydrophobic” residue, which determine its high hydrophobicity. Mutations of the TiPARP peptide were focused on those residues having minimal impact on the peptide antigenicity, e.g., P1, P3, P6. I employed two strategies for peptide mutation: substitution of hydrophobic residues by less hydrophobic residues that match the frequency matrix of V α 3S1/V β 13S1-TCR ligands (**Figure 4.4.4c**) and alanine mutagenesis, which utilizes the non-bulky and chemically inert nature of alanine and its methyl functional group mimicking the secondary structure preference of numerous amino acids.

I selected four mutants of the “YRILQILRV” peptide and one negative control peptide, “TiPARP-neg,” with a shuffled sequence of TiPARP peptide, to test their antigenicity after

improving their water solubility in culture medium (**Figure 4.7.3.2 a**). These synthetic peptides were added to the co-culture of V α 3S1/V β 13S1-TCR hybridoma and HLA-C*06:02-721.221. My observations indicate that solely the mutant “TiPARP-3A” induced a slight V α 3S1/V β 13S1 TCR stimulation, while other mutants lost their antigenicity (**Figure 4.7.3.2 b**) despite gaining favorable water solubility.

a

Human proteins	1	2	3	4	5	6	7	8	9	Estimated solubility by Peptide Solubility Calculator	Actual solubility in culture medium
TIPARP	Y	R	I	L	Q	I	L	R	V	Poor water solubility	Poor water solubility
TIPARP-neg	I	L	R	I	V	R	Q	L	Y	Poor water solubility	Good water solubility
TIPARP-36A	Y	R	A	L	Q	A	L	R	V	Good water solubility	Good water solubility
TIPARP-3A	Y	R	A	L	Q	I	L	R	V	Poor water solubility	Good water solubility
TIPARP-1R	R	R	I	L	Q	I	L	R	V	Good water solubility	Good water solubility
TIPARP-6S	Y	R	I	L	Q	S	L	R	V	Good water solubility	Good water solubility

b

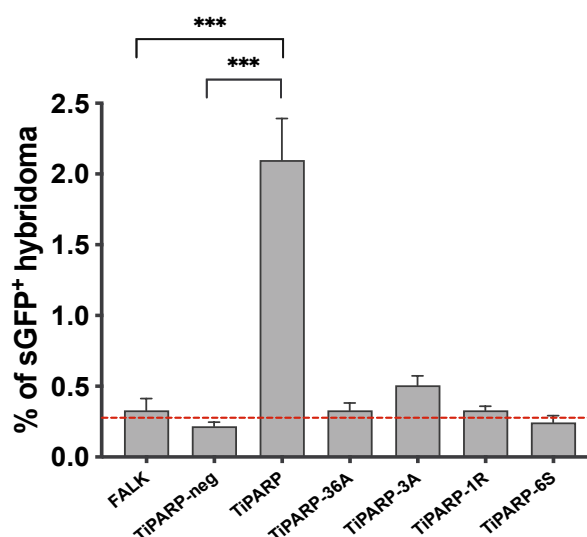


Figure 4.7.3.2 TCR activation by various mutants of TiPARP peptides in the form of synthetic peptides presented by HLA-C*06:02-721.221. Synthetic FALK peptide was employed as a negative control. Data were summarized from technical triplicates from two or three independent experiments, compared by nonpaired t-test, and shown as mean \pm SEM, with statistical significance indicated as *** $p < 0.001$. Amino acids are designated by the one-letter code.

The TiPARP peptide was classified as a non-shared ligand because it was only observed in the HLA-C*06:02 peptidome of GM20771. However, the peptidomes eluted through LC-MS/MS represent only a fraction of the total peptides presented by HLA-C*06:02 on the cell surface of the cell lines. According to the Human Protein Atlas, TiPARP is expressed during all differentiation stages of B cells (including plasma cells). Therefore, it should be presented by HLA-C*06:02 as an autoantigen of all B cells. Overall, my experiments thus identified 7

endogenous peptides in the HLA-C*06:02 peptidomes of B cells that are immunogenic for the V α 3S1/V β 13S1 TCR. Of them, the antigenicity of TiPARP was proven by stimulation with synthetic peptide.

5. Discussion

The major risk allele of psoriasis, HLA-C*06:02, mediates an autoimmune response against melanocytes through the presentation of an autoantigenic peptide from ADAMTSL5 as a key pathomechanism of the underlying genetic association. Streptococcal angina is the most common and best-characterized trigger of psoriasis in individuals carrying *HLA-C*06:02* (Mallbris *et al.*, 2009; Prinz, 2009; Thorleifsdottir, Eysteinsdóttir, *et al.*, 2016). Streptococcal infections of the tonsils can provoke the development of psoriasis in genetically predisposed individuals, maintain or worsen existing psoriasis, and induce psoriasis flare-ups. Despite various hypotheses, the pathomechanism of the association between streptococcal angina and the development of the psoriatic autoimmune response against melanocytes remains elusive.

In my thesis, I employed a V α 3S1/V β 13S1 TCR derived from a pathogenic lesional CD8⁺ T-cell clone to investigate how streptococcal angina can elicit an autoimmune response against melanocytes. This TCR had originally uncovered that HLA-C*06:02 mediates an autoimmune response against melanocytes in psoriasis through the presentation of an epitope from ADAMTSL5 as a melanocyte autoantigen (Arakawa *et al.*, 2015). Expressed in a mouse T-hybridoma reporter cell line with the induction of sGFP as a readout of TCR ligation (Siewert *et al.*, 2012), the V α 3S1/V β 13S1 TCR allows to reproduce the psoriatic autoimmune response in an *in vitro* assay. Through the results of my investigations, a completely new and unexpected concept of the triggering mechanism of psoriasis emerged. It reveals that during streptococcal angina, T lymphocytes may be specifically activated against B lymphocytes to subsequently react against melanocytes in the skin. This discovery is the outcome of a complex series of experimental approaches, as illustrated in the following flowchart (**Figure 5**).

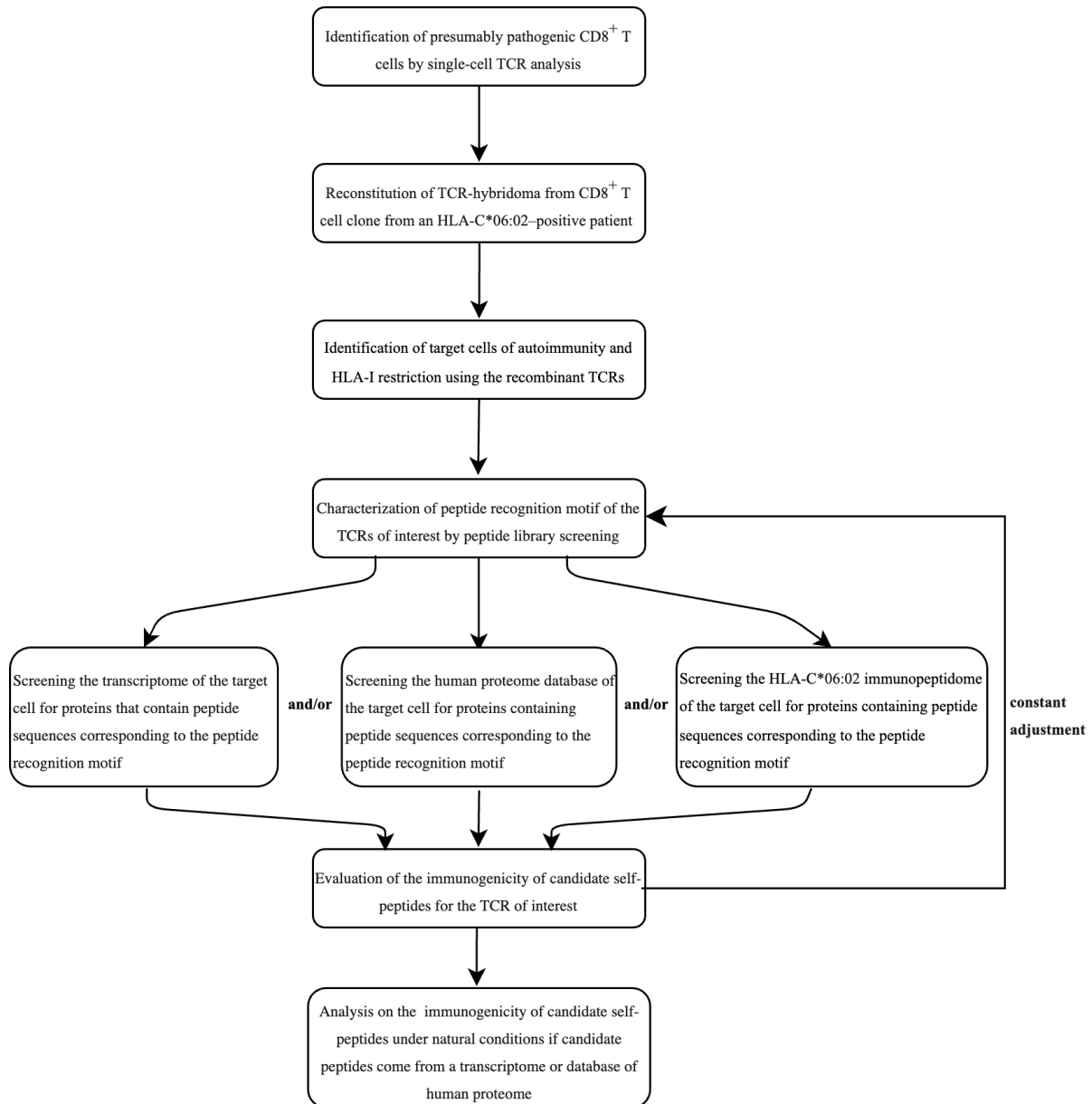


Figure 5 General overview of the main strategies to identify autoantigen(s) of the psoriatic autoimmune response using a Vα3S1/Vβ13S1 TCR from a lesional psoriatic CD8⁺ T-cell clone (Prinz, 2023).

5.1 Identification of B Cells as Initiators of the Psoriatic Autoimmune Response

According to streptococcal angina as the most common trigger of psoriasis, I commenced my research project by seeking evidence of a possible immunologic stimulus for the psoriatic autoimmune response in the tonsils using the melanocyte-specific psoriatic Vα3S1/Vβ13S1 TCR. I observed that the Vα3S1/Vβ13S1 TCR hybridoma was activated when co-cultured with tonsil cells from HLA-C*06:02-positive psoriasis patients who had undergone tonsillectomy for their streptococcal-induced psoriasis (**Figure 4.2.1.1**). This finding suggested the existence

of specific target cells or other stimulators of the V α 3S1/V β 13S1 TCR within the tonsil cells. Fractionation of tonsil cells into subpopulations and subsequent experiments using the TCR hybridoma assay indicated that tonsillar B cells were inducing the V α 3S1/V β 13S1 TCR stimulation (**Figure 4.2.1.2**).

Tonsils are lymphoid organs directly exposed to infections and other environmental conditions in the pharynx. Therefore, I had to consider that TCR stimulation by the tonsillar tissue might be induced by antigens or other exogenous triggers, such as streptococcal superantigens presented on the B cells, as formerly suggested (Leung *et al.*, 1995). However, the finding that the V α 3S1/V β 13S1 TCR was also activated by various EBV-transformed B cell lines made this assumption unlikely and rather indicated that the TCR response was directed against B cells themselves (Section 4.2.2). The observation that among the EBV-transformed B cell lines exhibiting diverse HLA-class I haplotypes, only HLA-C*06:02⁺ EBV-transformed B cell lines triggered activation of the TCR hybridoma revealed that the TCR stimulation by B cells was HLA-C*06:02 restricted. Blocking TCR stimulation with a pan-HLA-class I antibody further indicated that the V α 3S1/V β 13S1 TCR stimulation by B cells was specifically induced by antigens presented by HLA-C*06:02. The stimulation of the V α 3S1/V β 13S1 TCR by the EBV-transformed B cell lines further indicated that these indefinitely reproducible cell lines could replace primary B cells to search for the B cell antigens of the V α 3S1/V β 13S1 TCR, similar to the previous experiments identifying the melanocyte autoantigen, in which melanoma cell lines acted as surrogates of primary melanocytes (Arakawa *et al.*, 2015).

An essential question for utilizing EBV-transformed B cell lines in my study was whether these immortalized B cells had an altered expression of parental proteins of potential autoantigens or of molecules involved in the antigen processing and presenting pathways that might affect their immunogenicity. EBV infection can reprogram the transcriptome of resting B cells to an extensive transcriptional profile (Mrozek-Gorska *et al.*, 2019). Therefore, I investigated whether the antigenicity for the V α 3S1/V β 13S1 TCR was a general property of B cells. Like the fractionated tonsil B cells, blood B cells from HLA-C*06:02⁺ psoriasis patients, but not other cell types, stimulated the V α 3S1/V β 13S1 TCR. B cells from HLA-C*06:02⁺ healthy volunteers induced only a low activation of the V α 3S1/V β 13S1 TCR hybridoma, which hardly differed from the B cells from HLA-C*06:02-negative healthy donors (Section 4.2.3). The observation that B cells from psoriasis patients stimulated the V α 3S1/V β 13S1 TCR most may suggest that they present higher levels of autoantigens to the V α 3S1/V β 13S1 TCR. This would increase the risk for the induction of an autoimmune response. The stimulatory effect was

further enhanced when the B cells from blood or tonsils were conditioned with IFN- γ , which, as with melanocytes (Arakawa *et al.*, 2021), upregulates antigen processing and HLA-C expression. This might also be important for an increase in the immunogenicity of B cells in inflammatory conditions, such as streptococcal angina, and facilitate an autoimmune response against B cells in genetically predisposed patients.

These results raised the question of whether other cell types are immunogenic for V α 3S1/V β 13S1 TCR. Keratinocytes were formerly proposed as target cells of the autoimmune response in psoriasis, as psoriasis is restricted to the skin and characterized by the abnormal proliferation of keratinocytes. Earlier work, however, had already excluded keratinocytes as targets of the V α 3S1/V β 13S1 TCR (Arakawa *et al.*, 2015). My expanded search scope for target cells through TCR-hybridoma co-culture experiments with human cell lines of diverse origins failed to identify additional cell types that may stimulate the V α 3S1/V β 13S1 TCR. This supports that, in addition to melanocytes, only B cells are immunogenic for the V α 3S1/V β 13S1 TCR (Section 4.2.4).

We considered the V α 3S1/V β 13S1 TCR as paradigmatic for the psoriatic autoimmune response, given that immunohistology analysis of psoriatic skin lesions had confirmed that the lesional psoriatic autoimmune response of CD8⁺ T cells is generally directed against melanocytes (Arakawa *et al.*, 2015). My results, therefore, raised the question of whether the reactivity against B cells is a special property of the V α 3S1/V β 13S1 TCR or if autologous B cells are particularly immunogenic for psoriasis patients in general. I investigated this issue using different methods. At first, my results showed that PBMC from psoriasis patients displayed a significantly increased autoprolieration compared to healthy subjects. It was lost following the depletion of the B cells from the PBMC and restored by B-cell reconstitution. Measurement of the proliferating cell populations by CFSE dilution assays assigned the autoprolieration specifically to CD8⁺ T cells. Inhibition of HLA-class I antigen presentation by a pan-HLA-class I antibody effectively suppressed the autostimulatory activation of PBMCs, providing compelling evidence that autoprolieration is HLA-class I-restricted (Section 4.3). Thus, B cells may drive the autoprolieration of CD8⁺ T cells in psoriasis patients. My findings, therefore, indicate that the reactivity of V α 3S1/V β 13S1 TCR against B cells reflects a principal responsiveness of CD8⁺ T cells in psoriasis, and they propose that the B cell immunogenicity is related to self-peptides presented by HLA-C*06:02.

The conclusion of a B-cell-dependent autoimmune response against melanocytes in psoriasis is supported by several clinical observations. The elimination of tonsillar B cells by tonsillectomy

achieved symptom resolution in a substantial proportion of patients with recalcitrant psoriasis associated with episodes of streptococcal angina (Rachakonda *et al.*, 2015). Several case reports documented that treatment with B cell-depleting monoclonal CD20 antibodies alleviated symptoms of psoriasis, psoriatic arthritis, and pustular psoriasis and thus concluded on a role of B cells in psoriasis pathology (Chang, Y. S. *et al.*, 2012; Codrina *et al.*, 2014; Jimenez-Boj *et al.*, 2012; Singh and Weinberg, 2005; Toussi *et al.*, 2019). On the other hand, in isolated cases, psoriasis was induced by rituximab treatment of autoantibody-mediated autoimmune diseases (Ly *et al.*, 2023). A possible explanation would be the stimulation of pathogenic T cells by B-cell antigens and pro-inflammatory cytokines released from apoptotic B cells. Another supporting piece of evidence is a high proportion of circulating B cells observed in the early stage of psoriasis pathogenesis, while the ratio of B cells in PBMC in the later phase of the disease was no longer elevated, indicating that B cells may act as antigen-presenting cells to activate T cell in the early event (Gambichler *et al.*, 2013; Lu *et al.*, 2016; Niu *et al.*, 2015).

5.2 Attempts to Identify the Psoriatic Autoantigen(s) in B cells

HLA-class I molecules mediate immune responses of CD8⁺ T cells against target cells by presenting peptides derived from cytoplasmic or nuclear proteins (Neefjes *et al.*, 2011). HLA-C*06:02 is the primary risk allele for psoriasis (Nair *et al.*, 2006; Zhou *et al.*, 2016). The B-cell autoantigens stimulating the V α 3S1/V β 13S1 TCR should thus be contained in the transcriptome and proteome of B cells and be represented in the immunopeptidome of HLA-C*06:02.

Given that the melanocyte autoantigen of the V α 3S1/V β 13S1 TCR, ADAMTSL5, is present in the transcriptome of B cells and B cell lines, it was reasonable to speculate that ADAMTSL5 may also serve as an autoantigen of B cells. Various observations made this unlikely: i) The expression of ADAMTSL5 in B cells, according to the public data from “The Human Protein Atlas” and our own transcriptome analysis of a B cell line, is very low; ii) At the time of my experiments, HLA-C*06:02 immunopeptidomes from two B cell lines, C1R and 721.221, were available from the literature (Di Marco *et al.*, 2017; Mobbs *et al.*, 2017; Sarkizova *et al.*, 2020). The ADAMTSL5 peptide “VRSRRCLRL” was not observed in three publicly available HLA-C*06:02 peptidomes from B cell lines, and, in the later course of my experiments, the immunopeptidomes of four EBV-transformed B cell lines homozygous for HLA-C*06:02; iii) The antigenicity of B cells for the V α 3S1/V β 13S1 TCR was not affected following siRNA-mediated knockdown of ADAMTSL5 (Section 4.6.2). iiiii) While the immunogenicity of

ADAMTSL5 in melanocytes is increased by the psoriasis risk haplotype of ERAP1, Hap2, the B-cell line homozygous for HLA-C*06:02 and ERAP1 Hap2 had the lowest stimulatory capacity for the V α 3S1/V β 13S1 TCR, suggesting that the B-cell autoantigen of the V α 3S1/V β 13S1 TCR is destroyed rather than generated by Hap2.

We considered the B cell-reactive V α 3S1/V β 13S1 TCR as a specific tool for the identification of the putative HLA-C*06:02-presented B-cell autoantigens. For a precise search for corresponding peptide ligands, I therefore further characterized the peptide recognition motif of the V α 3S1/V β 13S1 TCR using TCR ligands that had already been identified in prior experiments (Section 4.4). This way, I defined a group of combinational recognition motifs of the V α 3S1/V β 13S1 TCR, which enabled efficient screening algorithms against the vast peptide repertoire, either in searching the human proteome and the B-cell transcriptome or HLA-C*06:02 peptidomes of B cells. The heat map of preferred amino acids at different peptide positions and the corresponding Sequence Logo of the V α 3S1/V β 13S1 TCR ligands clearly corresponded to the HLA-C*06:02 peptide-binding motifs (**Figure 4.7.2.2**).

The B cell antigen(s) should be contained in the HLA-C*06:02 peptidome. Therefore, I first screened the two HLA-C*06:02 immunopeptidomes obtained from the C1R and 721.221 cell lines (Di Marco *et al.*, 2017; Mobbs *et al.*, 2017) with the peptide recognition motifs of the V α 3S1/V β 13S1 TCR. The two cell lines share similarities, as they had lost the expression of HLA-A, -B, and -C molecules due to γ -ray-induced mutations (Shimizu *et al.*, 1988; Shimizu and DeMars, 1989). Transfection with HLA-C*06:02, therefore, allowed a selective analysis of the HLA-C*06:02 immunopeptidomes. With the peptide recognition motifs of the V α 3S1/V β 13S1 TCR, I identified several promising candidate peptide ligands. However, none of them stimulated the V α 3S1/V β 13S1 TCR. Subsequent examination of the two cell lines unveiled an unexpected finding that none of them stimulated the V α 3S1/V β 13S1 TCR in co-culture experiments. Therefore, I examined whether these cell lines had lost the ability for TCR ligation as a result of γ -ray irradiation. I found that both cell lines stimulated the V α 3S1/V β 13S1-TCR hybridoma after transfection with plasmids of established V α 3S1/V β 13S1 TCR ligands or loading with corresponding synthetic peptides. Thus, they were able to effectively present antigens by HLA-C*06:02 (Section 4.5.2). From this, I concluded that the antigen(s) of EBV-transformed or primary B-cells were not presented by HLA-C*06:02 on C1R or 721.221 cells. Accordingly, the HLA-C*06:02 immunopeptidomes of these cell lines were not suitable to search for the B-cell antigens of the V α 3S1/V β 13S1 TCR, as γ -ray irradiation may have altered either expression or processing of the potential autoantigen(s).

In the second attempt to search for B-cell autoantigens, I screened the *Homo sapiens* proteome in the Uniprot database for proteins that contain the V α 3S1/V β 13S1 TCR-recognition motifs and are expressed in the transcriptome of an EBV-transformed stimulatory B-cell line. This identified 13 stimulatory peptides. To differentiate which of them was naturally processed from the proteome of B cells and presented by HLA-C*06:02, I applied siRNAs suppressing the respective parental protein in the D22 B-cell line that activated the V α 3S1/V β 13S1-TCR hybridoma. However, none of the peptide antigens turned out to be naturally generated and presented to activate the V α 3S1/V β 13S1 TCR in these experiments (Section 4.6). The later analysis confirmed that none of these peptides were present in the four HLA-C*06:02 immunopeptidomes of the B-cell lines homozygous for HLA-C*06:02. Thus, several proteins of the B-cell proteome contained peptide sequences stimulating the V α 3S1/V β 13S1 TCR that were obviously not generated by antigen processing from the parental proteins.

After these extensive experiments, I focused my further antigen search on the peptidomes of four HLA-C*06:02 homozygous B cell lines, which we had obtained in the meantime from the Coriell Institute for Medical Research (Camden, NJ, USA). All four B cell lines stimulated the V α 3S1/V β 13S1 TCR (**Figure 4.7.1**) and were genetically well characterized, because they were samples from individuals included in the 1,000 Genomes project that created a catalogue of common human genetic variation (<https://www.genome.gov/27528684/1000-genomes-project>). This allowed us to determine the respective ERAP1 haplotype. I expanded these cell lines to have the HLA-C*06:02 immunopeptidomes determined by Prof. Andreas Schlosser (Rudolf-Virchow-Center, Center for Integrative and Translational Bioimaging, University of Würzburg). The yields of HLA-C*06:02 ligands from the four HLA-C*06:02-homozygous B cell lines were much lower than those from the HLA-C*06:02-transfected cell lines C1R and 721.221, and the shared ligands between the two groups were limited (**Figure 4.7.2.1.2 & 4.7.2.1.3**). According to my studies, these differences may involve the much higher expression of recombinant HLA-C*06:02 in the transfectants. In my further screening for stimulatory peptides in the four HLA-C*06:02 peptidomes, I excluded peptides found in the HLA-C*06:02 peptidomes from C1R and HLA-C*06:02-721.221, as these cell lines did not stimulate the V α 3S1/V β 13S1 TCR, and focused my analyses instead on the overlapping peptide repertoires from the four homozygous HLA-C*06:02 B cell lines (**Figure 4.7.2.1.3**). The search based on the V α 3S1/V β 13S1-TCR-ligand motif (Section 4.7.2.2) identified 78 potential V α 3S1/V β 13S1 TCR ligands, which I tested as plasmid-encoded peptides (see supplemental data 6.1.5 and 6.2.5).

During the initial phase of testing, I used HLA-C*06:02-transfected COS-7 cells as APCs. However, none of the plasmid-encoded peptides induced stimulation of the V α 3S1/V β 13S1 TCR. Therefore, I changed the antigen-presenting strategy and used the naturally HLA-C*06:02-positive melanoma cell line WM278 for antigen presentation in co-culture experiments with the V α 3S1/V β 13S1 TCR hybridoma. As a certain limitation of this approach, the activation of the V α 3S1/V β 13S1 TCR in response to peptide antigens presented in WM278 may not accurately reflect the activation level induced by the peptides alone. This is due to the natural immunogenicity of WM278 cells, which are targets of the V α 3S1/V β 13S1 TCR because they present the ADAMTSL5 self-peptide as the autoantigen. However, much of the immunogenicity of WM278 cells for the V α 3S1/V β 13S1 TCR depends on the presence of IFN- γ to increase ERAP1 and HLA-C*06:02 expression. In the absence of IFN- γ , WM278 induces only low levels of V α 3S1/V β 13S1-TCR stimulation and can be used for antigen presentation. To assess the actual antigen-specific hybridoma activation, I normalized the peptide-induced stimulation to the V α 3S1/V β 13S1-TCR stimulation by the ADAMTSL5 peptide, using the FALK peptide as negative control.

In this way, I identified 7 peptides contained in the HLA-C*06:02 immunopeptidomes that stimulated the V α 3S1/V β 13S1 TCR with different potency. The presence of 7 stimulatory peptides in the HLA-C*06:02 immunopeptidomes may explain why B cells activate the V α 3S1/V β 13S1 TCR even more strongly than melanocytes. At the same time, the surprisingly large number of stimulatory antigens in the same cell type did not allow knockdown experiments to verify their role as autoantigens, as this would only inhibit the expression of the protein silenced by siRNA, while the expression of the other 6 proteins would remain unaffected. For this reason, I used synthetic peptides to obtain additional evidence of their antigenicity. To this end, a 9-mer peptide from the TiPARP protein exhibited antigenicity when presented as synthetic peptide by HLA-C*06:02-721.221 and the melanoma cell line WM278. This peptide also elicited the strongest stimulation of the V α 3S1/V β 13S1 TCR as recombinant peptide (**Figure 4.7.3.1.1**).

Interestingly, the TiPARP peptide “YRILQILRV” stimulated a lesser frequency but induced substantially higher cellular intensity of sGFP in the V α 3S1/V β 13S1 TCR hybridoma cells than the ADAMTSL5 peptide, indicating intense TCR stimulation. The lower frequency of responding hybridoma cells may be attributed to the poor peptide solubility in the culture medium due to its high hydrophobicity. I attempted to test several mutants of “YRILQILRV” to improve the water solubility in the culture medium on the premises of unchanged antigenicity.

However, this was not successful, as the mutants exhibited improved water solubility but lost their immunogenicity after mutagenesis. Still, with the TCR activation by synthetic TiPARP peptide presented by HLA-C*06:02-721.221, I confirmed that TiPARP peptide “YRILQILRV” is a proven autoantigen derived from B cells, as it is contained in the HLA-C*06:02 immunopeptidome and stimulatory for the V α 3S1/V β 13S1 TCR. As determined by NetMHCpan-4.1, it is an extremely strong binder to HLA-C*06:02, with a predicted binding affinity % Rank of 0.007 compared to the distribution of affinities calculated on set of a random peptides (<https://services.healthtech.dtu.dk/services/NetMHCpan-4.1/>). Overall, these findings exemplify that different self-peptides can be recognized by the same autoreactive T-cell clone in different organs, i.e., the ADAMTSL5 peptide “VRSRRCLRL” in melanocytes and the TiPARP peptide “YRILQILRV” in tonsillar B cells. This may allow for cross-reactive immune responses between a stimulatory and a target cell type.

I observed the TiPARP peptide only in the HLA-C*06:02 peptidome of GM20771 cells. Nevertheless, its presence in the HLA-C*06:02 peptidomes of all four EBV-transformed B-LCL (**Figure 4.7.1**) can be assumed since the peptides eluted through LC-MS/MS represent only a fraction of the total peptidome presented by HLA-C*06:02 on the cell surface, and the TiPARP protein is constitutively expressed in B cells and plasma cells. In particular, peptides rich in arginine, such as the V α 3S1/V β 13S1 TCR ligands, may escape identification in the LC-MS analysis, as they usually don't have sufficient retention on the reversed-phase stationary phases due to the strong proton affinity and polarity of the side chain (Foettinger *et al.*, 2006). The analysis of the peptidomes from four different B cell lines, however, reduced the likelihood of missing antigenic peptides of the V α 3S1/V β 13S1 TCR.

5.3 Streptococcal Angina Triggers B-cell-dependent Autoimmunity Against Melanocytes

Infections caused by Lancefield's group A beta-haemolytic streptococci (*S. pyogenes*) trigger a range of post-streptococcal sequelae. They include rheumatic fever composed of myo- and endocarditis, poststreptococcal reactive arthritis, and erythema anulare rheumaticum, as well as poststreptococcal glomerulonephritis (Cunningham, M. W., 2000, 2012). They are furthermore blamed for causing acute and chronic tic and obsessive-compulsive disorders, which are summarized with the term “pediatric autoimmune neuropsychiatric disorders associated with streptococcal infection” (PANDAS) and include chorea minor Sydenham and Tourette's syndrome (Sims Sanyahumbi *et al.*, 2016).

As an underlying pathomechanism, streptococcal strains with certain rheumatogenic M proteins elicit cross-reactive cellular or humoral autoimmune responses against proteins with homologous peptide sequences from various organs, including myocardium and endocardium, joints, kidneys, and brain, based on molecular mimicry. Accordingly, the etiology of psoriasis has been hypothesized to involve cross-reactive immune responses between streptococcal M proteins and keratins, resulting in an autoimmune response against keratinocytes. This hypothesis was supported by increased T-cell reactivity against homologous peptides of M-proteins and keratins in patients with streptococci-associated psoriasis onset and flares. From today's perspective, however, various aspects challenge this hypothesis. Specifically, poststreptococcal diseases are highly specific to *S. pyogenes* strains with particular rheumatogenic M proteins, while psoriasis onset or flare-ups are often associated with streptococcal angina caused by group B, C, and G streptococci lacking the classical M proteins of group A streptococci (Sigurdardottir *et al.*, 2013). Moreover, homologous peptides of streptococcal M proteins and keratins were observed to activate predominantly CD4⁺ T cells, whereas psoriasis, as an HLA class I-restricted autoimmune disease, results from epidermal recruitment, activation, and clonal expansion of CD8⁺ T cells (Di Meglio *et al.*, 2016; Ortega *et al.*, 2009; Paukkonen *et al.*, 1992). In contrast to the HLA-C*06:02-restricted CD8⁺ T cell-mediated autoimmune response against melanocytes (Arakawa *et al.*, 2015), an autoimmune reaction against keratinocytes has never been demonstrated. Furthermore, sequence alignment of the seven B cell peptides stimulating the V α 3S1/V β 13S1 TCR with the protein databases for *Streptococcus* (taxid: 1301) and *Streptococcus pyogenes* (taxid:1314) did not find sufficient sequence homologies that would make a cross-reactive immune response between them and streptococcal antigens likely.

While the lesional psoriatic dermis is mainly infiltrated by CD4⁺ T cells, psoriasis lesions develop only upon epidermal infiltration of CD8⁺ T cells (Cheuk *et al.*, 2014; Di Meglio *et al.*, 2016; Paukkonen *et al.*, 1992). My findings that B cells stimulate the autoprolieration of CD8⁺ T cells within PBMC support that CD8⁺ T cells are the key effector cells in psoriasis (Section 4.3.3). The hypothesis that streptococcal superantigens trigger psoriasis (Leung *et al.*, 1995) is contradicted by the strong clonal expansion of CD8⁺ T cells in psoriasis lesions, which can only be explained by antigen-specific activation. The mechanism of CD8⁺ T cell activation by autologous B cells based on specific TCR reactivity that I have identified now provides a completely new explanation of the role of streptococcal angina in triggering the psoriatic autoimmune response.

Overall, therefore, it seems likely that the severe inflammation caused by streptococcal infection of the tonsils may create the inflammatory conditions necessary to break peripheral tolerance mechanisms against self-peptides and trigger the primary autoimmune response of autoreactive CD8⁺ T cells against B cells in the tonsils (**Figure 5.3**). This step likely involves an increase in the otherwise low expression of HLA-C and the HLA-C-restricted presentation of self-peptides by IFN- γ , as well as the provision of secondary signals leading to T-cell priming. Similar to primary melanocytes, pretreatment of primary B cells with IFN- γ markedly increased HLA-C*06:02 expression and V α 3S1/V β 13S1-TCR stimulation in my experiments (Section 4.2.1 & 4.2.3). The resulting enhanced presentation of self-peptides on B cells may then allow for the activation and expansion of self-peptide-specific pathogenic CD8⁺ T cells, followed by their homing to the skin via blood vessels due to the expression of the skin-homing receptor, cutaneous lymphocyte antigen (CLA) (Diluvio *et al.*, 2006). Here, they finally mediate a cross-reactive autoimmune response against melanocytes and induce psoriatic inflammation through the recognition of the ADAMTSL5 peptide.

Unlike the cytotoxic autoimmune attack against melanocytes in vitiligo, streptococcal infection in the tonsils may prime CD8⁺ T cells to express a Tc17 cytokine pattern that coordinates antimicrobial defense and wound healing (Arakawa *et al.*, 2015; Krueger, 2015). Following activation against melanocytes in the skin, the CD8⁺ T cells produce IL-17 and IL-22 that mediate the abnormal proliferation of keratinocytes (Cheuk *et al.*, 2017), the accumulation of neutrophilic granulocytes, as well as the production of antimicrobial peptides and other inflammatory cytokines and chemokines rather than serving as cytotoxic effectors (Prinz, 2017a). During the autoimmune response against B cells, T_{RM} cells may develop from CD8⁺ effector T cell precursors and mediate recurrences in previously inflamed sites upon withdrawal of treatment (Cheuk *et al.*, 2014; Owczarczyk-Saczonek *et al.*, 2020). Still, lesional psoriatic inflammation requires a constant supply of autoreactive effector T cells, since tonsillectomy or blocking of T cell emigration from secondary lymphoid organs via S₁P₁ agonists or of extravasation of T cells into skin lesions by an LFA-1 antibody can ameliorate psoriasis (D'Ambrosio *et al.*, 2016; Jullien *et al.*, 2004; Ryan and Menter, 2014).

The insights obtained here suggest that the inflammation during streptococcal angina may mediate the disruption of peripheral tolerance mechanisms, increase the presentation of self-peptides by HLA-C*06:02 on B cells in the tonsils and provide the proinflammatory environment for the activation of self-reactive T cells. An increased immunogenicity of B cells for pathogenic T cells has also been observed in multiple sclerosis (Jelcic *et al.*, 2018). Similar

to my observations, B cells drive the autoprolieration of pathogenic brain-homing T cells, which recognize antigens presented by the disease-associated HLA-DR5 molecules on both B cells and in multiple sclerosis brain lesions. B-cell-depleting antibodies are therapeutically effective in various autoantibody-mediated autoimmune diseases (Gürcan *et al.*, 2009). The therapeutic efficacy here is mainly attributed to the elimination of the autoantibody-producing B cells. In psoriasis, B cells may directly stimulate pathogenic CD8⁺ T cells. This may explain why B-cell depletion may improve but also initiate the onset of psoriasis in select cases. My results, as well as the observations in multiple sclerosis, suggest that the efficacy of B-cell depletion may involve reduced stimulation of pathogenic T cells by B lymphocytes. Therefore, it would be interesting to consider whether this mechanism might be implicated in the pathogenesis of other autoimmune disorders as well, including post-streptococcal disorders.

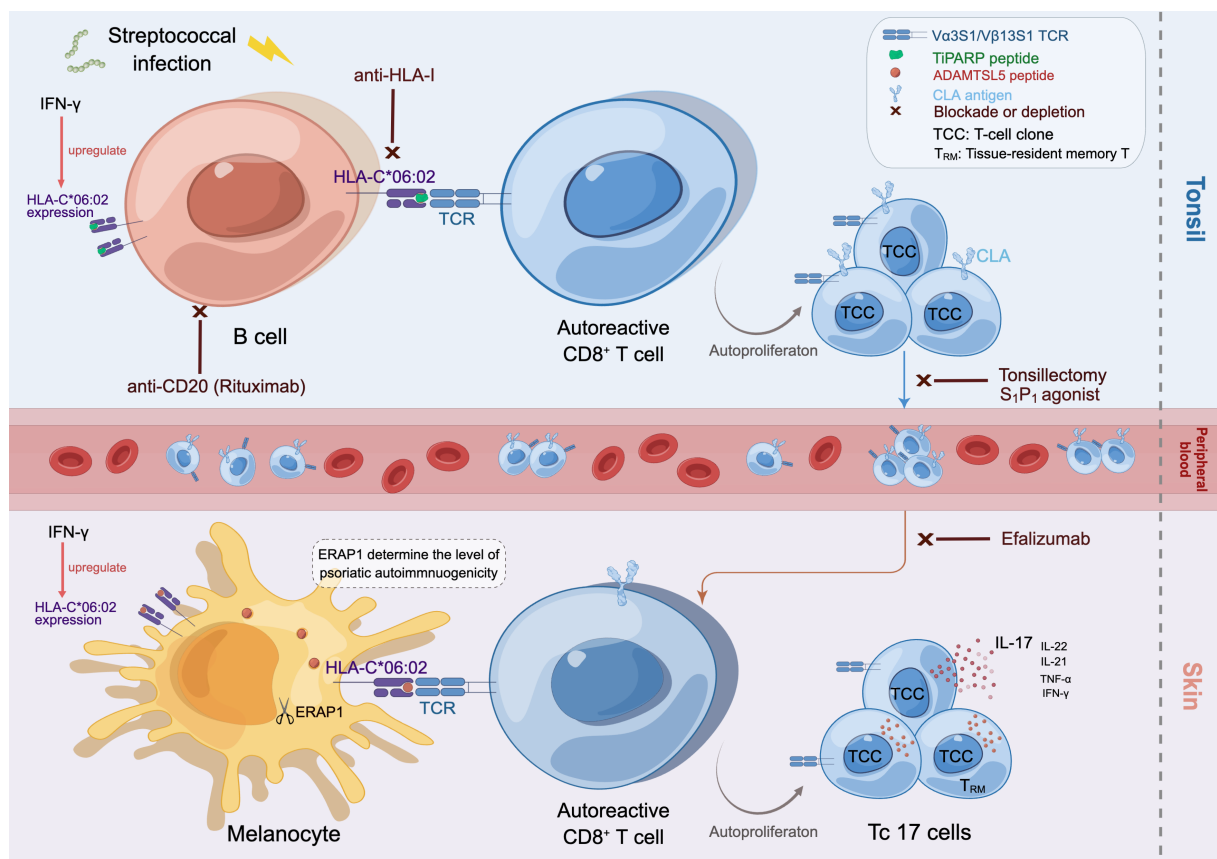


Figure 5.3 Schematic diagram of the potential cross-reactive autoimmune response between tonsillar B cells and epidermal melanocytes triggered by streptococcal infection (figure by Figdraw).

5.4 HLA-C*06:02 Peptidome Analysis Depending on ERAP1 Variants

HLA-class I molecules and ERAP1 cooperate in antigen processing and presentation. ERAP1 variants control the HLA-C*06:02-mediated risk for psoriasis in gene-gene interaction with

*HLA-C*06:02* (Strange *et al.*, 2010) by determining the amount of autoantigen for presentation (Arakawa *et al.*, 2021). Coding variants combine to encode different ERAP1 haplotypes that exhibit different enzymatic activities towards peptide substrates and differentially shape the immunopeptidome of MHC-I (Alvarez-Navarro and López de Castro, 2014; Kuiper *et al.*, 2018; López de Castro, 2018; Reeves *et al.*, 2020). In psoriasis, ERAP1 haplotypes control the level of autoimmunogenicity of melanocytes by different autoantigen yields: the generation of the autoantigenic ADAMTSL5 epitope from precursor peptides in melanocytes is ERAP1-dependent. The protective Hap10 was less effective in generating the autoantigenic ADAMTSL5 epitope from precursors than the risk haplotype Hap2 of ERAP1, leading to lower HLA-C expression and immunogenicity of melanocytes (Arakawa *et al.*, 2021).

Given that in psoriasis, CD8⁺ T cells may be activated by autologous B cells, I wondered if ERAP1 affected the immunogenicity of B cells for the V α 3S1/V β 13S1 TCR. Data from deep sequencing of the genomes of a large number of individuals in the 1000 Genomes Project allowed the determination of ERAP1 variants and haplotypes of the six *HLA-C*06:02*-homozygous B cell lines that I had used to stimulate the V α 3S1/V β 13S1 TCR (**Table 3.4.2**). Donors of *HLA-C*06:02*-homozygous B cell lines GM11930 and HG00142 turned out to be homozygous Hap2 or Hap10 haplotype carriers, respectively. I took this as an opportunity to address the above question using these *HLA-C*06:02* peptidomes.

First, it was striking that the B cell line homozygous for the ERAP1 risk haplotype Hap2 had the lowest stimulatory activity for the V α 3S1/V β 13S1 TCR of all six B cell lines. Furthermore, the B cell line homozygous for Hap10, HG00142, produced stronger V α 3S1/V β 13S1 TCR stimulation than the B cell line homozygous for Hap2, GM11930. Regarding the immunogenicity and HLA-C expression of B cell lines with respect to ERAP1 Hap2 or Hap10, my results are thus in contrast to the effect of ERAP1 haplotypes observed in melanocytes. This indicates that, unlike the autoantigenic ADAMTSL5 epitope of melanocytes, the B-cell autoantigen is rather destroyed by the high enzymatic activity of Hap2 and preserved in the presence of Hap10 with its low trimming efficacy. It is further evidence that the autoantigen(s) in B cells differ from the autoantigen in melanocytes and are subject to different processing by ERAP1. Accordingly, the risk haplotype Hap2 seems to mediate its pathogenic effect for psoriasis in melanocytes but not B cells.

To address this issue further, I analyzed the immunopeptidomes in relation to the ERAP1 haplotypes. ERAP1 strongly prefers peptides with hydrophobic C-terminal residues and generates the appropriate peptide length for binding into the MHC class I peptide binding

groove by N-terminal trimming of peptide precursors (Chang, S. C. *et al.*, 2005). Upon analyzing the residue composition at each position in the peptidomes from B cell lines either homozygous for *hap2* or *hap10*, I observed that both of them exhibit a marked preference for hydrophobic C-terminal residues but major differences in the preferred N-terminal residues. Specifically, the peptidome from the *hap2*-homozygous B cell line showed a preference for N-terminal basic residues (R, K), while the peptidome from the *hap10*-homozygous B cell line preferred hydrophilic neutral or hydrophobic residues (S, T, V, Y) at the N-termini (**Figure 4.7.2.3.3**).

Although GM11930 (Hap2/Hap2) had a lower immunogenicity or HLA-C expression compared to HG00142 (Hap10/Hap10), a greater diversity of peptides and a higher proportion of 8-mers in its HLA-C*06:02 peptidome still indicated a higher trimming efficiency of Hap2 (Section 4.7.2.3). By the alignment of hybridoma activation results and HLA expression of all HLA-C*06:02-homozygous B cell lines, I found that the expression of HLA-C, but not the expression of HLA-ABC, was highly positively correlated to the V α 3S1/V β 13S1-TCR hybridoma activation (**al**).

An extended comparison of the HLA-C*06:02 ligands in the data from seven peptidomes revealed that all HLA-C*06:02 peptidomes share common features. They showed the same strong preference for arginine and leucine at P2 and P9, respectively, and shared various ligands with each other. Still, there existed discernible differences in the characteristics of these peptidomes. Concerning the overlap within the four peptidomes from HLA-C*06:02 homozygous B cell lines, there was a certain proportion of unshared ligands in each peptidome. Moreover, there were minor differences between all HLA-C*06:02 immunopeptidomes regarding the preferred amino acid residues at P7: four peptidomes had a preference for arginine and two preferred leucine, while the others had no preference for P7 at all.

As a limitation of this comparison, GM11930 (Hap2/Hap2) and HG00142 (Hap10/Hap10) originate from different individuals who carry different HLA-A and HLA-B alleles, as well as other genetic variations that may affect the processing and presentation of HLA-C ligands. A rigorous scientific analysis of the effect of the two ERAP1 haplotypes on the HLA-C*06:02 immunopeptidome in B cells would need to be based on a strict control design involving the same cell line with different ERAP1 haplotypes (e.g., ERAP1^{-/-} B cells reconstituted with Hap2 or Hap10). The peptidome analyses performed in my thesis only provided an overall view for HLA-C*06:02 peptides, which is not sufficient to demonstrate a specific ERAP1 haplotype

trimming efficiency for precursor peptides of the autoantigenic B-cell peptides ligating the V α 3S1/V β 13S1 TCR.

Apart from the inherent genetic variations among individuals, various extrinsic factors also influence HLA-C*06:02 peptidome data. These factors include methodological differences in the elution of HLA-C*06:02 ligands, the methods of sample preparation, as well as variations in running parameters, such as the sensitivity and specificity of the mass spectrometry instrument and analysis software employed (Granados *et al.*, 2014). Furthermore, it certainly makes a difference whether genuinely HLA-C*06:02-positive or HLA-C*06:02-transfected and irradiated B cell lines are compared. It is imperative to consider these factors when comparing HLA-C*06:02 ligand profiles from diverse sources. This is also evident from the fact that all HLA-C*06:02-positive B-cell lines, but not HLA-C*06:02-transfected C1R and 721.221 cells, stimulated the V α 3S1/V β 13S1 TCR.

5.5 Impacts, Limitations, and Future Perspectives

The clarification of T-cell epitopes presented by specific HLA molecules is critical for a comprehensive understanding of T-cell-mediated HLA-associated autoimmune disorders. At present, very few autoantigens responsible for the pathogenesis of HLA-class I-associated autoimmune diseases have been determined due to the complexity of the discovery of self-peptides of autoimmune T-cell responses (Sharma *et al.*, 2019).

The workflow shown in **Figure 5** provides a possible strategy for the discovery of self-peptides for HLA-associated autoimmune T-cell responses that includes several categories of assays. My study provides an example of how the combination of two types of assays can be used to identify T cell autoantigens. It combines the analysis of MHC ligands isolated from natural target cells by elution and mass spectrometry with the investigation of TCR reactivity to identify target cells and TCR ligands selected from immunopeptidomes according to the peptide recognition motif of the TCR. The former assay enables us to address the naturally presented self-peptides, while the latter assay gives a direct read-out of the T-cell response to specific cells and epitopes (Peters *et al.*, 2020; Prinz, 2023). In my thesis, the V α 3S1/V β 13S1-TCR hybridoma reporter assay (Seitz *et al.*, 2006; Siewert *et al.*, 2012) allowed the identification of B cells as autoimmune triggers, while the V α 3S1/V β 13S1-TCR recognition motif enabled the identification of V α 3S1/V β 13S1 TCR ligands in the immunopeptidomes eluted from B cell lines homozygous for HLA-C*06:02.

Certain limitations in the present study result from technical issues. Though we obtained four EBV-transformed B cell lines from donors homozygous for HLA-C*06:02, the immunopeptidomes also contained peptide ligands of HLA-A and HLA-B according to the use of the pan-HLA class I antibody W6/32 for isolation. HLA-C*06:02 ligands were assigned by the MHC binding prediction tool NetMHC4.0, which may lead to misassignments due to limited prediction accuracy and the possibility that other HLA molecules may share ligands with HLA-C*06:02, e.g., HLA-C*02:05, HLA-B*14:02, and HLA-B*27:05 (according to similarity based on HLA allele motifs) (Di Marco *et al.*, 2017; Rasmussen *et al.*, 2014; Sarkizova *et al.*, 2020). In future studies, HLA-I knockout B cell lines other than the C1R and 721.221 cell lines, which may have deficits in antigen processing as they were not immunogenic for the V α 3S1/V β 13S1 TCR, should be developed to clarify the peptide repertoire of HLA-C*06:02 and other select HLA-class I alleles.

It is evident by the limited reproductivity among biological replicates that current protocols of LC-MS/MS may only identify a limited fraction of the total peptides presented by MHC molecules on the cell surface due to losses during the processes of IP and peptide purification or a low abundance of some peptides (Hassan *et al.*, 2014; Zhang, X. *et al.*, 2019). Further, the antigens of a given TCR have to be identified from the multitude of different peptides in the peptidome. As my experimental approaches show, a large number of candidate antigens selected according to the peptide recognition motif had to be loaded on HLA-C*06:02 in antigen-presenting cells and examined by the V α 3S1/V β 13S1-TCR. These experiments are time-consuming and labor-intensive. Not least, as observed here, the immunogenicity of select proteins and peptides may depend on the cell type presenting them as antigens. Therefore, high-throughput and unbiased computational strategies to efficiently determine which epitopes may be recognized by pathogenic CD8⁺ T cells are urgently required (De Mattos-Arruda *et al.*, 2020). Moreover, it would be interesting to investigate what makes HLA-C*06:02⁺ B cells from psoriasis patients but not healthy HLA-C*06:02 carriers particularly immunogenic for the V α 3S1/V β 13S1 TCR and whether certain B cell subpopulations mediate the stimulation of the CD8⁺ T cells against melanocytes in psoriasis. Specifically, immunophenotyping of the antigenic B cells and the validation of B-cell immunogenicity in different clinical classifications of psoriasis await to be elucidated. Hence, my results direct the avenue to experiments addressing novel questions related to the pathogenesis of psoriasis and other T-cell-mediated autoimmune diseases.

5.6 Conclusions

Overall, my study reveals that a pathogenic psoriatic V α 3S1/V β 13S1 TCR cross-reacts against B cells and melanocytes by recognizing different self-peptides of these cell types that are presented by HLA-C*06:02. Notably, B cells exhibited distinctive immunogenicity towards psoriatic CD8⁺ T cells, extending beyond the specific immunogenicity for the V α 3S1/V β 13S1 TCR. Since B cells are rarely seen in normal skin under homeostatic conditions and largely absent from psoriasis skin lesions (Egbuniwe *et al.*, 2015; Nihal *et al.*, 2000), it is plausible that the autoimmune response induced against B cells during streptococcal angina in the tonsils may give rise to an autoimmune activation of pathogenic CD8⁺ T cells against melanocytes in the skin. Autoimmunity against B cells in secondary lymphoid organs may then constantly provide novel effector CD8⁺ T cells for the psoriatic autoimmune response against melanocytes in the skin, which depends on a steady recruitment of pathogenic CD8⁺ T cells.

The identification of the cross-reactive autoimmune response against different self-peptides presented by HLA-C*06:02 on B cells and melanocytes uncovers a previously unrecognized pathomechanism that may underlie streptococcal angina as a triggering event of psoriasis. This may fundamentally change our understanding of psoriasis pathogenesis, but perhaps also of other streptococcal-induced autoimmune diseases. The identification of B cells as possible stimulators of the psoriatic autoimmune response against melanocytes opens up new therapeutic strategies. Therapies targeting specific autoantigens of B cells or B cells themselves may help develop new immunotherapies for the disease. By using antibodies or other small molecules that directly prevent access to MHC-I-peptide complexes, it may be feasible to specifically inhibit T cell contact with pMHC. The pathogenic T-cell engagement with autoantigens may also be prevented or altered by manipulating factors upstream of MHC-I, such as the cellular proteome, or by inhibiting or modifying the proteasome, TAP, or the antigen-loading complex pharmacologically. The therapeutic approaches addressing HLA-class I-restricted autoimmune responses against specific immunogenic peptides indeed hold great promise (Kuiper *et al.*, 2023).

6. Supplements

6.1 Primers for Double-strand DNA Coding Short Peptides

Primers for PCR reactions that produce double-strand DNA coding short peptides were designated with “for” (ward) to elongate the coding strand, and primers designated with “rev” (erse) elongate the non-coding strand of DNA. These primers are listed in three tables corresponding to three matrices of candidate peptides.

Table 6.1.1 Primers for alanine mutants of the ADAMTSL5₅₇₋₆₅ peptide.

Name	Primer sequences
VRSRRCLRL_for	5'- CACC ATG GTG CGC AGC CGG CGC TGC CTC CGG CTT TGA -3'
VRSRRCLRL_rev	5'- TCA AAG CCG GAG GCA GCG CCG GCT GCG CAC -3'
ARSRRCLRL_for	5'- CACC ATG GCC CGC AGC CGG CGC TGC CTC CGG CTT TGA -3'
ARSRRCLRL_rev	5'- TCA AAG CCG GAG GCA GCG CCG GCT GCG GGC -3'
VARSRRCLRL_for	5'- CACC ATG GTG GCC AGC CGG CGC TGC CTC CGG CTT TGA -3'
VARSRRCLRL_rev	5'- TCA AAG CCG GAG GCA GCG CCG GCT GGC CAC -3'
VRARRCLRL_for	5'- CACC ATG GTG CGC GCC CGG CGC TGC CTC CGG CTT TGA -3'
VRARRCLRL_rev	5'- TCA AAG CCG GAG GCA GCG CCG GGC GCG CAC -3'
VRSARCLRL_for	5'- CACC ATG GTG CGC AGC GCC CGC TGC CTC CGG CTT TGA -3'
VRSARCLRL_rev	5'- TCA AAG CCG GAG GCA GCG GGC GCT GCG CAC -3'
VRSRACLRL_for	5'- CACC ATG GTG CGC AGC CGG GCC TGC CTC CGG CTT TGA -3'
VRSRACLRL_rev	5'- TCA AAG CCG GAG GCA GGC CCG GCT GCG CAC -3'
VRSRRALRL_for	5'- CACC ATG GTG CGC AGC CGG CGC GCC CTC CGG CTT TGA -3'
VRSRRALRL_rev	5'- TCA AAG CCG GAG GGC GCG CCG GCT GCG CAC -3'
VRSRRCARL_for	5'- CACC ATG GTG CGC AGC CGG CGC TGC GCC CGG CTT TGA -3'
VRSRRCARL_rev	5'- TCA AAG CCG GGC GCA GCG CCG GCT GCG CAC -3'
VRSRRCLAL_for	5'- CACC ATG GTG CGC AGC CGG CGC TGC CTC GCC CTT TGA -3'
VRSRRCLAL_rev	5'- TCA AAG GGC GAG GCA GCG CCG GCT GCG CAC -3'
VRSRRCLRA_for	5'- CACC ATG GTG CGC AGC CGG CGC TGC CTC CGG GCC TGA -3'
VRSRRCLRA_rev	5'- TCA GGC CCG GAG GCA GCG CCG GCT GCG CAC -3'
VRSRACLAL_for	5'- CACC ATG GTG CGC AGC CGG GCC TGC CTC GCC CTT TGA -3'
VRSRACLAL_rev	5'- TCA AAG GGC GAG GCA GGC CCG GCT GCG CAC -3'
VRSRACAAL_for	5'- CACC ATG GTG CGC AGC CGG GCC TGC GCC GCC CTT TGA -3'
VRSRACAAL_rev	5'- TCA AAG GGC GGC GCA GGC CCG GCT GCG CAC -3'

Table 6.1.2 Primers for ADAMTSL5₅₇₋₆₅ peptide and the RASSF10₄₄₋₅₂ peptide mutants at HLA-C*06:02 anchor positions P2, P7, and P9, as well as Vα3S1/Vβ13S1 TCR-recognition positions P5 and P8.

Name	Primer sequences
SRSRRCLRL_for	5'- CACC ATG TCT CGC AGC CGG CGC TGC CTC CGG CTT TGA -3'
SRSRRCLRL_rev	5'- TCA AAG CCG GAG GCA GCG CCG GCT GCG AGA -3'
VGSRRCLRL_for	5'- CACC ATG GTG GGA AGC CGG CGG TGC CTG CGG CTG TGA -3'
VGSRRCLRL_rev	5'- TCA AAG CCG GAG GCA GCG CCG GCT TCC CAC -3'
VTSSRRCLRL_for	5'- CACC ATG GTG ACA AGC CGG CGC TGC CTC CGG CTT TGA -3'

VTSRRCLRL_rev	5'- TCA AAG CCG GAG GCA GCG CCG GCT TGT CAC -3'
VPSRRCLRL_for	5'- CACC ATG GTG CCT AGC CGG CGC TGC CTC CGG CTT TGA -3'
VPSRRCLRL_rev	5'- TCA AAG CCG GAG GCA GCG CCG GCT AGG CAC -3'
VYSRRCLRL_for	5'- CACC ATG GTG TAT AGC CGG CGC TGC CTC CGG CTT TGA -3'
VYSRRCLRL_rev	5'- TCA AAG CCG GAG GCA GCG CCG GCT ATA CAC -3'
VLSRRCLRL_for	5'- CACC ATG GTG CTT AGC CGG CGC TGC CTC CGG CTT TGA -3'
VLSRRCLRL_rev	5'- TCA AAG CCG GAG GCA GCG CCG GCT AAG CAC -3'
VRSRCRLRL_for	5'- CACC ATG GTG CGC AGC CGG TGC CGC CTC CGG CTT TGA -3'
VRSRCRLRL_rev	5'- TCA AAG CCG GAG GCG GCA CCG GCT GCG CAC -3'
VRSRKCLRL_for	5'- CACC ATG GTG CGC AGC CGG AAG TGC CTC CGG CTT TGA -3'
VRSRKCLRL_rev	5'- TCA AAG CCG GAG GCA CTT CCG GCT GCG CAC -3'
VRSRHCLRL_for	5'- CACC ATG GTG CGC AGC CGG CAC TGC CTC CGG CTT TGA -3'
VRSRHCLRL_rev	5'- TCA AAG CCG GAG GCA GTG CCG GCT GCG CAC -3'
VRSRSCLRL_for	5'- CACC ATG GTG CGC AGC CGG AGC TGC CTC CGG CTT TGA -3'
VRSRSCLRL_rev	5'- TCA AAG CCG GAG GCA GCT CCG GCT GCG CAC -3'
VRSRLCLRL_for	5'- CACC ATG GTG CGC AGC CGG CTT TGC CTC CGG CTT TGA -3'
VRSRLCLRL_rev	5'- TCA AAG CCG GAG GCA AAG CCG GCT GCG CAC -3'
VRSRFCLRL_for	5'- CACC ATG GTG CGC AGC CGG TTT TGC CTC CGG CTT TGA -3'
VRSRFCLRL_rev	5'- TCA AAG CCG GAG GCA AAA CCG GCT GCG CAC -3'
VRSRICLRL_for	5'- CACC ATG GTG CGC AGC CGG ATA TGC CTC CGG CTT TGA -3'
VRSRICLRL_rev	5'- TCA AAG CCG GAG GCA TAT CCG GCT GCG CAC -3'
VRSRVCLRL_for	5'- CACC ATG GTG CGC AGC CGG GTA TGC CTC CGG CTT TGA -3'
VRSRVCLRL_rev	5'- TCA AAG CCG GAG GCA TAC CCG GCT GCG CAC -3'
VRSRGCLRL_for	5'- CACC ATG GTG CGC AGC CGG GGA TGC CTC CGG CTT TGA -3'
VRSRGCLRL_rev	5'- TCA AAG CCG GAG GCA TCC CCG GCT GCG CAC -3'
VRSRRCKRL_for	5'- CACC ATG GTG CGC AGC CGG CGC TGC AAA CGG CTT TGA -3'
VRSRRCKRL_rev	5'- TCA AAG CCG TTT GCA GCG CCG GCT GCG CAC -3'
VRSRRCQRL_for	5'- CACC ATG GTG CGC AGC CGG CGC TGC CAG CGG CTT TGA -3'
VRSRRCQRL_rev	5'- TCA AAG CCG CTG GCA GCG CCG GCT GCG CAC -3'
VRSRRCIRL_for	5'- CACC ATG GTG CGC AGC CGG CGC TGC ATA CGG CTT TGA -3'
VRSRRCIRL_rev	5'- TCA AAG CCG TAT GCA GCG CCG GCT GCG CAC -3'
VRSRRCVRL_for	5'- CACC ATG GTG CGC AGC CGG CGC TGC GTA CGG CTT TGA -3'
VRSRRCVRL_rev	5'- TCA AAG CCG TAC GCA GCG CCG GCT GCG CAC -3'
VRSRRCLKL_for	5'- CACC ATG GTG CGC AGC CGG CGC TGC CTC AAG CTT TGA -3'
VRSRRCLKL_rev	5'- TCA AAG CTT GAG GCA GCG CCG GCT GCG CAC -3'
VRSRRCLHL_for	5'- CACC ATG GTG CGC AGC CGG CGC TGC CTC CAC CTT TGA -3'
VRSRRCLHL_rev	5'- TCA AAG GTG GAG GCA GCG CCG GCT GCG CAC -3'
VRSRRCLLL_for	5'- CACC ATG GTG CGC AGC CGG CGC TGC CTC CTT CTT TGA -3'
VRSRRCLLL_rev	5'- TCA AAG AAG GAG GCA GCG CCG GCT GCG CAC -3'
VRSRRCLRY_for	5'- CACC ATG GTG CGC AGC CGG CGC TGC CTC CGG TAT TGA -3'
VRSRRCLRY_rev	5'- TCA ATA CCG GAG GCA GCG CCG GCT GCG CAC -3'
VRSRRCLRv_for	5'- CACC ATG GTG CGC AGC CGG CGC TGC CTC CGG GTT TGA -3'
VRSRRCLRv_rev	5'- TCA AAC CCG GAG GCA GCG CCG GCT GCG CAC -3'
VRSRRCLRf_for	5'- CACC ATG GTG CGC AGC CGG CGC TGC CTC CGG TTT TGA -3'
VRSRRCLRf_rev	5'- TCA AAA CCG GAG GCA GCG CCG GCT GCG CAC -3'
VRSRRCLRI_for	5'- CACC ATG GTG CGC AGC CGG CGC TGC CTC CGG ATC TGA -3'
VRSRRCLRI_rev	5'- TCA GAT CCG GAG GCA GCG CCG GCT GCG CAC -3'
VRSRRCLRM_for	5'- CACC ATG GTG CGC AGC CGG CGC TGC CTC CGG ATG TGA -3'
VRSRRCLRM_rev	5'- TCA CAT CCG GAG GCA GCG CCG GCT GCG CAC -3'
RYQRRSRRL_for	5'- CACC ATG CGG TAC CAG CGG CGG AGC CGG CTG TGA -3'
RYQRRSRRL_rev	5'- TCA CAG CCG CCG GCT CCG CCG CTG GTA CCG -3'
RGQRRSRRL_for	5'- CACC ATG CGG GGG CAG CGG CGG AGC CGG CTG TGA -3'

RGQRRSRRL_rev	5'- TCA CAG CCG CCG GCT CCG CCG CTG CCC CCG -3'
RTQRRSRRL_for	5'- CACC ATG CGG ACG CAG CGG CGG AGC CGG CGG CTG TGA -3'
RTQRRSRRL_rev	5'- TCA CAG CCG CCG GCT CCG CCG CTG CGT CCG -3'
RAQRRSRRL_for	5'- CACC ATG CGG GCT CAG CGG CGG AGC CGG CGG CTG TGA -3'
RAQRRSRRL_rev	5'- TCA CAG CCG CCG GCT CCG CCG CTG AGC CCG -3'
RPQRRSRRL_for	5'- CACC ATG CGG CCT CAG CGG CGG AGC CGG CGG CTG TGA -3'
RPQRRSRRL_rev	5'- TCA CAG CCG CCG GCT CCG CCG CTG AGG CCG -3'
RQQRRSRRL_for	5'- CACC ATG CGG CAG CAG CGG CGG AGC CGG CGG CTG TGA -3'
RQQRRSRRL_rev	5'- TCA CAG CCG CCG GCT CCG CCG CTG CTG CCG -3'
RRQRGSRL_for	5'- CACC ATG CGG CGG CAG CGG GGG AGC CGG CGG CTG TGA -3'
RRQRGSRL_rev	5'- TCA CAG CCG CCG GCT CCC CCG CTG CCG CCG -3'
RRQRRSRM_for	5'- CACC ATG CGG CGG CAG CGG CGG AGC CGG CGG ATG TGA -3'
RRQRRSRM_rev	5'- TCA CAT CCG CCG GCT CCG CCG CTG CCG CCG -3'
RRQRRSRT_for	5'- CACC ATG CGG CGG CAG CGG CGG AGC CGG CGG ACC TGA -3'
RRQRRSRT_rev	5'- TCA GGT CCG CCG GCT CCG CCG CTG CCG CCG -3'
RRQRRSRG_for	5'- CACC ATG CGG CGG CAG CGG CGG AGC CGG CGG GGC TGA -3'
RRQRRSRG_rev	5'- TCA GCC CCG CCG GCT CCG CCG CTG CCG CCG -3'
RRQRRSRI_for	5'- CACC ATG CGG CGG CAG CGG CGG AGC CGG CGG ATC TGA -3'
RRQRRSRI_rev	5'- TCA GAT CCG CCG GCT CCG CCG CTG CCG CCG -3'
RRQRRSRA_for	5'- CACC ATG CGG CGG CAG CGG CGG AGC CGG CGG GCC TGA -3'
RRQRRSRA_rev	5'- TCA GGC CCG CCG GCT CCG CCG CTG CCG CCG -3'
RRQRRSRV_for	5'- CACC ATG CGG CGG CAG CGG CGG AGC CGG CGG GTG TGA -3'
RRQRRSRV_rev	5'- TCA CAC CCG CCG GCT CCG CCG CTG CCG CCG -3'
RRQRRSRY_for	5'- CACC ATG CGG CGG CAG CGG CGG AGC CGG CGG TAC TGA -3'
RRQRRSRY_rev	5'- TCA GTA CCG CCG GCT CCG CCG CTG CCG CCG -3'
RRQRRSRF_for	5'- CACC ATG CGG CGG CAG CGG CGG AGC CGG CGG TTC TGA -3'
RRQRRSRF_rev	5'- TCA GAA CCG CCG GCT CCG CCG CTG CCG CCG -3'
RRQRRSRP_for	5'- CACC ATG CGG CGG CAG CGG CGG AGC CGG CGG CCT TGA -3'
RRQRRSRP_rev	5'- TCA AGG CCG CCG GCT CCG CCG CTG CCG CCG -3'

Table 6.1.3 Primers for candidate peptide antigens from peptides eluted from HLA-C*06:02-C1R or HLA-C*06:02-721.221.

Name	Primer sequences
LRHPNILRL_for	5'- CACC ATG CTT CGG CAT CCT AAT ATT CTT AGA CTG TGA -3'
LRHPNILRL_rev	5'- TCA CAG TCT AAG AAT ATT AGG ATG CCG AAG -3'
QRAWQERRL_for	5'- CACC ATG CAG CGC GCC TGG CAA GAG CGG CGC CTG TGA -3'
QRAWQERRL_rev	5'- TCA CAG GCG CCG CTC TTG CCA GGC GCG CTG -3'
LRNFNLFRL_for	5'- CACC ATG CTA AGG AAC TTT AAC CTC TTC CGC TTA TGA -3'
LRNFNLFRL_rev	5'- TCA TAA GCG GAA GAG GTT AAA GTT CCT TAG -3'
FRPEHVSRL_for	5'- CACC ATG TTC CGG CCA GAG CAC GTG TCC AGG CTG TGA -3'
FRPEHVSRL_rev	5'- TCA CAG CCT GGA CAC GTG CTC TGG CCG GAA -3'
IRPEHVLRL_for	5'- CACC ATG ATC CGG CCC GAG CAC GTC CTG CGC CTC TGA -3'
IRPEHVLRL_rev	5'- TCA GAG GCG CAG GAC GTG CTC GGG CCG GAT -3'
ERFAKERRL_for	5'- CACC ATG GAG AGG TTT GCC AAA GAG CGC AGG CTG TGA -3'
ERFAKERRL_rev	5'- TCA CAG CCT GCG CTC TTT GGC AAA CCT CTC -3'
SRPVKLFRV_for	5'- CACC ATG TCC CGT CCT GTG AAG CTC TTC CGA GTC TGA -3'
SRPVKLFRV_rev	5'- TCA GAC TCG GAA GAG CTT CAC AGG ACG GGA -3'
LRYDHQSRL_for	5'- CACC ATG CTG CGA TAT GAC CAC CAG TCA CGG CTT TGA -3'
LRYDHQSRL_rev	5'- TCA AAG CCG TGA CTG GTG GTC ATA TCG CAG -3'
ERFPKLLRL_for	5'- CACC ATG GAA CGA TTT CCC AAG TTA CTA CGC CTG TGA -3'

ERFPKLLRL_rev	5'- TCA CAG GCG TAG TAA CTT GGG AAA TCG TTC -3'
SRFPEALRL_for	5'- CACC ATG AGC CGC TTC CCT GAA GCT CTG AGA TTG TGA -3'
SRFPEALRL_rev	5'- TCA CAA TCT CAG AGC TTC AGG GAA GCG GCT -3'
KRASYILRL_for	5'- CACC ATG AAA CGT GCA AGT TAC ATC TTG CGT CTT TGA -3'
KRASYILRL_rev	5'- TCA AAG ACG CAA GAT GTA ACT TGC ACG TTT -3'
YRKAFESRL_for	5'- CACC ATG TAC CGC AAA GCG TTT GAG AGC AGA CTA TGA -3'
YRKAFESRL_rev	5'- TCA TAG TCT GCT CTC AAA CGC TTT GCG GTA -3'
SRPELIFRL_for	5'- CACC ATG TCA AGG CCT GAA CTT ATT TTT AGA CTA TGA -3'
SRPELIFRL_rev	5'- TCA TAG TCT AAA AAT AAG TTC AGG CCT TGA -3'
NRNFWVLRL_for	5'- CACC ATG AAC AGG AAC TTC TGG GTC CTG CGG CTG TGA -3'
NRNFWVLRL_rev	5'- TCA CAG CCG CAG GAC CCA GAA GTT CCT GTT -3'
SRSISLLRL_for	5'- CACC ATG TCC CGT AGC ATC AGC CTG CTG CGT CTC TGA -3'
SRSISLLRL_rev	5'- TCA GAG ACG CAG CAG GCT GAT GCT ACG GGA -3'
FRNERAIRF_for	5'- CACC ATG TTT CGA AAT GAA CGT GCA ATT AGA TTC TGA -3'
FRNERAIRF_rev	5'- TCA GAA TCT AAT TGC ACG TTC ATT TCG AAA -3'
VRFHRPYRL_for	5'- CACC ATG GTG CGT TTT CAC CGT CCT TAC CGC CTG TGA -3'
VRFHRPYRL_rev	5'- TCA CAG GCG GTA AGG ACG GTG AAA ACG CAC -3'
GAYGQAVRY_for	5'- CACC ATG GGC GCC TAT GGG CAG GCG GTG CGC TAC TGA -3'
GAYGQAVRY_rev	5'- TCA GTA GCG CAC CGC CTG CCC ATA GGC GCC -3'
YRIATSKRY_for	5'- CACC ATG TAC CGT ATC GCC ACC TCC AAG AGG TAC TGA -3'
YRIATSKRY_rev	5'- TCA GTA CCT CTT GGA GGT GGC GAT ACG GTA -3'
LRYDHQQL_for	5'- CACC ATG CTG CGA TAC GAC CAT CAA CAG AGA CTG TGA -3'
LRYDHQQL_rev	5'- TCA CAG TCT CTG TTG ATG GTC GTA TCG CAG -3'
FRIEKIERI_for	5'- CACC ATG TTC AGA ATA GAG AAG ATT GAG AGG ATC TGA -3'
FRIEKIERI_rev	5'- TCA GAT CCT CTC AAT CTT CTC TAT TCT GAA -3'
KLYGKPIRV_for	5'- CACC ATG AAA CTC TAT GGG AAG CCA ATA CGG GTG TGA -3'
KLYGKPIRV_rev	5'- TCA CAC CCG TAT TGG CTT CCC ATA GAG TTT -3'
HRFEHDARI_for	5'- CACC ATG CAT CGT TTT GAG CAC GAT GCA AGA ATA TGA -3'
HRFEHDARI_rev	5'- TCA TAT TCT TGC ATC GTG CTC AAA ACG ATG -3'
VHVGHVVRF_for	5'- CACC ATG GTC CAC GTT GGG CAT GTT GTT CGC TTT TGA -3'
VHVGHVVRF_rev	5'- TCA AAA GCG AAC AAC ATG CCC AAC GTG GAC -3'
IRHTHVPRL_for	5'- CACC ATG ATT CGG CAT ACT CAT GTA CCC AGA CTT TGA -3'
IRHTHVPRL_rev	5'- TCA AAG TCT GGG TAC ATG AGT ATG CCG AAT -3'
VRKDHENRL_for	5'- CACC ATG GTT CGA AAG GAT CAC GAA AAC AGA TTG TGA -3'
VRKDHENRL_rev	5'- TCA CAA TCT GTT TTC GTG ATC CTT TCG AAC -3'
KRHEKDVRI_for	5'- CACC ATG AAA CGA CAT GAA AAG GAC GTA AGG ATA TGA -3'
KRHEKDVRI_rev	5'- TCA TAT CCT TAC GTC CTT TTC ATG TCG TTT -3'
SRFGKFIRI_for	5'- CACC ATG TCT CGC TTT GGT AAA TTC ATC AGG ATC TGA -3'
SRFGKFIRI_rev	5'- TCA GAT CCT GAT GAA TTT ACC AAA GCG AGA -3'
KYIDKTIRV_for	5'- CACC ATG AAG TAC ATC GAC AAG ACG ATC CGG GTA TGA -3'
KYIDKTIRV_rev	5'- TCA TAC CCG GAT CGT CTT GTC GAT GTA CTT -3'

Table 6.1.4 Primers for candidate peptides from human proteome screening.

Names	Primer sequences
HRKQRALRI_for	5'- CACC ATG CAC AGA AAG CAA AGG GCA CTC AGA ATC TGA -3'
HRKQRALRI_rev	5'- TCA GAT TCT GAG TGC CCT TTG CTT TCT GTG -3'
NRNHNSSRF_for	5'- CACC ATG AAC CGC AAT CAC AAC TCC AGC CGC TTT TGA -3'
NRNHNSSRF_rev	5'- TCA AAA GCG GCT GGA GTT GTG ATT GCG GTT -3'
SRSSQDSRF_for	5'- CACC ATG TCC CGC TCC AGC CAG GAC TCC CGC TTC TGA -3'
SRSSQDSRF_rev	5'- TCA GAA GCG GGA GTC CTG GCT GGA GCG GGA -3'

WRRPRLRRL_for	5'- CACC ATG TGG CGG CGG CCA CGG CTG AGG CGT CTA TGA -3'
WRRPRLRRL_rev	5'- TCA TAG ACG CCT CAG CCG TGG CCG CCG CCA -3'
IRAARRSRL_for	5'- CACC ATG ATT CGA GCG GCC AGG AGG TCC CGG CTT TGA -3'
IRAARRSRL_rev	5'- TCA AAG CCG GGA CCT CCT GGC CGC TCG AAT -3'
DRIERMLRRL_for	5'- CACC ATG GAT AGA ATA GAA AGA ATG CTT CGC CTC TGA -3'
DRIERMLRRL_rev	5'- TCA GAG GCG AAG CAT TCT TTC TAT TCT ATC -3'
LRHQQRGLRRL_for	5'- CACC ATG CTA AGG CAC CAA AGG GGT CTA AGG TTA TGA -3'
LRHQQRGLRRL_rev	5'- TCA TAA CCT TAG ACC CCT TTG GTG CCT TAG -3'
RRFLRTLRL_for	5'- CACC ATG CGC CGC TTC CTG CGC ACA TTG CGC CTC TGA -3'
RRFLRTLRL_rev	5'- TCA GAG GCG CAA TGT GCG CAG GAA GCG GCG -3'
RRCPLRLRRL_for	5'- CACC ATG CGC CGC TGC CCT CGT CTA CGC CGC CTA TGA -3'
RRCPLRLRRL_rev	5'- TCA TAG GCG GCG TAG ACG AGG GCA GCG GCG -3'
QRLSRRRRL_for	5'- CACC ATG CAG CGC CTG TCG CGG CGC CGG CGG CTG TGA -3'
QRLSRRRRL_rev	5'- TCA CAG CCG CCG GCG CCG CGA CAG GCG CTG -3'
GRRSRGRRRL_for	5'- CACC ATG GGG CGG CGG TCG CGG GGT CGG CGG CTC TGA -3'
GRRSRGRRRL_rev	5'- TCA GAG CCG CCG ACC CCG CGA CCG CCG CCC -3'
SRAERNRRL_for	5'- CACC ATG TCC AGA GCA GAG AGG AAC CGG CGC CTG TGA -3'
SRAERNRRL_rev	5'- TCA CAG GCG CCG GTT CCT CTC TGC TCT GGA -3'
LRSVRPLRRL_for	5'- CACC ATG CTG CGG TCA GTG AGG CCC CTA CGG TTG TGA -3'
LRSVRPLRRL_rev	5'- TCA CAA CCG TAG GGG CCT CAC TGA CCG CAG -3'
HRADRMRRRL_for	5'- CACC ATG CAC CGG GCC GAC CGC ATG AGG CGC CTG TGA -3'
HRADRMRRRL_rev	5'- TCA CAG GCG CCT CAT GCG GTC GGC CCG GTG -3'
DRFQKRRL_for	5'- CACC ATG GAC CGC TTC CAG CGA AAG CGG CGA TTG TGA -3'
DRFQKRRL_rev	5'- TCA CAA TCG CCG CTT TCG CTG GAA GCG GTC -3'
MRVVRLRL_for	5'- CACC ATG ATG CGC GTG GTG CGG CTG CTG CGG CTC TGA -3'
MRVVRLRL_rev	5'- TCA GAG CCG CAG CAG CCG CAC CAC GCG CAT -3'
TRLPRGRRL_for	5'- CACC ATG ACG CGA CTG CCC CGC GGG CGG AGA CTG TGA -3'
TRLPRGRRL_rev	5'- TCA CAG TCT CCG CCC GCG GGG CAG TCG CGT -3'
TRSSRRRL_for	5'- CACC ATG ACC CGC AGC TCC CGG CGC CGC CGG CTG TGA -3'
TRSSRRRL_rev	5'- TCA CAG CCG GCG GCG CCG GGA GCT GCG GGT -3'
IRRGRVRRRL_for	5'- CACC ATG ATC AGG CGG GGG CGA GTT AGG CGA CTT TGA -3'
IRRGRVRRRL_rev	5'- TCA AAG TCG CCT AAC TCG CCC CCG CCT GAT -3'
ARIGRILRL_for	5'- CACC ATG GCC AGG ATT GGC CGA ATC CTA CGT CTA TGA -3'
ARIGRILRL_rev	5'- TCA TAG ACG TAG GAT TCG GCC AAT CCT GGC -3'
FRVLRPLRL_for	5'- CACC ATG TTC CGC GTG CTG CGC CCC CTG CGG CTG TGA -3'
FRVLRPLRL_rev	5'- TCA CAG CCG CAG GGG GCG CAG CAC GCG GAA -3'
ERIQLRLRL_for	5'- CACC ATG GAG CGC ATC CAG CGC CTC CGC CGT CTC TGA -3'
ERIQLRLRL_rev	5'- TCA GAG ACG GCG GAG GCG CTG GAT GCG CTC -3'
ARSKRGLRRL_for	5'- CACC ATG GCT CGT TCA AAG AGA GGC TTG AGA CTC TGA -3'
ARSKRGLRRL_rev	5'- TCA GAG TCT CAA GCC TCT CTT TGA ACG AGC -3'
LRFLRALRRL_for	5'- CACC ATG TTG AGA TTT TTA AGA GCT CTG AGA CTG TGA -3'
LRFLRALRRL_rev	5'- TCA CAG TCT CAG AGC TCT TAA AAA TCT CAA -3'
SREDTPSRL_for	5'- CACC ATG TCC AGA GAG GAC ACG CCG AGC AGA TTG TGA -3'
SREDTPSRL_rev	5'- TCA CAA TCT GCT CGG CGT GTC CTC TCT GGA -3'
ARQRRQSRL_for	5'- CACC ATG GCG CGG CAG CGC AGG CAG AGC CGC CTA TGA -3'
ARQRRQSRL_rev	5'- TCA TAG GCG GCT CTG CCT GCG CTG CCG CGC -3'
PRETRERRL_for	5'- CACC ATG CCG AGG GAG ACC AGA GAG AGG AGG CTG TGA -3'
PRETRERRL_rev	5'- TCA CAG CCT CCT CTC TCT GGT CTC CCT CGG -3'
ERVERERRL_for	5'- CACC ATG GAG AGA GTG GAG AGA GAG AGA CGC TTA TGA -3'
ERVERERRL_rev	5'- TCA TAA GCG TCT CTC TCT CTC CAC TCT CTC -3'
RRDHRALRRL_for	5'- CACC ATG AGA AGA GAT CAT CGT GCT CTC AGA CTC TGA -3'
RRDHRALRRL_rev	5'- TCA GAG TCT GAG AGC ACG ATG ATC TCT TCT -3'

GREARRRRL_for	5'- CACC ATG GGT CGC GAG GCC CGG CGC CGG CGG CTT TGA -3'
GREARRRRL_rev	5'- TCA AAG CCG CCG GCG CCG GGC CTC GCG ACC -3'
ARVARWRRL_for	5'- CACC ATG GCC CGG GTG GCG CGG TGG CGG CGG CTG TGA -3'
ARVARWRRL_rev	5'- TCA CAG CCG CCG CCA CCG CGC CAC CCG GGC -3'
PRRRRRRRL_for	5'- CACC ATG CCT CGC CGC CGC CGT CGT CGC CGG TTA TGA -3'
PRRRRRRRL_rev	5'- TCA TAA CCG GCG ACG ACG GCG GCG GCG AGG -3'
LRALRHLRL_for	5'- CACC ATG CTG AGA GCT TTA CGT CAT CTT CGA TTA TGA -3'
LRALRHLRL_rev	5'- TCA TAA TCG AAG ATG ACG TAA AGC TCT CAG -3'
GRKWRKLRL_for	5'- CACC ATG GGA AGA AAG TGG AGG AAG CTG AGG TTG TGA -3'
GRKWRKLRL_rev	5'- TCA CAA CCT CAG CTT CCT CCA CTT TCT TCC -3'
ERALRLLRL_for	5'- CACC ATG GAG CGA GCC CTC CGC CTT CTC AGA CTA TGA -3'
ERALRLLRL_rev	5'- TCA TAG TCT GAG AAG GCG GAG GGC TCG CTC -3'
ARALRGRRRL_for	5'- CACC ATG GCC CGC GCC CTG CGT GGC CGG CGC CTG TGA -3'
ARALRGRRRL_rev	5'- TCA CAG GCG CCG GCC ACG CAG GGC GCG GGC -3'
QRERRGRRRL_for	5'- CACC ATG CAG CGG GAG AGA CGT GGT CGC CGT CTC TGA -3'
QRERRGRRRL_rev	5'- TCA GAG ACG GCG ACC ACG TCT CTC CCG CTG -3'
VRGSRCLRL_for	5'- CACC ATG GTC CGT GGG TCG CGC TGC TTG CGG CTG TGA -3'
VRGSRCLRL_rev	5'- TCA CAG CCG CAA GCA GCG CGA CCC ACG GAC -3'
LRPKRTLRL_for	5'- CACC ATG CTG CGT CCA AAG AGG ACT CTG CGG CTG TGA -3'
LRPKRTLRL_rev	5'- TCA CAG CCG CAG AGT CCT CTT TGG ACG CAG -3'
RRRSTGLRL_for	5'- CACC ATG CGG CGG CGC AGC ACA GGA CTC CGG CTG TGA -3'
RRRSTGLRL_rev	5'- TCA CAG CCG GAG TCC TGT GCT GCG CCG CCG -3'
LRQGQSRRV_for	5'- CACC ATG CTC CGG CAG GGG CAG TCC CGG AGA GTT TGA -3'
LRQGQSRRV_rev	5'- TCA AAC TCT CCG GGA CTG CCC CTG CCG GAG -3'
MRVDRESRF_for	5'- CACC ATG ATG CGG GTA GAC AGG GAG AGC AGG TTT TGA -3'
MRVDRESRF_rev	5'- TCA AAA CCT GCT CTC CCT GTC TAC CCG CAT -3'
ARGGRGRRRL_for	5'- CACC ATG GCG CGC GGT GGC CGC GGC CGC CGC CTG TGA -3'
ARGGRGRRRL_rev	5'- TCA CAG GCG GCG GCC GCG GCC ACC GCG CGC -3'
ARLLRALRL_for	5'- CACC ATG GCG CGA TTG CTC CGG GCT CTG CGC CTG TGA -3'
ARLLRALRL_rev	5'- TCA CAG GCG CAG AGC CCG GAG CAA TCG CGC -3'
GRPRRRRRL_for	5'- CACC ATG GGA AGA CCC AGG AGA AGG CGG AGG CTC TGA -3'
GRPRRRRRL_rev	5'- TCA GAG CCT CCG CCT TCT CCT GGG TCT TCC -3'
RRLARFLRL_for	5'- CACC ATG CGC CGT CTG GCA CGC TTC CTG AGG CTC TGA -3'
RRLARFLRL_rev	5'- TCA GAG CCT CAG GAA GCG TGC CAG ACG GCG -3'
HRPLRPLRL_for	5'- CACC ATG CAT CGC CCG CTG CGG CCC CTG CGG CTC TGA -3'
HRPLRPLRL_rev	5'- TCA GAG CCG CAG GGG CCG CAG CGG GCG ATG -3'
YRNPRFLRL_for	5'- CACC ATG TAC AGG AAC CCC CGG TTC CTC AGG TTA TGA -3'
YRNPRFLRL_rev	5'- TCA TAA CCT GAG GAA CCG GGG GTT CCT GTA -3'
RRRRRRRRL_for	5'- CACC ATG CGC CGA CGC CGC CGC CGC CGT CGC CTG TGA -3'
RRRRRRRRL_rev	5'- TCA CAG GCG ACG GCG GCG GCG GCG TCG GCG -3'
ARIGRVLRL_for	5'- CACC ATG GCG CGG ATT GGG CGT GTC CTG CGG CTG TGA -3'
ARIGRVLRL_rev	5'- TCA CAG CCG CAG GAC ACG CCC AAT CCG CGC -3'
RRPYRRRRF_for	5'- CACC ATG CGC CGG CCC TAC CGC AGG CGA AGG TTC TGA -3'
RRPYRRRRF_rev	5'- TCA GAA CCT TCG CCT GCG GTA GGG CCG GCG -3'
VRRDRPLRV_for	5'- CACC ATG GTT CGA CGA GAC CGG CCA CTA CGT GTC TGA -3'
VRRDRPLRV_rev	5'- TCA GAC ACG TAG TGG CCG GTC TCG TCG AAC -3'
SRHERSLRM_for	5'- CACC ATG TCC AGG CAT GAG CGG TCT CTT AGG ATG TGA -3'
SRHERSLRM_rev	5'- TCA CAT CCT AAG AGA CCG CTC ATG CCT GGA -3'
VRRDRLRRM_for	5'- CACC ATG GTG CGC CGA GAT CGC CTC CGC AGG ATG TGA -3'
VRRDRLRRM_rev	5'- TCA CAT CCT GCG GAG GCG ATC TCG GCG CAC -3'
ERIERVRRRI_for	5'- CACC ATG GAG CGG ATC GAG CGC GTG CGG AGG ATC TGA -3'
ERIERVRRRI_rev	5'- TCA GAT CCT CCG CAC GCG CTC GAT CCG CTC -3'

RRIPRGRRR_for	5'- CACC ATG CGC CGG ATT CCC CGG GGC CGG CGC ATC TGA -3'
RRIPRGRRR_rev	5'- TCA GAT GCG CCG GCC CCG GGG AAT CCG GCG -3'
RRRVRRRRM_for	5'- CACC ATG CGA AGG AGA GTT CGC CGC CGT CGA ATG TGA -3'
RRRVRRRRM_rev	5'- TCA CAT TCG ACG GCG GCG AAC TCT CCT TCG -3'
RRPRRRRRV_for	5'- CACC ATG CGG CGG CCC CGG CGG CGG CGG CGG GTG TGA -3'
RRPRRRRRV_rev	5'- TCA CAC CCG CCG CCG CCG CCG GGG CCG CCG -3'
RRYWRSRLRV_for	5'- CACC ATG CGC AGA TAC TGG CGC AGC TTA CGG GTC TGA -3'
RRYWRSRLRV_rev	5'- TCA GAC CCG TAA GCT GCG CCA GTA TCT GCG -3'
RRSPRGRRR_for	5'- CACC ATG CGC AGA TCT CCA CGC GGC CGG AGG ATC TGA -3'
RRSPRGRRR_rev	5'- TCA GAT CCT CCG GCC GCG TGG AGA TCT GCG -3'
QRAQRILRV_for	5'- CACC ATG CAG CGG GCT CAG CGG ATC CTC CGC GTG TGA -3'
QRAQRILRV_rev	5'- TCA CAC GCG GAG GAT CCG CTG AGC CCG CTG -3'
FRCSRVLRV_for	5'- CACC ATG TTT AGA TGT TCC AGA GTC CTC AGA GTC TGA -3'
FRCSRVLRV_rev	5'- TCA GAC TCT GAG GAC TCT GGA ACA TCT AAA -3'
FRMVRGRRV_for	5'- CACC ATG TTC CGG ATG GTC CGT GGC CGC CGG GTG TGA -3'
FRMVRGRRV_rev	5'- TCA CAC CCG GCG GCC ACG GAC CAT CCG GAA -3'
LREPRLRRI_for	5'- CACC ATG CTT CGA GAG CCC AGG TTA CGA CGG ATT TGA -3'
LREPRLRRI_rev	5'- TCA AAT CCG TCG TAA CCT GGG CTC TCG AAG -3'
RRPPRERRF_for	5'- CACC ATG AGG CGA CCA CCT CGT GAA CGA AGA TTC TGA -3'
RRPPRERRF_rev	5'- TCA GAA TCT TCG TTC ACG AGG TGG TCG CCT -3'
VRILRLLRI_for	5'- CACC ATG GTA CGA ATT TTG CGG TTA TTA AGA ATT TGA -3'
VRILRLLRI_rev	5'- TCA AAT TCT TAA TAA CCG CAA AAT TCG TAC -3'
ARLIRHRRR_for	5'- CACC ATG GCA CGA CTC ATT AGA CAC CGG AGA ATC TGA -3'
ARLIRHRRR_rev	5'- TCA GAT TCT CCG GTG TCT AAT GAG TCG TGC -3'
RRQRRERRF_for	5'- CACC ATG CGC CGC CAA CGC CGA GAA CGT CGC TTT TGA -3'
RRQRRERRF_rev	5'- TCA AAA GCG ACG TTC TCG GCG TTG GCG GCG -3'
ARQYRSLRV_for	5'- CACC ATG GCC AGG CAG TAC CGA AGC CTT CGG GTG TGA -3'
ARQYRSLRV_rev	5'- TCA CAC CCG AAG GCT TCG GTA CTG CCT GGC -3'
RRLRLRLRV_for	5'- CACC ATG CGT CGA CTA CTG AGA TTG CTG AGA GTG TGA -3'
RRLRLRLRV_rev	5'- TCA CAC TCT CAG CAA TCT CAG TAG TCG ACG -3'
QRVARRRRF_for	5'- CACC ATG CAG AGA GTG GCT CGG CGG CGA AGG TTT TGA -3'
QRVARRRRF_rev	5'- TCA AAA CCT TCG CCG CCG AGC CAC TCT CTG -3'
NREHRVRRR_for	5'- CACC ATG AAC CGA GAG CAC CGT GTC CGC AGG ATC TGA -3'
NREHRVRRR_rev	5'- TCA GAT CCT GCG GAC ACG GTG CTC TCG GTT -3'
LREARGLRV_for	5'- CACC ATG CTG CGC GAG GCC CGG GGG CTC AGG GTA TGA -3'
LREARGLRV_rev	5'- TCA TAC CCT GAG CCC CCG GGC CTC GCG CAG -3'
LRTLRLPLRV_for	5'- CACC ATG CTG CGG ACC CTG CGC CCG CTC AGG GTG TGA -3'
LRTLRLPLRV_rev	5'- TCA CAC CCT GAG CGG GCG CAG GGT CCG CAG -3'
LRVLRALRI_for	5'- CACC ATG CTG CGC GTG CTG CGG GCG CTG CGC ATC TGA -3'
LRVLRALRI_rev	5'- TCA GAT GCG CAG CGC CCG CAG CAC GCG CAG -3'
SRGRRQRRM_for	5'- CACC ATG TCC CGG GGA AGG CGC CAG CGA AGA ATG TGA -3'
SRGRRQRRM_rev	5'- TCA CAT TCT TCG CTG GCG CCT TCC CCG GGA -3'
DRVERVRRR_for	5'- CACC ATG GAC AGA GTA GAA CGT GTA CGC AGA ATC TGA -3'
DRVERVRRR_rev	5'- TCA GAT TCT GCG TAC ACG TTC TAC TCT GTC -3'
DRAGRRLRV_for	5'- CACC ATG GAC CGC GCC GGG CGG AGG CTG CGG GTT TGA -3'
DRAGRRLRV_rev	5'- TCA AAC CCG CAG CCT CCG CCC GGC GCG GTC -3'

Table 6.1.5 Candidate peptides from HLA-C*06:02 peptidomes eluted from four homozygous EBV-transformed B cell lines.

Names	Primer sequences
-------	------------------

KRNPRLIRV_for	5'- CACC ATG AAA CGG AAC CCC AGG TTA ATT CGT GTT TGA -3'
KRNPRLIRV_rev	5'- TCA AAC ACG AAT TAA CCT GGG GTT CCG TTT -3'
RQIDRQNRL_for	5'- CACC ATG CGC CAG ATC GAT CGC CAG AAC CGC CTC TGA -3'
RQIDRQNRL_rev	5'- TCA GAG GCG GTT CTG GCG ATC GAT CTG GCG -3'
RVTDRYFRI_for	5'- CACC ATG CGC GTC ACC GAC CGC TAC TTT CGG ATC TGA -3'
RVTDRYFRI_rev	5'- TCA GAT CCG AAA GTA GCG GTC GGT GAC GCG -3'
KLRDRAERI_for	5'- CACC ATG AAG CTT CGC GAC AGG GCC GAG CGG ATC TGA -3'
KLRDRAERI_rev	5'- TCA GAT CCG CTC GGC CCT GTC GCG AAG CTT -3'
KLYDRILRV_for	5'- CACC ATG AAG CTG TAC GAT CGC ATC CTG CGG GTG TGA -3'
KLYDRILRV_rev	5'- TCA CAC CCG CAG GAT GCG ATC GTA CAG CTT -3'
KLNDRVMRV_for	5'- CACC ATG AAA CTC AAT GAT CGT GTC ATG AGA GTG TGA -3'
KLNDRVMRV_rev	5'- TCA CAC TCT CAT GAC ACG ATC ATT GAG TTT -3'
ALYGRALRV_for	5'- CACC ATG GCG CTC TAC GGC CGC GCG CTG CGG GTG TGA -3'
ALYGRALRV_rev	5'- TCA CAC CCG CAG CGC GCG GCC GTA GAG CGC -3'
FLTDREVRL_for	5'- CACC ATG TTC TTA ACA GAT AGG GAG GTA CGA CTT TGA -3'
FLTDREVRL_rev	5'- TCA AAG TCG TAC CTC CCT ATC TGT TAA GAA -3'
RLSNRVVRV_for	5'- CACC ATG CGG CTG TCC AAT CGA GTC GTG CGT GTG TGA -3'
RLSNRVVRV_rev	5'- TCA CAC ACG CAC GAC TCG ATT GGA CAG CCG -3'
RYQGRQYRL_for	5'- CACC ATG AGA TAC CAG GGC AGA CAG TAC AGA CTG TGA -3'
RYQGRQYRL_rev	5'- TCA CAG TCT GTA CTG TCT GCC CTG GTA TCT -3'
KILSRLFRV_for	5'- CACC ATG AAG ATC CTG TCG CGG CTG TTC CGC GTG TGA -3'
KILSRLFRV_rev	5'- TCA CAC GCG GAA CAG CCG CGA CAG GAT CTT -3'
ERRRCHRL_for	5'- CACC ATG GAG AGG CGG CGA TGC CAC AGG TTG TGA -3'
ERRRCHRL_rev	5'- TCA CAA CCT GTG GCA TCG CCG CCT CTC -3'
RVPRAVRV_for	5'- CACC ATG CGA GTC CCA CGG GCC GTG CGC GTG TGA -3'
RVPRAVRV_rev	5'- TCA CAC GCG CAC GGC CCG TGG GAC TCG -3'
VALRALRL_for	5'- CACC ATG GTG GCC CTG CGC GCG CTG CGC CTG TGA -3'
VALRALRL_rev	5'- TCA CAG GCG CAG CGC GCG CAG GGC CAC -3'
KQQRKERL_for	5'- CACC ATG AAG CAG CAG CGG AAG GAG CGG CTG TGA -3'
KQQRKERL_rev	5'- TCA CAG CCG CTC CTT CCG CTG CTG CTT -3'
RISTARRV_for	5'- CACC ATG CGG ATC TCC ACG GCC AGG AGG GTC TGA -3'
RISTARRV_rev	5'- TCA GAC CCT CCT GGC CGT GGA GAT CCG -3'
GVIRTQRRRL_for	5'- CACC ATG GGT GTG ATT CGC ACC CAG CGC CGG CTG TGA -3'
GVIRTQRRRL_rev	5'- TCA CAG CCG GCG CTG GGT GCG AAT CAC ACC -3'
RSVRAIRI_for	5'- CACC ATG CGT AGT GTC CGT GCC ATC CGG ATT TGA -3'
RSVRAIRI_rev	5'- TCA AAT CCG GAT GGC ACG GAC ACT ACG -3'
LYASNVRV_for	5'- CACC ATG CTG TAT GCC AGC AAC GTG CGG CGA GTC TGA -3'
LYASNVRV_rev	5'- TCA GAC TCG CCG CAC GTT GCT GGC ATA CAG -3'
QYYPNGIRL_for	5'- CACC ATG CAG TAC TAC CCC AAT GGC ATC CGG CTC TGA -3'
QYYPNGIRL_rev	5'- TCA GAG CCG GAT GCC ATT GGG GTA GTA CTG -3'
KISLRLKRA_for	5'- CACC ATG AAG ATT TCT CTT CGG CTG AAG AGG GCT TGA -3'
KISLRLKRA_rev	5'- TCA AGC CCT CTT CAG CCG AAG AGA AAT CTT -3'
RIRRDVRV_for	5'- CACC ATG CGC ATC CGG CGG GAC GTC AGG GTC TGA -3'
RIRRDVRV_rev	5'- TCA GAC CCT GAC GTC CCG CCG GAT GCG -3'
VRNGHIKRI_for	5'- CACC ATG GTA CGG AAT GGC CAC ATC AAA AGA ATC TGA -3'
VRNGHIKRI_rev	5'- TCA GAT TCT TTT GAT GTG GCC ATT CCG TAC -3'
ARYYKTKRV_for	5'- CACC ATG GCT CGA TAT TAT AAG ACC AAG CGA GTC TGA -3'
ARYYKTKRV_rev	5'- TCA GAC TCG CTT GGT CTT ATA ATA TCG AGC -3'
KMKEKVERI_for	5'- CACC ATG AAA ATG AAG GAG AAA GTT GAA CGT ATT TGA -3'
KMKEKVERI_rev	5'- TCA AAT ACG TTC AAC TTT CTC CTT CAT TTT -3'
RSYPHLRRV_for	5'- CACC ATG CGG AGC TAT CCG CAC CTC CGG AGA GTC TGA -3'
RSYPHLRRV_rev	5'- TCA GAC TCT CCG GAG GTG CGG ATA GCT CCG -3'

RSYSRRIKI_for	5'- CACC ATG AGA AGC TAT TCT CGC AGA ATT AAA ATA TGA -3'
RSYSRRIKI_rev	5'- TCA TAT TTT AAT TCT GCG AGA ATA GCT TCT -3'
FSATQTRKV_for	5'- CACC ATG TTT TCT GCC ACC CAA ACT CGA AAA GTT TGA -3'
FSATQTRKV_rev	5'- TCA AAC TTT TCG AGT TTG GGT GGC AGA AAA -3'
RVVDQPLKL_for	5'- CACC ATG AGA GTA GTA GAC CAG CCC CTT AAA CTT TGA -3'
RVVDQPLKL_rev	5'- TCA AAG TTT AAG GGG CTG GTC TAC TAC TCT -3'
IRGNVKKL_for	5'- CACC ATG ATC AGA GGC AAC GTG AAG AAA CTT TGA -3'
IRGNVKKL_rev	5'- TCA AAG TTT CTT CAC GTT GCC TCT GAT -3'
KAYKQSSHL_for	5'- CACC ATG AAA GCC TAT AAG CAG TCC TCA CAC CTT TGA -3'
KAYKQSSHL_rev	5'- TCA AAG GTG TGA GGA CTG CTT ATA GGC TTT -3'
MRREQVLKV_for	5'- CACC ATG ATG CGA AGA GAA CAA GTA CTA AAA GTG TGA -3'
MRREQVLKV_rev	5'- TCA CAC TTT TAG TAC TTG TTC TCT TCG CAT -3'
KRKENAIKL_for	5'- CACC ATG AAA AGA AAA GAA AAT GCC ATT AAA TTG TGA -3'
KRKENAIKL_rev	5'- TCA CAA TTT AAT GGC ATT TTC TTT TCT TTT -3'
SQFEKTRKV_for	5'- CACC ATG TCC CAG TTT GAA AAA ACG AGA AAA GTG TGA -3'
SQFEKTRKV_rev	5'- TCA CAC TTT TCT CGT TTT TTC AAA CTG GGA -3'
MMPNKVRKI_for	5'- CACC ATG ATG ATG CCC AAC AAG GTC AGG AAG ATT TGA -3'
MMPNKVRKI_rev	5'- TCA AAT CTT CCT GAC CTT GTT GGG CAT CAT -3'
TRGDHVKHY_for	5'- CACC ATG ACC AGA GGC GAT CAT GTG AAG CAT TAC TGA -3'
TRGDHVKHY_rev	5'- TCA GTA ATG CTT CAC ATG ATC GCC TCT GGT -3'
VRSSKFRHV_for	5'- CACC ATG GTC CGC TCC AGC AAG TTC CGC CAC GTG TGA -3'
VRSSKFRHV_rev	5'- TCA CAC GTG GCG GAA CTT GCT GGA GCG GAC -3'
KRISKTTKL_for	5'- CACC ATG AAA AGA ATT TCA AAG ACT ACT AAG TTG TGA -3'
KRISKTTKL_rev	5'- TCA CAA CTT AGT AGT CTT TGA AAT TCT TTT -3'
FQTSHTLHL_for	5'- CACC ATG TTC CAA ACA TCC CAC ACA CTT CAC CTG TGA -3'
FQTSHTLHL_rev	5'- TCA CAG GTG AAG TGT GTG GGA TGT TTG GAA -3'
HAPDHTRHL_for	5'- CACC ATG CAC GCC CCA GAC CAC ACA AGG CAC TTG TGA -3'
HAPDHTRHL_rev	5'- TCA CAA GTG CCT TGT GTG GTC TGG GGC GTG -3'
IIFETPLRV_for	5'- CACC ATG ATT ATT TTT GAG ACT CCC CTC CGA GTG TGA -3'
IIFETPLRV_rev	5'- TCA CAC TCG GAG GGG AGT CTC AAA AAT AAT -3'
KLFTQILRV_for	5'- CACC ATG AAG CTC TTC ACG CAG ATT CTG CGG GTC TGA -3'
KLFTQILRV_rev	5'- TCA GAC CCG CAG AAT CTG CGT GAA GAG CTT -3'
AAAETELRV_for	5'- CACC ATG GCT GCA GCT GAA ACT GAG CTC AGG GTG TGA -3'
AAAETELRV_rev	5'- TCA CAC CCT GAG CTC AGT TTC AGC TGC AGC -3'
AQFTTALRL_for	5'- CACC ATG GCC CAG TTC ACC ACG GCC CTG CGG CTC TGA -3'
AQFTTALRL_rev	5'- TCA GAG CCG CAG GGC CGT GGT GAA CTG GGC -3'
QYVTQINRL_for	5'- CACC ATG CAA TAT GTC ACC CAG ATC AAC AGG CTG TGA -3'
QYVTQINRL_rev	5'- TCA CAG CCT GTT GAT CTG GGT GAC ATA TTG -3'
KLQEQIHRV_for	5'- CACC ATG AAG CTT CAG GAA CAA ATT CAC AGA GTT TGA -3'
KLQEQIHRV_rev	5'- TCA AAC TCT GTG AAT TTG TTC CTG AAG CTT -3'
YLYDRLLRI_for	5'- CACC ATG TAC CTG TAT GAC CGC TTG CTT CGG ATC TGA -3'
YLYDRLLRI_rev	5'- TCA GAT CCG AAG CAA GCG GTC ATA CAG GTA -3'
VRFGQQKRY_for	5'- CACC ATG GTG CGA TTT GGT CAA CAA AAG CGA TAC TGA -3'
VRFGQQKRY_rev	5'- TCA GTA TCG CTT TTG TTG ACC AAA TCG CAC -3'
YRILQILRV_for	5'- CACC ATG TAC AGA ATT TTG CAG ATA TTG AGA GTC TGA -3'
YRILQILRV_rev	5'- TCA GAC TCT CAA TAT CTG CAA AAT TCT GTA -3'
YTDATPLRV_for	5'- CACC ATG TAC ACA GAT GCC ACA CCT CTG AGA GTC TGA -3'
YTDATPLRV_rev	5'- TCA GAC TCT CAG AGG TGT GGC ATC TGT GTA -3'
RYADRARKI_for	5'- CACC ATG CGC TAT GCT GAC AGA GCA AGA AAA ATC TGA -3'
RYADRARKI_rev	5'- TCA GAT TTT TCT TGC TCT GTC AGC ATA GCG -3'
VLYDRPLKI_for	5'- CACC ATG GTG CTC TAT GAC CGG CCT CTG AAG ATA TGA -3'
VLYDRPLKI_rev	5'- TCA TAT CTT CAG AGG CCG GTC ATA GAG CAC -3'

KLWSRSLKL_for	5'- CACC ATG AAA CTC CCT CCA AAG GAT CTAAGAATC TGA -3'
KLWSRSLKL_rev	5'- TCA GAT TCT TAG ATC CTT TGG AGG GAG TTT -3'
SLSGRPLKV_for	5'- CACC ATG ACA TTC ATG GAT CAT GTG TTA CGC TAT TGA -3'
SLSGRPLKV_rev	5'- TCA ATA GCG TAA CAC ATG ATC CAT GAA TGT -3'
FLFRRGLKV_for	5'- CACC ATG ACT TAT GCA GAA AAG TTG CAC AGA TTA TGA -3'
FLFRRGLKV_rev	5'- TCA TAA TCT GTG CAA CTT TTC TGC ATA AGT -3'
VLYDRVLYKY_for	5'- CACC ATG CGG GAG ATC CGT CTG CAG AGG CTG TGA -3'
VLYDRVLYKY_rev	5'- TCA CAG CCT CTG CAG ACG GAT CTC CCG -3'
RTFGHLLRY_for	5'- CACC ATG AGG TCG CAG AGG CCT GTC CGC TGG TGA -3'
RTFGHLLRY_rev	5'- TCA CCA GCG GAC AGG CCT CTG CGA CCT -3'
VLYLKPLRI_for	5'- CACC ATG CGC AAG AGG CAG ACT TTG CGG CTA TGA -3'
VLYLKPLRI_rev	5'- TCA TAG CCG CAA AGT CTG CCT CTT GCG -3'
KLPPKDLRI_for	5'- CACC ATG CGG ACG GTC ACG CCT CTG CGG TGG TGA -3'
KLPPKDLRI_rev	5'- TCA CCA CCG CAG AGG CGT GAC CGT CCG -3'
TFMDHVLRY_for	5'- CACC ATG CGG TCC ATG AAA GGC CTC CGC TGG TGA -3'
TFMDHVLRY_rev	5'- TCA CCA GCG GAG GCC TTT CAT GGA CCG -3'
TYAEKHLRL_for	5'- CACC ATG ATC CGC AAA GAC TCC CTG CGG CTG GTG TGA -3'
TYAEKHLRL_rev	5'- TCA CAC CAG CCG CAG GGA GTC TTT GCG GAT -3'
REIRLQRL_for	5'- CACC ATG ACC AGG TGT CCG CTG GTG CTG AAA CTG TGA -3'
REIRLQRL_rev	5'- TCA CAG TTT CAG CAC CAG CGG ACA CCT GGT -3'
RSQRPVRW_for	5'- CACC ATG CAC CGG GTG TAC CTG GTG CGG AAG CTC TGA -3'
RSQRPVRW_rev	5'- TCA GAG CTT CCG CAC CAG GTA CAC CCG GTG -3'
RKRQTLRL_for	5'- CACC ATG ACC TAC AGC GAG CTG CTC AGG CGC ATC TGA -3'
RKRQTLRL_rev	5'- TCA GAT GCG CCT GAG CAG CTC GCT GTA GGT -3'
RTVTPLRW_for	5'- CACC ATG CGC TAC TTC AAA ACC CCT CGC AAG TTT TGA -3'
RTVTPLRW_rev	5'- TCA AAA CTT GCG AGG GGT TTT GAA GTA GCG -3'
RSMKGLRW_for	5'- CACC ATG AAG TAT TTT GCA CAG GCA TTG AAA CTG TGA -3'
RSMKGLRW_rev	5'- TCA CAG TTT CAA TGC CTG TGC AAA ATA CTT -3'
IRKDSLRLV_for	5'- CACC ATG CGT GAA TTT AAA CTC AGC AAA GTC TGA -3'
IRKDSLRLV_rev	5'- TCA GAC TTT GCT GAG TTT AAA TTC ACG -3'
TRCPLVLKL_for	5'- CACC ATG CGA GAC CTG CGC AAG TCC AAG TTC TGA -3'
TRCPLVLKL_rev	5'- TCA GAA CTT GGA CTT GCG CAG GTC TCG -3'
HRVYLVRKL_for	5'- CACC ATG AAG CGA CAT AAC TAT GTT CGG AAA GTA TGA -3'
HRVYLVRKL_rev	5'- TCA TAC TTT CCG AAC ATA GTT ATG TCG CTT -3'
TYSELLRRI_for	5'- CACC ATG AAA CGA AGT CAA TTG GTA AAG AAG CTG TGA -3'
TYSELLRRI_rev	5'- TCA CAG CTT CTT TAC CAA TTG ACT TCG TTT -3'
RYFKTPRKF_for	5'- CACC ATG TAT CAG AGG GAC CCC CTG AAG CTG TGA -3'
RYFKTPRKF_rev	5'- TCA CAG CTT CAG GGG GTC CCT CTG ATA -3'
KYFAQALKL_for	5'- CACC ATG GTT TAC TCT CAA ATC TTG AGA AAA CTC TGA -3'
KYFAQALKL_rev	5'- TCA GAG TTT TCT CAA GAT TTG AGA GTAAAC -3'
REFKLSKV_for	5'- CACC ATG CGG CGC TAC CTG CGG CGC AAG GAG TGA -3'
REFKLSKV_rev	5'- TCA CTC CTT GCG CCG CAG GTA GCG CCG -3'
RDLRKSKE_for	5'- CACC ATG CGG AGA CTT CCA TGC AGA AAG AGA TGA -3'
RDLRKSKE_rev	5'- TCA TCT CTT TCT GCA TGG AAG TCT CCG -3'
KRHNYVRKV_for	5'- CACC ATG GTC CGT TAC CGT CTG CCC CTG CGC GTG TGA -3'
KRHNYVRKV_rev	5'- TCA CAC GCG CAG GGG CAG ACG GTA ACG GAC -3'
KRSQVLKKL_for	5'- CACC ATG AAA CTC CCT CCA AAG GAT CTAAGAATC TGA -3'
KRSQVLKKL_rev	5'- TCA GAT TCT TAG ATC CTT TGG AGG GAG TTT -3'
YQRDPLKL_for	5'- CACC ATG ACA TTC ATG GAT CAT GTG TTA CGC TAT TGA -3'
YQRDPLKL_rev	5'- TCA ATA GCG TAA CAC ATG ATC CAT GAA TGT -3'
VYSQILRKL_for	5'- CACC ATG ACT TAT GCA GAA AAG TTG CAC AGA TTA TGA -3'
VYSQILRKL_rev	5'- TCA TAA TCT GTG CAA CTT TTC TGC ATA AGT -3'

RRYLRRKE_for	5'- CACC ATG CGG GAG ATC CGT CTG CAG AGG CTG TGA -3'
RRYLRRKE_rev	5'- TCA CAG CCT CTG CAG ACG GAT CTC CCG -3'
RRLPCRKR_for	5'- CACC ATG AGG TCG CAG AGG CCT GTC CGC TGG TGA -3'
RRLPCRKR_rev	5'- TCA CCA GCG GAC AGG CCT CTG CGA CCT -3'
VRYLPLRV_for	5'- CACC ATG CGC AAG AGG CAG ACT TTG CGG CTA TGA -3'
VRYLPLRV_rev	5'- TCA TAG CCG CAAAGT CTG CCT CTT GCG -3'

6.2 Plasmids

All peptide-encoding plasmids were generated with empty vector pcDNA3.1D/V5-His-TOPO™ and listed in three tables corresponding to three matrices of candidate peptides.

Table 6.2.1 Plasmids coding sequences of alanine mutants of the ADAMTSL5₅₇₋₆₅ peptide.

Plasmid	Size	Resistance Genes	Application
pcDNA3.1D/V5-His-VRSRRCLRL	5.5kb	amp ^R , neo ^R	Expression of VRSRRCLRL peptide in APCs
pcDNA3.1D/V5-His-ARSRRCLRL	5.5kb	amp ^R , neo ^R	Expression of ARSRRCLRL peptide in APCs
pcDNA3.1D/V5-His-VASRRCLRL	5.5kb	amp ^R , neo ^R	Expression of VASRRCLRL peptide in APCs
pcDNA3.1D/V5-His-VRARRCLRL	5.5kb	amp ^R , neo ^R	Expression of VRARRCLRL peptide in APCs
pcDNA3.1D/V5-His-VRSARCLRL	5.5kb	amp ^R , neo ^R	Expression of VRSARCLRL peptide in APCs
pcDNA3.1D/V5-His-VRSRACLRL	5.5kb	amp ^R , neo ^R	Expression of VRSRACLRL peptide in APCs
pcDNA3.1D/V5-His-VRSRRALRL	5.5kb	amp ^R , neo ^R	Expression of VRSRRALRL peptide in APCs
pcDNA3.1D/V5-His-VRSRRCARL	5.5kb	amp ^R , neo ^R	Expression of VRSRRCARL peptide in APCs
pcDNA3.1D/V5-His-VRSRRCLAL	5.5kb	amp ^R , neo ^R	Expression of VRSRRCLAL peptide in APCs
pcDNA3.1D/V5-His-VRSRRCLRA	5.5kb	amp ^R , neo ^R	Expression of VRSRRCLRA peptide in APCs
pcDNA3.1D/V5-His-VRSRACLAL	5.5kb	amp ^R , neo ^R	Expression of VRSRACLAL peptide in APCs
pcDNA3.1D/V5-His-VRSRACAAL	5.5kb	amp ^R , neo ^R	Expression of VRSRACAAL peptide in APCs

Table 6.2.1 Plasmids coding ADAMTSL5₅₇₋₆₅ peptide and the RASSF10₄₄₋₅₂ peptide mutants at HLA-C*06:02 anchor positions P2, P7, and P9, as well as Vα3S1/Vβ13S1 TCR-recognition positions P5 and P8.

Plasmid	Size	Resistance Genes	Application
pcDNA3.1D/V5-His-SRSRRCLRL	5.5kb	amp ^R , neo ^R	Expression of SRSRRCLRL peptide in APCs
pcDNA3.1D/V5-His-VGSRRCLRL	5.5kb	amp ^R , neo ^R	Expression of VGSRRCLRL peptide in APCs
pcDNA3.1D/V5-His-VTSRRCLRL	5.5kb	amp ^R , neo ^R	Expression of VTSRRCLRL peptide in APCs
pcDNA3.1D/V5-His-VPSRRCLRL	5.5kb	amp ^R , neo ^R	Expression of VPSRRCLRL peptide in APCs
pcDNA3.1D/V5-His-VYSRRCLRL	5.5kb	amp ^R , neo ^R	Expression of VYSRRCLRL peptide in APCs
pcDNA3.1D/V5-His-VLSRRCLRL	5.5kb	amp ^R , neo ^R	Expression of VLSRRCLRL peptide in APCs
pcDNA3.1D/V5-His-VRSRCRLRL	5.5kb	amp ^R , neo ^R	Expression of VRSRCRLRL peptide in APCs
pcDNA3.1D/V5-His-VRSRKCLRL	5.5kb	amp ^R , neo ^R	Expression of VRSRKCLRL peptide in APCs
pcDNA3.1D/V5-His-VRSRHCLRL	5.5kb	amp ^R , neo ^R	Expression of VRSRHCLRL peptide in APCs

pcDNA3.1D/V5-His-VRSR S CLRL	5.5kb	amp ^R , neo ^R	Expression of VRSR S CLRL peptide in APCs
pcDNA3.1D/V5-His-VRSR L CLRL	5.5kb	amp ^R , neo ^R	Expression of VRSR L CLRL peptide in APCs
pcDNA3.1D/V5-His-VRSR F CLRL	5.5kb	amp ^R , neo ^R	Expression of VRSR F CLRL peptide in APCs
pcDNA3.1D/V5-His-VRSR I CLRL	5.5kb	amp ^R , neo ^R	Expression of VRSR I CLRL peptide in APCs
pcDNA3.1D/V5-His-VRSR V CLRL	5.5kb	amp ^R , neo ^R	Expression of VRSR V CLRL peptide in APCs
pcDNA3.1D/V5-His-VRSR G CLRL	5.5kb	amp ^R , neo ^R	Expression of VRSR G CLRL peptide in APCs
pcDNA3.1D/V5-His-VRSR R C K RL	5.5kb	amp ^R , neo ^R	Expression of VRSR R C K RL peptide in APCs
pcDNA3.1D/V5-His-VRSR R C Q RL	5.5kb	amp ^R , neo ^R	Expression of VRSR R C Q RL peptide in APCs
pcDNA3.1D/V5-His-VRSR R C I RL	5.5kb	amp ^R , neo ^R	Expression of VRSR R C I RL peptide in APCs
pcDNA3.1D/V5-His-VRSR R C V RL	5.5kb	amp ^R , neo ^R	Expression of VRSR R C V RL peptide in APCs
pcDNA3.1D/V5-His-VRSR R CL K L	5.5kb	amp ^R , neo ^R	Expression of VRSR R CL K L peptide in APCs
pcDNA3.1D/V5-His-VRSR R CL H L	5.5kb	amp ^R , neo ^R	Expression of VRSR R CL H L peptide in APCs
pcDNA3.1D/V5-His-VRSR R CL L L	5.5kb	amp ^R , neo ^R	Expression of VRSR R CL L L peptide in APCs
pcDNA3.1D/V5-His-VRSR R CL R Y	5.5kb	amp ^R , neo ^R	Expression of VRSR R CL R Y peptide in APCs
pcDNA3.1D/V5-His-VRSR R CL R V	5.5kb	amp ^R , neo ^R	Expression of VRSR R CL R V peptide in APCs
pcDNA3.1D/V5-His-VRSR R CL R F	5.5kb	amp ^R , neo ^R	Expression of VRSR R CL R F peptide in APCs
pcDNA3.1D/V5-His-VRSR R CL R I	5.5kb	amp ^R , neo ^R	Expression of VRSR R CL R I peptide in APCs
pcDNA3.1D/V5-His-VRSR R CL R M	5.5kb	amp ^R , neo ^R	Expression of VRSR R CL R M peptide in APCs
pcDNA3.1D/V5-His- R Y QRRSRRL	5.5kb	amp ^R , neo ^R	Expression of R Y QRRSRRL peptide in APCs
pcDNA3.1D/V5-His- R G QRRSRRL	5.5kb	amp ^R , neo ^R	Expression of R G QRRSRRL peptide in APCs
pcDNA3.1D/V5-His- R T QRRSRRL	5.5kb	amp ^R , neo ^R	Expression of R T QRRSRRL peptide in APCs
pcDNA3.1D/V5-His- R A QRRSRRL	5.5kb	amp ^R , neo ^R	Expression of R A QRRSRRL peptide in APCs
pcDNA3.1D/V5-His- R P QRRSRRL	5.5kb	amp ^R , neo ^R	Expression of R P QRRSRRL peptide in APCs
pcDNA3.1D/V5-His- R Q QRRSRRL	5.5kb	amp ^R , neo ^R	Expression of R Q QRRSRRL peptide in APCs
pcDNA3.1D/V5-His-RRQR G SRRL	5.5kb	amp ^R , neo ^R	Expression of RRQR G SRRL peptide in APCs
pcDNA3.1D/V5-His-RRQR S SR M	5.5kb	amp ^R , neo ^R	Expression of RRQR S SR M peptide in APCs
pcDNA3.1D/V5-His-RRQR S SR T	5.5kb	amp ^R , neo ^R	Expression of RRQR S SR T peptide in APCs
pcDNA3.1D/V5-His-RRQR S SR G	5.5kb	amp ^R , neo ^R	Expression of RRQR S SR G peptide in APCs
pcDNA3.1D/V5-His-RRQR S SR I	5.5kb	amp ^R , neo ^R	Expression of RRQR S SR I peptide in APCs
pcDNA3.1D/V5-His-RRQR S SR A	5.5kb	amp ^R , neo ^R	Expression of RRQR S SR A peptide in APCs
pcDNA3.1D/V5-His-RRQR S SR V	5.5kb	amp ^R , neo ^R	Expression of RRQR S SR V peptide in APCs
pcDNA3.1D/V5-His-RRQR S SR Y	5.5kb	amp ^R , neo ^R	Expression of RRQR S SR Y peptide in APCs
pcDNA3.1D/V5-His-RRQR S SR F	5.5kb	amp ^R , neo ^R	Expression of RRQR S SR F peptide in APCs
pcDNA3.1D/V5-His-RRQR S SR P	5.5kb	amp ^R , neo ^R	Expression of RRQR S SR P peptide in APCs

Table 6.2.3 Plasmids coding sequences of peptides from HLA-C*06:02-C1R or HLA-C*06:02-721.221 peptidomes.

Plasmid	Size	Resistance Genes	Application
pcDNA3.1D/V5-His-LRHPNILRL	5.5kb	amp ^R , neo ^R	Expression of LRHPNILRL peptide in APCs
pcDNA3.1D/V5-His-QRAWQERRL	5.5kb	amp ^R , neo ^R	Expression of QRAWQERRL peptide in APCs

pcDNA3.1D/V5-His-LRNFNLFRL	5.5kb	amp ^R , neo ^R	Expression of LRNFNLFRL peptide in APCs
pcDNA3.1D/V5-His-FRPEHVSRL	5.5kb	amp ^R , neo ^R	Expression of FRPEHVSRL peptide in APCs
pcDNA3.1D/V5-His-IRPEHVLRL	5.5kb	amp ^R , neo ^R	Expression of IRPEHVLRL peptide in APCs
pcDNA3.1D/V5-His-ERFAKERRL	5.5kb	amp ^R , neo ^R	Expression of ERFAKERRL peptide in APCs
pcDNA3.1D/V5-His-SRPVKLFRV	5.5kb	amp ^R , neo ^R	Expression of SRPVKLFRV peptide in APCs
pcDNA3.1D/V5-His-LRYDHQSRL	5.5kb	amp ^R , neo ^R	Expression of LRYDHQSRL peptide in APCs
pcDNA3.1D/V5-His-ERFPKLLRL	5.5kb	amp ^R , neo ^R	Expression of ERFPKLLRL peptide in APCs
pcDNA3.1D/V5-His-SRFPEALRL	5.5kb	amp ^R , neo ^R	Expression of SRFPEALRL peptide in APCs
pcDNA3.1D/V5-His-KRASYILRL	5.5kb	amp ^R , neo ^R	Expression of KRASYILRL peptide in APCs
pcDNA3.1D/V5-His-YRKAFESRL	5.5kb	amp ^R , neo ^R	Expression of YRKAFESRL peptide in APCs
pcDNA3.1D/V5-His-SRPELIFRL	5.5kb	amp ^R , neo ^R	Expression of SRPELIFRL peptide in APCs
pcDNA3.1D/V5-His-NRNFWVLRL	5.5kb	amp ^R , neo ^R	Expression of NRNFWVLRL peptide in APCs
pcDNA3.1D/V5-His-SRSISLLRL	5.5kb	amp ^R , neo ^R	Expression of SRSISLLRL peptide in APCs
pcDNA3.1D/V5-His-FRNERAIRF	5.5kb	amp ^R , neo ^R	Expression of FRNERAIRF peptide in APCs
pcDNA3.1D/V5-His-VRFHRPYRL	5.5kb	amp ^R , neo ^R	Expression of VRFHRPYRL peptide in APCs
pcDNA3.1D/V5-His-GAYGQAVRY	5.5kb	amp ^R , neo ^R	Expression of GAYGQAVRY peptide in APCs
pcDNA3.1D/V5-His-YRIATSKRY	5.5kb	amp ^R , neo ^R	Expression of YRIATSKRY peptide in APCs
pcDNA3.1D/V5-His-LRYDHQQRL	5.5kb	amp ^R , neo ^R	Expression of LRYDHQQRL peptide in APCs
pcDNA3.1D/V5-His-FRIEKIERI	5.5kb	amp ^R , neo ^R	Expression of FRIEKIERI peptide in APCs
pcDNA3.1D/V5-His-KLYGKPIRV	5.5kb	amp ^R , neo ^R	Expression of KLYGKPIRV peptide in APCs
pcDNA3.1D/V5-His-HRFEHDARI	5.5kb	amp ^R , neo ^R	Expression of HRFEHDARI peptide in APCs
pcDNA3.1D/V5-His-VHVGHVVRV	5.5kb	amp ^R , neo ^R	Expression of VHVGHVVRV peptide in APCs
pcDNA3.1D/V5-His-IRHTHVPRL	5.5kb	amp ^R , neo ^R	Expression of IRHTHVPRL peptide in APCs
pcDNA3.1D/V5-His-VRKDHENRL	5.5kb	amp ^R , neo ^R	Expression of VRKDHENRL peptide in APCs
pcDNA3.1D/V5-His-KRHEKDVI	5.5kb	amp ^R , neo ^R	Expression of KRHEKDVI peptide in APCs
pcDNA3.1D/V5-His-SRFGKFIRI	5.5kb	amp ^R , neo ^R	Expression of SRFGKFIRI peptide in APCs
pcDNA3.1D/V5-His-KYIDKTIRV	5.5kb	amp ^R , neo ^R	Expression of KYIDKTIRV peptide in APCs

Table 6.2.4 Plasmids coding sequences of peptides from human proteome screening.

Plasmid	Size	Resistance Genes	Application
pcDNA3.1D/V5-His-HRKQRALRI	5.5kb	amp ^R , neo ^R	Expression of HRKQRALRI peptide in APCs
pcDNA3.1D/V5-His-NRNHNSSRF	5.5kb	amp ^R , neo ^R	Expression of NRNHNSSRF peptide in APCs
pcDNA3.1D/V5-His-SRSSQDSRF	5.5kb	amp ^R , neo ^R	Expression of SRSSQDSRF peptide in APCs
pcDNA3.1D/V5-His-WRRPRLRRL	5.5kb	amp ^R , neo ^R	Expression of WRRPRLRRL peptide in APCs
pcDNA3.1D/V5-His-IRAARRSRL	5.5kb	amp ^R , neo ^R	Expression of IRAARRSRL peptide in APCs
pcDNA3.1D/V5-His-DRIERMLRL	5.5kb	amp ^R , neo ^R	Expression of DRIERMLRL peptide in APCs
pcDNA3.1D/V5-His-LRHQRGLRL	5.5kb	amp ^R , neo ^R	Expression of LRHQRGLRL peptide in APCs
pcDNA3.1D/V5-His-RRFLRTLRL	5.5kb	amp ^R , neo ^R	Expression of RRFLRTLRL peptide in APCs
pcDNA3.1D/V5-His-RRCPRLRRL	5.5kb	amp ^R , neo ^R	Expression of RRCPLRRL peptide in APCs
pcDNA3.1D/V5-His-QRLSRRRRL	5.5kb	amp ^R , neo ^R	Expression of QRLSRRRRL peptide in APCs

pcDNA3.1D/V5-His-GRRSRGRRL	5.5kb	amp ^R , neo ^R	Expression of GRRSRGRRL peptide in APCs
pcDNA3.1D/V5-His-SRAERNRRL	5.5kb	amp ^R , neo ^R	Expression of SRAERNRRL peptide in APCs
pcDNA3.1D/V5-His-LRSVRPLRL	5.5kb	amp ^R , neo ^R	Expression of LRSVRPLRL peptide in APCs
pcDNA3.1D/V5-His-HRADRMRL	5.5kb	amp ^R , neo ^R	Expression of HRADRMRL peptide in APCs
pcDNA3.1D/V5-His-DRFQRKRRL	5.5kb	amp ^R , neo ^R	Expression of DRFQRKRRL peptide in APCs
pcDNA3.1D/V5-His-MRVVRLRL	5.5kb	amp ^R , neo ^R	Expression of MRVVRLRL peptide in APCs
pcDNA3.1D/V5-His-TRLPRGRRL	5.5kb	amp ^R , neo ^R	Expression of TRLPRGRRL peptide in APCs
pcDNA3.1D/V5-His-TRSSRRRL	5.5kb	amp ^R , neo ^R	Expression of TRSSRRRL peptide in APCs
pcDNA3.1D/V5-His-IRRGRVRRL	5.5kb	amp ^R , neo ^R	Expression of IRRGRVRRL peptide in APCs
pcDNA3.1D/V5-His-ARIGRILRL	5.5kb	amp ^R , neo ^R	Expression of ARIGRILRL peptide in APCs
pcDNA3.1D/V5-His-FRVLRLPLRL	5.5kb	amp ^R , neo ^R	Expression of FRVLRLPLRL peptide in APCs
pcDNA3.1D/V5-His-ERIQRLRL	5.5kb	amp ^R , neo ^R	Expression of ERIQRLRL peptide in APCs
pcDNA3.1D/V5-His-ARSKRGLRL	5.5kb	amp ^R , neo ^R	Expression of ARSKRGLRL peptide in APCs
pcDNA3.1D/V5-His-LRFLRALRL	5.5kb	amp ^R , neo ^R	Expression of LRFLRALRL peptide in APCs
pcDNA3.1D/V5-His-SREDTPSRL	5.5kb	amp ^R , neo ^R	Expression of SREDTPSRL peptide in APCs
pcDNA3.1D/V5-His-ARQRRQSRL	5.5kb	amp ^R , neo ^R	Expression of ARQRRQSRL peptide in APCs
pcDNA3.1D/V5-His-PRETRERRL	5.5kb	amp ^R , neo ^R	Expression of PRETRERRL peptide in APCs
pcDNA3.1D/V5-His-ERVERERRL	5.5kb	amp ^R , neo ^R	Expression of ERVERERRL peptide in APCs
pcDNA3.1D/V5-His-RRDHRALRL	5.5kb	amp ^R , neo ^R	Expression of RRDHRALRL peptide in APCs
pcDNA3.1D/V5-His-GREARRRRL	5.5kb	amp ^R , neo ^R	Expression of GREARRRRL peptide in APCs
pcDNA3.1D/V5-His-ARVARWRRL	5.5kb	amp ^R , neo ^R	Expression of ARVARWRRL peptide in APCs
pcDNA3.1D/V5-His-PRRRRRRRL	5.5kb	amp ^R , neo ^R	Expression of PRRRRRRRRL peptide in APCs
pcDNA3.1D/V5-His-LRALRHLRL	5.5kb	amp ^R , neo ^R	Expression of LRALRHLRL peptide in APCs
pcDNA3.1D/V5-His-GRKWRKLRL	5.5kb	amp ^R , neo ^R	Expression of GRKWRKLRL peptide in APCs
pcDNA3.1D/V5-His-ERALRLLRL	5.5kb	amp ^R , neo ^R	Expression of ERALRLLRL peptide in APCs
pcDNA3.1D/V5-His-ARALRGRRL	5.5kb	amp ^R , neo ^R	Expression of ARALRGRRL peptide in APCs
pcDNA3.1D/V5-His-QRERRGRRL	5.5kb	amp ^R , neo ^R	Expression of QRERRGRRL peptide in APCs
pcDNA3.1D/V5-His-VRGSRCLRL	5.5kb	amp ^R , neo ^R	Expression of VRGSRCLRL peptide in APCs
pcDNA3.1D/V5-His-LRPKRTLRL	5.5kb	amp ^R , neo ^R	Expression of LRPKRTLRL peptide in APCs
pcDNA3.1D/V5-His-RRRSTGLRL	5.5kb	amp ^R , neo ^R	Expression of RRRSTGLRL peptide in APCs
pcDNA3.1D/V5-His-LRQGQSRRV	5.5kb	amp ^R , neo ^R	Expression of LRQGQSRRV peptide in APCs
pcDNA3.1D/V5-His-MRVDRESRF	5.5kb	amp ^R , neo ^R	Expression of MRVDRESRF peptide in APCs
pcDNA3.1D/V5-His-ARGGRGRRL	5.5kb	amp ^R , neo ^R	Expression of ARGGRGRRL peptide in APCs
pcDNA3.1D/V5-His-ARLLRALRL	5.5kb	amp ^R , neo ^R	Expression of ARLLRALRL peptide in APCs
pcDNA3.1D/V5-His-GRPRRRRRL	5.5kb	amp ^R , neo ^R	Expression of GRPRRRRRL peptide in APCs
pcDNA3.1D/V5-His-RRLARFLRL	5.5kb	amp ^R , neo ^R	Expression of RRLARFLRL peptide in APCs
pcDNA3.1D/V5-His-HRPLRPLRL	5.5kb	amp ^R , neo ^R	Expression of HRPLRPLRL peptide in APCs
pcDNA3.1D/V5-His-YRNPRFLRL	5.5kb	amp ^R , neo ^R	Expression of YRNPRFLRL peptide in APCs
pcDNA3.1D/V5-His-RRRRRRRRL	5.5kb	amp ^R , neo ^R	Expression of RRRRRRRRRL peptide in APCs
pcDNA3.1D/V5-His-ARIGRVLRL	5.5kb	amp ^R , neo ^R	Expression of ARIGRVLRL peptide in APCs
pcDNA3.1D/V5-His-RRPYRRRRF	5.5kb	amp ^R , neo ^R	Expression of RRPYRRRRF peptide in APCs

pcDNA3.1D/V5-His-VRRDRPLRV	5.5kb	amp ^R , neo ^R	Expression of VRRDRPLRV peptide in APCs
pcDNA3.1D/V5-His-SRHERSLRM	5.5kb	amp ^R , neo ^R	Expression of SRHERSLRM peptide in APCs
pcDNA3.1D/V5-His-VRRDRLRRM	5.5kb	amp ^R , neo ^R	Expression of VRRDRLRRM peptide in APCs
pcDNA3.1D/V5-His-ERIERVRRRI	5.5kb	amp ^R , neo ^R	Expression of ERIERVRRRI peptide in APCs
pcDNA3.1D/V5-His-RRIPRGRRRI	5.5kb	amp ^R , neo ^R	Expression of RRIPRGRRRI peptide in APCs
pcDNA3.1D/V5-His-RRRVRRRRM	5.5kb	amp ^R , neo ^R	Expression of RRRVRRRRM peptide in APCs
pcDNA3.1D/V5-His-RRPRRRRRV	5.5kb	amp ^R , neo ^R	Expression of RRPRRRRRV peptide in APCs
pcDNA3.1D/V5-His-RRYWRSLRV	5.5kb	amp ^R , neo ^R	Expression of RRYWRSLRV peptide in APCs
pcDNA3.1D/V5-His-RRSPRGRRRI	5.5kb	amp ^R , neo ^R	Expression of RRSPRGRRRI peptide in APCs
pcDNA3.1D/V5-His-QRAQRILRV	5.5kb	amp ^R , neo ^R	Expression of QRAQRILRV peptide in APCs
pcDNA3.1D/V5-His-FRCSRVLRV	5.5kb	amp ^R , neo ^R	Expression of FRCSRVLRV peptide in APCs
pcDNA3.1D/V5-His-FRMVRGRRV	5.5kb	amp ^R , neo ^R	Expression of FRMVRGRRV peptide in APCs
pcDNA3.1D/V5-His-LREPRLRRI	5.5kb	amp ^R , neo ^R	Expression of LREPRLRRI peptide in APCs
pcDNA3.1D/V5-His-RRPPRERRF	5.5kb	amp ^R , neo ^R	Expression of RRPPRERRF peptide in APCs
pcDNA3.1D/V5-His-VRILRLLRI	5.5kb	amp ^R , neo ^R	Expression of VRILRLLRI peptide in APCs
pcDNA3.1D/V5-His-ARLIRHRRI	5.5kb	amp ^R , neo ^R	Expression of ARLIRHRRI peptide in APCs
pcDNA3.1D/V5-His-RRQRRERRF	5.5kb	amp ^R , neo ^R	Expression of RRQRRERRF peptide in APCs
pcDNA3.1D/V5-His-ARQYRSLRV	5.5kb	amp ^R , neo ^R	Expression of ARQYRSLRV peptide in APCs
pcDNA3.1D/V5-His-RRLRLLRV	5.5kb	amp ^R , neo ^R	Expression of RRLRLLRV peptide in APCs
pcDNA3.1D/V5-His-QRVARRRRF	5.5kb	amp ^R , neo ^R	Expression of QRVARRRRF peptide in APCs
pcDNA3.1D/V5-His-NREHRVRRRI	5.5kb	amp ^R , neo ^R	Expression of NREHRVRRRI peptide in APCs
pcDNA3.1D/V5-His-LREARGLRV	5.5kb	amp ^R , neo ^R	Expression of LREARGLRV peptide in APCs
pcDNA3.1D/V5-His-LRTLRLRV	5.5kb	amp ^R , neo ^R	Expression of LRTLRLRV peptide in APCs
pcDNA3.1D/V5-His-LRVLRALRI	5.5kb	amp ^R , neo ^R	Expression of LRVLRALRI peptide in APCs
pcDNA3.1D/V5-His-SRGRRQRRM	5.5kb	amp ^R , neo ^R	Expression of SRGRRQRRM peptide in APCs
pcDNA3.1D/V5-His-DRVERVRRRI	5.5kb	amp ^R , neo ^R	Expression of DRVERVRRRI peptide in APCs
pcDNA3.1D/V5-His-DRAGRRLRV	5.5kb	amp ^R , neo ^R	Expression of DRAGRRLRV peptide in APCs

Table 6.2.5 Plasmids coding sequences of peptides from HLA-C*06:02 peptidomes eluted from four homozygous EBV-transformed B cell lines.

Plasmid	Size	Resistance Genes	Application
pcDNA3.1D/V5-His-KRNPRLIRV	5.5kb	amp ^R , neo ^R	Expression of KRNPRLIRV peptide in APCs
pcDNA3.1D/V5-His-RQIDRQNRL	5.5kb	amp ^R , neo ^R	Expression of RQIDRQNRL peptide in APCs
pcDNA3.1D/V5-His-RVTDRYFRI	5.5kb	amp ^R , neo ^R	Expression of RVTDRYFRI peptide in APCs
pcDNA3.1D/V5-His-KLRDRAERI	5.5kb	amp ^R , neo ^R	Expression of KLRDRAERI peptide in APCs
pcDNA3.1D/V5-His-KLYDRILRV	5.5kb	amp ^R , neo ^R	Expression of KLYDRILRV peptide in APCs
pcDNA3.1D/V5-His-KLNDRVMRV	5.5kb	amp ^R , neo ^R	Expression of KLNDRVMRV peptide in APCs
pcDNA3.1D/V5-His-ALYGRALRV	5.5kb	amp ^R , neo ^R	Expression of ALYGRALRV peptide in APCs
pcDNA3.1D/V5-His-FLTDREVRL	5.5kb	amp ^R , neo ^R	Expression of FLTDREVRL peptide in APCs
pcDNA3.1D/V5-His-RLSNRVVRV	5.5kb	amp ^R , neo ^R	Expression of RLSNRVVRV peptide in APCs

pcDNA3.1D/V5-His-RYQGRQYRL	5.5kb	amp ^R , neo ^R	Expression of RYQGRQYRL peptide in APCs
pcDNA3.1D/V5-His-KILSRLFRV	5.5kb	amp ^R , neo ^R	Expression of KILSRLFRV peptide in APCs
pcDNA3.1D/V5-His-ERRRCHRL	5.5kb	amp ^R , neo ^R	Expression of ERRRCHRL peptide in APCs
pcDNA3.1D/V5-His-RVPRAVRV	5.5kb	amp ^R , neo ^R	Expression of RVPRAVRV peptide in APCs
pcDNA3.1D/V5-His-VALRALRL	5.5kb	amp ^R , neo ^R	Expression of VALRALRL peptide in APCs
pcDNA3.1D/V5-His-KQQRKERL	5.5kb	amp ^R , neo ^R	Expression of KQQRKERL peptide in APCs
pcDNA3.1D/V5-His-RISTARRV	5.5kb	amp ^R , neo ^R	Expression of RISTARRV peptide in APCs
pcDNA3.1D/V5-His-GVIRTQRRRL	5.5kb	amp ^R , neo ^R	Expression of GVIRTQRRRL peptide in APCs
pcDNA3.1D/V5-His-RSVRAIRI	5.5kb	amp ^R , neo ^R	Expression of RSVRAIRI peptide in APCs
pcDNA3.1D/V5-His-LYASNVRV	5.5kb	amp ^R , neo ^R	Expression of LYASNVRV peptide in APCs
pcDNA3.1D/V5-His-QYYPNGIRL	5.5kb	amp ^R , neo ^R	Expression of QYYPNGIRL peptide in APCs
pcDNA3.1D/V5-His-KISLRLKRA	5.5kb	amp ^R , neo ^R	Expression of KISLRLKRA peptide in APCs
pcDNA3.1D/V5-His-RIRRDVRV	5.5kb	amp ^R , neo ^R	Expression of RIRRDVRV peptide in APCs
pcDNA3.1D/V5-His-VRNGHIKRI	5.5kb	amp ^R , neo ^R	Expression of VRNGHIKRI peptide in APCs
pcDNA3.1D/V5-His-ARYYKTKRV	5.5kb	amp ^R , neo ^R	Expression of ARYYKTKRV peptide in APCs
pcDNA3.1D/V5-His-KMKEKVERI	5.5kb	amp ^R , neo ^R	Expression of KMKEKVERI peptide in APCs
pcDNA3.1D/V5-His-RSYPHLRRV	5.5kb	amp ^R , neo ^R	Expression of RSYPHLRRV peptide in APCs
pcDNA3.1D/V5-His-RSYSRRIKI	5.5kb	amp ^R , neo ^R	Expression of RSYSRRIKI peptide in APCs
pcDNA3.1D/V5-His-FSATQTRKV	5.5kb	amp ^R , neo ^R	Expression of FSATQTRKV peptide in APCs
pcDNA3.1D/V5-His-RVVDQPLKL	5.5kb	amp ^R , neo ^R	Expression of RVVDQPLKL peptide in APCs
pcDNA3.1D/V5-His-IRGNVKKL	5.5kb	amp ^R , neo ^R	Expression of IRGNVKKL peptide in APCs
pcDNA3.1D/V5-His-KAYKQSSHL	5.5kb	amp ^R , neo ^R	Expression of KAYKQSSHL peptide in APCs
pcDNA3.1D/V5-His-MRREQVLKV	5.5kb	amp ^R , neo ^R	Expression of MRREQVLKV peptide in APCs
pcDNA3.1D/V5-His-KRKENAIKL	5.5kb	amp ^R , neo ^R	Expression of KRKENAIKL peptide in APCs
pcDNA3.1D/V5-His-SQFEKTRKV	5.5kb	amp ^R , neo ^R	Expression of SQFEKTRKV peptide in APCs
pcDNA3.1D/V5-His-MMPNKVRKI	5.5kb	amp ^R , neo ^R	Expression of MMPNKVRKI peptide in APCs
pcDNA3.1D/V5-His-TRGDHVKHY	5.5kb	amp ^R , neo ^R	Expression of TRGDHVKHY peptide in APCs
pcDNA3.1D/V5-His-VRSSKFRHV	5.5kb	amp ^R , neo ^R	Expression of VRSSKFRHV peptide in APCs
pcDNA3.1D/V5-His-KRISKTTKL	5.5kb	amp ^R , neo ^R	Expression of KRISKTTKL peptide in APCs
pcDNA3.1D/V5-His-FQTSHTLHL	5.5kb	amp ^R , neo ^R	Expression of FQTSHTLHL peptide in APCs
pcDNA3.1D/V5-His-HAPDHTRHL	5.5kb	amp ^R , neo ^R	Expression of HAPDHTRHL peptide in APCs
pcDNA3.1D/V5-His-IIFETPLRV	5.5kb	amp ^R , neo ^R	Expression of IIFETPLRV peptide in APCs
pcDNA3.1D/V5-His-KLFTQILRV	5.5kb	amp ^R , neo ^R	Expression of KLFTQILRV peptide in APCs
pcDNA3.1D/V5-His-AAAE TELRV	5.5kb	amp ^R , neo ^R	Expression of AAAE TELRV peptide in APCs
pcDNA3.1D/V5-His-AQFTTALRL	5.5kb	amp ^R , neo ^R	Expression of AQFTTALRL peptide in APCs
pcDNA3.1D/V5-His-QYVTQINRL	5.5kb	amp ^R , neo ^R	Expression of QYVTQINRL peptide in APCs
pcDNA3.1D/V5-His-KLQEIQHRV	5.5kb	amp ^R , neo ^R	Expression of KLQEIQHRV peptide in APCs
pcDNA3.1D/V5-His-PLYDRLLRI	5.5kb	amp ^R , neo ^R	Expression of PLYDRLLRI peptide in APCs
pcDNA3.1D/V5-His-VRFGQQKRY	5.5kb	amp ^R , neo ^R	Expression of VRFGQQKRY peptide in APCs
pcDNA3.1D/V5-His-YRILQILRV	5.5kb	amp ^R , neo ^R	Expression of YRILQILRV peptide in APCs
pcDNA3.1D/V5-His-YTDATPLRV	5.5kb	amp ^R , neo ^R	Expression of YTDATPLRV peptide in APCs

pcDNA3.1D/V5-His-RYADRARKI	5.5kb	amp ^R , neo ^R	Expression of RYADRARKI peptide in APCs
pcDNA3.1D/V5-His-VLYDRPLKI	5.5kb	amp ^R , neo ^R	Expression of VLYDRPLKI peptide in APCs
pcDNA3.1D/V5-His-KLWSRSLKL	5.5kb	amp ^R , neo ^R	Expression of KLWSRSLKL peptide in APCs
pcDNA3.1D/V5-His-SLSGRPLKV	5.5kb	amp ^R , neo ^R	Expression of SLSGRPLKV peptide in APCs
pcDNA3.1D/V5-His-FLFRRGLKV	5.5kb	amp ^R , neo ^R	Expression of FLFRRGLKV peptide in APCs
pcDNA3.1D/V5-His-VLYDRVLYKY	5.5kb	amp ^R , neo ^R	Expression of VLYDRVLYKY peptide in APCs
pcDNA3.1D/V5-His-RTFGHLLRY	5.5kb	amp ^R , neo ^R	Expression of RTFGHLLRY peptide in APCs
pcDNA3.1D/V5-His-VLYLKPLRI	5.5kb	amp ^R , neo ^R	Expression of VLYLKPLRI peptide in APCs
pcDNA3.1D/V5-His-KLPPKDLRI	5.5kb	amp ^R , neo ^R	Expression of KLPPKDLRI peptide in APCs
pcDNA3.1D/V5-His-TFMDHVLRY	5.5kb	amp ^R , neo ^R	Expression of TFMDHVLRY peptide in APCs
pcDNA3.1D/V5-His-TYAEKLHRL	5.5kb	amp ^R , neo ^R	Expression of TYAEKLHRL peptide in APCs
pcDNA3.1D/V5-His-REIRLQRL	5.5kb	amp ^R , neo ^R	Expression of REIRLQRL peptide in APCs
pcDNA3.1D/V5-His-RSQRPVVRW	5.5kb	amp ^R , neo ^R	Expression of RSQRPVVRW peptide in APCs
pcDNA3.1D/V5-His-RKRQTLRL	5.5kb	amp ^R , neo ^R	Expression of RKRQTLRL peptide in APCs
pcDNA3.1D/V5-His-RTVTPLRW	5.5kb	amp ^R , neo ^R	Expression of RTVTPLRW peptide in APCs
pcDNA3.1D/V5-His-RSMKGLRW	5.5kb	amp ^R , neo ^R	Expression of RSMKGLRW peptide in APCs
pcDNA3.1D/V5-His-IRKDSLRLV	5.5kb	amp ^R , neo ^R	Expression of IRKDSLRLV peptide in APCs
pcDNA3.1D/V5-His-TRCPLVLKL	5.5kb	amp ^R , neo ^R	Expression of TRCPLVLKL peptide in APCs
pcDNA3.1D/V5-His-HRVYLVRKL	5.5kb	amp ^R , neo ^R	Expression of HRVYLVRKL peptide in APCs
pcDNA3.1D/V5-His-TYSELLRRI	5.5kb	amp ^R , neo ^R	Expression of TYSELLRRI peptide in APCs
pcDNA3.1D/V5-His-RYFKTPRKF	5.5kb	amp ^R , neo ^R	Expression of RYFKTPRKF peptide in APCs
pcDNA3.1D/V5-His-KYFAQALKL	5.5kb	amp ^R , neo ^R	Expression of KYFAQALKL peptide in APCs
pcDNA3.1D/V5-His-REFKLSKV	5.5kb	amp ^R , neo ^R	Expression of REFKLSKV peptide in APCs
pcDNA3.1D/V5-His-RDLRKSKE	5.5kb	amp ^R , neo ^R	Expression of RDLRKSKE peptide in APCs
pcDNA3.1D/V5-His-KRHNYVRKV	5.5kb	amp ^R , neo ^R	Expression of KRHNYVRKV peptide in APCs
pcDNA3.1D/V5-His-KRSQVLVKKL	5.5kb	amp ^R , neo ^R	Expression of KRSQVLVKKL peptide in APCs
pcDNA3.1D/V5-His-YQRDPLKL	5.5kb	amp ^R , neo ^R	Expression of YQRDPLKL peptide in APCs
pcDNA3.1D/V5-His-VYSQILRKL	5.5kb	amp ^R , neo ^R	Expression of VYSQILRKL peptide in APCs
pcDNA3.1D/V5-His-RRYLRRKE	5.5kb	amp ^R , neo ^R	Expression of RRYLRRKE peptide in APCs
pcDNA3.1D/V5-His-RRLPCRKR	5.5kb	amp ^R , neo ^R	Expression of RRLPCRKR peptide in APCs
pcDNA3.1D/V5-His-VRYRLPLRV	5.5kb	amp ^R , neo ^R	Expression of VRYRLPLRV peptide in APCs

6.3 Information on Psoriasis Patients or Healthy Donors

Numbers	Age	Gender	HLA-C*06:02	Donations
HCB01	50	Female	+	blood
HCB02	84	Male	+	blood
HCB03	62	Female	+	blood
HCB04	65	Male	-	blood
HCB05	43	Female	-	blood

HCB06	30	Female	-	blood
HCB07	40	Male	-	blood
HCB08	32	Male	N/A	blood
HCB09	51	Male	N/A	blood
HCB10	55	Female	-	blood
HCB11	22	Female	N/A	blood
HCB12	36	Male	+	blood
HCB13	61	Female	Female	blood
PVB01	43	Male	+	blood
PVB02	41	Male	+	tonsil
PVB03	51	Female	+	tonsil
PVB04	43	Female	+	tonsil
PVB05	51	Female	+	blood
PVB06	53	Male	+	blood
PVB07	72	Male	+	blood
PVB08	33	Female	+	blood
PVB09	71	Female	+	blood
PVB10	55	Male	N/A	blood
PVB11	75	Male	+	blood
PVB12	53	Male	+	blood
PVB13	19	Male	N/A	blood
PVB14	44	Male	N/A	blood
PVB15	34	Male	N/A	blood
PVB16	54	Female	N/A	blood
PVB17	56	Female	N/A	blood
PVB18	27	Male	N/A	blood
PVB19	23	Female	N/A	blood
PVB20	48	Female	N/A	blood
PVB21	48	Female	N/A	blood
PVB22	28	Male	N/A	blood
PVB23	35	Male	+	blood
PVB24	68	Male	N/A	blood

*HC: healthy controls; PV: patients with psoriasis vulgaris.

6.4 Sequences of siRNAs for Target Proteins

Sequences of Silencer[®] Select Validated siRNAs and Silencer[®] Select Pre-designed siRNAs from ThermoFisher Scientific are available at PubChem Database by the IDs (<https://pubchem.ncbi.nlm.nih.gov>).

Target Proteins	Sense siRNA Sequences
TAOK3 (ID: s27996)	5'- GCA UGA CUU UGU UCG ACG A TT -3'
HDAC6 (ID: s19459)	5'- CCG UGA GAG UUC CAA CUU U TT -3'
B2M (ID: s1854)	5'- CAU CCG ACA UUG AAG UUG A TT -3'
PIF1(ID: s36919)	5'- UCA UAU CUG CUA AAG CGA A TT -3'
PIF1(ID: s36920)	5'- GGG CGA UGU CCA UCC ACA A TT -3'
PIF1(ID: s36921)	5'- GAU GCC CAG UGU CCU GUU A TT -3'
LRRC28 (ID: s42641)	5'- GGA ACU CCC UGA CAU CCU U TT -3'
LRRC28 (ID: s42642)	5'- CCA AUC UCA UUA CCC AGA A TT -3'
LRRC28 (ID: s42643)	5'- GCA CUC AAA UAA CAU AGU U TT -3'
ZNF670 (ID: s41144)	5'- GGA AUG UCC AGA GAA GUU A TT -3'
ZNF670 (ID: s41145)	5'- CCU UCA AAU AUU CUA GUA A TT -3'
ZNF670 (ID: s41146)	5'- GCC UUU AUC UCU CUC ACC A TT -3'
KIFC2 (ID: s40543)	5'- UAG CCU CUU UGG AUC CAU U TT -3'
KIFC2 (ID: s40544)	5'- GCG ACG GAC UCA GAG AAA A TT -3'
FBXL19 (ID: s458471)	5'- CAA GGG UUC AGG GAA CAA A TT -3'
FBXL19 (ID: s458473)	5'- CAA UAC GGU UUG CUA UAA A TT -3'

6.5 Raw Data of HLA-C*06:02 Peptidomes

A full list of HLA-I peptides eluted from four HLA-C*06:02 homozygous EBV-transformed B cell lines, integrating the HLA-C*06:02 ligands unveiled by Di Marco and Sarkizova (Di Marco *et al.*, 2017; Sarkizova *et al.*, 2020), has been generated by Prof. Andreas Schlosser and Melissa Bernhardt from the Center for Integrative and Translational Bioimaging at Universität Würzburg, Würzburg). Raw data of these peptides can be found on Figshare (<https://figshare.com/s/e2dedc1983b26488367a>). The dataset of HLA-C*06:02 ligands uncovered by Mobbs *et al.* is available in the supplementary data of the study (Mobbs *et al.*, 2017).

References

- Abi-Rached, L., Gouret, P., Yeh, J.-H., Di Cristofaro, J., Pontarotti, P., Picard, C., & Paganini, J. (2018). Immune diversity sheds light on missing variation in worldwide genetic diversity panels. *PLoS One*, 13(10), e0206512.
- Ahmad, T. A., Eweida, A. E., & El-Sayed, L. H. (2016). T-cell epitope mapping for the design of powerful vaccines. *Vaccine Rep*, 6, 13-22.
- Alvarez-Navarro, C., & López de Castro, J. A. (2014). ERAP1 structure, function and pathogenetic role in ankylosing spondylitis and other MHC-associated diseases. *Mol Immunol*, 57(1), 12-21.
- Arakawa, A., Siewert, K., Stöhr, J., Besgen, P., Kim, S. M., Rühl, G., Nickel, J., Vollmer, S., Thomas, P., Krebs, S., Pinkert, S., Spannagl, M., Held, K., Kammerbauer, C., Besch, R., Dornmair, K., & Prinz, J. C. (2015). Melanocyte antigen triggers autoimmunity in human psoriasis. *J Exp Med*, 212(13), 2203-2212.
- Arakawa, A., Reeves, E., Vollmer, S., Arakawa, Y., He, M., Galinski, A., Stöhr, J., Dornmair, K., James, E., & Prinz, J. C. (2021). ERAP1 Controls the Autoimmune Response against Melanocytes in Psoriasis by Generating the Melanocyte Autoantigen and Regulating Its Amount for HLA-C*06:02 Presentation. *J Immunol*, 207(9), 2235-2244.
- Auton, A., Abecasis, G. R., Altshuler, D. M., Durbin, R. M., Abecasis, G. R., Bentley, D. R., Chakravarti, A., Clark, A. G., Donnelly, P., Eichler, E. E., Flicek, P., Gabriel, S. B., Gibbs, R. A., Green, E. D., Hurles, M. E., Knoppers, B. M., Korbel, J. O., Lander, E. S., Lee, C., Lehrach, H., Mardis, E. R., Marth, G. T., McVean, G. A., Nickerson, D. A., Schmidt, J. P., Sherry, S. T., Wang, J., Wilson, R. K., Gibbs, R. A., Boerwinkle, E., Doddapaneni, H., Han, Y., Korchina, V., Kovar, C., Lee, S., Muzny, D., Reid, J. G., Zhu, Y., Wang, J., Chang, Y., Feng, Q., Fang, X., Guo, X., Jian, M., Jiang, H., Jin, X., Lan, T., Li, G., Li, J., Li, Y., Liu, S., Liu, X., Lu, Y., Ma, X., Tang, M., Wang, B., Wang, G., Wu, H., Wu, R., Xu, X., Yin, Y., Zhang, D., Zhang, W., Zhao, J., Zhao, M., Zheng, X., Lander, E. S., Altshuler, D. M., Gabriel, S. B., Gupta, N., Gharani, N., Toji, L. H., Gerry, N. P., Resch, A. M., Flicek, P., Barker, J., Clarke, L., Gil, L., Hunt, S. E., Kelman, G., Kulesha, E., Leinonen, R., McLaren, W. M., Radhakrishnan, R., Roa, A., Smirnov, D., Smith, R. E., Streeter, I., Thormann, A., Toneva, I., Vaughan, B., Zheng-Bradley, X., Bentley, D. R., Grocock, R., Humphray, S., James, T., Kingsbury, Z., Lehrach, H., Sudbrak, R., Albrecht, M. W., Amstislavskiy, V. S., Borodina, T. A., Lienhard, M., Mertes, F., Sultan, M., Timmermann, B., Yaspo, M.-L., Mardis, E. R., Wilson, R. K., Fulton, L., Fulton, R., Sherry, S. T., Ananiev, V., Belaia, Z., Beloslyudtsev, D., Bouk, N., Chen, C., Church, D., Cohen, R., Cook, C., Garner, J., Hefferon, T., Kimelman, M., Liu, C., Lopez, J., Meric, P., O'Sullivan, C., Ostapchuk, Y., Phan, L., Ponomarov, S., Schneider, V., Shekhtman, E., Sirotkin, K., Slotta, D., Zhang, H., McVean, G. A., Durbin, R. M., Balasubramaniam, S., Burton, J., Danecek, P., Keane, T. M., Kolb-Kokocinski, A., McCarthy, S., Stalker, J., Quail, M., Schmidt, J. P., Davies, C. J., Gollub, J., Webster, T., Wong, B., Zhan, Y., Auton, A., Campbell, C. L., Kong, Y., Marcketta, A., Gibbs, R. A., Yu, F., Antunes, L., Bainbridge, M., Muzny, D., Sabo, A., Huang, Z., Wang, J., Coin, L. J. M., Fang, L., Guo, X., Jin, X., Li, G., Li, Q., Li, Y., Li, Z., Lin, H., Liu, B., Luo, R., Shao, H., Xie, Y., Ye, C., Yu, C., Zhang, F., Zheng, H., Zhu, H., Alkan, C., Dal, E., Kahveci, F., Marth, G. T., Garrison, E. P., Kural, D., Lee, W.-P., Fung Leong, W., Stromberg, M., Ward, A. N., Wu, J., Zhang, M., Daly, M. J., DePristo, M. A., Handsaker, R. E., Altshuler, D. M., Banks, E., Bhatia, G., del Angel, G., Gabriel, S. B., Genovese, G., Gupta, N., Li, H., Kashin, S., Lander, E. S., McCarroll, S. A., Nemesh, J. C., Poplin, R. E., Yoon, S. C., Lihm, J., Makarov, V., Clark, A. G., Gottipati, S., Keinan, A., Rodriguez-Flores, J. L., Korbel, J. O., Rausch, T., Fritz, M. H., Stütz, A. M., Flicek, P., Beal, K., Clarke, L., Datta, A., Herrero, J., McLaren, W. M., Ritchie, G. R. S., Smith, R. E., Zerbino, D., Zheng-Bradley, X., Sabeti, P. C., Shlyakhter, I., Schaffner, S. F., Vitti, J., Cooper, D. N., Ball, E. V., Stenson, P. D., Bentley, D. R., Barnes, B., Bauer, M., Keira Cheetham, R., Cox, A., Eberle, M., Humphray, S., Kahn, S., Murray, L., Peden, J., Shaw, R., Kenny, E. E., Batzer, M. A., Konkel, M. K., Walker, J. A., MacArthur, D. G., Lek, M., Sudbrak, R., Amstislavskiy, V. S., Herwig, R., Mardis, E. R., Ding, L., Koboldt, D. C., Larson, D., Ye, K., Gravel, S., The Genomes Project, C., Corresponding, a.,

- Steering, c., Production, g., Baylor College of, M., Shenzhen, B. G. I., Broad Institute of, M. I. T., Harvard, Coriell Institute for Medical, R., European Molecular Biology Laboratory, E. B. I., Illumina, Max Planck Institute for Molecular, G., McDonnell Genome Institute at Washington, U., Health, U. S. N. I. o., University of, O., Wellcome Trust Sanger, I., Analysis, g., Affymetrix, Albert Einstein College of, M., Bilkent, U., Boston, C., Cold Spring Harbor, L., Cornell, U., European Molecular Biology, L., Harvard, U., Human Gene Mutation, D., Icahn School of Medicine at Mount, S., Louisiana State, U., Massachusetts General, H., McGill, U., & National Eye Institute, N. I. H. (2015). A global reference for human genetic variation. *Nature*, 526(7571), 68-74.
- Barker, D. J., Maccari, G., Georgiou, X., Cooper, M. A., Flicek, P., Robinson, J., & Marsh, S. G. E. (2023). The IPD-IMGT/HLA Database. *Nucleic Acids Res*, 51(D1), D1053-d1060.
- Bowcock, A. M., & Krueger, J. G. (2005). Getting under the skin: the immunogenetics of psoriasis. *Nat Rev Immunol*, 5(9), 699-711.
- Boyman, O., Hefti, H. P., Conrad, C., Nickoloff, B. J., Suter, M., & Nestle, F. O. (2004). Spontaneous development of psoriasis in a new animal model shows an essential role for resident T cells and tumor necrosis factor- α . *J Exp Med*, 199(5), 731-736.
- Burden, A. D., Javed, S., Bailey, M., Hodgins, M., Connor, M., & Tillman, D. (1998). Genetics of psoriasis: paternal inheritance and a locus on chromosome 6p. *J Invest Dermatol*, 110(6), 958-960.
- Calis, J. J., Maybeno, M., Greenbaum, J. A., Weiskopf, D., De Silva, A. D., Sette, A., Keşmir, C., & Peters, B. (2013). Properties of MHC class I presented peptides that enhance immunogenicity. *PLoS Comput Biol*, 9(10), e1003266.
- Capon, F. (2017). The Genetic Basis of Psoriasis. *Int J Mol Sci*, 18(12), 2526.
- Chang, J. C., Smith, L. R., Froning, K. J., Schwabe, B. J., Laxer, J. A., Caralli, L. L., Kurland, H. H., Karasek, M. A., Wilkinson, D. I., & Carlo, D. J. (1994). CD8+ T cells in psoriatic lesions preferentially use T-cell receptor V beta 3 and/or V beta 13.1 genes. *Proc Natl Acad Sci U S A*, 91(20), 9282-9286.
- Chang, S. C., Momburg, F., Bhutani, N., & Goldberg, A. L. (2005). The ER aminopeptidase, ERAP1, trims precursors to lengths of MHC class I peptides by a "molecular ruler" mechanism. *Proc Natl Acad Sci U S A*, 102(47), 17107-17112.
- Chang, Y. S., Lee, H. T., Chen, W. S., Hsiao, K. H., Chen, M. H., Tsai, C. Y., & Chou, C. T. (2012). Treatment of psoriasis with rituximab. *J Am Acad Dermatol*, 66(5), e184-185.
- Cheuk, S., Wikén, M., Blomqvist, L., Nylén, S., Talme, T., Ståhle, M., & Eidsmo, L. (2014). Epidermal Th22 and Tc17 Cells Form a Localized Disease Memory in Clinically Healed Psoriasis. *J Immunol*, 192(7), 3111-3120.
- Cheuk, S., Schlums, H., Gallais Sérézal, I., Martini, E., Chiang, S. C., Marquardt, N., Gibbs, A., Detlofsson, E., Introini, A., Forkel, M., Höög, C., Tjernlund, A., Michaëlsson, J., Folkersen, L., Mjösberg, J., Blomqvist, L., Ehrström, M., Ståhle, M., Bryceson, Y. T., & Eidsmo, L. (2017). CD49a Expression Defines Tissue-Resident CD8(+) T Cells Poised for Cytotoxic Function in Human Skin. *Immunity*, 46(2), 287-300.
- Codrina, A., Chiriac, A., Smaranda, M., & Ancuta, E. (2014). A role for B-cell -depleting agents in treating psoriatic skin lesions induced by tumor necrosis factor- α antagonists. Case report and literature review. *Arch Biol Sci*, 66.
- Conrad, C., Boyman, O., Tonel, G., Tun-Kyi, A., Laggner, U., de Fougères, A., Koteliński, V., Gardner, H., & Nestle, F. O. (2007). $\alpha 1\beta 1$ integrin is crucial for accumulation of epidermal T cells and the development of psoriasis. *Nat Med*, 13(7), 836-842.
- Crotzer, V. L., & Blum, J. S. (2009). Autophagy and its role in MHC-mediated antigen presentation. *J Immunol*, 182(6), 3335-3341.
- Cunningham, B. C., & Wells, J. A. (1989). High-resolution epitope mapping of hGH-receptor interactions by alanine-scanning mutagenesis. *Science*, 244(4908), 1081-1085.
- Cunningham, M. W. (2000). Pathogenesis of group A streptococcal infections. *Clin Microbiol Rev*, 13(3), 470-511.

- Cunningham, M. W. (2012). Streptococcus and rheumatic fever. *Curr Opin Rheumatol*, 24(4), 408-416.
- Curtsinger, J. M., Lins, D. C., & Mescher, M. F. (1998). CD8+ memory T cells (CD44^{high}, Ly-6C⁺) are more sensitive than naive cells to (CD44^{low}, Ly-6C⁻) to TCR/CD8 signaling in response to antigen. *J Immunol*, 160(7), 3236-3243.
- D'Orsogna, L. J., Roelen, D. L., Doxiadis, II, & Claas, F. H. (2010). Alloreactivity from human viral specific memory T-cells. *Transpl Immunol*, 23(4), 149-155.
- D'Ambrosio, D., Freedman, M. S., & Prinz, J. (2016). Ponesimod, a selective S1P1 receptor modulator: a potential treatment for multiple sclerosis and other immune-mediated diseases. *Ther Adv Chronic Dis*, 7(1), 18-33.
- De Mattos-Arruda, L., Vazquez, M., Finotello, F., Lepore, R., Porta, E., Hundal, J., Amengual-Rigo, P., Ng, C. K. Y., Valencia, A., Carrillo, J., Chan, T. A., Guallar, V., McGranahan, N., Blanco, J., & Griffith, M. (2020). Neoantigen prediction and computational perspectives towards clinical benefit: recommendations from the ESMO Precision Medicine Working Group. *Ann Oncol*, 31(8), 978-990.
- den Haan, J. M., Arens, R., & van Zelm, M. C. (2014). The activation of the adaptive immune system: cross-talk between antigen-presenting cells, T cells and B cells. *Immunol Lett*, 162(2 Pt B), 103-112.
- Di Marco, M., Schuster, H., Backert, L., Ghosh, M., Rammensee, H.-G., & Stevanović, S. (2017). Unveiling the Peptide Motifs of HLA-C and HLA-G from Naturally Presented Peptides and Generation of Binding Prediction Matrices. *J Immunol*, 199(8), 2639-2651.
- Di Meglio, P., Villanova, F., Navarini, A. A., Mylonas, A., Tosi, I., Nestle, F. O., & Conrad, C. (2016). Targeting CD8+ T cells prevents psoriasis development. *J Allergy Clin Immunol*, 138(1), 274-276.e276.
- Diluvio, L., Vollmer, S., Besgen, P., Ellwart, J. W., Chimenti, S., & Prinz, J. C. (2006). Identical TCR beta-chain rearrangements in streptococcal angina and skin lesions of patients with psoriasis vulgaris. *J Immunol*, 176(11), 7104-7111.
- Dranoff, G. (2004). Cytokines in cancer pathogenesis and cancer therapy. *Nat Rev Cancer*, 4(1), 11-22.
- Dupic, T., Marcou, Q., Walczak, A. M., & Mora, T. (2019). Genesis of the $\alpha\beta$ T-cell receptor. *PLoS Comput Biol*, 15(3), e1006874.
- Durand, M., & Segura, E. (2016). Dendritic Cell Subset Purification from Human Tonsils and Lymph Nodes. *Methods Mol Biol*, 1423, 89-99.
- Egbuniwe, I. U., Karagiannis, S. N., Nestle, F. O., & Lacy, K. E. (2015). Revisiting the role of B cells in skin immune surveillance. *Trends Immunol*, 36(2), 102-111.
- Falk, K., Rötzschke, O., Stevanović, S., Jung, G., & Rammensee, H.-G. (1991). Allele-specific motifs revealed by sequencing of self-peptides eluted from MHC molecules. *Nature*, 351(6324), 290-296.
- Falk, K., Rötzschke, O., Grahovac, B., Schendel, D., Stevanović, S., Gnau, V., Jung, G., Strominger, J. L., & Rammensee, H. G. (1993). Allele-specific peptide ligand motifs of HLA-C molecules. *Proc Natl Acad Sci U S A*, 90(24), 12005-12009.
- Foettinger, A., Leitner, A., & Lindner, W. (2006). Derivatisation of arginine residues with malondialdehyde for the analysis of peptides and protein digests by LC-ESI-MS/MS. *J Mass Spectrom*, 41(5), 623-632.
- Gaide, O., Emerson, R. O., Jiang, X., Gulati, N., Nizza, S., Desmarais, C., Robins, H., Krueger, J. G., Clark, R. A., & Kupper, T. S. (2015). Common clonal origin of central and resident memory T cells following skin immunization. *Nat Med*, 21(6), 647-653.
- Gambichler, T., Zhang, Y., Höxtermann, S., & Kreuter, A. (2013). Natural killer cells and B lymphocytes in peripheral blood of patients with psoriasis. *Br J Dermatol*, 168(4), 894-896.
- Granados, D. P., Sriranganadane, D., Daouda, T., Zieger, A., Laumont, C. M., Caron-Lizotte, O., Boucher, G., Hardy, M.-P., Gendron, P., Côté, C., Lemieux, S., Thibault, P., & Perreault, C. (2014). Impact of genomic polymorphisms on the repertoire of human MHC class I-associated peptides. *Nat Commun*, 5(1), 3600.

- Griffiths, C. E. M., Armstrong, A. W., Gudjonsson, J. E., & Barker, J. (2021). Psoriasis. *Lancet*, 397(10281), 1301-1315.
- Grijbovski, A. M., Olsen, A. O., Magnus, P., & Harris, J. R. (2007). Psoriasis in Norwegian twins: contribution of genetic and environmental effects. *J Eur Acad Dermatol Venereol*, 21(10), 1337-1343.
- Gürçan, H. M., Keskin, D. B., Stern, J. N., Nitzberg, M. A., Shekhani, H., & Ahmed, A. R. (2009). A review of the current use of rituximab in autoimmune diseases. *Int Immunopharmacol*, 9(1), 10-25.
- Haapasalo, K., Koskinen, L. L. E., Suvilehto, J., Jousilahti, P., Wolin, A., Suomela, S., Trembath, R., Barker, J., Vuopio, J., Kere, J., Jokiranta, T. S., & Saavalainen, P. (2018). The Psoriasis Risk Allele HLA-C*06:02 Shows Evidence of Association with Chronic or Recurrent Streptococcal Tonsillitis. *Infect Immun*, 86(10).
- Hassan, C., Kester, M. G. D., Oudgenoeg, G., de Ru, A. H., Janssen, G. M. C., Drijfhout, J. W., Spaapen, R. M., Jiménez, C. R., Heemskerk, M. H. M., Falkenburg, J. H. F., & van Veelen, P. A. (2014). Accurate quantitation of MHC-bound peptides by application of isotopically labeled peptide MHC complexes. *J Proteomics*, 109, 240-244.
- Heberle, H., Meirelles, G. V., da Silva, F. R., Telles, G. P., & Minghim, R. (2015). InteractiVenn: a web-based tool for the analysis of sets through Venn diagrams. *BMC Bioinform*, 16(1), 169.
- Hodne, K., & Weltzien, F. A. (2015). Single-Cell Isolation and Gene Analysis: Pitfalls and Possibilities. *Int J Mol Sci*, 16(11), 26832-26849.
- Hooijberg, E., Bakker, A. Q., Ruizendaal, J. J., & Spits, H. (2000). NFAT-controlled expression of GFP permits visualization and isolation of antigen-stimulated primary human T cells. *Blood*, 96(2), 459-466.
- Ishimoto, T., Arakawa, Y., Vural, S., Stöhr, J., Vollmer, S., Galinski, A., Siewert, K., Rühl, G., Poluektov, Y., Delcommenne, M., Horvath, O., He, M., Summer, B., Pohl, R., Alharbi, R., Dornmair, K., Arakawa, A., & Prinz, J. C. (2024). Multiple environmental antigens may trigger autoimmunity in psoriasis through T-cell receptor polyspecificity. *Front Immunol*, 15.
- Jelcic, I., Al Nimer, F., Wang, J., Lentsch, V., Planas, R., Jelcic, I., Madjovski, A., Ruhrmann, S., Faigle, W., Frauenknecht, K., Pinilla, C., Santos, R., Hammer, C., Ortiz, Y., Opitz, L., Grönlund, H., Rogler, G., Boyman, O., Reynolds, R., Lutterotti, A., Khademi, M., Olsson, T., Piehl, F., Sospedra, M., & Martin, R. (2018). Memory B Cells Activate Brain-Homing, Autoreactive CD4(+) T Cells in Multiple Sclerosis. *Cell*, 175(1), 85-100.e123.
- Jerne, N. K. (1955). THE NATURAL-SELECTION THEORY OF ANTIBODY FORMATION. *Proc Natl Acad Sci U S A*, 41(11), 849-857.
- Jimenez-Boj, E., Stamm, T. A., Sadlonova, M., Rovensky, J., Raffayová, H., Leeb, B., Machold, K. P., Graninger, W. B., & Smolen, J. S. (2012). Rituximab in psoriatic arthritis: an exploratory evaluation. *Ann Rheum Dis*, 71(11), 1868-1871.
- Jullien, D., Prinz, J. C., Langley, R. G., Caro, I., Dummer, W., Joshi, A., Dedrick, R., & Natta, P. (2004). T-cell modulation for the treatment of chronic plaque psoriasis with efalizumab (Raptiva): mechanisms of action. *Dermatology*, 208(4), 297-306.
- Kim, S.-M. (2011). *Analyse der T-Zell-Spezifität der pathogenen psoriatischen Immunantwort (In German)*. (Dr. rer. biol. hum. Dissertation). Ludwig-Maximilians-Universität München, Munich.
- Kim, S.-M., Bhonsle, L., Besgen, P., Nickel, J., Backes, A., Held, K., Vollmer, S., Dornmair, K., & Prinz, J. C. (2012). Analysis of the Paired TCR α - and β -chains of Single Human T Cells. *PLoS One*, 7(5), e37338.
- Krueger, J. G. (2015). An autoimmune "attack" on melanocytes triggers psoriasis and cellular hyperplasia. *J Exp Med*, 212(13), 2186-2186.
- Kuiper, J. J. W., Setten, J. V., Devall, M., Cretu-Stancu, M., Hiddingh, S., Ophoff, R. A., Missotten, T., Velthoven, M. V., Den Hollander, A. I., Hoyng, C. B., James, E., Reeves, E., Cordero-Coma, M., Fonollosa, A., Adán, A., Martín, J., Koeleman, B. P. C., Boer, J. H., Pulit, S. L., Márquez, A., & Radstake, T. (2018). Functionally distinct ERAP1 and ERAP2 are a hallmark of HLA-A29- (Birdshot) Uveitis. *Hum Mol Genet*, 27(24), 4333-4343.

- Kuiper, J. J. W., Prinz, J. C., Stratikos, E., Kuśnierczyk, P., Arakawa, A., Springer, S., Mintoff, D., Padjen, I., Shumnalieva, R., Vural, S., Kötter, I., Sande, M. G. v. d., Boyvat, A., Boer, J. H. d., Bertsias, G., Vries, N. d., Krieckaert, C. L., Leal, I., Valentinčič, N. V., Tugal-Tutkun, I., Ahanach, H. e. K., Costantino, F., Glatigny, S., Zimak, D. M., Lötscher, F., Kerstens, F. G., Bakula, M., Sousa, E. V., Böhm, P., Bosman, K., Kenna, T. J., Powis, S. J., Breban, M., Gul, A., Bowes, J., Lories, R. J., Nowatzky, J., Wolbink, G. J., McGonagle, D. G., & Turkstra, F. (2023). EULAR study group on 'MHC-I-opathy': identifying disease-overarching mechanisms across disciplines and borders. *Ann Rheum Dis*, annrheumdis-2022-222852.
- Letourneur, F., & Malissen, B. (1989). Derivation of a T cell hybridoma variant deprived of functional T cell receptor alpha and beta chain transcripts reveals a nonfunctional alpha-mRNA of BW5147 origin. *Eur J Immunol*, 19(12), 2269-2274.
- Leung, D. Y., Travers, J. B., Giorno, R., Norris, D. A., Skinner, R., Aelion, J., Kazemi, L. V., Kim, M. H., Trumble, A. E., Kotb, M., & et al. (1995). Evidence for a streptococcal superantigen-driven process in acute guttate psoriasis. *J Clin Invest*, 96(5), 2106-2112.
- López de Castro, J. A. (2018). How ERAP1 and ERAP2 Shape the Peptidomes of Disease-Associated MHC-I Proteins. *Front Immunol*, 9(2463).
- Lu, J., Ding, Y., Yi, X., & Zheng, J. (2016). CD19+ B cell subsets in the peripheral blood and skin lesions of psoriasis patients and their correlations with disease severity. *Braz J Med Biol Res*, 49(9), e5374.
- Ly, S., Nedosekin, D., & Wong, H. K. (2023). Review of an Anti-CD20 Monoclonal Antibody for the Treatment of Autoimmune Diseases of the Skin. *Am J Clin Dermatol*, 24(2), 247-273.
- Mallbris, L., Wolk, K., Sánchez, F., & Ståhle, M. (2009). HLA-Cw*0602 associates with a twofold higher prevalence of positive streptococcal throat swab at the onset of psoriasis: a case control study. *BMC Dermatol*, 9(1), 5.
- Medzhitov, R., & Janeway, C., Jr. (2000). Innate immune recognition: mechanisms and pathways. *Immunol Rev*, 173, 89-97.
- Mobbs, J. I., Illing, P. T., Dudek, N. L., Brooks, A. G., Baker, D. G., Purcell, A. W., Rossjohn, J., & Vivian, J. P. (2017). The molecular basis for peptide repertoire selection in the human leucocyte antigen (HLA) C*06:02 molecule. *J Biol Chem*, 292(42), 17203-17215.
- Monera, O. D., Sereda, T. J., Zhou, N. E., Kay, C. M., & Hodges, R. S. (1995). Relationship of sidechain hydrophobicity and alpha-helical propensity on the stability of the single-stranded amphipathic alpha-helix. *J Pept Sci*, 1(5), 319-329.
- Mrozek-Gorska, P., Buschle, A., Pich, D., Schwarzmayer, T., Fechtner, R., Scialdone, A., & Hammerschmidt, W. (2019). Epstein-Barr virus reprograms human B lymphocytes immediately in the prelatent phase of infection. *Proc Natl Acad Sci U S A*, 116(32), 16046-16055.
- Nair, R. P., Stuart, P. E., Nistor, I., Hiremagalore, R., Chia, N. V. C., Jenisch, S., Weichenthal, M., Abecasis, G. R., Lim, H. W., Christophers, E., Voorhees, J. J., & Elder, J. T. (2006). Sequence and Haplotype Analysis Supports HLA-C as the Psoriasis Susceptibility 1 Gene. *Am J Hum Genet*, 78(5), 827-851.
- Neefjes, J., Jongsma, M. L. M., Paul, P., & Bakke, O. (2011). Towards a systems understanding of MHC class I and MHC class II antigen presentation. *Nat Rev Immunol*, 11(12), 823-836.
- Nihal, M., Mikkola, D., & Wood, G. S. (2000). Detection of clonally restricted immunoglobulin heavy chain gene rearrangements in normal and lesional skin: analysis of the B cell component of the skin-associated lymphoid tissue and implications for the molecular diagnosis of cutaneous B cell lymphomas. *J Mol Diagn*, 2(1), 5-10.
- Nikamo, P., Lysell, J., & Ståhle, M. (2015). Association with Genetic Variants in the IL-23 and NF-κB Pathways Discriminates between Mild and Severe Psoriasis Skin Disease. *J Invest Dermatol*, 135(8), 1969-1976.
- Niu, J., Song, Z., Yang, X., Zhai, Z., Zhong, H., & Hao, F. (2015). Increased circulating follicular helper T cells and activated B cells correlate with disease severity in patients with psoriasis. *J Eur Acad Dermatol Venereol*, 29(9), 1791-1796.

- Ogawa, K., & Okada, Y. (2020). The current landscape of psoriasis genetics in 2020. *J Dermatol Sci*, 99(1), 2-8.
- Ombrello, M. J., Kastner, D. L., & Remmers, E. F. (2015). Endoplasmic reticulum-associated aminopeptidase 1 and rheumatic disease: genetics. *Curr Opin Rheumatol*, 27(4), 349-356.
- Ortega, C., Fernández-A, S., Carrillo, J. M., Romero, P., Molina, I. J., Moreno, J. C., & Santamaría, M. (2009). IL-17-producing CD8+ T lymphocytes from psoriasis skin plaques are cytotoxic effector cells that secrete Th17-related cytokines. *J Leukoc Biol*, 86(2), 435-443.
- Owczarczyk-Saczonek, A., Krajewska-Włodarczyk, M., Kaspruwicz-Furmańczyk, M., & Placek, W. (2020). Immunological Memory of Psoriatic Lesions. *Int J Mol Sci*, 21(2), 625.
- Parkes, M., Cortes, A., van Heel, D. A., & Brown, M. A. (2013). Genetic insights into common pathways and complex relationships among immune-mediated diseases. *Nat Rev Genet*, 14(9), 661-673.
- Paukkonen, K., Naukkarinen, A., & Horsmanheimo, M. (1992). The development of manifest psoriatic lesions is linked with the invasion of CD8 + T cells and CD11c + macrophages into the epidermis. *Arch Dermatol Res*, 284(7), 375-379.
- Perera, G. K., Di Meglio, P., & Nestle, F. O. (2012). Psoriasis. *Annu Rev Pathol*, 7, 385-422.
- Peters, B., Nielsen, M., & Sette, A. (2020). T Cell Epitope Predictions. *Annu Rev Immunol*, 38(1), 123-145.
- Prinz, J. C. (1997). Psoriasis vulgaris, streptococci and the immune system: a riddle to be solved soon? *Scand J Immunol*, 45(6), 583-586.
- Prinz, J. C. (2009). Bedeutung von Streptokokken für die Psoriasispathogenese. *Hautarzt*, 60(2), 109-115.
- Prinz, J. C. (2017a). Melanocytes: Target Cells of an HLA-C*06:02-Restricted Autoimmune Response in Psoriasis. *J Invest Dermatol*, 137(10), 2053-2058.
- Prinz, J. C. (2017b). Autoimmune aspects of psoriasis: Heritability and autoantigens. *Autoimmun Rev*, 16(9), 970-979.
- Prinz, J. C. (2018). Human Leukocyte Antigen-Class I Alleles and the Autoreactive T Cell Response in Psoriasis Pathogenesis. *Front Immunol*, 9, 954-954.
- Prinz, J. C. (2022). Antigen Processing, Presentation, and Tolerance: Role in Autoimmune Skin Diseases. *J Invest Dermatol*, 142(3 Pt B), 750-759.
- Prinz, J. C. (2023). Immunogenic self-peptides - the great unknowns in autoimmunity: Identifying T-cell epitopes driving the autoimmune response in autoimmune diseases. *Front Immunol*, 13.
- Rachakonda, T. D., Dhillon, J. S., Florek, A. G., & Armstrong, A. W. (2015). Effect of tonsillectomy on psoriasis: a systematic review. *J Am Acad Dermatol*, 72(2), 261-275.
- Rasmussen, M., Harndahl, M., Stryhn, A., Boucherma, R., Nielsen, L. L., Lemonnier, F. A., Nielsen, M., & Buus, S. (2014). Uncovering the Peptide-Binding Specificities of HLA-C: A General Strategy To Determine the Specificity of Any MHC Class I Molecule. *J Immunol*, 193(10), 4790-4802.
- Rausch, C., Weber, T., Kohlbacher, O., Wohlleben, W., & Huson, D. H. (2005). Specificity prediction of adenylation domains in nonribosomal peptide synthetases (NRPS) using transductive support vector machines (TSVMs). *Nucleic Acids Res*, 33(18), 5799-5808.
- Reeves, E., Islam, Y., & James, E. (2020). ERAP1: a potential therapeutic target for a myriad of diseases. *Expert Opin Ther Targets*, 24(6), 535-544.
- Riley, T. P., Keller, G. L. J., Smith, A. R., Davancaze, L. M., Arbuiso, A. G., Devlin, J. R., & Baker, B. M. (2019). Structure Based Prediction of Neoantigen Immunogenicity. *Front Immunol*, 10(2047).
- Roche, P. A., & Furuta, K. (2015). The ins and outs of MHC class II-mediated antigen processing and presentation. *Nat Rev Immunol*, 15(4), 203-216.
- Rock, K. L., Reits, E., & Neefjes, J. (2016). Present Yourself! By MHC Class I and MHC Class II Molecules. *Trends Immunol*, 37(11), 724-737.
- Ryan, C., & Menter, A. (2014). Ponesimod--a future oral therapy for psoriasis? *Lancet*, 384(9959), 2006-2008.
- Sanchez-Trincado, J. L., Gomez-Perosanz, M., & Reche, P. A. (2017). Fundamentals and Methods for T- and B-Cell Epitope Prediction. *J Immunol Res*, 2017, 2680160.

- Sarkizova, S., Klaeger, S., Le, P. M., Li, L. W., Oliveira, G., Keshishian, H., Hartigan, C. R., Zhang, W., Braun, D. A., Ligon, K. L., Bachiredy, P., Zervantonakis, I. K., Rosenbluth, J. M., Ouspenskaia, T., Law, T., Justesen, S., Stevens, J., Lane, W. J., Eisenhaure, T., Lan Zhang, G., Clauser, K. R., Hacohen, N., Carr, S. A., Wu, C. J., & Keskin, D. B. (2020). A large peptidome dataset improves HLA class I epitope prediction across most of the human population. *Nat Biotechnol*, 38(2), 199-209.
- Sattler, S. (2017). The Role of the Immune System Beyond the Fight Against Infection. In S. Sattler & T. Kennedy-Lydon (Eds.), *The Immunology of Cardiovascular Homeostasis and Pathology* (pp. 3-14). Cham: Springer International Publishing.
- Schmidt, J., Smith, A. R., Magnin, M., Racle, J., Devlin, J. R., Bobisse, S., Cesbron, J., Bonnet, V., Carmona, S. J., Huber, F., Ciriello, G., Speiser, D. E., Bassani-Sternberg, M., Coukos, G., Baker, B. M., Harari, A., & Gfeller, D. (2021). Prediction of neo-epitope immunogenicity reveals TCR recognition determinants and provides insight into immunoediting. *Cell Rep Med*, 2(2), 100194.
- Seitz, S., Schneider, C. K., Malotka, J., Nong, X., Engel, A. G., Wekerle, H., Hohlfeld, R., & Dornmair, K. (2006). Reconstitution of paired T cell receptor alpha- and beta-chains from microdissected single cells of human inflammatory tissues. *Proc Natl Acad Sci U S A*, 103(32), 12057-12062.
- Sette, A., Vitiello, A., Reheman, B., Fowler, P., Nayarsina, R., Kast, W. M., Melief, C. J., Oseroff, C., Yuan, L., Ruppert, J., Sidney, J., del Guercio, M. F., Southwood, S., Kubo, R. T., Chesnut, R. W., Grey, H. M., & Chisari, F. V. (1994). The relationship between class I binding affinity and immunogenicity of potential cytotoxic T cell epitopes. *J Immunol*, 153(12), 5586-5592.
- Sewell, A. K. (2012). Why must T cells be cross-reactive? *Nat Rev Immunol*, 12(9), 669-677.
- Sharma, G., & Holt, R. A. (2014). T-cell epitope discovery technologies. *Hum Immunol*, 75(6), 514-519.
- Sharma, G., Rive, C. M., & Holt, R. A. (2019). Rapid selection and identification of functional CD8+ T cell epitopes from large peptide-coding libraries. *Nat Commun*, 10(1), 4553.
- Shimizu, Y., Geraghty, D. E., Koller, B. H., Orr, H. T., & DeMars, R. (1988). Transfer and expression of three cloned human non-HLA-A,B,C class I major histocompatibility complex genes in mutant lymphoblastoid cells. *Proc Natl Acad Sci U S A*, 85(1), 227-231.
- Shimizu, Y., & DeMars, R. (1989). Production of human cells expressing individual transferred HLA-A,-B,-C genes using an HLA-A,-B,-C null human cell line. *J Immunol*, 142(9), 3320-3328.
- Siewert, K., Malotka, J., Kawakami, N., Wekerle, H., Hohlfeld, R., & Dornmair, K. (2012). Unbiased identification of target antigens of CD8+ T cells with combinatorial libraries coding for short peptides. *Nat Med*, 18(5), 824-828.
- Sigurdardottir, S. L., Thorleifsdottir, R. H., Valdimarsson, H., & Johnston, A. (2013). The association of sore throat and psoriasis might be explained by histologically distinctive tonsils and increased expression of skin-homing molecules by tonsil T cells. *Clin Exp Immunol*, 174(1), 139-151.
- Sims Sanyahumbi, A., Colquhoun, S., Wyber, R., & Carapetis, J. R. (2016). Global Disease Burden of Group A Streptococcus. In J. J. Ferretti, D. L. Stevens, & V. A. Fischetti (Eds.), *Streptococcus pyogenes: Basic Biology to Clinical Manifestations*. University of Oklahoma Health Sciences Center: © The University of Oklahoma Health Sciences Center.
- Singh, F., & Weinberg, J. M. (2005). Partial remission of psoriasis following rituximab therapy for non-Hodgkin lymphoma. *Cutis*, 76(3), 186-188.
- Stern, L. J., & Santambrogio, L. (2016). The melting pot of the MHC II peptidome. *Curr Opin Immunol*, 40, 70-77.
- Storkus, W. J., Alexander, J., Payne, J. A., Dawson, J. R., & Cresswell, P. (1989). Reversal of natural killing susceptibility in target cells expressing transfected class I HLA genes. *Proc Natl Acad Sci U S A*, 86(7), 2361-2364.
- Strange, A., Capon, F., Spencer, C. C., Knight, J., Weale, M. E., Allen, M. H., Barton, A., Band, G., Bellenguez, C., Bergboer, J. G., Blackwell, J. M., Bramon, E., Bumpstead, S. J., Casas, J. P., Cork, M. J., Corvin, A., Deloukas, P., Dilthey, A., Duncanson, A., Edkins, S., Estivill, X., Fitzgerald, O., Freeman, C., Giardina, E., Gray, E., Hofer, A., Hüffmeier, U., Hunt, S. E., Irvine, A. D., Jankowski, J., Kirby, B., Langford, C., Lascorz, J., Leman, J., Leslie, S., Mallbris, L., Markus, H. S., Mathew, C. G., McLean, W. H., McManus, R., Mössner, R., Moutsianas, L.,

- Naluai, A. T., Nestle, F. O., Novelli, G., Onoufriadis, A., Palmer, C. N., Perricone, C., Pirinen, M., Plomin, R., Potter, S. C., Pujol, R. M., Rautanen, A., Riveira-Munoz, E., Ryan, A. W., Salmhofer, W., Samuelsson, L., Sawcer, S. J., Schalkwijk, J., Smith, C. H., Stähle, M., Su, Z., Tazi-Ahnini, R., Traupe, H., Viswanathan, A. C., Warren, R. B., Weger, W., Wolk, K., Wood, N., Worthington, J., Young, H. S., Zeeuwen, P. L., Hayday, A., Burden, A. D., Griffiths, C. E., Kere, J., Reis, A., McVean, G., Evans, D. M., Brown, M. A., Barker, J. N., Peltonen, L., Donnelly, P., & Trembath, R. C. (2010). A genome-wide association study identifies new psoriasis susceptibility loci and an interaction between HLA-C and ERAP1. *Nat Genet*, 42(11), 985-990.
- Taylor, W. R. (1986). The classification of amino acid conservation. *J Theor Biol*, 119(2), 205-218.
- Ten Bergen, L. L., Petrovic, A., Aarebrot, A. K., & Appel, S. (2020). Current knowledge on autoantigens and autoantibodies in psoriasis. *Scand J Immunol*, 92(4), e12945.
- The International Psoriasis Genetics Consortium. (2003). The International Psoriasis Genetics Study: assessing linkage to 14 candidate susceptibility loci in a cohort of 942 affected sib pairs. *Am J Hum Genet*, 73(2), 430-437.
- Thomsen, M. C. F., & Nielsen, M. (2012). Seq2Logo: a method for construction and visualization of amino acid binding motifs and sequence profiles including sequence weighting, pseudo counts and two-sided representation of amino acid enrichment and depletion. *Nucleic Acids Res*, 40(W1), W281-W287.
- Thorleifsdottir, R., Eysteinsdóttir, J., Olafsson, J., Sigurdsson, M., Johnston, A., Valdimarsson, H., & Sigurgeirsson, B. (2016). Throat Infections are Associated with Exacerbation in a Substantial Proportion of Patients with Chronic Plaque Psoriasis. *Acta Derm Venereol*, 96.
- Thorleifsdottir, R., Sigurdardottir, S., Sigurgeirsson, B., Olafsson, J., Petersen, H., Sigurdsson, M., Gudjonsson, J., Johnston, A., & Valdimarsson, H. (2016). HLA-Cw6 homozygosity in plaque psoriasis is associated with streptococcal throat infections and pronounced improvement after tonsillectomy: A prospective case series. *J Am Acad Dermatol*, 75.
- Toussi, A., Merleev, A., Barton, V. R., Le, S. T., Marusina, A., Luxardi, G., Kirma, J., Xing, X., Adamopoulos, I. E., Fung, M. A., Raychaudhuri, S. P., Shimoda, M., Gudjonsson, J. E., & Maverakis, E. (2019). Transcriptome mining and B cell depletion support a role for B cells in psoriasis pathophysiology. *J Dermatol Sci*, 96(3), 181-184.
- Trolle, T., & Nielsen, M. (2014). NetTepi: an integrated method for the prediction of T cell epitopes. *Immunogenetics*, 66(7), 449-456.
- Tsoi, L. C., Spain, S. L., Knight, J., Ellinghaus, E., Stuart, P. E., Capon, F., Ding, J., Li, Y., Tejasvi, T., Gudjonsson, J. E., Kang, H. M., Allen, M. H., McManus, R., Novelli, G., Samuelsson, L., Schalkwijk, J., Stähle, M., Burden, A. D., Smith, C. H., Cork, M. J., Estivill, X., Bowcock, A. M., Krueger, G. G., Weger, W., Worthington, J., Tazi-Ahnini, R., Nestle, F. O., Hayday, A., Hoffmann, P., Winkelmann, J., Wijmenga, C., Langford, C., Edkins, S., Andrews, R., Blackburn, H., Strange, A., Band, G., Pearson, R. D., Vukcevic, D., Spencer, C. C., Deloukas, P., Mrowietz, U., Schreiber, S., Weidinger, S., Koks, S., Kingo, K., Esko, T., Metspalu, A., Lim, H. W., Voorhees, J. J., Weichenthal, M., Wichmann, H. E., Chandran, V., Rosen, C. F., Rahman, P., Gladman, D. D., Griffiths, C. E., Reis, A., Kere, J., Nair, R. P., Franke, A., Barker, J. N., Abecasis, G. R., Elder, J. T., & Trembath, R. C. (2012). Identification of 15 new psoriasis susceptibility loci highlights the role of innate immunity. *Nat Genet*, 44(12), 1341-1348.
- Tsoi, L. C., Spain, S. L., Ellinghaus, E., Stuart, P. E., Capon, F., Knight, J., Tejasvi, T., Kang, H. M., Allen, M. H., Lambert, S., Stoll, S. W., Weidinger, S., Gudjonsson, J. E., Koks, S., Kingo, K., Esko, T., Das, S., Metspalu, A., Weichenthal, M., Enerback, C., Krueger, G. G., Voorhees, J. J., Chandran, V., Rosen, C. F., Rahman, P., Gladman, D. D., Reis, A., Nair, R. P., Franke, A., Barker, J., Abecasis, G. R., Trembath, R. C., & Elder, J. T. (2015). Enhanced meta-analysis and replication studies identify five new psoriasis susceptibility loci. *Nat Commun*, 6, 7001.
- Veiga-Fernandes, H., Walter, U., Bourgeois, C., McLean, A., & Rocha, B. (2000). Response of naïve and memory CD8+ T cells to antigen stimulation in vivo. *Nat Immunol*, 1(1), 47-53.
- Vural, S., Kerl, K., Ertop Doğan, P., Vollmer, S., Puchta, U., He, M., Arakawa, Y., Heper, A. O., Karal-Öktem, A., Hartmann, D., Boyvat, A., Prinz, J. C., & Arakawa, A. (2021). Lesional activation of

- Tc17 cells in Behçet disease and psoriasis supports HLA class I-mediated autoimmune responses*. *Br J Dermatol*, 185(6), 1209-1220.
- Vyas, J. M., Van der Veen, A. G., & Ploegh, H. L. (2008). The known unknowns of antigen processing and presentation. *Nat Rev Immunol*, 8(8), 607-618.
- Wang, G., Wan, H., Jian, X., Li, Y., Ouyang, J., Tan, X., Zhao, Y., Lin, Y., & Xie, L. (2020). INeo-Epp: A Novel T-Cell HLA Class-I Immunogenicity or Neoantigenic Epitope Prediction Method Based on Sequence-Related Amino Acid Features. *Biomed Res Int*, 2020, 5798356-5798356.
- Watkins, T. S., & Miles, J. J. (2021). The human T-cell receptor repertoire in health and disease and potential for omics integration. *Immunol Cell Biol*, 99(2), 135-145.
- Wieczorek, M., Abualrous, E. T., Sticht, J., Álvaro-Benito, M., Stolzenberg, S., Noé, F., & Freund, C. (2017). Major Histocompatibility Complex (MHC) Class I and MHC Class II Proteins: Conformational Plasticity in Antigen Presentation. *Front Immunol*, 8(292).
- Wilson, J. K., Al-Suwaidan, S. N., Krowchuk, D., & Feldman, S. R. (2003). Treatment of psoriasis in children: is there a role for antibiotic therapy and tonsillectomy? *Pediatr Dermatol*, 20(1), 11-15.
- Wu, P., Zhang, T., Liu, B., Fei, P., Cui, L., Qin, R., Zhu, H., Yao, D., Martinez, R. J., Hu, W., An, C., Zhang, Y., Liu, J., Shi, J., Fan, J., Yin, W., Sun, J., Zhou, C., Zeng, X., Xu, C., Wang, J., Evavold, B. D., Zhu, C., Chen, W., & Lou, J. (2019). Mechano-regulation of Peptide-MHC Class I Conformations Determines TCR Antigen Recognition. *Mol Cell*, 73(5), 1015-1027.e1017.
- Youming, Z. (2018). Gene Expression during the Activation of Human B Cells. In U. Fumiaki (Ed.), *Gene Expression and Regulation in Mammalian Cells* (pp. Ch. 9). Rijeka: IntechOpen.
- Zhang, X., Qi, Y., Zhang, Q., & Liu, W. (2019). Application of mass spectrometry-based MHC immunopeptidome profiling in neoantigen identification for tumor immunotherapy. *Biomed Pharmacother*, 120, 109542.
- Zhang, X. W. (2013). A combination of epitope prediction and molecular docking allows for good identification of MHC class I restricted T-cell epitopes. *Comput Biol Chem*, 45, 30-35.
- Zhou, F., Cao, H., Zuo, X., Zhang, T., Zhang, X., Liu, X., Xu, R., Chen, G., Zhang, Y., Zheng, X., Jin, X., Gao, J., Mei, J., Sheng, Y., Li, Q., Liang, B., Shen, J., Shen, C., Jiang, H., Zhu, C., Fan, X., Xu, F., Yue, M., Yin, X., Ye, C., Zhang, C., Liu, X., Yu, L., Wu, J., Chen, M., Zhuang, X., Tang, L., Shao, H., Wu, L., Li, J., Xu, Y., Zhang, Y., Zhao, S., Wang, Y., Li, G., Xu, H., Zeng, L., Wang, J., Bai, M., Chen, Y., Chen, W., Kang, T., Wu, Y., Xu, X., Zhu, Z., Cui, Y., Wang, Z., Yang, C., Wang, P., Xiang, L., Chen, X., Zhang, A., Gao, X., Zhang, F., Xu, J., Zheng, M., Zheng, J., Zhang, J., Yu, X., Li, Y., Yang, S., Yang, H., Wang, J., Liu, J., Hammarström, L., Sun, L., Wang, J., & Zhang, X. (2016). Deep sequencing of the MHC region in the Chinese population contributes to studies of complex disease. *Nat Genet*, 48(7), 740-746.

Appendixes

1. Abbreviations

AA	<u>A</u> mino <u>A</u> cid
Amp	<u>A</u> mpicillin
APC	Allophycocyanin (a fluorescent dye)
APCs	<u>A</u> ntigen <u>P</u> resenting <u>C</u> ells
bp	<u>B</u> ase <u>P</u> airs
CD	<u>C</u> luster of <u>D</u> ifferentiation
cDNA	<u>C</u> omplementary DNA
CDR	<u>C</u> omplementarity <u>D</u> etermining <u>R</u> egion
CLA	<u>C</u> utaneous <u>L</u> ymphocyte-Associated <u>A</u> ntigen
CSC	<u>C</u> hina <u>S</u> cholarship <u>C</u> ouncil
CTLs	Cytotoxic T cells
DAPI	4',6-diamidino-2-phenylindole (a fluorescent dye)
DCs	<u>D</u> endritic <u>C</u> ells
DMEM	<u>D</u> ulbecco's <u>M</u> odified <u>E</u> agle <u>M</u> edium
DMSO	<u>D</u> imethyl <u>S</u> ulfoxide
DNA	<u>D</u> eoxyribonucleic <u>A</u> cid
dNTP	<u>D</u> esoxy- <u>n</u> ucleoside-triphosphat
<i>E. coli</i>	<i><u>E</u>scherichia <u>c</u>oli</i>
EB	<u>E</u> lution <u>B</u> uffer
EBV	<u>E</u> pstein- <u>B</u> arr- <u>V</u> irus
EDTA	<u>E</u> thylenediamine tetraacetic <u>a</u> cid
ER	<u>E</u> ndoplasmic <u>R</u> eticulum
ERAP1	<u>E</u> ndoplasmic <u>R</u> eticulum <u>A</u> minopeptidase 1
FACS	<u>F</u> luorescence-activated <u>C</u> ell <u>S</u> orting
FCS	<u>F</u> etal <u>C</u> alf <u>S</u> erum
FITC	<u>F</u> luorescein- <u>I</u> sothiocyanate (a fluorescent dye)
FT	<u>F</u> ast-growing, highly <u>T</u> ransfectable
G418	Geneticin
GFP	<u>G</u> reen <u>F</u> luorescent <u>P</u> rotein
HLA	<u>H</u> uman <u>L</u> eucocyte <u>A</u> ntigen
HPLC	<u>H</u> igh <u>P</u> erformance <u>L</u> iquid <u>C</u> hromatography
Ig	<u>I</u> mmunoglobulin
IL	<u>I</u> nterleukin
IL12B	<u>I</u> nterleukin <u>12</u> Subunit <u>B</u> eta
IL23A	<u>I</u> nterleukin <u>23</u> Subunit <u>A</u> lpha
IL23R	<u>I</u> nterleukin <u>23</u> <u>R</u> eceptor

IMiDS	<u>I</u> mmune <u>M</u> ediated <u>I</u> nflammatory <u>D</u> isorders
IFN- γ	<u>I</u> nterferon- <u>g</u> amma
kb	<u>K</u> ilo <u>b</u> ase pairs
LB-Medium	<u>L</u> uria- <u>B</u> ertani-Medium
LC	<u>L</u> iquid <u>C</u> hromatography
LC-MS/MS	<u>L</u> iquid <u>C</u> hromatography <u>T</u> andem <u>M</u> ass <u>S</u> pectrometry
MACS	<u>M</u> agnetic- <u>a</u> ctivated <u>C</u> ell <u>S</u> orting
MHC	<u>M</u> ajor <u>H</u> istocompatibility <u>A</u> ntigen
MS	<u>M</u> ass <u>S</u> pectrometry
ND	<u>N</u> ot <u>D</u> etermined
NFAT	<u>N</u> uclear <u>F</u> actor of <u>A</u> ctivated <u>T</u> Cells
NF κ B	<u>N</u> uclear <u>F</u> actor ' <u>\kappa</u> -light-chain-enhancer' of activated <u>B</u> -cells
NK cells	<u>N</u> atural <u>K</u> iller cells
OD	<u>O</u> ptical <u>D</u> ensity
PBL	<u>P</u> eripheral <u>B</u> lood <u>L</u> ymphocytes
PBMC	<u>P</u> eripheral <u>B</u> lood <u>M</u> ononuclear <u>C</u> ell
PBS	<u>P</u> hosphate <u>B</u> uffered <u>S</u> aline
PCR	<u>P</u> olymerase <u>C</u> hain <u>R</u> eaction
pDCs	<u>P</u> lasmacytoid <u>D</u> endritic <u>C</u> ells
PE	<u>P</u> hycoerythrin (a fluorescent dye)
PECP library	<u>P</u> lasmi <u>d</u> - <u>E</u> ncoded <u>C</u> ombinatorial <u>P</u> eptide library
PE/Cyanine7	<u>P</u> hycoerythrin- <u>C</u> yanine 7 (a fluorescent dye)
PerCP/Cyanine5.5	<u>P</u> eridinin <u>C</u> hlorophyll <u>P</u> rotein- <u>C</u> yanine 5.5 (a fluorescent dye)
pMHC	<u>P</u> eptide- <u>M</u> HC complex
RNA	<u>R</u> ibonucleic <u>A</u> cid
RNase	Ribonuclease
rpm	<u>R</u> evolutions per <u>m</u> inute
RPMI medium	<u>R</u> oswell <u>P</u> ark <u>M</u> emorial <u>I</u> nstitute medium
RT	<u>R</u> oom temperature
sGFP	superfolder <u>G</u> reen <u>F</u> luorescent <u>P</u> rotein
S ₁ P ₁	<u>S</u> phingosine- <u>1</u> -phosphate receptor- <u>1</u>
SNPs	<u>S</u> ingle <u>N</u> ucleotide <u>P</u> olymorphisms
TAP	Transporter associated with antigen processing transporter
TBE	<u>T</u> ris- <u>B</u> orat- <u>E</u> DTA
Tc cell	<u>C</u> ytotoxic <u>T</u> cell
TCR	<u>T</u> Cell <u>R</u> eceptor
TE buffer	<u>T</u> ris- <u>E</u> DTA buffer
TGF- β	<u>T</u> ransforming <u>G</u> rowth <u>F</u> actor- β
Th cell	<u>T</u> helper cell
T _m	<u>M</u> elting <u>T</u> emperature
TNF	<u>T</u> umor <u>n</u> ecrosis <u>f</u> actor
TNF- α	<u>T</u> umor <u>n</u> ecrosis <u>f</u> actor- <u>\alpha</u>

Tris	Tris-(hydroxymethyl)aminomethan
U	<u>U</u> nit
UV	<u>U</u> ltravio <u>l</u> et Light

2. Index of Figures

Figure 1.1.4.1	10
Figure 1.1.4.2	11
Figure 1.1.5	13
Figure 1.2.1	14
Figure 1.2.2	16
Figure 1.2.3.1	17
Figure 1.2.3.2	18
Figure 1.3.3.1	21
Figure 1.3.3.2	22
Figure 3.1.5	37
Figure 3.1.7.3.1	40
Figure 3.1.7.3.2	41
Figure 3.1.11.....	45
Figure 3.2.6.2	52
Figure 3.4.1.1	57
Figure 3.4.1.2	58
Figure 4.1	63
Figure 4.2.1.1	64
Figure 4.2.1.2	65
Figure 4.2.2	67
Figure 4.2.3	70
Figure 4.3.1	72
Figure 4.3.2	73
Figure 4.3.3	74
Figure 4.3.4	75
Figure 4.4.1	78
Figure 4.4.2	80

Figure 4.4.3.1	81
Figure 4.4.3.2	83
Figure 4.4.4	85
Figure 4.5.1	88
Figure 4.5.2.1	89
Figure 4.5.2.2	90
Figure 4.5.2.3	91
Figure 4.6.1.1	93
Figure 4.6.1.2	94
Figure 4.6.2	95
Figure 4.7.1	97
Figure 4.7.2.1.1	99
Figure 4.7.2.1.2	100
Figure 4.7.2.1.3	101
Figure 4.7.2.2	103
Figure 4.7.2.3.1	104
Figure 4.7.2.3.2	104
Figure 4.7.2.3.3	106
Figure 4.7.3.1.1	108
Figure 4.7.3.1.2	109
Figure 4.7.3.2	111
Figure 5	114
Figure 5.3	124

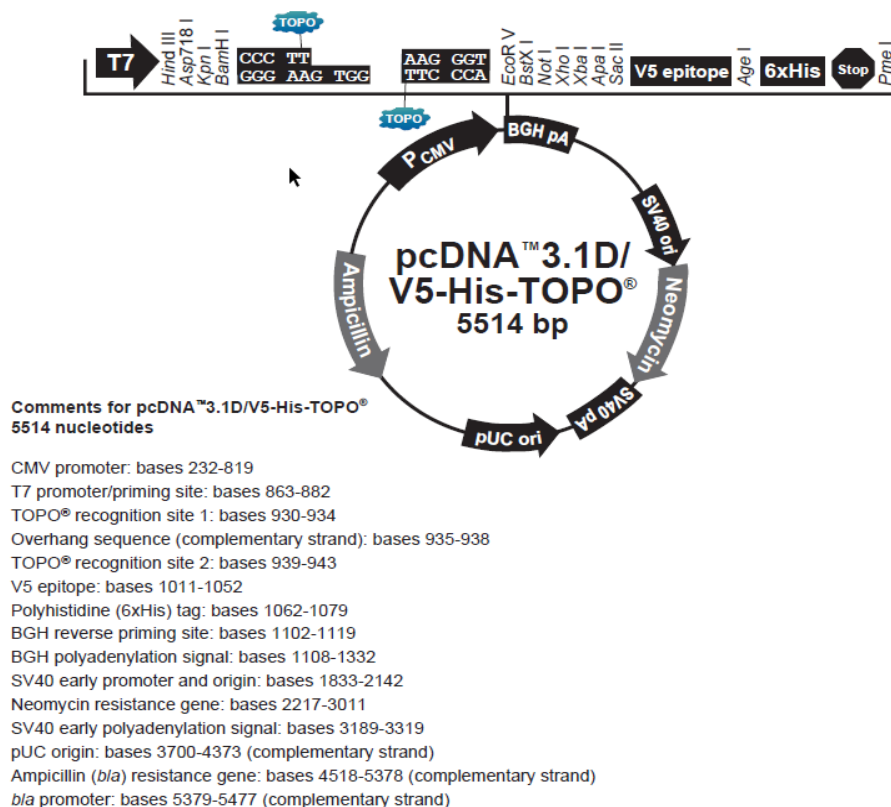
3. Index of Tables

Table 3.1.7.3	41
Table 3.2.2.1	47
Table 3.4.2	59
Table 4.2.2	66
Table 4.2.4	71
Table 4.4.5	86
Table 4.7.2.1	99

Table 4.7.3.2	110
Table 6.1.1	130
Table 6.1.2	130
Table 6.1.3	132
Table 6.1.4	133
Table 6.1.5	136
Table 6.2.1	140
Table 6.2.2	140
Table 6.2.3	141
Table 6.2.4	142
Table 6.2.5	144

4. Vector Map

The Map of pcDNA™3.1D/V5-His-TOPO®:



Acknowledgements

I could not have undertaken this journey without my supervisor, Prof. Dr. med. Jörg C. Prinz, who not only offered technical and professional advice but also provided assistance with everyday challenges. I express my sincere gratitude to him, particularly for his unwavering trust, great patience, constant encouragement, and unreserved support throughout my study and subsequent thesis writing. Under his mentorship, I have grown into a “mastermind” of my project, as he always expected.

I am deeply appreciative of the valuable contributions made by Dr. Akiko Arakawa, who provided extremely meticulous technical guidance in executing each experiment. She always engaged in enlightening discussions with me, and her astute insights on experimental design and data analysis guaranteed the reliability of this study’s findings. Besides supporting my studies, Akiko and her partner Atsushi always offered me countless concerns about my daily life.

The working atmosphere within our group is pleasant and amicable. I consider myself fortunate to have had the opportunity to work with colleagues with whom I could engage in conversations, share laughter, and discuss scientific inquiries. Within our laboratory team, I would like to extend my sincere appreciation to Sigrid Vollmer for being an outstanding custodian of everything in the lab and the best steward for daily laboratory activities. Despite the age disparity, she has become my closest confidant. Our group has dedicated over three decades to investigating the underlying pathogenesis of psoriasis, which has continuously fueled my motivation and inspiration to explore scientific questions.

I would like to express my gratitude to Prof. Andreas Schlosser and Melissa Bernhardt, our esteemed collaborators from the Center for Integrative and Translational Bioimaging at Universität Würzburg. Their exceptional expertise in mass spectrometry-based MHC immunopeptidome profiling has played a crucial role in the successful identification of the specific autoantigen originating from immunogenic B cells. Without their invaluable collaboration, this achievement would not have been possible.

Furthermore, I would like to extend my heartfelt thanks to many colleagues in our research group: Seçil Vural, Yukiyasu Arakawa, and Tatsushi Ishimoto, as well as the colleagues in our clinic: Burkard Summer, Ralf Pohl, Claudia Kammerbauer, Takashi Satoh, et al. Their unwavering kindness and support have greatly contributed to the completion of my research work.

I would further like to thank the Chairman of the Department of Dermatology and Allergy, Prof. Dr. med. Lars French, for the support, scientific atmosphere and research motivation he has created at the Clinic.

I would also like to acknowledge the China Scholarship Council (CSC) for providing financial support for the CSC-LMU Joint Program throughout my study in Germany, which enabled me to engage in research activities abroad. Additionally, this thesis was carried out in the framework of the German Research Foundation grants PR 241/5-1 and 5-2.

Finally, I am very grateful to my family for their unconditional support throughout my academic journey. They fully support my decision to study abroad for four years. Their unwavering presence and encouragement have served as a constant source of inspiration, particularly during the toughest periods of the global COVID-19 pandemic.

Affidavit



Promotionsbüro
Medizinische Fakultät



Affidavit

He, Mengwen

Surname, first name

Street

Zip code, town, country

I hereby declare, that the submitted thesis entitled:

Role of B-cell antigenicity in the psoriatic autoimmune response against melanocytes

is my own work. I have only used the sources indicated and have not made unauthorized use of services of a third party. Where the work of others has been quoted or reproduced, the source is always given.

I further declare that the submitted thesis or parts thereof have not been presented as part of an examination degree to any other university.

Zhuhai, 02/11/2024
place, date

Mengwen He
Signature doctoral candidate